DISS. ETH NO. 27604

MECHANISTIC ASSESSMENT OF FIBROBLAST GROWTH FACTOR RECEPTOR SIGNALING AND FUNCTION IN KERATINOCYTES

A thesis submitted to attain the degree of

DOCTOR OF SCIENCES of ETH Zurich

(Dr. sc. ETH Zurich)

presented by

THERESA RAUSCHENDORFER

M.Sc., University of Bayreuth

born 15.05.1990

citizen of Germany

accepted on the recommendation of

Prof. Dr. Sabine Werner, examiner

Prof. Dr. Nancy Hynes, co-examiner

Prof. Dr. Michael Detmar, co-examiner

2021

Table of contents

Summary **1**

Zusammenfassung **3**

1 Introduction **5**

1. The skin 5

1.1 The epidermis *5*

1.2 The dermis and hypodermis *7*

1.3 Skin defects and wound healing *9*

2. Cell communication 11

2.1 Fibroblast growth factors (FGFs) *11*

2.2 FGF receptors *12*

2.3 Canonical FGF signaling *14*

2.4 Importance of FGF signaling in skin *16*

2.5 Complexity of FGF signaling *17*

3. Optogenetics 19

3.1 Optogenetic systems *19*

3.2 Optogenetics in cell signaling research *21*

3.3 Optogenetic modification of FGFRs *22*

3.4 OptoR2 *23*

4. Objectives 24

References 25

2 Materials **36**

1. Chemicals and solid biologicals 36

2. Prefabricated products and kits 40

3. Buffers and solutions 42

4. Oligonucleotides 47

5. Primary antibodies 50

6. Secondary and coupled antibodies 53

3 Methods 54

1. Mouse methods 54

1.1 Mouse genotyping 54

1.2 Illumination of mice 54

1.3 Excisional wounding 55

1.4 Tape stripping 55

1.5 Preparation of tail explants 55

1.6 Establishment of murine primary keratinocyte cultures 56

2. Cell culture 57

2.1 Cell lines and cell types 57

2.2 Passaging of cells 58

2.3 Cryopreservation of cells 58

2.4 Generation of lentivirus particles and lentiviral transduction 59

2.5 Starvation and illumination experiment 60

2.6 MTT assay 60

2.7 Scratch assay 61

2.8 Chelation of FBS 62

3. Cell stains 63

3.1 Crystal violet cell stain 63

3.2 Immunofluorescence staining of cells 63

3.3 BrdU staining 64

3.4 Staining for flow cytometry 64

3.5 Cell cycle analysis by flow cytometry 65

3.6 Microscopy 66

4. Histological stains 67

4.1 Tissue processing for paraffin sections 67

4.2 H&E stain 68

4.3 Herovici's stain 68

4.4 Masson-Goldner Trichrome stain 69

4.5 Immunohistochemistry staining of tissue sections *70*
4.6 Immunofluorescence staining of tissue sections *70*
4.7 Microscopy *71*
5. DNA methods 72
5.1 KAPA PCR for genotyping *72*
5.2 Agarose gel *72*
5.3 Measurement of the concentration of nucleic acids by Nanodrop *73*
5.4 Molecular cloning using restriction enzymes *73*
5.5 Molecular cloning using Topoisomerase Ligation and Gateway strategy *75*
5.6 Isolation of genomic DNA (HotShot) *76*
5.7 Analysis of viral DNA by qPCR *76*
6. RNA methods 78
6.1 Isolation of RNA from tissue *78*
6.2 Isolation of RNA from cells *79*
6.3 Reverse transcription *79*
6.4 Analysis of the RNA content by qPCR *80*
7. Protein methods 81
7.1 Preparation of protein lysates from tissue *81*
7.2 Preparation of protein lysates from cultured cells *81*
7.3 Nuclear-cytoplasmic fractionation of cells *82*
7.4 Immunoprecipitation *82*
7.5 Measurement of the protein concentration using BCA assay *83*
7.6 Western blot *83*
7.7 ELISA for phospho-ERK1/2 and total ERK1/2 *84*
8. Analysis and statistics 86
8.1 qPCR analysis *86*
8.2 Statistical analysis *86*
References 87
4 Results **89**
1. Optogenetic activation of FGFR2 89
Abstract *91*

1.1 Introduction *92*
1.2 Materials and Methods *94*
1.3 Results *102*
1.4 Discussion *115*
Acknowledgements *118*
Author contributions *118*
Disclosure *118*
Supplementary figures *119*
References *123*

2. FGF, interferon and antiviral defence 128
The paper explained *130*
Graphical abstract *131*
Abstract *132*
2.1 Introduction *133*
2.2 Materials and Methods *134*
2.3 Results *141*
2.4 Discussion *161*
Acknowledgments *164*
Author contributions *164*
Conflict of interest *164*
Tables *165*
Extended data *167*
Appendix *170*
References *175*

3. FGF receptor triple knockout in skin 181
Abstract *183*
3.1 Introduction *184*
3.2 Materials and Methods *186*
3.3 Results *192*
3.4 Discussion *201*
Acknowledgements *203*
Author contributions *203*
Disclosure *203*

Supplementary figures *204*
References *208*

5 Conclusions and Outlook **211**

1. Optogenetic activation of FGFR2 211
1.1 Reduction in the cellular response to OptoR2 in keratinocytes *212*
1.2 Optogenetic alternatives *215*
2. FGF, interferon and antiviral defence 217
2.1 Mechanism of ISG regulation by FGFs *217*
2.2 Beneficial and detrimental FGF effects *218*
2.3 FGFR inhibition as a novel antiviral strategy *219*
3. Loss of FGF signaling in keratinocytes 221
3.1 Overlapping functions of different FGFRs in keratinocytes *221*
3.2 Barrier defect and skin fibrosis in the absence of FGFR signaling in keratinocytes *222*
4. Complexity in biological signaling systems 223
4.1 Degrees of complexity in cellular signaling networks *223*
4.2 Reductionist approaches *225*
4.3 Holistic approaches *226*

References *227*

Appendix **235**

Abbreviations **239**

Acknowledgements **244**

Complete bibliography **245**

Summary

The skin protects the body from environmental insults by forming an indispensable barrier. When it gets disrupted by wounding or upon development of certain skin diseases, different cell types have to act together to restore the barrier. Therefore, cellular communication via secretion of growth factors and other signaling molecules, which bind to receptors on the receiving cell, is essential. Major players in the communication between keratinocytes and fibroblasts, the main cell types of epidermis and dermis, respectively, are fibroblast growth factors (FGFs) and their receptors (FGFRs). However, FGFR signaling is complex and involves a large variety of ligands, which activate different splice variants of four high-affinity FGFRs. Additionally, the intracellular signal transduction molecules are not exclusive for FGF signaling, but are shared with and influenced by other signaling pathways. This complexity is a major obstacle when investigating effects of different FGFs and FGF receptors.

To reduce the complexity and to investigate the effect of only one FGFR, we modified the major FGFR expressed in keratinocytes, FGFR2, to be activated by blue light (OptoR2) instead of its endogenous ligands. In HEK 293T cells expressing OptoR2, illumination activated the downstream signaling pathways with remarkable temporal precision, and induced cell migration and proliferation. Keratinocytes expressing OptoR2 also responded to blue light with activation of their downstream pathways, regulation of known FGF target genes and increased migration. However, in all keratinocyte *in vitro* and *in vivo* systems that we generated, the cells lost the responsiveness to OptoR2 over time through receptor down-regulation or desensitisation to FGFR signaling. Therefore, a novel optogenetic strategy is required to further study FGFR signaling in the skin.

Another means to reduce complexity is removal of a single signaling component and analysis of the effect that this loss exerts in the cells. However, receptors and downstream signaling molecules are frequently redundant. Keratinocytes, for example, express FGFR1, FGFR2 and FGFR3. When FGFR1 and FGFR2 are lost in keratinocytes, mice develop a skin phenotype resembling Atopic Dermatitis in humans, with epidermal thickening, barrier defects and inflammation. These abnormalities are absent or reduced in mice lacking only a single FGFR. However, FGFR3 might compensate at least in part for the loss of the other two FGFRs. Therefore, we generated mice lacking FGFR1, FGFR2 and FGFR3 in keratinocytes to determine the effect of complete loss of FGFR signaling in this cell type. I contributed to the

analysis of the phenotype of these mice, which revealed that loss of FGFR3 alone does not affect skin homeostasis and repair. Surprisingly, the phenotype of mice lacking all three receptors was not much stronger compared to the abnormalities seen in the absence of FGFR1 and FGFR2. It is possible that other receptor tyrosine kinases compensate for the loss of FGFR signaling in keratinocytes.

Finally, we discovered an unexpected interaction between FGF and type I interferon signaling, which depends on FGFR kinase and proteasomal activity, but not on type I interferon receptors. Consequently, FGF7-stimulated keratinocytes produce less antiviral proteins and are more prone to viral infection. *Vice versa*, inhibition of FGFR signaling strongly reduces the infection of keratinocytes with different viruses. This finding opens the possibility of treating viral infections with FGFR inhibitors, which should be further explored in the future.

Overall, my work contributed to the understanding of FGFR signaling at multiple levels and identified strengths and weaknesses of optogenetic approaches to study growth factor function. Finally, it opened potential new avenues for the treatment of viral infections in humans using FGFR kinase inhibitors.

Zusammenfassung

Die Haut bildet eine schützende Barriere und verhindert so, dass Umwelteinflüsse in unseren Körper eindringen. Wenn diese geschädigt ist, zum Beispiel durch eine Wunde oder bestimmte Hautkrankheiten, müssen verschiedene Zelltypen zusammenarbeiten, um die Barriere schnell wiederherzustellen. Dafür ist die Kommunikation zwischen den Zellen über Wachstumsfaktoren und andere Signalmoleküle entscheidend. Diese werden von einer Zelle ausgeschieden und binden an Rezeptoren auf einer Zielzelle, die das Signal empfängt und in ihrem Inneren charakteristische Signalwege anschaltet. In der Kommunikation zwischen Keratinozyten und Fibroblasten, den beiden häufigsten Zelltypen in der Epidermis beziehungsweise Dermis, spielen *Fibroblast growth factors* (FGFs) und ihre Rezeptoren (FGFRs) eine herausragende Rolle. Der FGF Signalweg ist jedoch sehr komplex: er beinhaltet eine grosse Anzahl an Liganden, die verschiedene Varianten der vier FGFRs mit unterschiedlicher Affinität binden. Zusätzlich werden die Signalmoleküle, die das Signal innerhalb der Zelle weiterleiten, nicht nur durch FGFs reguliert, sondern auch von anderen Wachstumsfaktoren beeinflusst. Wenn man dieses Netzwerk von Signalwegen untersuchen will, ist Komplexität also ein grosses Problem.

Deshalb versucht man, das Netzwerk auf einzelne Signalwege herunterzubrechen und so die Komplexität zu reduzieren. Dafür haben wir FGFR2, den wichtigsten FGF Rezeptor in Keratinozyten, so modifiziert, dass er durch blaues Licht anstatt seiner üblichen Liganden aktiviert wird (OptoR2). Wenn OptoR2 in HEK 293T Zellen vorhanden war, wurden die klassischen FGF Signalwege durch die Beleuchtung der Zellen aktiviert. Dies erfolgte mit bemerkenswerter Genauigkeit und brachte die Zellen dazu, mehr zu wandern und sich zu teilen. Auch die Beleuchtung von Keratinozyten, die OptoR2 auf ihrer Zelloberfläche hatten, schaltete die bekannten Signalwege an. Zusätzlich veränderte das Licht die Expression bekannter FGF Zielgene, und führte dazu, dass die Zellen schneller wanderten. Doch in allen Keratinozyten-Systemen, die wir herstellten, verloren die Zellen über die Zeit ihre Reaktivität gegenüber OptoR2. Sie regulierten entweder den Rezeptor herunter oder reagierten nicht mehr so stark auf das FGFR Signal. Deshalb benötigt man eine neue Strategie, um diesen Signalweg in der Haut mit Licht zu untersuchen.

Um die Komplexität zu reduzieren, ist es auch möglich, eine Signalkomponente zu entfernen und zu untersuchen, was dies in den Zellen bewirkt. Doch oft sind die Signalwege redundant

und können den Ausfall eines einzelnen Signalweges kompensieren. In Keratinozyten zum Beispiel gibt es FGFR1, FGFR2 und FGFR3. Wenn FGFR1 und FGFR2 in diesen Zellen fehlen, entwickeln die Mäuse Veränderungen in der Haut, die an Neurodermitis im Menschen erinnern. Ihre Epidermis verdickt sich, die Hautbarriere wird durchlässiger und es entstehen Entzündungen. Diese Effekte sind sehr reduziert oder fehlen ganz, wenn nur einer der Rezeptoren verloren geht – ein Hinweis darauf, dass die Rezeptoren Aufgaben von einander übernehmen können. Auch FGFR3 könnte den Ausfall der anderen beiden Rezeptoren zumindest teilweise kompensieren. Deshalb haben wir Mäuse so verändert, dass in ihren Keratinozyten alle drei FGFRs fehlen und sie damit überhaupt kein FGF Signal mehr wahrnehmen können. Ich trug mit meiner Arbeit zur Analyse dieser Mäuse bei, die zeigte, dass der alleinige Verlust von FGFR3 keine Wirkung auf die Haut im Ruhezustand und während der Wundheilung hat. Überraschenderweise war die Haut der Mäuse, bei denen alle drei FGFRs fehlen, nicht viel anders als die Haut der Mäuse ohne FGFR1 und FGFR2. Möglicherweise kompensieren nochmals andere Wachstumsfaktoren den kompletten Ausfall des FGF Signalwegs.

Zuletzt entdeckten wir, dass der FGF Signalweg unerwarteterweise den Typ I Interferon Signalweg beeinflusst. Dieser Signalweg ist wichtig, wenn Zellen sich gegen die Infektion mit einem Virus verteidigen. Demzufolge produzieren Keratinozyten, die mit FGF7 stimuliert werden, weniger antivirale Proteine und werden darum leichter von Viren infiziert. Anders herum können sich verschiedene Viren in den Keratinozyten nicht so stark vermehren, wenn deren FGFRs gehemmt werden. Der Effekt von FGF auf den Interferon Signalweg benötigt die Aktivität der FGFR Kinase sowie des Proteasoms, während der Typ I Interferon-Rezeptor selbst nicht daran beteiligt ist. Diese bisher unbekannte Funktion von FGFs eröffnet die Möglichkeit, zukünftig virale Infekte mit FGFR Inhibitoren zu behandeln. Dies sollte in weiteren Experimenten genauer erforscht werden.

Insgesamt trug meine Arbeit auf unterschiedlichen Ebenen zum Verständnis des FGFR Signalwegs bei. Weiterhin konnten wir durch Aktivierung bestimmter FGFR Signalwege durch Licht die Stärken und Schwächen dieser Methode aufzeigen. Zu guter Letzt eröffnen die in dieser Dissertation erzielten Ergebnisse mögliche neue Wege zur Behandlung viraler Infektionen.

1 Introduction

1. The skin

The skin, which is the largest and outermost organ of the mammalian body, has many essential functions. It regulates temperature and fluid balance by insulating the body and by sweat production, and, when exposed to light, it synthesizes vitamin D. It is also an important sensory organ, which perceives temperature and mechanical pressure, for example touch and other mechanical cues. The key function of the skin, however, is to form a barrier against the environment, both inside-out, protecting from excessive water loss, as well as outside-in, preventing the entrance of a plethora of environmental agents, including irritants, allergens, toxins and pathogens [1].

These diverse functions of the skin are distributed amongst its different layers. The outermost one, the epidermis, is decisive for the formation of the protective barrier against the environment and consists of several layers of densely packed keratinocytes as the main cell type. It is separated from the dermis by the basement membrane, which is a testimony of the separate origin of these tissues from two different germ layers: The epidermis develops from ectoderm, whereas dermis and hypodermis are of mesenchymal origin [2]. The dermis includes fibroblasts as the main cell type, which produce a complex extracellular matrix (ECM). Embedded in this matrix are the vascular system and different types of immune cells. Underneath the dermis is the hypodermis, which mainly consists of adipocytes and serves as an insulator and energy storage compartment (Figure 1) [3]. Skin homeostasis is highly important and is maintained by a very fine-tuned interaction between the different cell types present in the different skin layers.

1.1 The epidermis

The epidermis consists of several cell layers, which can be subdivided into four *strata*. Right above the basement membrane, which separates the dermis from the epidermis, is the *stratum basale* (Figure 1). It contains transiently amplifying cells with a high proliferative capacity and keratinocyte stem cells with low proliferation rate. These cells continuously renew the entire human epidermis within approximately four weeks throughout the entire life time [4-10]. The

basal keratinocytes are anchored to the basement membrane by integrin receptor binding to laminin proteins in the basement membrane. By asymmetric mitosis, differentiating keratinocytes are generated and travel upwards towards the *stratum spinosum*, where they start to synthesize a different pattern of structural proteins and lipids. Along their journey towards the outside, they further change their morphology and maturate into keratinocytes of the *stratum granulosum*, which are connected by tight junctions. In the end, keratinocytes of this layer differentiate in a process called cornification to become inviable, anucleated corneocytes, held together by proteins and lipids to form the *stratum corneum*. This outermost layer of the epidermis is most exposed to the environment and is constantly shed off and renewed from the differentiating keratinocytes, maintaining a fine balance of proliferation and desquamation, whose disturbance is a symptom of many skin diseases [11].

These changes in cell location and morphology correlate with expression patterns of different structural proteins. As the name suggests, keratinocytes express keratins. These are structural proteins, which form a web-like structure in the cytoplasm and terminate at desmosomes and hemi-desmosomes, which in turn connect keratinocytes with each other or with the basement membrane, respectively [12, 13]. While basal keratinocytes mainly express keratin (K) 5 and K14, more mature keratinocytes in the suprabasal layers switch and express K1 and K10 [14, 15]. In the late stages of differentiation, keratin fibres are bundled and stabilised by filaggrin and the cells express late differentiation markers like involucrin or loricrin. In parallel to these expression changes, differentiating keratinocytes produce lipids, which are stored in lamellar bodies. These vesicles are secreted as soon as the cells reach the *stratum corneum*, resulting in corneocytes, which are embedded like bricks in a “mortar” of lipids (ceramide, cholesterol) [16].

Keratinocytes make up the vast majority of cells in the epidermis, but also other cell types can be found in this tissue layer. Langerhans cells and lymphocytes are part of the adaptive immune system, mediating specific immune responses against invading pathogens [17, 18]. Soft mechanical pressure like touch can be perceived via a sensory system, of which Merkel cells comprise an important element located in the epidermis [19, 20]. Last but not least, the epidermis harbours melanocytes, which migrate into the skin early in embryogenesis [21]. These cells transfer melanin to keratinocytes, thereby shielding their nuclei from ultraviolet (UV) radiation and protecting them against damage, with the aesthetic side effect of skin tanning [22, 23].

All in all, there are many components of physical, chemical and immune barriers residing in the epidermis. The immune barriers include soluble factors, for example pro-inflammatory cytokines and antimicrobial peptides, as well as immune cells, such as Langerhans cells and lymphocytes, and under inflammation conditions also macrophages and neutrophils [17]. Physical barriers are formed by the network of structural proteins within the cells as well as by tight junctions, desmosomes, and adherens junctions. They connect the viable cell layers firmly and make them resistant to mechanical stress. Between the keratinocytes of the *stratum granulosum* tight junctions are located, which are made up of proteins like occludin, claudins and zonal occluding proteins. They form a tight seal between cells, thereby preventing the passage of different molecules and excessive water loss. The physically and chemically strongest barrier is formed by the *stratum corneum*: The vast majority of the cell content of corneocytes are protein bundles of keratins and filaggrin, which together constitute more than 80% of the protein content of the mammalian epidermis. Additional chemical barrier constituents are the extracellular lipids, as well as the acidic pH and secreted antimicrobial peptides in the *stratum corneum*. Last but not least, the desquamation itself as well as colonisation of the skin with commensal bacteria form a barrier against invasion of pathogens [11, 24].

Defects at many different levels of the barrier are the underlying cause of many skin diseases and one of the biggest challenges that the skin faces after wounding [5, 25]. These aspects will be further discussed later.

1.2 The dermis and hypodermis

The dermis mainly consists of connective tissue, including an ECM of collagen and elastic fibres, which is produced and constantly remodelled by fibroblasts (Figure 1). These fibres are responsible for the mechanical strength and elasticity of the skin. The thickness of the collagen fibres divides the dermis into upper papillary dermis and lower reticular dermis [26-29]. Hair follicles along with their affiliated sebaceous glands as well as sweat glands are embedded in the ECM. The dermis is highly vascularised, both with blood and lymphatic vessels. This allows the supply with nutrients and oxygen not only of the dermis, but also of the epidermis, which is not vascularised. Additionally, the blood supply facilitates the recruitment of many innate and adaptive immune cells [17]. Some of these cells reside in the skin constitutively, but in case of

injury or pathogen invasion, their number drastically increases by local proliferation and in particular by chemoattraction and extravasation of immune cells from the blood [18].

Below the dermis resides the hypodermis, which is comprised of adipocytes capable of storing fat (Figure 1). Furthermore, the hypodermis contains big blood vessels and the lowest part of the appendages. Mouse skin is further confined by an underlying muscle layer called *panniculus carnosus*. The hypodermis insulates the body against extreme temperatures and stores energy [11].

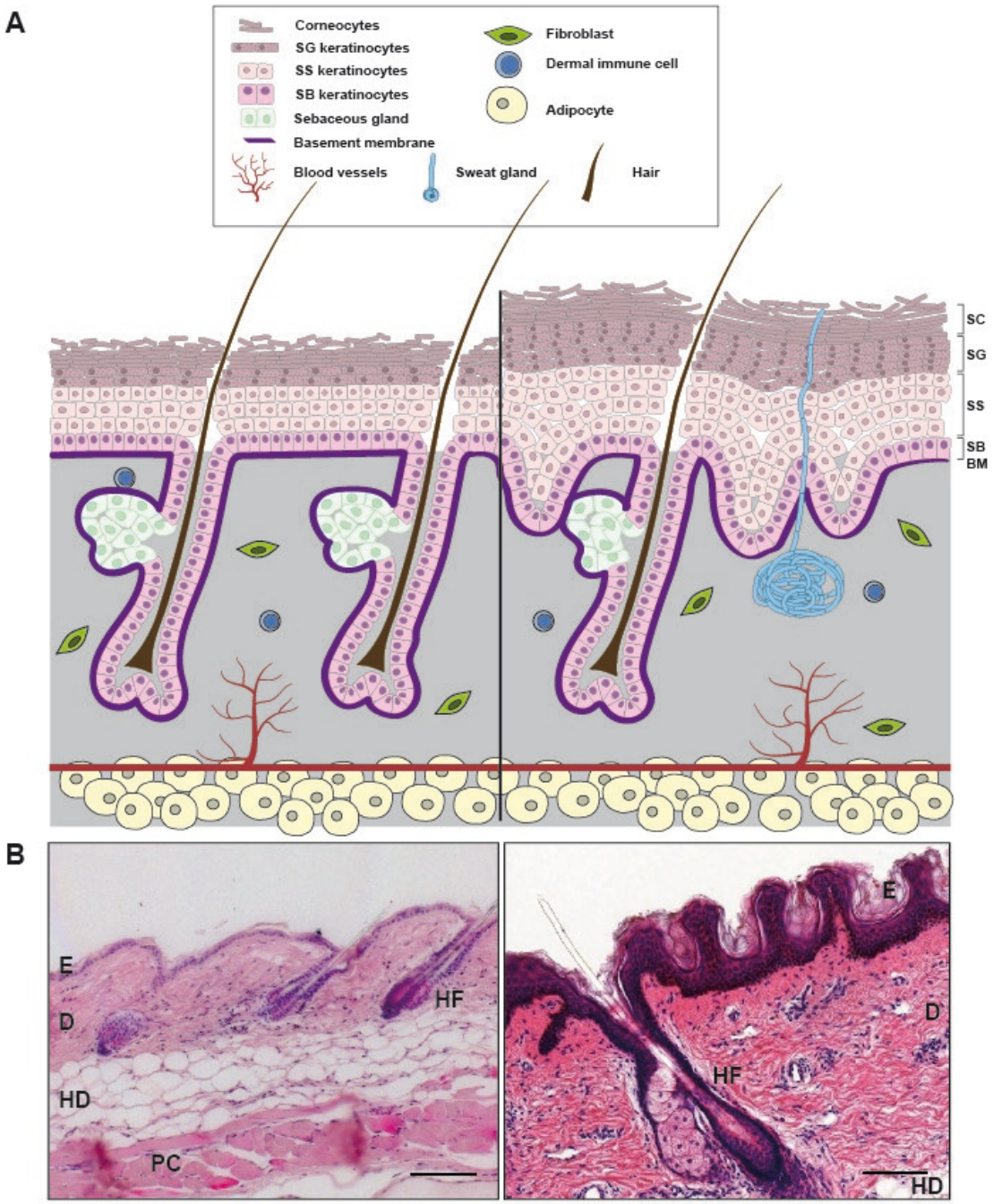

Figure 1: Comparison of mouse (left) and human (right) skin. A: The outermost layer, the epidermis, can be subdivided into four keratinocyte-harbouring layers: *stratum basale* (SB) right above the

basement membrane (BM), *stratum spinosum* (SS), *stratum granulosum* (SG), and *stratum corneum* (SC) which contains corneocytes. In the dermis, hair follicles with sebaceous glands, sweat glands, fibroblasts and immune cells are embedded within the extracellular matrix (grey). It is highly vascularized with large blood vessels residing in the lowest layer, the hypodermis with the adipocytes. B: Hematoxylin and eosin-stained photomicrographs of mouse (left) and human (right) skin. Marked are epidermis (E), dermis (D), hypodermis (HD), hair follicle (HF) and *panniculus carnosus* (PC). Scale bar: 100 µm.

Mouse and human skin are similar in terms of both structure as well as functions. However, some differences can be found. For example, while mouse skin contains more hair follicles per area, sweat glands are only present in the foot pads of mouse skin, but are present in most areas of human skin. In addition, the human epidermis is thicker, consisting of 6 to 10 cell layers compared to 3 layers in mouse skin. Moreover, human epidermis forms extensions into the dermis, which are called rete ridges (Figure 1).

1.3 Skin defects and wound healing

Defects in different barrier components, e.g. those resulting from mutations in genes that encode structural or cell-cell contact proteins, disrupt the balance between proliferation of the basal keratinocytes and corneocyte shedding. This is the case in several inherited skin diseases, which are characterised by severe blistering in the case of epidermolysis bullosa or by hyperkeratosis and keratoderma in the case of ichthyosis [15]. In addition, acquired skin diseases like eczema, contact and atopic dermatitis have a skin barrier defect as an underlying cause [30-35]. In many cases, disruption of the barrier also causes activation of immune responses, may it be because of hyperosmotic stress due to water loss or, more often, increased invasion of environmental substances like irritants, allergens and pathogens [17].

Apart from these pathology-associated defects in skin architecture, skin integrity can be damaged by wounding. Upon injury, a provisional barrier is immediately restored within minutes by formation of a blood clot, which not only prevents fluid loss, but also serves as a reservoir for different factors [25]. Tissue damage and platelet degranulation release mediators, which initiate the first phase of wound healing, the inflammatory phase. Here, different immune cells are attracted, extravasate at the injury site and defend the organism against invading pathogens [36]. The immune cells secrete growth factors, cytokines and proteases, thereby initiating the tissue formation phase [37, 38]. Keratinocytes from the wound edge or from hair follicles migrate and hyperproliferate to re-epithelialise the wound. Fibroblasts migrate into the wound bed; they proliferate and a large percentage of them differentiates into myofibroblasts

to contract the wound and form new ECM. In addition, neo-vascularisation occurs at this stage. After some days, the wound is completely re-epithelialised and the barrier is restored. In this last phase of wound healing, named the remodelling phase, the majority of the immune cells in the newly formed granulation tissue undergo apoptosis, while the ECM in the granulation tissue is remodelled [39]. This results in a scar with reduced tensile strength and elasticity and lack of appendages in adult mammalian skin. However, wounds in mammalian embryos until the end of the second trimester heal without scar formation, and some organisms even have the capacity to completely regenerate amputated limbs [40-42].

2. Cell communication

To orchestrate complex cellular functions with multiple cell types involved, for example the healing of a skin wound, cell-cell communication is crucial. To achieve this, one cell produces and secretes signaling molecules, which are recognised by receptors located on the same cell (autocrine signaling), on neighbouring cells (paracrine signaling) or cells that are located far away at another site of the body, after the signaling molecule has been transported through the blood stream (endocrine signaling). Hormones, which can influence selected organs or the whole organism, typically signal via the endocrine pathway. For example, growth hormone is produced in the pituitary gland and distributed via the blood, increasing body growth by acting on many different tissues, for example the skeleton and the cartilage [43]. Paracrine signaling plays a major role in local processes like skin wound healing, and therefore will be discussed in more detail later, especially in the context of fibroblast growth factors (FGFs). Autocrine signaling sounds paradoxical at first glance – why would a cell secrete a signaling molecule to signal back to itself? However, autocrine signaling is crucial for enhancing signaling, for example in "emergency" situations like viral infection. When a cell senses viral molecules or other signs of viral entry, it produces and secretes type I interferons (IFN I), which signal back to the cell and thereby amplify the expression of antiviral defence molecules [44].

2.1 Fibroblast growth factors (FGFs)

FGFs are evolutionary highly conserved signaling molecules and in mice and humans comprise a group of 22 proteins, which are divided into seven subgroups according to phylogeny (Figure 2A). Most of them, the canonical FGFs, share a core homology domain composed of ca. 125 amino acids folded into 12 anti-parallel β-strands. However, they differ both in length and sequence in their C- and N-terminal regions, which determine their affinity to different FGF receptors [45, 46].

Several of these β-strands exhibit moderate to high affinity to heparan sulphate proteoglycans (HSPGs), which are located at the cell surface as well as in the ECM. Binding to these molecules traps the FGFs within the vicinity of the secreting cell, therefore resulting in paracrine signaling. Additionally, the HSPGs also play an active role in receptor binding, acting as cofactors for the regulation of receptor activation [47].

Some FGFs, however, do not bind HSPGs and therefore act as endocrine growth factors, which require members of the klotho family for receptor activation (FGF19 subfamily). Another atypical subgroup of the FGF family is the FGF11 subfamily. FGFs of this subfamily are not secreted and do not bind to FGFRs, but instead interact with other proteins like voltage-gated sodium channels in axons. They are still counted as members of the FGF family due to their remarkable sequence and structural homology to the other FGFs [48].

2.2 FGF receptors

Most of the FGFs signal through one or more of the four tyrosine kinase receptors (FGFR1-4). They are single-pass transmembrane receptor tyrosine kinases with an extracellular and an intracellular part. The extracellular portion is composed of three immunoglobulin-like (Ig) domains (Ig I-III) and an acid box (AB) domain, which is located between Ig I and Ig II. The N-terminal part of the receptor, which is located around the AB domain, is thought to be important for receptor autoinhibition, whereas Ig II, Ig III and the linker between them determine the ligand binding specificity. The transmembrane (TM) domain spans the plasma membrane and is C-terminally followed by a cytoplasmic split tyrosine kinase (TK) domain [46, 49, 50].

For FGFR1-3, alternative splicing in the Ig III domain generates “b” and “c” variants, dramatically altering the ligand binding specificity, as shown in Figure 2B for FGFR2b and FGFR2c [42]. The b isoform is mainly expressed in epithelial cells, whereas the c isoform is predominant in mesenchymal and immune cells. Most FGFs bind to either epithelial or mesenchymal receptor isoforms, except FGF1, which is thought to be a “universal” FGFR ligand [50].

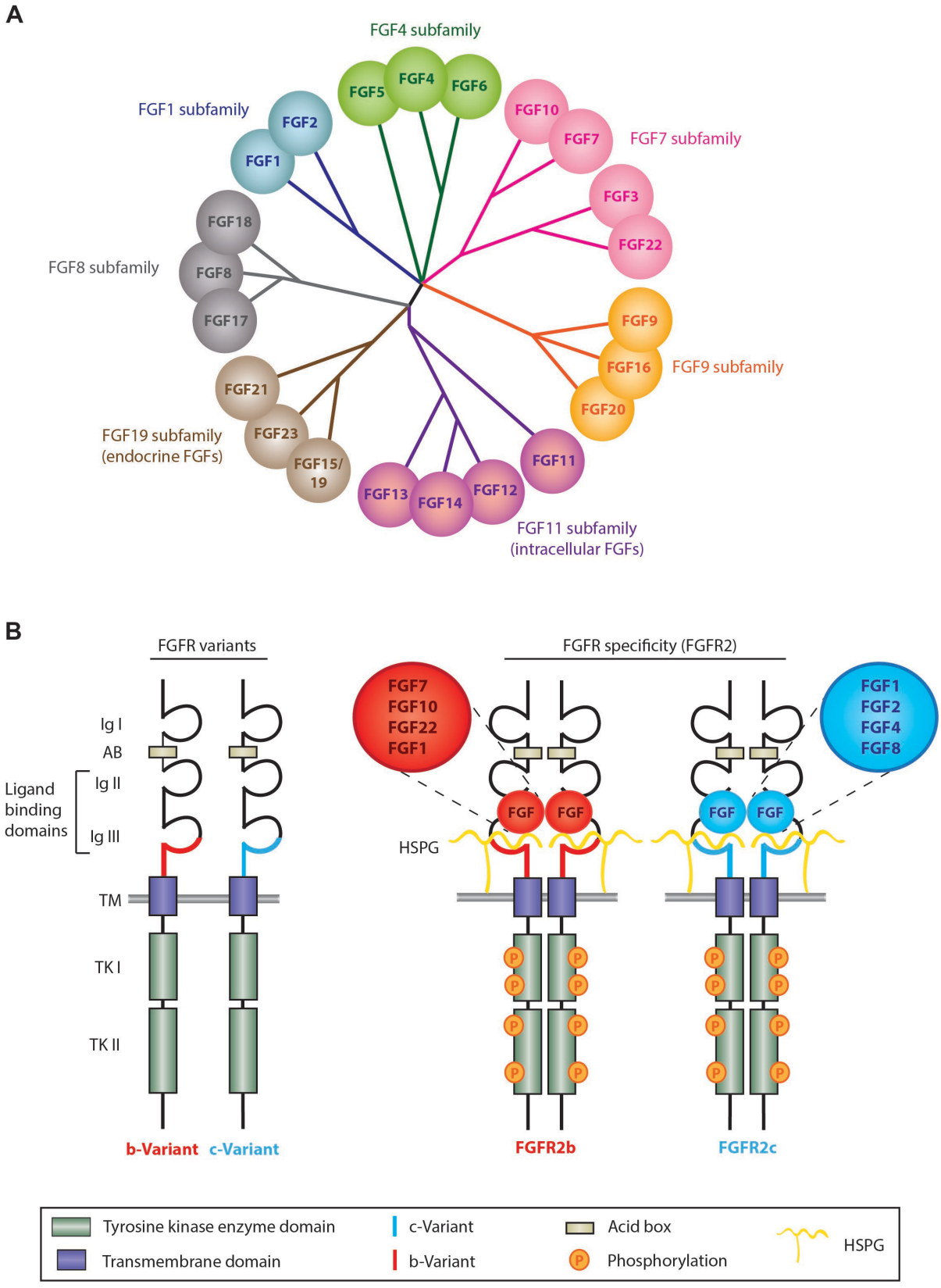

Figure 1: The FGF family and its receptors. A: The 22 FGFs are subdivided into seven subfamilies based on phylogenetic analysis. FGF15 and FGF19 are mouse and human homologues. **B:** The left schematic shows the general difference between FGFR "b" and "c" variants in red and blue, respectively, whereas on the right, the specific situation for FGFR2b and FGFR2c with their respective ligand binding properties are depicted. Adapted from [42].

2.3 Canonical FGF signaling

The canonical, autocrine/paracrine-acting FGFs bind together with HSPGs to the ligand-binding domains of the FGFR in 2:2:2 ratios. This induces a conformational change and dimerisation of the FGFR, which brings the intracellular tyrosine kinase domains into close proximity. Thereby, the kinase domains are activated and cross-phosphorylate each other at different tyrosine residues (human FGFR2: Y466, Y586, Y588, Y656, Y657, Y769 [51]), in a process called trans-autophosphorylation.

The phosphotyrosine residues, which are created in the tyrosine kinase domain of FGFRs, serve as docking sites for intracellular signaling and adaptor proteins, which bind them via their Src homology 2 (SH2) or phosphotyrosine-binding (PTB) domains. Thereby, three major pathways are activated: the mitogen-activated protein kinase (MAPK) pathway, the phosphoinositide 3-kinase (PI3K) pathway, and the phopholipase Cγ (PLCγ) pathway (Figure 3). Additionally, other pathways can be activated depending on the cell type or the context, for example the signal transducer and activator of transcription (STAT) pathway [52-54].

2.3.1 The MAPK pathway

The MAPK pathway is activated via several adaptor proteins. FGFR substrate 2α (FRS2α) binds constitutively to FGFR and, when the receptor is activated, is phosphorylated and binds growth factor receptor bound protein 2 (GRB2) via its SH2 domain [55]. This in turn recruits son of sevenless (SOS), which is a nucleotide exchange protein for rat sarcoma (RAS), activating RAS by stimulating the exchange of guanosine 5-diphosphate (GDP) to guanosine 5-triphosphate (GTP). RAS is a monomeric G protein with intrinsic GTPase activity and switches between the inactive state with GDP bound and the active state, when GTP is bound. RAS is an important and well-studied proto-oncogene with hyperactive mutants found in many malignancies. RAS in turn activates rapidly accelerated fibrosarcoma (RAF) by inducing conformational changes and recruiting it to the plasma membrane. RAF is a mitogen activated protein (MAP) kinase kinase kinase and upstream of a cascade of kinases: The MAP kinase kinase kinase RAF phosphorylates and activates the MAP kinase kinase MAPK/ERK kinase (MEK), which in turn phosphorylates and activates the MAP kinases extracellular signal-regulated kinases 1 and 2 (ERK1/2). Finally, ERK phosphorylates other downstream proteins, including gene regulatory proteins, thereby causing complex changes in cell behaviour.

The basic principle of the MAPK signaling is similar for mitogens like FGFs and for stress signals or cytokines. In every case it is composed of three consecutive kinases. This principle leads to strong amplification of the signal at every step of the cascade, which is advantageous for weak input signals and for integration of different signaling pathways. Depending on the cell context, other MAPK pathways can be activated by FGFR signaling, as will be discussed later. The MAPK pathway is inhibited at several stages by phosphatases, such as dual-specific phosphatase 6 (DUSP6), which remove the phosphates and therefore dampen MAPK signaling.

2.3.2 The PI3K pathway

PI3K consists of two subunits: The regulatory subunit is recruited to the plasma membrane by FRS2α, GRB2 and GRB2 associated binding protein 1 (GAB1), so that the catalytic subunit can phosphorylate membrane-bound phosphatidylinositol 4,5-bisphosphate (PIP_2) to generate phosphatidylinositol 3,4,5-trisphosphate (PIP_3). PIP_3 in turn recruits pleckstrin homology (PH) domain harbouring proteins like phosphoinositide-dependent kinase (PDK) and Akt8 virus oncogene cellular homologue (AKT) to the membrane. PDK phosphorylates and activates AKT, a serine/threonine kinase that stimulates translation, glycolysis, production of glycogen and glucose uptake. Additionally, it protects cells from apoptosis, for example by inhibition of BCL2 associated agonist of cell death (BAD), and therefore it is often upregulated in malignant tumours. It is antagonised by the tumour suppressor phosphatase and tensin homologue (PTEN), which dephosphorylates PIP_3 and therefore inhibits AKT pathway activation [56].

2.3.3 The PLCγ pathway

PLCγ is directly recruited to the FGFR via its SH2 domain and gets phosphorylated by the receptor. This activates its enzymatic activity, resulting in hydrolysis of membrane bound PIP_2 to diacylglycerol (DAG) and inositol trisphosphate (IP_3). The latter leaves the membrane and via IP_3 receptors promotes calcium ion (Ca^{2+}) influx from the endoplasmatic reticulum (ER). The elevated levels of cytosolic Ca^{2+} activate Ca^{2+}-dependent effector kinases like calmodulin and protein kinase C (PKC).

2.3.4 Context-dependent pathways

Depending on the cellular context, additional pathways can be activated by FGFR phosphorylation. Amongst them is the STAT pathway, where STAT proteins get

phosphorylated by FGFR and translocate to the nucleus to act as transcription factors. Alternatively, other MAPK pathways can be influenced by FGFR signaling, in particular the p38 and c-Jun N-terminal kinase (JNK) pathways [48].

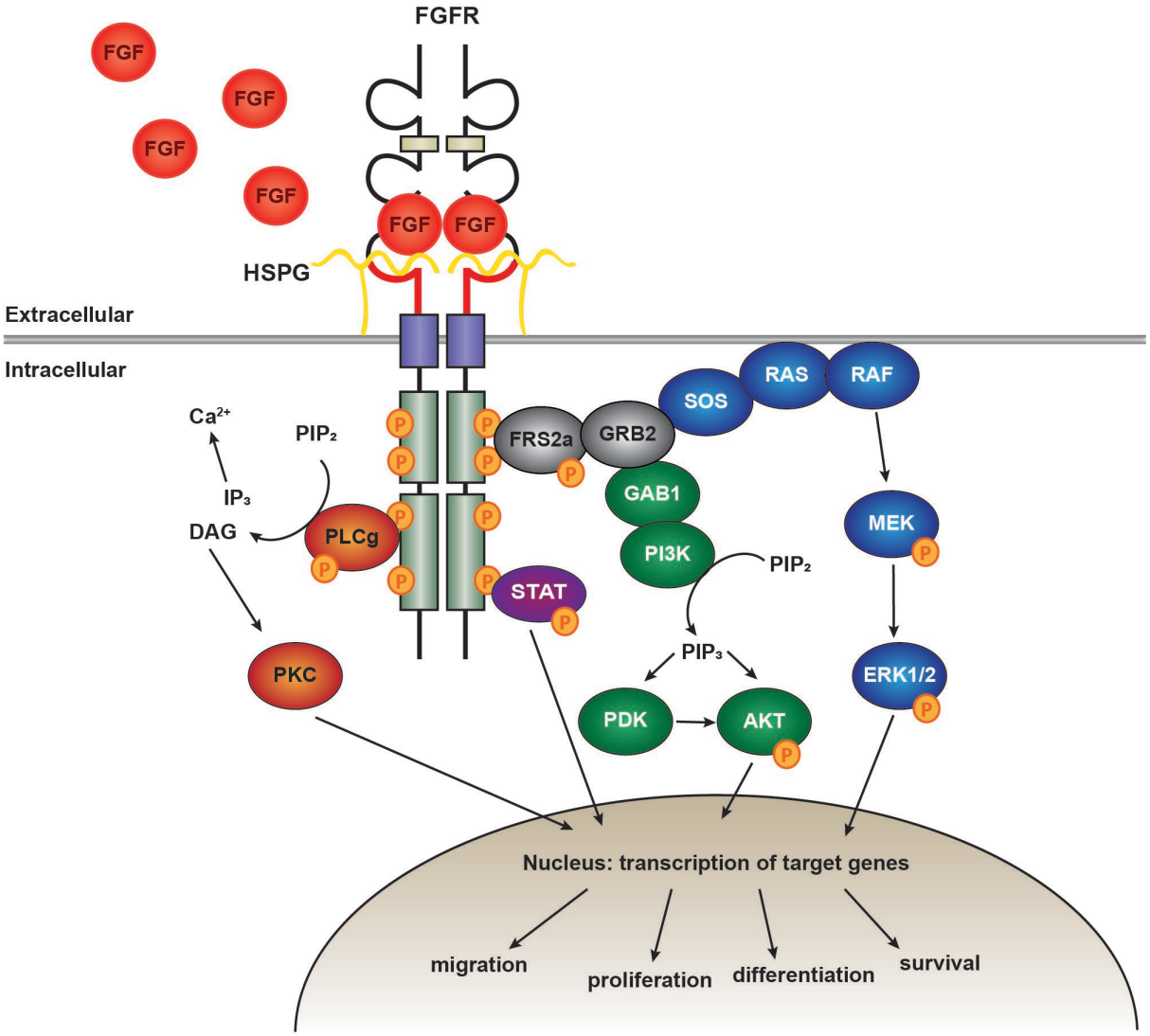

Figure 2: The FGF signaling pathways. FGF binding to FGFRs together with their cofactors HSPGs induces dimerisation and trans-autophosphorylation of the receptors. This leads to activation of three main pathways, the MAPK pathway (blue), the PI3K pathway (green) and the PLCγ pathway (red). Additionally, the STAT pathway (pink) is activated in a cell context-dependent manner.

2.4 Importance of FGF signaling in skin

Acidic and basic FGF (FGF1 and FGF2, respectively) were found to increase proliferation of fibroblasts in the 1970s and were named after this fibroblast growth-stimulating activity. However, their effect is not limited to this cell type. These and other FGFs orchestrate migration, proliferation, differentiation and survival of multiple cell types and therefore play

crucial roles not only during development, but also in homeostasis, repair and disease of a variety of tissues [42, 57-60].

In the skin, the signaling by members of the FGF7 subfamily (FGF7, FGF10, FGF22 and FGF3) is crucial both for epidermal homeostasis as well as repair. FGF7, also named keratinocyte growth factor (KGF), has been described already in 1991 to stimulate proliferation of keratinocytes, but not of fibroblasts or endothelial cells [61]. Expression of a dominant-negative mutant of FGFR2b, the main receptor of FGF7, in keratinocytes of transgenic mice, revealed an important role of FGF signaling in epidermal homeostasis [62] . Keratinocytes do not express FGF7 themselves, and fibroblasts and also γδ T cells were identified as the source of FGF7 in the skin [63]. Furthermore, FGF7 was shown to have a cytoprotective effect on keratinocytes, which were stressed by UV irradiation or treatment with chemotherapeutic or cytotoxic agents [64].

The role of FGFR signaling in skin homeostasis as well as wound healing was further underlined by the phenotype of mice lacking FGFR1 and FGFR2 in keratinocytes (Cre recombinase expressed under control of the K5 promoter). These mice have a strong skin phenotype, which includes 1) progressive hair loss due to a failure of hair follicle stem cells to initiate a new hair cycle; 2) development of a progressive inflammatory skin disease due to formation of abnormal tight junctions that resulted in excessive water loss; 3) severe wound healing defects, mainly due to impaired keratinocyte migration; 4) hyperthickened and hyperkeratotic epidermis, similar to atopic dermatitis [65, 66]. The role of FGFs and other growth factors in skin homeostasis as well as during wound healing have been reviewed extensively [42, 67-69].

2.5 Complexity of FGF signaling

The biological output of FGF signaling depends on the cell type, the type of receptor and the presence of HSPGs on the cell surface, which are required for specific FGF signaling [47, 70]. For example, FGF7 and FGF10 both act on FGFR2b, but while FGF7 leads to receptor degradation and cell proliferation, FGF10 stimulation induces receptor recycling and cell migration [71]. Little is known on how different cellular responses can be induced by stimulation of the same receptor with different FGFs or by stimulation of different receptors with the same ligand. Additionally, there are unsolved issues regarding possible synergistic

effects of different types of FGFRs and in combination with other cellular receptors or other downstream signaling pathways. This is particularly relevant for cells, which express multiple FGF receptors, such as keratinocytes of the skin. These cells were shown to express FGFR1-3 with FGFR2 being the most relevant receptor and FGFR1 having a "back-up" function [65, 66]. By contrast, endogenous FGFR3 is dispensable for skin homeostasis as reported in Chapter 3 of this thesis. To specifically test the function of an individual FGF receptor, it is necessary to break down the signaling system, ideally by activating only one receptor with high temporal and spatial precision. This is not possible using the ligands, because firstly, they do not offer spatial and temporal precision, and secondly, they are promiscuous and bind to different FGFRs with different affinities and kinetics [57]. A promising alternative approach is optogenetics, where photoactivatable protein domains are used to tightly control and manipulate cellular signaling networks [72-74].

3. Optogenetics

The term “optogenetics” refers to the use of light-responsive proteins to modulate cellular behaviour. Following the 2005 discovery of light-responsive ion channels in plants (channelrhodopsins), optogenetics has had a huge impact, particularly in the field of neurobiology [75, 76]. By expressing these natural channelrhodopsins in animal nerve cells, neurons can be activated or inactivated by de- or hyperpolarisation of the cell membrane with light [77-79]. The use of natural as well as engineered light-responsive proteins has therefore transformed the field of neurobiology in many respects, even allowing complex behavioural studies in transgenic animals [80-91]. Due to these ground-breaking discoveries, optogenetics was named the method of the year 2010 by the scientific journal *Nature* [92].

After the remarkable success of this technology in neurobiology, biologists in many other fields have identified optogenetics as a useful tool. These include basic and translational cell biologists, who use optogenetics to modify cell signaling proteins, rendering them light-responsive. With these novel tools at hand, the complex jungle of cellular signaling networks looks less impenetrable [93-101].

3.1 Optogenetic systems

While the activation principle of neurons is rather uniform (ion flux changes the membrane potential), in the broader context of cell signaling research there is a wide range of manipulations necessary to control different cellular functions. Therefore, it relies heavily on the versatility of the optogenetic toolkit, which features several light-responsive domains with different wavelengths, kinetics and modes of activation [72]. Although there are many more systems that can be exploited for special applications, the most commonly used systems are the phytochrome B (PHYB) system, the cryptochrome 2 (CRY2) system and the light-oxygen-voltage domain (LOV) system (Figure 4).

3.1.1 PHYB

The PHYB protein is derived from *Arabidopsis thaliana*, where it controls seedling stem elongation [72]. The PHYB system is a hetero-dimerisation system, which is activated by red light (650 nm) and inactivated by infrared light (750 nm). Its chromophore is phycocyanobilin

(PCB), which must be delivered exogenously in animal cells. After illumination with red light, PHYB binds to its hetero-dimerisation partner phytochrome interacting factor (PIF) and this dimerisation is stable in the dark for hours, until it is illuminated with infrared light. This system can be used for hetero-dimerisation of different proteins, as well as translocation of proteins to specific compartments of the cell, like the cell membrane. The major advantage of the PHYB system is the light-induced reversibility, which allows controlled termination of signaling. However, the requirement of exogenous PCB, which has to be isolated from bacterial cultures and supplemented to animal cells, can be a cumbersome obstacle [102-104].

3.1.2 CRY2

CRY2 is a plant protein, also from *A. thaliana*, which naturally mediates floral initiation. It is a homo-oligomerisation and hetero-dimerisation system, which responds to blue light (450 nm). Its chromophore is flavin, which is ubiquitously expressed also in animal cells. Upon illumination, it homo-oligomerises and binds to cryptochrome-interacting basic helix-loop-helix 1 (CIB1). This makes the system suitable for homo- and hetero-dimerisation of proteins, protein recruitment and sequestration-based inhibition. Although this system is very versatile, its broad activation spectrum complicates its combination with other common fluorophores like green-fluorescent protein (GFP) [105-107].

3.1.3 LOV

LOV domain proteins can be found in several different taxa and regulate phototropism in plants and microbes. They are all sensitive to blue light (450 nm) and, like the CRY2 system, use endogenous flavin as a chromophore. LOV domains belong to the period-ARNT-singleminded (PAS) domain family with a consensus amino acid motif (GXNCRFLQ). The PAS fold is composed of a 5-stranded antiparallel β-sheet and a helical part that binds the flavin chromophore. In the dark state, the flavin co-factor is oxidised and has its absorption peak at 450 nm. Illumination with light of this wavelength establishes a covalent linkage between the C4a position of flavin and the thiol moiety of the cysteine residue at the active site of the LOV domain. This leads to conformational changes, which either induce homo-dimerisation or unfolding of its C-terminal Jα helix, depending on the LOV domain. In the dark, this photocycle is thermally reversible with a half-life of seconds to days [101, 108, 109].

This system is mostly utilised to induce homo- or hetero-dimerisation, but can be also used for uncaging signal peptides, such as a nuclear localisation signal. Due to their variability, LOV

domains are useful in a broad range of applications and are easy to engineer for specific desired properties, which allows most drawbacks of this system, such as the broad activation wavelength spectrum, to be circumvented. However, for some applications, the half-life of the activated state has to be engineered, because it cannot be turned off like the PHYB system [110-114].

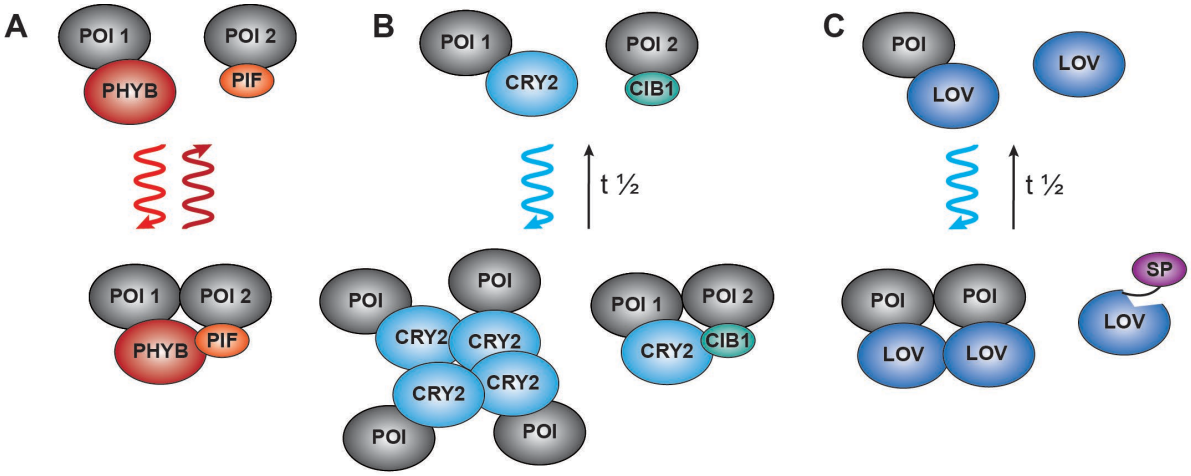

Figure 3: The most common optogenetic systems. All interactions bring proteins of interest (POI) into close proximity, thereby leading to physical interaction. **A:** PHYB hetero-dimerises with PIF upon red light illumination and dissociates again with infrared illumination. **B:** CRY2 homo-oligomerises with itself or hetero-dimerises with CIB1 under blue light. The interaction is terminated spontaneously with a certain half-life. **C:** LOV domains homo-dimerise upon illumination with blue light, however, the conformational change can also be used for uncaging certain peptides (SP: signal peptide).

3.2 Optogenetics in cell signaling research

Given the wealth of optogenetic tools that are available, it is important to first compare different systems and choose the most optimal tool prior to beginning a research project [72]. Most optogenetic systems are activated within seconds and, as illumination can also be spatially restricted using focused light, share precision both in space and time [74, 101, 115]. Together with advanced microscopy tools like multi-photon microscopy or total internal reflection fluorescence (TIRF) microscopy, optogenetics is an extremely powerful tool to investigate cell signaling, for example by only activating molecules at the surface of the cell, like receptors [116, 117]. A selection of exciting studies is highlighted below.

In a 2018 study by Morri et al., optogenetics was used to decipher the previously unknown functions of orphan G-protein coupled receptors (GPCRs). They were fused with the light-sensitive domain of rhodopsin, allowing for their activation with light. By analysing their

downstream signaling properties, conclusions about their protein functions could be drawn [118]. In a different study, the CRY2 system was used to understand the difference in signaling between nerve growth factor and epidermal growth factor (NGF and EGF) in a neuronal cell line. Activation by either ligand led to cell cycle arrest or proliferation, respectively, although both factors activated the same downstream signaling pathways [119]. Additionally, researchers have unravelled the spatiotemporal regulation of ERK during larval development in *Drosophila* using the PHYB system, allowing them to activate the RAS/ERK module with light [120-123].

Light-controlled domains have also been used successfully to activate or inhibit receptor tyrosine kinase signaling using tropomyosin receptor kinase (TRK) [124] or protein tyrosine phosphatase 1B (PTP1B) [125], respectively. Downstream pathways like MAPK pathway components RAF and MEK and a cyclin-dependent kinase (CDK) were also studied using photo-switchable versions. This led to the identification of previously unknown negative feedback loops and enabled light-inducible synaptic vesicle transport [126]. Finally, a CRY2-coupled version of PI3K was used to examine downstream targets of transforming growth factor β (TGFβ) signaling and to investigate its impact on epithelial-mesenchymal transition (EMT), a hallmark of cancer [127].

3.3 Optogenetic modification of FGFRs

Optogenetic tools have also been used successfully in FGF signaling research. Two different versions of a light-activated FGFR1 had previously been generated and characterized *in vitro* [128, 129]. One tool took advantage of LOV domains for receptor homo-dimerisation of FGFR1, and was able to activate the canonical intracellular signaling cascades. This induced proliferation and migration in different tumour cell lines and *in vitro* capillary formation by endothelial cells [128]. The other receptor system used CRY2 homo-dimerisation to induce receptor interaction and activation. Experiments in HeLa tumour cells and human umbilical vein endothelial cells (HUVECs) showed that this system could be used to activate downstream signaling pathways, induce cytoskeletal reorganisation, alter cell polarity and direct cell migration [129]. In addition to receptor activation, FGFR1 was also inactivated with light, which inhibited downstream signaling. This strategy was used to rescue growth defects due to excessive FGFR1 signaling in zebrafish embryos [130].

3.4 OptoR2

To study the important function of FGFR receptors, particularly FGFR2, in keratinocytes, we generated a LOV-modified version of FGFR2, the OptoR2 (Figure 5). The intracellular domain of human FGFR2 was fused to a LOV domain of aureochrome 1 from the alga *Vaucheria frigida*. We used this optogenetic system, because 1) the half-life of its activated state is around 500 seconds, similar to endogenous FGFR2; 2) this LOV domain is located in its natural context at the C-terminus, so in the engineered OptoR2 the overall domain arrangement can be maintained; 3) it has previously been shown to be suitable for FGFR1 activation [128]. The OptoR2 is anchored in the membrane by a myristoylation domain and is fused to a hemagglutinin (HA) -tag. As the extracellular ligand binding domain was removed, OptoR2 responds specifically to blue light, and is not affected by natural FGFR2 ligands (e.g. FGF7, FGF10). This enables us to use the OptoR2 system to precisely mimic FGFR2 signaling and control cell behaviour in space and time [74, 115].

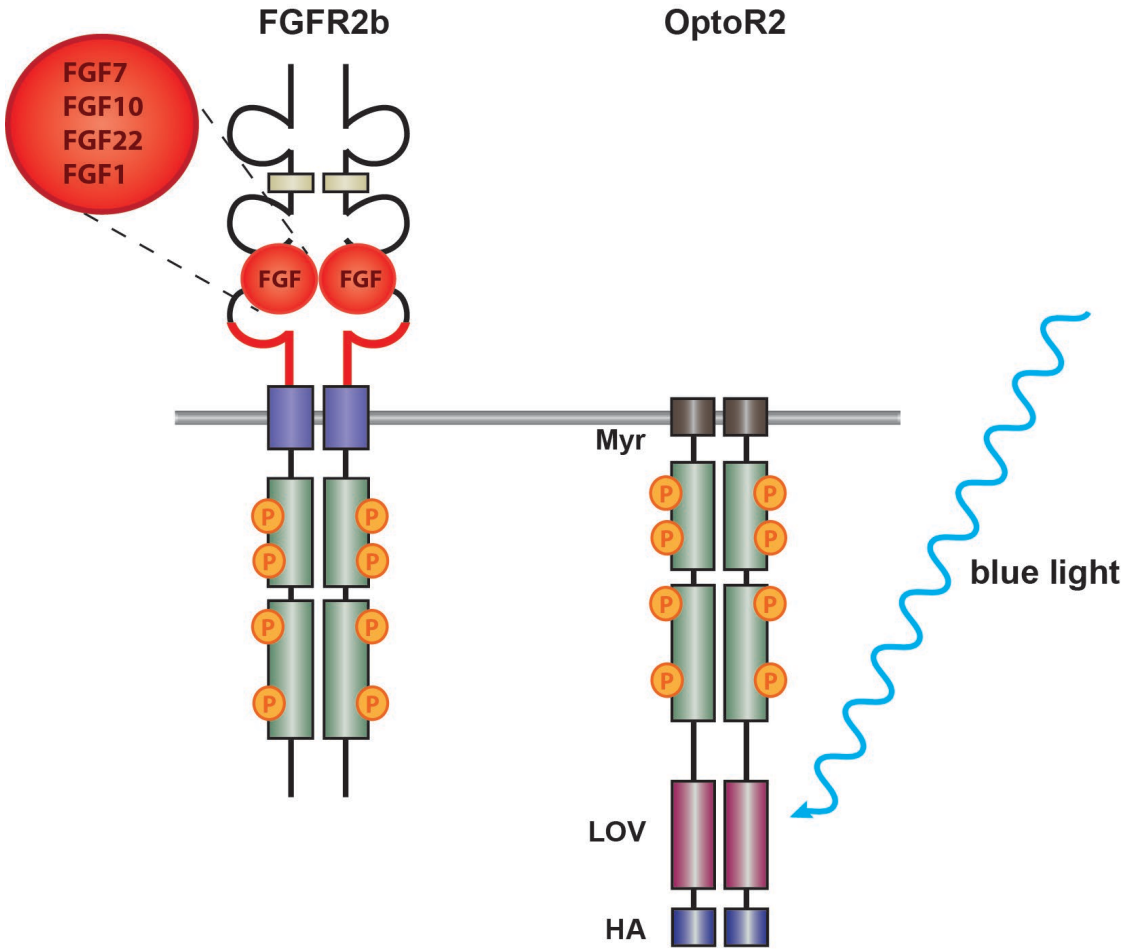

Figure 4: Design of the OptoR2. The intracellular part of the endogenous FGFR2b is fused to light-responsive LOV domains, which dimerise upon illumination with blue light. OptoR2 is anchored in the membrane with a myristoylation signal (Myr) that is fused to a hemagglutinin (HA) tag.

4. Objectives

As FGF signaling is crucial both for skin homeostasis and repair following injury, it was the goal of my thesis to further characterise FGF signaling and function in keratinocytes.

In the major part of my thesis project I used optogenetics to generate a modified FGFR2, OptoR2, that is only activated by light. I showed that activation of OptoR2 with blue light robustly activates the FGFR2 signaling cascade, which induces migration and proliferation in human embryonic kidney (HEK) 293 T cells. A doxycycline (Dox)-inducible expression system allowed me to investigate OptoR2 signaling in keratinocytes (see Chapter 1).

An exciting novel function of FGFs in keratinocytes is the suppression of the IFN type I response, which we discovered in our laboratory. Therefore, the second part of my thesis project aimed to determine the effect of FGF7 or of FGFR kinase inhibitors on IFN I signaling and viral replication in keratinocytes (see Chapter 2).

Finally, I contributed to the characterization of mice lacking FGFR1, FGFR2 and FGFR3 in keratinocytes. This work showed that FGFR3 is dispensable for epidermal homeostasis and repair (see Chapter 3).

References

1 **Proksch, E., Brandner, J. M. & Jensen, J.-M. (2008)** *The skin: an indispensable barrier*. Experimental Dermatology 17, 1063-1072.

2 **Fuchs, E. & Raghavan, S. (2002)** *Getting under the skin of epidermal morphogenesis*. Nature Reviews Genetics 3, 199-209.

3 **Gould, J. (2018)** *Superpowered skin*. Nature 563, S84-S85.

4 **Cotsarelis, G., Sun, T. T. & Lavker, R. M. (1990)** *Label-retaining cells reside in the bulge area of pilosebaceous unit: implications for follicular stem cells, hair cycle, and skin carcinogenesis*. Cell 61, 1329-1337.

5 **Roop, D. (1995)** *Defects in the barrier*. Science 267, 474.

6 **Heenen, M. & Galand, P. (1997)** *The growth fraction of normal human epidermis*. Dermatology 194, 313-317.

7 **Webb, A., Li, A. & Kaur, P. (2004)** *Location and phenotype of human adult keratinocyte stem cells of the skin*. Differentiation 72, 387-395.

8 **Blanpain, C. & Fuchs, E. (2006)** *Epidermal stem cells of the skin*. Annual Review of Cell and Developmental Biology 22, 339-373.

9 **Blanpain, C. & Fuchs, E. (2009)** *Epidermal homeostasis: a balancing act of stem cells in the skin*. Nature Reviews Molecular Cell Biology 10, 207-217.

10 **Hsu, Y. C., Pasolli, H. A. & Fuchs, E. (2011)** *Dynamics between stem cells, niche, and progeny in the hair follicle*. Cell 144, 92-105.

11 **Baroni, A., Buommino, E., De Gregorio, V., Ruocco, E., Ruocco, V. & Wolf, R. (2012)** *Structure and function of the epidermis related to barrier properties*. Clinical Dermatology 30, 257-262.

12 **Hopkinson, S. B., Hamill, K. J., Wu, Y., Eisenberg, J. L., Hiroyasu, S. & Jones, J. C. (2014)** *Focal contact and hemidesmosomal proteins in keratinocyte migration and wound repair*. Advances in Wound Care (New Rochelle) 3, 247-263.

13 **Walko, G., Castanon, M. J. & Wiche, G. (2015)** *Molecular architecture and function of the hemidesmosome*. Cell and Tissue Research 360, 529-544.

14 **Fuchs, E. (1993)** *Epidermal differentiation and keratin gene expression*. Journal of Cell Science 17, 197-208.

15 **Simpson, C. L., Patel, D. M. & Green, K. J. (2011)** *Deconstructing the skin: cytoarchitectural determinants of epidermal morphogenesis*. Nature Reviews Molecular Cell Biology 12, 565-580.

16 **Nemes, Z. & Steinert, P. M. (1999)** *Bricks and mortar of the epidermal barrier*. Experimental & Molecular Medicine 31, 5-19.

17 **Bangert, C., Brunner, P. M. & Stingl, G. (2011)** *Immune functions of the skin*. Clinical Dermatology 29, 360-376.

18 **Richmond, J. M. & Harris, J. E. (2014)** *Immunology and skin in health and disease*. Cold Spring Harbor Perspectives in Medicine 4, a015339.

19 **Maricich, S. M., Wellnitz, S. A., Nelson, A. M., Lesniak, D. R., Gerling, G. J., Lumpkin, E. A. & Zoghbi, H. Y. (2009)** *Merkel cells are essential for light-touch responses*. Science 324, 1580-1582.

20 **Zimmerman, A., Bai, L. & Ginty, D. D. (2014)** *The gentle touch receptors of mammalian skin*. Science 346, 950-954.

21 **Dupin, E. & Le Douarin, N. M. (2003)** *Development of melanocyte precursors from the vertebrate neural crest*. Oncogene 22, 3016-3023.

22 **Brenner, M. & Hearing, V. J. (2008)** *The protective role of melanin against UV damage in human skin*. Photochemistry and Photobiology 84, 539-549.

23 **Singh, S. K., Kurfurst, R., Nizard, C., Schnebert, S., Perrier, E. & Tobin, D. J. (2010)** *Melanin transfer in human skin cells is mediated by filopodia - a model for homotypic and heterotypic lysosome-related organelle transfer*. The FASEB Journal 24, 3756-3769.

24 **Stacy, A. & Belkaid, Y. (2019)** *Microbial guardians of skin health*. Science 363, 227-228.

25 **Singer, A. J. & Clark, R. A. (1999)** *Cutaneous wound healing*. The New England Journal of Medicine 341, 738-746.

26 **Sorrell, J. M. & Caplan, A. I. (2004)** *Fibroblast heterogeneity: more than skin deep*. Journal of Cell Science 117, 667-675.

27 **Kurita, M., Okazaki, M., Kaminishi-Tanikawa, A., Niikura, M., Takushima, A. & Harii, K. (2012)** *Differential expression of wound fibrotic factors between facial and trunk dermal fibroblasts*. Connective Tissue Research 53, 349-354.

28 **Tracy, L. E., Minasian, R. A. & Caterson, E. J. (2016)** *Extracellular matrix and dermal fibroblast function in the healing wound*. Advances in Wound Care 5, 119-136.

29 **Lynch, M. D. & Watt, F. M. (2018)** *Fibroblast heterogeneity: implications for human disease*. The Journal of Clinical Investigation 128, 26-35.

30 **Proksch, E., Fölster-Holst, R. & Jensen, J.-M. (2006)** *Skin barrier function, epidermal proliferation and differentiation in eczema*. Journal of Dermatological Science 43, 159-169.

31 **O'Regan, G. M., Sandilands, A., McLean, W. H. & Irvine, A. D. (2008)** *Filaggrin in atopic dermatitis*. Journal of Allergy and Clinical Immunology 124, R2-6.

32 **Guttman-Yassky, E., Suarez-Farinas, M., Chiricozzi, A., Nograles, K. E., Shemer, A., Fuentes-Duculan, J., Cardinale, I., Lin, P., Bergman, R., Bowcock, A. M. & Krueger, J. G. (2009)** *Broad defects in epidermal cornification in atopic dermatitis identified through genomic analysis*. Journal of Allergy and Clinical Immunology 124, 1235-1244.e1258.

33 **Boguniewicz, M. & Leung, D. Y. M. (2011)** *Atopic dermatitis: A disease of altered skin barrier and immune dysregulation*. Immunological Reviews 242, 233-246.

34 **Kezic, S., Novak, N., Jakasa, I., Jungersted, J. M., Simon, M., Brandner, J. M., Middelkamp-Hup, M. A. & Weidinger, S. (2014)** *Skin barrier in atopic dermatitis*. Frontiers in Bioscience 19, 542-556.

35 **Peng, W. & Novak, N. (2015)** *Pathogenesis of atopic dermatitis*. Clinical & Experimental Allergy 45, 566-574.

36 **Härtel, E., Werner, S. & Schäfer, M. (2014)** *Transcriptional regulation of wound inflammation*. Seminars in Immunology 26, 321-328.

37 **Werner, S. & Grose, R. (2003)** *Regulation of wound healing by growth factors and cytokines*. Physiological Reviews 83, 835-870.

38 **Bünemann, E., Hoff, N. P., Buhren, B. A., Wiesner, U., Meller, S., Bolke, E., Muller-Homey, A., Kubitza, R., Ruzicka, T., Zlotnik, A., Homey, B. & Gerber, P. A. (2018)** *Chemokine ligand-receptor interactions critically regulate cutaneous wound healing*. European Journal of Medical Research 23, 4.

39 **Schäfer, M. & Werner, S. (2008)** *Cancer as an overhealing wound: an old hypothesis revisited*. Nature Reviews Molecular Cell Biology 9, 628-638.

40 **Brockes, J. P. & Kumar, A. (2008)** *Comparative aspects of animal regeneration*. Annual Review of Cell and Developmental Biology 24, 525-549.

41 **Larson, B. J., Longaker, M. T. & Lorenz, H. P. (2010)** *Scarless fetal wound healing: A basic science review*. Plastic and Reconstructive Surgery 126, 1172-1180.

42 **Maddaluno, L., Urwyler, C. & Werner, S. (2017)** *Fibroblast growth factors: Key players in regeneration and tissue repair*. Development 144, 4047-4060.

43 **Lanning, N. J. & Carter-Su, C. (2006)** *Recent advances in growth hormone signaling*. Reviews in Endocrine and Metabolic Disorders 7, 225-235.

44 **Chen, K., Liu, J. & Cao, X. (2017)** *Regulation of type I interferon signaling in immunity and inflammation: A comprehensive review*. Journal of Autoimmunity 83, 1-11.

45 **Beenken, A. & Mohammadi, M. (2009)** *The FGF family: Biology, pathophysiology and therapy*. Nature Reviews Drug Discovery 8, 235-253.

46 **Belov, A. A. & Mohammadi, M. (2013)** *Molecular mechanisms of fibroblast growth factor signaling in physiology and pathology*. Cold Spring Harbor Perspectives in Biology 5, 1-24.

47 **Makarenkova, H. P., Hoffman, M. P., Beenken, A., Eliseenkova, A. V., Meech, R., Tsau, C., Patel, V. N., Lang, R. A. & Mohammadi, M. (2009)** *Differential interactions of FGFs with heparan sulfate control gradient formation and branching morphogenesis*. Science Signaling 2, ra55.

48 **Ornitz, D. M. & Itoh, N. (2015)** *The fibroblast growth factor signaling pathway*. Wiley Interdisciplinary Reviews: Developmental Biology 4, 215-266.

49 **Eswarakumar, V. P., Lax, I. & Schlessinger, J. (2005)** *Cellular signaling by fibroblast growth factor receptors*. Cytokine & Growth Factor Reviews 16, 139-149.

50 **Zhang, X., Ibrahimi, O. A., Olsen, S. K., Umemori, H., Mohammadi, M. & Ornitz, D. M. (2006)** *Receptor specificity of the fibroblast growth factor family. The complete mammalian FGF family*. Journal of Biological Chemistry 281, 15694-15700.

51 in *Encyclopedia of Genetics, Genomics, Proteomics and Informatics* 2064-2064 (Springer Netherlands, 2008).

52 **Lemmon, M. A. & Schlessinger, J. (2010)** *Cell signaling by receptor tyrosine kinases*. Cell 141, 1117-1134.

53 **Tiong, K. H., Mah, L. Y. & Leong, C.-O. (2013)** *Functional roles of fibroblast growth factor receptors (FGFRs) signaling in human cancers*. Apoptosis 18, 1447-1468.

54 **Touat, M., Ileana, E., Postel-Vinay, S., André, F. & Soria, J.-C. (2015)** *Targeting FGFR Signaling in Cancer*. Clinical Cancer Research 21, 2684-2694.

55 **Ong, S. H., Guy, G. R., Hadari, Y. R., Laks, S., Gotoh, N., Schlessinger, J. & Lax, I. (2000)** *FRS2 Proteins Recruit Intracellular Signaling Pathways by Binding to Diverse*

Targets on Fibroblast Growth Factor and Nerve Growth Factor Receptors. Molecular and Cellular Biology 20, 979-989.

56 **Hertzler-Schaefer, K., Mathew, G., Somani, A. K., Tholpady, S., Kadakia, M. P., Chen, Y., Spandau, D. F. & Zhang, X. (2014)** *Pten loss induces autocrine FGF signaling to promote skin tumorigenesis*. Cell Reports 6, 818-826.

57 **Mason, I. (2007)** *Initiation to end point: The multiple roles of fibroblast growth factors in neural development*. Nature Reviews Neuroscience 8, 583-596.

58 **Turner, N. & Grose, R. (2010)** *Fibroblast growth factor signalling: From development to cancer*. Nature Reviews Cancer 10, 116-129.

59 **Coutu, D. L. & Galipeau, J. (2011)** *Roles of FGF signaling in stem cell self-renewal, senescence and aging*. Aging 3, 920-933.

60 **Fearon, A. E., Gould, C. R. & Grose, R. P. (2013)** *FGFR signalling in women's cancers*. International Journal of Biochemistry & Cell Biology 45, 2832-2842.

61 **Aaronson, S. A., Bottaro, D. P., Miki, T., Ron, D., Finch, P. W., Fleming, T. P., Ahn, J., Taylor, W. G. & Rubin, J. S. (1991)** *Keratinocyte growth factor: A fibroblast growth factor family member with unusual target cell specificity*. Annals of the New York Academy of Sciences 638, 62-77.

62 **Werner, S., Weinberg, W., Liao, X., Peters, K., Blessing, M., Yuspa, S., Weiner, R. & Williams, L. (1993)** *Targeted expression of a dominant-negative FGF receptor mutant in the epidermis of transgenic mice reveals a role of FGF in keratinocyte organization and differentiation*. The EMBO Journal 12, 2635-2643.

63 **Boismenu, R. & Havran, W. L. (1994)** *Modulation of epithelial cell growth by intraepithelial gamma delta T cells*. Science 266, 1253-1255.

64 **Braun, S., Krampert, M., Bodo, E., Kumin, A., Born-Berclaz, C., Paus, R. & Werner, S. (2006)** *Keratinocyte growth factor protects epidermis and hair follicles from cell death induced by UV irradiation, chemotherapeutic or cytotoxic agents*. Journal of Cell Science 119, 4841-4849.

65 **Yang, J., Meyer, M., Muller, A. K., Bohm, F., Grose, R., Dauwalder, T., Verrey, F., Kopf, M., Partanen, J., Bloch, W., Ornitz, D. M. & Werner, S. (2010)** *Fibroblast growth factor receptors 1 and 2 in keratinocytes control the epidermal barrier and cutaneous homeostasis*. Journal of Cell Biology 188, 935-952.

66 **Meyer, M., Muller, A. K., Yang, J., Moik, D., Ponzio, G., Ornitz, D. M., Grose, R. & Werner, S. (2012)** *FGF receptors 1 and 2 are key regulators of keratinocyte migration in vitro and in wounded skin*. Journal of Cell Science 125, 5690-5701.

67 **Müller, A. K., Meyer, M. & Werner, S. (2012)** *The roles of receptor tyrosine kinases and their ligands in the wound repair process*. Seminars in Cell & Developmental Biology 23, 963-970.

68 **Meyer, M., Maddaluno, L. & Werner, S.** in *Fibroblast growth factors: biology and clinical application* 187-209 (2017).

69 **de Araujo, R., Lobo, M., Trindade, K., Silva, D. F. & Pereira, N. (2019)** *Fibroblast growth factors: A controlling mechanism of skin aging*. Skin Pharmacology and Physiology 32, 275-282.

70 **Dailey, L., Ambrosetti, D., Mansukhani, A. & Basilico, C. (2005)** *Mechanisms underlying differential responses to FGF signaling*. Cytokine & Growth Factor Reviews 16, 233-247.

71 **Francavilla, C., Rigbolt, K. T., Emdal, K. B., Carraro, G., Vernet, E., Bekker-Jensen, D. B., Streicher, W., Wikstrom, M., Sundstrom, M., Bellusci, S., Cavallaro, U., Blagoev, B. & Olsen, J. V. (2013)** *Functional proteomics defines the molecular switch underlying FGF receptor trafficking and cellular outputs*. Molecular Cell 51, 707-722.

72 **Tischer, D. & Weiner, O. D. (2014)** *Illuminating cell signalling with optogenetic tools*. Nature Reviews Molecular Cell Biology 15, 551-558.

73 **Zhang, K. & Cui, B. (2015)** *Optogenetic control of intracellular signaling pathways*. Trends in Biotechnology 33, 92-100.

74 **Kwon, E. & Heo, W. D. (2020)** *Optogenetic tools for dissecting complex intracellular signaling pathways*. Biochemical and Biophysical Research Communications 527, 331-336.

75 **Nagel, G., Ollig, D., Fuhrmann, M., Kateriya, S., Musti, A. M., Bamberg, E. & Hegemann, P. (2002)** *Channelrhodopsin-1: A light-gated proton channel in green algae*. Science 296, 2395-2398.

76 **Nagel, G., Szellas, T., Huhn, W., Kateriya, S., Adeishvili, N., Berthold, P., Ollig, D., Hegemann, P. & Bamberg, E. (2003)** *Channelrhodopsin-2, a directly light-gated cation-selective membrane channel*. Proceedings of the National Academy of Sciences 100, 13940-13945.

77 **Boyden, E. S., Zhang, F., Bamberg, E., Nagel, G. & Deisseroth, K. (2005)** *Millisecond-timescale, genetically targeted optical control of neural activity*. Nature Neuroscience 8, 1263-1268.

78 **Nagel, G., Brauner, M., Liewald, J. F., Adeishvili, N., Bamberg, E. & Gottschalk, A. (2005)** *Light activation of channelrhodopsin-2 in excitable cells of Caenorhabditis elegans triggers rapid behavioral responses*. Current Biology 15, 2279-2284.

79 **Ishizuka, T., Kakuda, M., Araki, R. & Yawo, H. (2006)** *Kinetic evaluation of photosensitivity in genetically engineered neurons expressing green algae light-gated channels*. Neuroscience Research 54, 85-94.

80 **Miesenböck, G. (2009)** *The optogenetic catechism*. Science 326, 395-399.

81 **Covington, H. E., 3rd, Lobo, M. K., Maze, I., Vialou, V., Hyman, J. M., Zaman, S., LaPlant, Q., Mouzon, E., Ghose, S., Tamminga, C. A., Neve, R. L., Deisseroth, K. & Nestler, E. J. (2010)** *Antidepressant effect of optogenetic stimulation of the medial prefrontal cortex*. Journal of Neuroscience 30, 16082-16090.

82 **Deisseroth, K. (2011)** *Optogenetics*. Nature Methods 8, 26-29.

83 **Fenno, L., Yizhar, O. & Deisseroth, K. (2011)** *The development and application of optogenetics*. Annual Review of Neuroscience 34, 389-412.

84 **Lin, D., Boyle, M. P., Dollar, P., Lee, H., Lein, E. S., Perona, P. & Anderson, D. J. (2011)** *Functional identification of an aggression locus in the mouse hypothalamus*. Nature 470, 221-226.

85 **Dugue, G. P., Akemann, W. & Knopfel, T. (2012)** *A comprehensive concept of optogenetics*. Progress in Brain Research 196, 1-28.

86 **Rein, M. L. & Deussing, J. M. (2012)** *The optogenetic (r)evolution*. Molecular Genetics and Genomics 287, 95-109.

87 **Yizhar, O. (2012)** *Optogenetic insights into social behavior function*. Biological Psychiatry 71, 1075-1080.

88 **Daou, I., Tuttle, A. H., Longo, G., Wieskopf, J. S., Bonin, R. P., Ase, A. R., Wood, J. N., De Koninck, Y., Ribeiro-da-Silva, A., Mogil, J. S. & Seguela, P. (2013)** *Remote optogenetic activation and sensitization of pain pathways in freely moving mice*. Journal of Neuroscience 33, 18631-18640.

89 **Bryson, J. B., Machado, C. B., Crossley, M., Stevenson, D., Bros-Facer, V., Burrone, J., Greensmith, L. & Lieberam, I. (2014)** *Optical control of muscle function by transplantation of stem cell–derived motor neurons in mice*. Science 344, 94-97.

90 **Deisseroth, K., Etkin, A. & Malenka, R. C. (2015)** *Optogenetics and the circuit dynamics of psychiatric disease*. Journal of the American Medical Association 313, 2019-2020.

91 **Lüscher, C. (2016)** *The emergence of a circuit model for addiction*. Annual Review of Neuroscience 39, 257-276.

92 **Editorial. (2010)** *Method of the year 2010*. Nature Methods 8, 1.

93 **Gorostiza, P. & Isacoff, E. Y. (2008)** *Optical switches for remote and noninvasive control of cell signaling*. Science 322, 395-399.

94 **Airan, R. D., Thompson, K. R., Fenno, L. E., Bernstein, H. & Deisseroth, K. (2009)** *Temporally precise in vivo control of intracellular signalling*. Nature 458, 1025-1029.

95 **Bacchus, W. & Fussenegger, M. (2012)** *The use of light for engineered control and reprogramming of cellular functions*. Current Opinion in Biotechnology 23, 695-702.

96 **Chow, B. Y. & Boyden, E. S. (2013)** *Optogenetics and translational medicine*. Science Translational Medicine 5, 177ps175.

97 **Ingles-Prieto, A., Reichhart, E., Schelch, K., Janovjak, H. & Grusch, M. (2014)** *The optogenetic promise for oncology: Episode I.* Molecular & Cellular Oncology 1, e964045.

98 **Iyer, S. M. & Delp, S. L. (2014)** *Optogenetic regeneration*. Science 344, 44-45.

99 **Kushibiki, T., Okawa, S., Hirasawa, T. & Ishihara, M. (2014)** *Optogenetics: Novel tools for controlling mammalian cell functions with light*. International Journal of Photoenergy 2014, 1-10.

100 **Agus, V. & Janovjak, H. (2017)** *Optogenetic methods in drug screening: Technologies and applications*. Current Opinion in Biotechnology 48, 8-14.

101 **Rogers, K. W. & Muller, P. (2020)** *Optogenetic approaches to investigate spatiotemporal signaling during development*. Current Topics in Developmental Biology 137, 37-77.

102 **Ni, M., Tepperman, J. M. & Quail, P. H. (1999)** *Binding of phytochrome B to its nuclear signalling partner PIF3 is reversibly induced by light*. Nature 400, 781-784.

103 **Shimizu-Sato, S., Huq, E., Tepperman, J. M. & Quail, P. H. (2002)** *A light-switchable gene promoter system*. Nature Biotechnology 20, 1041-1044.

104 **Levskaya, A., Weiner, O. D., Lim, W. A. & Voigt, C. A. (2009)** *Spatiotemporal control of cell signalling using a light-switchable protein interaction*. Nature 461, 997-1001.

105 **Liu, H., Yu, X., Li, K., Klejnot, J., Yang, H., Lisiero, D. & Lin, C. (2008)** *Photoexcited CRY2 interacts with CIB1 to regulate transcription and floral initiation in Arabidopsis*. Science 322, 1535-1539.

106 **Kennedy, M. J., Hughes, R. M., Peteya, L. A., Schwartz, J. W., Ehlers, M. D. & Tucker, C. L. (2010)** *Rapid blue-light-mediated induction of protein interactions in living cells*. Nature Methods 7, 973-975.

107 **Bugaj, L. J., Choksi, A. T., Mesuda, C. K., Kane, R. S. & Schaffer, D. V. (2013)** *Optogenetic protein clustering and signaling activation in mammalian cells*. Nature Methods 10, 249-252.

108 **Pudasaini, A., El-Arab, K. K. & Zoltowski, B. D. (2015)** *LOV-based optogenetic devices: Light-driven modules to impart photoregulated control of cellular signaling*. Frontiers in Molecular Biosciences 2, 18.

109 **Glantz, S. T., Carpenter, E. J., M., M., Gardner, K. H., Boydeng, E. S., Wong, G. K.-S. & Chow, B. Y. (2016)** *Functional and topological diversity of LOV domain photoreceptors*. Proceedings of the National Academy of Sciences of the United States of America 113, E1442-E1451.

110 **Christie, J. M., Salomon, M., Nozue, K., Wada, M. & Briggs, W. R. (1999)** *LOV (light, oxygen, or voltage) domains of the blue-light photoreceptor phototropin (nph1): Binding sites for the chromophore flavin mononucleotide*. Proceedings of the National Academy of Sciences 96, 8779-8783.

111 **Harper, S. M., Neil, L. C. & Gardner, K. H. (2003)** *Structural basis of a phototropin light switch*. Science 301, 1541-1544.

112 **Wu, Y. I., Frey, D., Lungu, O. I., Jaehrig, A., Schlichting, I., Kuhlman, B. & Hahn, K. M. (2009)** *A genetically encoded photoactivatable Rac controls the motility of living cells*. Nature 461, 104-108.

113 **Strickland, D., Yao, X., Gawlak, G., Rosen, M. K., Gardner, K. H. & Sosnick, T. R. (2010)** *Rationally improving LOV domain-based photoswitches*. Nature Methods 7, 623-626.

114 **Strickland, D., Lin, Y., Wagner, E., Hope, C. M., Zayner, J., Antoniou, C., Sosnick, T. R., Weiss, E. L. & Glotzer, M. (2012)** *TULIPs: Tunable, light-controlled interacting protein tags for cell biology*. Nature Methods 9, 379-384.

115 **Toettcher, J. E., Voigt, C. A., Weiner, O. D. & Lim, W. A. (2011)** *The promise of optogenetics in cell biology: Interrogating molecular circuits in space and time*. Nature Methods 8, 35-38.

116 **Prakash, R., Yizhar, O., Grewe, B., Ramakrishnan, C., Wang, N., Goshen, I., Packer, A. M., Peterka, D. S., Yuste, R., Schnitzer, M. J. & Deisseroth, K. (2012)** *Two-photon optogenetic toolbox for fast inhibition, excitation and bistable modulation*. Nature Methods 9, 1171-1179.

117 **Fish, K. N. (2009)** *Total internal reflection fluorescence (TIRF) microscopy*. Current Protocols in Cytometry 50, 12.18.11-12.18.13.

118 **Morri, M., Sanchez-Romero, I., Tichy, A. M., Kainrath, S., Gerrard, E. J., Hirschfeld, P. P., Schwarz, J. & Janovjak, H. (2018)** *Optical functionalization of human class A orphan G-protein-coupled receptors*. Nature Communications 9, 1950.

119 **Zhang, K., Duan, L., Ong, Q., Lin, Z., Varman, P. M., Sung, K. & Cui, B. (2014)** *Light-mediated kinetic control reveals the temporal effect of the Raf/MEK/ERK pathway in PC12 cell neurite outgrowth*. PLoS One 9, e92917.

120 **Toettcher, J. E., Weiner, O. D. & Lim, W. A. (2013)** *Using optogenetics to interrogate the dynamic control of signal transmission by the Ras/Erk module*. Cell 155, 1422-1434.

121 **Goglia, A. G., Wilson, M. Z., DiGiorno, D. B. & Toettcher, J. E. (2017)** *Optogenetic control of Ras/Erk signaling using the Phy-PIF system*. Methods in Molecular Biology 1636, 3-20.

122 **Johnson, H. E., Goyal, Y., Pannucci, N. L., Schupbach, T., Shvartsman, S. Y. & Toettcher, J. E. (2017)** *The spatiotemporal limits of developmental Erk signaling*. Developmental Cell 40, 185-192.

123 **Wilson, M. Z., Ravindran, P. T., Lim, W. A. & Toettcher, J. E. (2017)** *Tracing information flow from Erk to target gene induction reveals mechanisms of dynamic and combinatorial control*. Molecular Cell 67, 757-769.e755.

124 **Leopold, A. V., Chernov, K. G., Shemetov, A. A. & Verkhusha, V. V. (2019)** *Neurotrophin receptor tyrosine kinases regulated with near-infrared light*. Nature Communications 10, 1129.

125 **Hongdusit, A., Zwart, P. H., Sankaran, B. & Fox, J. M. (2020)** *Minimally disruptive optical control of protein tyrosine phosphatase 1B*. Nature Communications 11, 788.

126 **Zhou, X. X., Fan, L. Z., Li, P., Shen, K. & Lin, M. Z. (2017)** *Optical control of cell signaling by single-chain photoswitchable kinases*. Science 355, 836-842.

127 **Zhou, X., Wang, J., Chen, J., Qi, Y., Di, N., Jin, L., Qian, X., Wang, X., Chen, Q., Liu, X. & Xu, Y. (2018)** *Optogenetic control of epithelial-mesenchymal transition in cancer cells*. Scientific Reports 8, 14098.

128 **Grusch, M., Schelch, K., Riedler, R., Reichhart, E., Differ, C., Berger, W., Ingles-Prieto, A. & Janovjak, H. (2014)** *Spatio-temporally precise activation of engineered receptor tyrosine kinases by light*. The EMBO Journal 33, 1713-1726.

129 **Kim, N., Kim, J. M., Lee, M., Kim, C. Y., Chang, K.-Y. & Heo, W. D. (2014)** *Spatiotemporal control of fibroblast growth factor receptor signals by blue light*. Chemistry & Biology 21, 903-912.

130 **Kainrath, S., Stadler, M., Reichhart, E., Distel, M. & Janovjak, H. (2017)** *Green-light-induced inactivation of receptor signaling using cobalamin-binding domains*. Angewandte Chemie International Edition 56, 4608-4611.

2 Materials

1. Chemicals and solid biologicals

Chemical	Catalogue no.	Manufacturer
Acetic acid	1.00063	Merck, Darmstadt, Germany
Acid fuchsin	A3908	Sigma, St Louis, USA
Acrylamide 4K-solution 30% 37,5:1	A1672	AppliChem, Darmstadt, Germany
Agarose	BS20.46	BioSell, Nürnberg, Germany
Ammonium persulfate (APS)	215589	Sigma
Ammonium thiocyanate	31120	Sigma
Ampicillin sodium salt	A9518	Sigma
Aniline blue, water soluble	340034C	Merck
Biebrich scarlett (Ponceau BS)	B6008	Sigma
Boric acid	B0394	Sigma
Bovine serum albumin (BSA) Fraction V	P06-1391100	PAN Biotech, Aidenbach, Germany
5'-Bromo-2'-deoxyuridine (BrdU)	B5002	Sigma
Bromophenol blue sodium salt	B2026	Sigma
Calcium dichloride ($CaCl_2$)	A331685	Sigma
Celestine blue	206342	Sigma
Chloroform	132950	Sigma
Cholera toxin from *Vibrio cholerae*	C8052	Sigma
Collagen from human placenta type IV	C7521	Sigma
Collagenase/Dispase	10269638001	Roche, Basel, Switzerland
Diethyl pyrocarbonate (DEPC)	40718	Sigma
Dimethyl sulfoxide (DMSO)	1.02952	Merck
Disodium hydrogen phosphate (Na_2HPO_4)	1.06580	Merck
DNase (Deoxyribonuclease I from bovine pancreas)	DN25	Sigma
Dithiothreitol (DTT)	A1101	AppliChem
Doxycycline monohydrate	D1822	Sigma
Eosin Y disodium salt	E4382	Sigma

Chemical	Catalogue no.	Manufacturer
Epidermal growth factor (EGF) from murine submaxillary gland	E4127	Sigma
Ethanol	1.00983	Merck
Ethanolamine	E0135	Sigma
Ethidium bromide	E1510	Sigma
Ethylenediamine tetraacetic acid (EDTA)	A2937	AppliChem
Ferric chloride ($FeCl_3$)	31232	Sigma
Ferrous sulphate	215422	Sigma
FGF1 (recombinant human FGF-acidic)	100-17A	PeproTech, Rocky Hill, USA
FGF7 (recombinant human KGF)	100-19	PeproTech
FGF10 (recombinant human FGF-10)	100-26	PeproTech
Formaldehyde solution	47608	Sigma
Geneticin (G418) sulphate	11811031	ThermoFisher Scientific, Waltham, USA
Glycerol	211339	AppliChem
Glycine	A1067	AppliChem
Guanidine thiocyanate	G9277	Sigma
Hematoxylin	3816.3	Roth, Karlsruhe, Germany
Hoechst 33342	14533	Sigma
Hydrochloric acid (HCl) fuming 37%	1.00317	Merck
Hydrocortisone	H0888	Sigma
Hydrogen peroxide (H_2O_2) 30%	1.07209	Merck
Insulin from bovine pancreas	I6634	Sigma
Iron alum (Aluminum potassium sulphate dodecahydrate)	31242	Sigma
Isopropanol (2-propanol)	1.09634	Merck
Kanamycin sulphate from *Streptomyces kanamyceticus*	K1377	Sigma
Ketamine (Ketanarkon)	1370031A	Streuli Pharma, Uznach, Switzerland
LB broth (Difco™ LB broth, Miller)	244610	BD Biosciences, Franklin Lakes, USA
Lithium carbonate (Li_2CO_3)	62470	Sigma
Magnesium chloride ($MgCl_2$) hexahydrate	M9272	Sigma
Metanil yellow	202029	Sigma
Methanol	1.06009	Merck
Methyl blue	M5528	Sigma
Mineral oil	M8410	Sigma

Chemical	Catalogue no.	Manufacturer
Mitomycin C from *Streptomyces caespitosus*	M4287	Sigma
Mowiol® 4-88	81381	Sigma
MTT (Thiazolyl blue tetrazolium bromide)	M2128	Sigma
NP-40 (IGEPAL® CA-630)	I3021	Sigma
Paraffin (Surgipath Paraplast)	39601006	Leica Biosystems, Wetzlar, Germany
Paraformaldehyde (PFA)	P6148	Sigma
Phenol	1.00206	Merck
Phosphoethanolamine	P3531	Sigma
Phosphomolybdic acid	221856	Sigma
Phosphotungstic acid	P4006	Sigma
Picric acid (saturated)	P6744	Sigma
Ponceau S red	P3504	Sigma
Potassium chloride (KCl)	1.04936	Merck
Potassium dihydrogen phosphate (KH_2PO_4)	1.04873	Merck
Propidium iodide	P1304MP	ThermoFisher
Puromycin dihydrochloride from *Streptomyces alboniger*	P8833	Sigma
Saponin	47036	Sigma
Skim milk powder	150141000000	Rapilait, Basel, Switzerland
Sodium acetate trihydrate	1.06267	Merck
Sodium hydrogen carbonate ($NaHCO_3$)	1.06329	Merck
Sodium tetraborate decahydrate	S9640	Sigma
Sodium chloride (NaCl)	S9888	Sigma
Sodium citrate tribasic hydrate	71405	Fluka, St Louis, USA
Sodium deoxycholate	D6750	Sigma
Sodium dodecyl sulphate (SDS)	L5750	Sigma
Sodium hydroxide (NaOH)	1.06498	Merck
TEMED (N,N,N′,N′-Tetramethylethylenediamine)	T9281	Sigma
Transferrin (human holo-Transferrin)	T0665	Sigma
Tris base	A2264	AppliChem
Tris-HCl	A3452	AppliChem
Triton X-100	3051	Roth
Trypsin solid 1:250	27250-018	ThermoFisher
Tween 20	P2287	Sigma
Urea	GEPURE00-67	Eurobio Scientific, Les Ulis, France

Chemical	**Catalogue no.**	**Manufacturer**
Xylazine	1170202A	Streuli Pharma
Xylene	534056	Sigma

2. Prefabricated products and kits

Product/Kit	Catalogue no.	Manufacturer
Anti-HA Magnetic Beads	88836	ThermoFisher Scientific
BCA Protein Assay Kit	23225	ThermoFisher Scientific
Chelex 100 Chelating Resin	142-2832	BioRad, Hercules, USA
cOmplete™, EDTA-free Protease Inhibitor Cocktail	11873580001	Roche
DAB Peroxidase substrate Kit	SK-4100	Maravai Life Sciences, San Diego, USA
Defined Keratinocyte SFM (1X)	10744019	ThermoFisher Scientific
Dulbecco's modified eagle medium (DMEM)	D6429	Merck
DNA Gel Loading Dye (6X)	R0611	ThermoFisher Scientific
Erk1/2 ELISA Kit	ADI-900-152	Enzo Life Sciences, Farmingdale, USA
Eukitt Quick-hardening mounting medium	03989	Sigma
Fetal bovine serum (FBS), qualified, One Shot	A3160802 LOT 2166297	ThermoFisher Scientific
Gateway™ LR Clonase™ II Enzyme mix	11791100	ThermoFisher Scientific
GeneRuler 100 bp Plus DNA Ladder	SM0322	ThermoFisher Scientific
HindIII	R0104	New England Biolabs (NEB), Ipswich, USA
iScript cDNA synthesis Kit	1708890	BioRad
KAPA2G Fast HotStart Genotyping Mix	KK5620	Roche
L-Glutamine solution 200mM	G7513	Sigma
LightCycler® 480 SYBR Green I Master	04887352001	Roche
Lipofectamine 2000 Transfection Reagent	11668030	Thermo Fisher Scientific
Mayer`s hematoxylin solution	MHS32	Sigma
Mini Total RNA Kit (Tissue)	IB47300	IBI Scientific, Dubuque, USA
Minimum Essential Medium Eagle	M8167	Sigma
NucleoSpin™ Gel and PCR Clean-up Kit	740609.250	Macherey-Nagel, Düren, Germany
NucleoSpin Plasmid, Mini kit	740588.50	Macherey-Nagel
Opti-MEM reduced serum medium	31985047	Thermo Fisher Scientific
PageRuler PLUS Protein Ladder	26619	Thermo Fisher Scientific
PCR Mycoplasma Test Kit I/C	PK-CA91-1024	PromoCell, Heidelberg, Germany
Penicillin/Streptomycin	P0781	Merck

Product/Kit	**Catalogue no.**	**Manufacturer**
pENTR™/D-TOPO™ Cloning Kit	K240020	ThermoFisher Scientific
PhosSTOP	4906845001	Roche
Phusion® High-Fidelity DNA Polymerase	M0530L	NEB
Plasmid Plus Maxi Kit	12963	Qiagen, Venlo, The Netherlands
ProLong™ Gold Antifade Mountant	P36934	ThermoFisher Scientific
Proteinase K, recombinant, PCR grade	A3830	AppliChem
Protran™ Premium NC Nitrocellulose Membranes	GE10600001	GE Healthcare, Chicago, USA
[pThr202/Tyr204]Erk1/2 ELISA Kit	ADI-900-098A-0001	Enzo Life Sciences
RNase A	10109169001	Roche
RNaseZAP™	R2020	Sigma
Shrimp Alkaline Phosphatase (rSAP)	M0371	NEB
Sma I	R0141	NEB
0.9% sodium chloride solution	534530	B.Braun, Melsungen, Germany
T4 DNA Ligase	M0202	NEB
T4 Polynucleotide Kinase (PNK)	M0201	NEB
Trypan blue solution	T8154	Sigma
Trypsin-EDTA Solution	T4174	Sigma
VECTASTAIN® Elite® ABC Kit, Peroxidase (Standard)	PK-4000	Maravai Life Sciences
WesternBright Sirius HRP substrate	K-12043	Advansta, San Jose, USA

3. Buffers and solutions

For the preparation of buffers and solutions, small amounts of chemicals were weighed with a fine balance (XS104 from Mettler Toledo, Columbus, USA), whereas for weights more than 1g, the precision balance (XS4002S from Mettler Toledo) was used. All buffers were set up in ddH_2O and stored at room temperature (RT), unless stated otherwise.

Buffer	Chemical	Concentration
Preparation of murine primary keratinocytes, cell culture methods		
PBS	NaCl	137mM
	KCl	2.7mM
	Na_2HPO_4	2.7mM
	KH_2PO_4	1.8mM
	Adjust pH with HCl to 7.4	
Murine keratinocyte growth medium	Defined keratinocyte serum-free medium,	75% (v/v)
	with supplements	25% (v/v)
	Minimal essential medium	100 U,
	Penicillin/Streptamycin	0.1mg/ml
	Cholera toxin	4.2pg/ml
	Insulin	10mg/ml
	Phosphoethanolamine	2.5µM
	Ethanolamine	2.5µM
	Transferrin	5ng/ml
	Hydrocortisone	6.5pg/ml
	Glutamine	500µM
	Chelated FBS	2% (v/v)
	$CaCl_2$	11.3µM
Murine keratinocyte starvation medium	Penicillin/Streptomycin	100 U,
	Cholera toxin	0.1mg/ml
		4.2pg/ml
	Set up with defined keratinocyte serum-free medium (without supplements)	
	Store at 4°C	
Immunofluorescence stain on cells		
Blocking solution	BSA	2% (w/v)
	Triton X-100	0.05% (v/v)

Buffer	Chemical	Concentration
	Set up with PBS Prepare fresh, do not store	
Cell cycle analysis by flow cytometry		
Staining solution	Triton X-100	1% (v/v)
	RNase A	200µg/ml
	Propidium iodide	20µg/ml
	Set up with PBS Prepare fresh, do not store	
H&E stain		
Eosin solution	Eosin	1% (w/v)
	Ethanol	90% (v/v)
Scott water	$MgCl_2$	98.4mM
	$NaHCO_3$	23.8mM
Herovici's stain		
Solution A	Celestine blue	3.4mg/ml
	Iron alum	42mg/ml
	Glycerol	17% (v/v)
Solution B	Hematoxylin	2.5mg/ml
	Ethanol	25% (v/v)
	Ferrous sulphate	40.5mM
	Ferric chloride ($FeCl_3$)	23.1mM
	HCl	0.2% (v/v)
Solution C	Metanil yellow	11mM
	Acetic acid	1 drop / 10ml
Solution D	Acetic acid	0.45% (v/v)
Solution E	Saturated aqueous Li_2CO_3 solution	0.2% (v/v)
Solution F	Methyl blue	0.45mg/ml
	Acid fuchsin	0.6mg/ml
	Glycerol	9% (v/v)
	Saturated aqueous Li_2CO_3 solution	0.045% (v/v)
Solution G	Acetic acid	1% (v/v)

Buffer	Chemical	Concentration
Masson-Goldner Trichrome stain		
Bouin's solution	Picric acid (saturated)	70% (v/v)
	Formaldehyde	9.25% (v/v)
	Acetic acid	5% (v/v)
Weigert's hematoxylin	Hematoxylin	0.5mg/ml
	Ethanol	50% (v/v)
	HCl	0.06% (v/v)
	$FeCl_3$	0.6% (w/v)
BSAF solution	Biebrich Scarlett	0.36% (w/v)
	Acid fuchsin	0.04% (w/v)
	Acetic acid	0.4% (v/v)
PMPT solution	Phosphomolybdic acid	2.5% (w/v)
	Phosphotungstic acid	2.5% (w/v)
Aniline blue solution	Aniline blue	2.5% (w/v)
	Acetic acid	2% (v/v)
Immunohistochemistry		
Mowiol	Mowiol	10.9% (w/v)
	Glyerol	18% (v/v)
	Tris-HCl pH 8.5	109µM
KAPA PCR for genotyping		
Tissue lysis buffer	Tris-HCl pH 8.8	50mM
	KCl	50mM
	EDTA	2.5mM
	NP-40	0.45% (v/v)
	Tween 20	0.45% (v/v)
Agarose gel		
SBA buffer	NaOH	20mM
	Boric acid	80.8mM
Isolation of genomic DNA (HotShot)		
Alkaline lysis buffer (pH 12)	Sodium hydroxide	25mM
	Disodium EDTA	0.2mM

Buffer	Chemical	Concentration
Neutralisation buffer (pH 5)	Tris-HCl	40mM
Isolation of RNA from tissue		
Trizol reagent	Phenol (molten for 1h at 60°C)	38% (v/v)
	Guanidine thiocyanate	800mM
	Ammonium thiocyanate	420mM
	Sodium acetate pH 5.0	0.1mM
	Glycerol	0.05% (v/v)
	Set up with DEPC water Store at 4°C in the dark	
Protein methods		
Sample buffer 2x	Tris-HCl pH 6.8	240mM
	SDS	280mM
	Glycerol	40% (v/v)
Isolation of protein from tissue		
T-Per lysis buffer	Tris-HCl pH 8	10mM
	Urea	8M
	EDTA	2mM
	Add protease and phosphatase inhibitor tablets Prepare fresh, do not store	
Nuclear cytoplasmic fractionation		
NP-40 lysis buffer	NP-40	0.1% (v/v)
	Set up with PBS Freshly add protease and phosphatase inhibitor tablets	
Immunopreciptiation using the HA tag		
IP buffer	NaCl	150mM
	HEPES pH 7.4	5mM
	EDTA	5mM
	Glycerol	10% (v/v)
	Sodium deoxycholate	0.25% (w/v)
	NP-40	0.05% (v/v)

Buffer	Chemical	Concentration
	Freshly add protease and phosphatase inhibitor tablets	
Tris buffered saline (TBS)	Tris base	25mM
	NaCl	137mM
	KCl	2.7mM
	Adjust pH with HCl to 8.0	
Western Blot		
Separation gel (12%)	Acrylamide solution 30%	36% (v/v)
	Tris-HCl pH 8.8	375mM
	SDS	0.1% (w/v)
	APS	0.1% (w/v)
	TEMED	0.04% (v/v)
Stacking gel (6%)	Acrylamide solution 30%	17% (v/v)
	Tris-HCl pH 6.8	127mM
	SDS	0.1% (w/v)
	APS	0.1% (w/v)
	TEMED	0.1% (v/v)
SDS running buffer	Tris base	25mM
	Glycine	192mM
	SDS	3.5mM
Transfer buffer	Tris base	25mM
	Glycine	192 mM
	Methanol	20% (v/v)
	Store at 4°C in the dark	
Ponceau S solution	Ponceau S red	0.1% (w/v)
	Acetic acid	0.5% (v/v)
TBS with Tween 20 (TBS-T)	Tris base	25mM
	NaCl	137mM
	KCl	2.7mM
	Tween 20	0.1% (v/v)
	Adjust pH with HCl to 8.0	

4. Oligonucleotides

Gene	Sequence	Application
ACTB (human)	5'-TAC TCC TGC TTG CTG ATC CAC-3'	DNA qPCR
	5'-TGT GTG GGG AGC TGT CAC AT-3'	
Cdh1 (mouse)	5'-GCG CAC TAC TGA GTT CCC A-3'	RNA qPCR
	5'-AAA TCT CAC TCT GCC CAG GA-3'	
Cre	5'-AAC ATG CTT CAT CGT CGG-3'	Genotyping
	5'-TTC GGA TCA TCA GCT ACA CC-3'	PCR
	5'-CGA CCA GGT TCG TTC ACT CA-3'	RNA qPCR
	5'-CGA GTT GAT AGC TGG CTG GT-3'	
DDX58 / *Ddx58* (human and mouse)	5'-ATC CCA GTG TAT GAA CAG CAG-3'	RNA qPCR
	5'-GCC TGT AAC TCT ATA CCC ATG TC-3'	
DUSP6 / *Dusp6* (human and mouse)	5'-GTT CTA CCT GGA AGG TGG CT-3'	RNA qPCR
	5'-AGT CCG TTG CAC TAT TGG GG-3'	
Fgfr1 (mouse)	5'-CGA ATG GAC AAG CCC AGT AAC-3'	Genotyping
	5'-CTC CTG CTT CCT TCA GAG C-3'	PCR
	5'-CAA CCG TGT GAC CAA AGT GG-3'	RNA qPCR
	5'-TCC GAC AGG TCC TTC TCC G-3'	
FGFR2 (human)	5'-AGC TGG GGT CGT TTC ATC TG-3'	RNA qPCR
	5'-TTG GTT GGT GGC TCT TCT GG-3'	
Fgfr2 (mouse)	5'-TTC CTG TTC GAC TAT AGG AGC AAC AGG CGG-3'	Genotyping PCR
	5'-GAG AGC AGG GTG CAA GAG GCG ACC AGT CAG-3'	
	5'-ATC CCC CTG CGG AGA CA-3'	RNA qPCR
	5'-GAG GAC AGA CGC GTT GTT ATC C-3'	
Fgfr2b (mouse)	5'-AAG GTT TAC AGC GAT GCC CA-3'	RNA qPCR
	5'-AGA GCC AGC ACT TCT GCA TT-3'	
Fgfr2c (mouse)	5'-GTG TTA ACA CCA CGG ACA AA-3'	RNA qPCR
	5'-TGG CAG AAC TGT CAA CCA TG-3'	
Fgfr3 (mouse)	5'-CAC AAG GTC TCT CGC TTC CCG-3'	Genotyping
	5'-AGG ACA CCT GCT TGG GTC ATC-3'	PCR
	5'-GTG GCT GGA GCT ACT TCC GA-3'	RNA qPCR
	5'-ATC CTT AGC CCA GAC CGT GG-3'	
Fgfr3b (mouse)	5'-ACT CAA GTC CTG GAT CAG TGA GA-3'	RNA qPCR
	5'-CCT TCT CAG CCA CGC CTA TG-3'	
Fgfr3c (mouse)	5'-ACT CAA GAC TGC AGG CGC TA-3'	RNA qPCR
	5'-GTC CTC AAA GGT GAC ATT GTG C-3'	
GlycB (HSV)	5'-CGC ATC AAG ACC ACC TCC TC-3'	DNA qPCR
	5'-GCT CGC ACC ACG CGA-3'	

Gene	Sequence	Application
HBEGF (human)	5'-TTA GTC ATG CCC AAC TTC ACT TT-3'	RNA qPCR
	5'-ATC GTG GGG CTT CTC ATG TTT-3'	
IFIT1 (human)	5'-AGC TTA CAC CAT TGG CTG CT-3'	RNA qPCR
	5'-CCA TTT GTA CTC ATG GTT GCT GT-3'	
Ifit1 (mouse)	5'-AGC AAC CAT GGG AGA GAA TGC-3'	RNA qPCR
	5'-CTT TCA GGT GCC TCA CGT A-3'	
IFNB (human)	5'-TGG GAG GAT TCT GCA TTA CC-3'	RNA qPCR
	5'-CAG CAT CTG CTG GTT GAA GA-3'	
Ifnb (mouse)	5'-CTG GCT TCC ATC ATG AAC AA-3'	RNA qPCR
	5'-CAT TTC CGA ATG TTC GTC CT-3'	
IFNL (human)	5'-GGT GAC TTT GGT GCT AGG-3'	RNA qPCR
	5'-TGA GTG ACT CTT CCA AGG-3'	
Ifnl (mouse)	5'-GGT TGG AGG TGA CAG AGT-3'	RNA qPCR
	5'-AAG GGT GCC ATC GAG AAG-3'	
IRF1 (human)	5'-CTC TGA AGC TAC AAC AGA TGA G-3'	RNA qPCR
	5'-GTA GAC TCA GCC CAA TAT CCC-3'	
IRF3 (human)	5'-TCG TGA TGG TCA AGG TTG T-3'	RNA qPCR
	5'AGG TCC ACA GTA TTC TCC AG-3'	
IRF7 (human)	5'-AGC TGT GCT GGC GAG AAG-3'	RNA qPCR
	5'-CTC TCC AGG AGC CTT GGT TG-3'	
Irf7 (mouse)	5'-AGC TTG GAT CTA CTG TGC GC-3'	RNA qPCR
	5'-GGG TTC CTC GTA AAC ACG GT-3'	
ISG15 (human)	5'-ACT CAT CTT TGC CAG TAC AGG AG-3'	RNA qPCR
	5'-CAG CAT CTT CAC CGT CAG GTC-3'	
Krt14 (mouse)	5'-AAC CAC GAG GAG GAA ATG G-3'	RNA qPCR
	5'-CCG GAG CTC AGA AAT CTC AC-3'	
M13	5'-TGT AAA ACG ACG GCC AG-3'	Sequencing
	5'-CAG GAA ACA GCT ATG AC-3'	
OAS2 (human)	5'-GGG CTA TTT CCA GAC AAC GC-3'	RNA qPCR
	5'-GAA AAC CAG GCC TGT GAT CTT GG-3'	
Oasl2 (mouse)	5'-TGC CTG GGA GAG AAT CGA AG-3'	RNA qPCR
	5'-AGC CTC CCT TCA CCA CCT TA-3'	
OptoR2	5'-CTC CCT CCC AGA CAA CCC TA-3'	Colony
	5'-CTC TGA GTC CAG CCA CGA AG-3'	PCR
	5'-CAC CGG GAG ACA CAA GCT GGC TAG-3'	Gateway
	5'-GCA ACT AGA AGG CAC AGT CGA GGC TG-3'	cloning
	5'-TGA CCA GCA GCT TGG CAT AA-3'	Genotyping
	5'-GCT CTG CAA ATG GCA CAA CA-3'	PCR
	5'-GGG AGA CAC AAG CTG GCT AG-3'	Restriction
	5'-GCA ACT AGA AGG CAC AGT CG-3'	cloning
	5'-GCT CTG CAA ATG GCA CAA CA-3'	RNA qPCR
	5'-TGA CCA GCA GCT TGG CAT AA-3'	

Gene	Sequence	Application
	5‘-CCA ACT GCA CCA ACG AAC TG-3’	Sequencing
	5’-TCG AGA GGT TGG CTG AGG TC-3’	
	5’-CAA GGG CCA GAA ACA GAC CC-3’	
	5’-GGT ATT CTC GGA GGT TGC CT-3’	
RPL27 (human)	5’-TCA CCT AAT GCC CAC AAG GTA-3’	RNA qPCR
	5’-CCA CTT GTT CTT GCC TGT CTT-3’	
Rps29 (mouse)	5’-GGT CAC CAG CAG CTC TAC TG-3’	RNA qPCR
	5’-GTC CAA CTT AAT GAA GCC TAT GTC C-3’	
RSAD2 (human)	5’-GCT GCT AGC TAC CAA GAG GAG-3’	RNA qPCR
	5’-ATC TTC TCC ATA CCA GCT TCC T-3’	
Rsad2 (mouse)	5’-GGA AAA CCT TCC AGC GCA CA-3’	RNA qPCR
	5’-GGA GGT GGT GCA GGG ATT AC-3’	
Snai2 (mouse)	5’-AGA AGC CCA ACT ACA GCG AA-3’	RNA qPCR
	5’-GCC CCA AGG ATG AGG AGT AT-3’	
SOCS1 (human)	5’-GGA ACT GCT TTT TCG CCC TTA-3’	RNA qPCR
	5’-AGC AGC TCG AAG AGG CAG TC-3’	
SOCS3 (human)	5’-GGC CAC TCT TCA GCA TCT C-3’	RNA qPCR
	5’-ATC GTA CTG GTC CAG GAA CTC-3’	
STAT1 (human)	5’-AAA GGA AGC ACC AGA GCC AAT-3’	RNA qPCR
	5’-TCC GAG ACA CCT CGT CAA AC-3’	
Stat1 (mouse)	5’-GGA TCG CTT GCC CAA CTC T-3’	RNA qPCR
	5’-GCA GAG CTG AAA CGA CCT AGA-3’	
STAT2 (human)	5’-GGA TCC TAC CCA GTT GGC TG-3’	RNA qPCR
	5’-GAG GGT GTC TTC CCT TTG GC-3’	
Stat2 (mouse)	5’-CTT TTG CAA GCG AGA GAG CC-3’	RNA qPCR
	5’-TGA AGC GCA GTA GGA AGG TG-3’	
VEGF (human)	Hs_VEGFA_6_SG, QuantiTect Primer Assay (QT01682072)	RNA qPCR
Vimentin (mouse)	5’-CCT GTA CGA GGA GGA GAT GC-3’	RNA qPCR
	5’-GTG CCA GAG AAG CAT TGT CA-3’	

5. Primary antibodies

Antigen	Host	Dilution	Application	Catalogue no.	Manufacturer
AKT	rabbit	1:1.000	Western blot	9272	Cell Signaling Technologies, Danvers, USA
AKT (phospho T308)	rabbit	1:1.000	Western blot	9275	Cell Signaling Technologies
AKT (phospho S473)	rabbit	1:1.000	Western blot	3787	Cell Signaling Technologies
ATF2	rabbit	1:1.000	Western blot	35031	Cell Signaling Technologies
ATF2 (phospho T71)	rabbit	1:1.000	Western blot	9221	Cell Signaling Technologies
BrdU	mouse	1:500	BrdU staining	1202693	Roche
c-Cbl	rabbit	1:1.000	Western blot	8447	Cell Signaling Technologies
c-Jun	mouse	1:1.000	Western blot	610326	BD Biosciences
c-Jun (phospho S73)	rabbit	1:1.000	Western blot	9164	Cell Signaling Technologies
Cadherin	mouse	1:100 1:500	Immunofluorescence Western blot	610181	BD Biosciences
Cbl-b	rabbit	1:1.000	Western blot	9498	Cell Signaling Technologies
CD3	rabbit	1:100	Immunohisto-chemistry	A0452	Agilent Technologies, Santa Clara, USA
CD31	rat	1:100	Immunofluorescence	553370	BD Biosciences
EGFR (phospho Y1068)	rabbit	1:1.000	Western blot	3777	Cell Signaling Technologies
EGFR (phospho Y1173)	rabbit	1:1.000	Western blot	4407	Cell Signaling Technologies
ERK	rabbit	1:1.000	Western Blot	9102	Cell Signaling Technologies
ERK (phospho T202/Y204)	mouse	1:100	Immunofluorescence	sc-136521	Santa Cruz Biotechnology, Dallas, USA
	rabbit	1:100	Immunofluorescence	9101	Cell Signaling Technologies

Antigen	Host	Dilution	Application	Catalogue no.	Manufacturer
		1:1.000	Western blot		
FGFR2 (BEK)	mouse	1:100	Western blot	sc-6930	Santa Cruz Biotechnology
FRS2α (phospho Y196)	rabbit	1:1.000	Western blot	3864	Cell Signaling Technologies
FRS2α (phospho Y436)	rabbit	1:1.000	Western blot	3861	Cell Signaling Technologies
GAPDH	mouse	1:5.000	Western blot	5G4cc	HyTest, Turku, Finland
GSK3β	rabbit	1:1.000	Western blot	9315	Cell Signaling Technologies
GSK3β (phospho S9)	rabbit	1:1.000	Western blot	9336	Cell Signaling Technologies
HA (OptoR2)	goat	1:1.000	Immunofluorescence	NB600-362	Novus Biologicals, Littleton, USA
	mouse	1:100	Immunofluorescence	sc-7392	Santa Cruz Biotechnology
	rabbit	1:100	Immunofluorescence Flow cytometry	3724	Cell Signaling Technologies
		1:1.000	Western blot		
Ikk α/β	rabbit	1:1.000	Western blot	2678	Cell Signaling Technologies
Ikk α/β (phospho S180/S181)	rabbit	1:1.000	Western blot	2681	Cell Signaling Technologies
IRF1	rabbit	1:1.000	Western blot	8478	Cell Signaling Technologies
IRF3	rabbit	1:1.000	Western blot	11904	Cell Signaling Technologies
IRF3 (phospho S396)	rabbit	1:1.000	Western blot	4947	Cell Signaling Technologies
IRF9	rabbit	1:1.000	Western blot	76684	Cell Signaling Technologies
Keratin 10	mouse	1:100	Immunofluorescence	M700201	Agilent Technologies
Keratin 14	mouse	1:100	Immunofluorescence	ab7800	Abcam, Cambridge, UK
	rabbit	1:5.000	Immunofluorescence	PRB-155P	BioLegend, San Diego, USA

Antigen	**Host**	**Dilution**	**Application**	**Catalogue no.**	**Manufacturer**
Ki67	rabbit	1:500	Immunohisto-chemistry Immunofluorescence	ab16667	Abcam
Ly6G	rat	1:500	Immunohisto-chemistry	551459	BD Biosciences
NFκB	mouse	1:1.000	Western blot	6956	Cell Signaling Technologies
NF-κB (phospho S536)	rabbit	1:1.000	Western blot	3033	Cell Signaling Technologies
p38	rabbit	1:1.000	Western blot	9212	Cell Signaling Technologies
p38 (phospho T180/Y182)	rabbit	1:1.000	Western blot	9211	Cell Signaling Technologies
PLCγ (phospho S1248)	rabbit	1:1.000	Western blot	4510	Cell Signaling Technologies
RIG-I	rabbit	1:1.000	Western blot	3743	Cell Signaling Technologies
RSAD2	rabbit	1:1.000	Western blot	13996	Cell Signaling Technologies
SAPK/JNK (phospho T183/Y185)	mouse	1:1.000	Western blot	9255	Cell Signaling Technologies
STAT1	rabbit	1:1.000	Western blot	14994	Cell Signaling Technologies
STAT1 (phospho Y701)	rabbit	1:1.000	Western blot	9167	Cell Signaling Technologies
STAT1 (phospho S727)	rabbit	1:1.000	Western blot	8826	Cell Signaling Technologies
STAT2	rabbit	1:1.000	Western blot	4594	Cell Signaling Technologies
STAT2 (phospho Y690)	rabbit	1:1.000	Western blot	88410	Cell Signaling Technologies
STAT3	rabbit	1:1.000	Western blot	4904	Cell Signaling Technologies
STAT3 (phospho Y705)	rabbit	1:1.000	Western blot	9131	Cell Signaling Technologies
Tyrosine (all phospho residues)	rabbit	1:1.000	Western blot	8954	Cell Signaling Technologies

6. Secondary and coupled antibodies

Antigen species	coupled with	Dilution	Application	Catalogue no.	Manufacturer
goat	Cy3	1:500	Immunofluorescence	805-165-180	Jackson ImmunoResearch, West Grove, USA
HA (OptoR2)	DyLight 650	1:100	Flow cytometry	26183-D650	ThermoFisher Scientific
mouse	Cy2	1:200	Immunofluorescence BrdU staining	115-225-003	Jackson ImmunoResearch
mouse	Cy3	1:200	Immunofluorescence	111-225-003	Jackson ImmunoResearch
mouse	HRP	1:5.000	Western blot	W4021	Promega, Madison, USA
rabbit	biotin	1:500	Immunohisto-chemistry	111-065-003	Jackson ImmunoResearch
rabbit	Cy2	1:200	Immunofluorescence	111-225-144	Jackson ImmunoResearch
rabbit	Cy3	1:200	Immunofluorescence	111-165-003	Jackson ImmunoResearch
rabbit	HRP	1:5.000	Western blot	W4011	Promega
rat	biotin	1:500	Immunohisto-chemistry	112-065-003	Jackson ImmunoResearch
rat	Cy3	1:200	Immunofluorescence	712-165-153	Jackson ImmunoResearch

3 Methods

1. Mouse methods

Mice were kept under specific pathogen free (SPF) conditions in the ETH Phenomics Center (EPIC) according to federal guidelines with food and water *ad libitum* and a 12h light-dark cycle. All mouse experiments were approved by the local veterinary authorities of Zurich, Switzerland (Kantonales Veterinäramt der Stadt Zürich).

1.1 Mouse genotyping

Skin samples obtained by ear clipping were digested with 200µl tissue lysis buffer containing 2.5µl Proteinase K for at least 3h or overnight at 55°C. Afterwards, the enzyme was inhibited by incubating the samples for 5min at 95°C, and remaining skin parts were removed by centrifugation for 5min at 13.000g. Then the samples were used as source of genomic deoxyribonucleic acid (DNA) for the genotyping polymerase chain reaction (PCR) as described in the DNA methods section.

1.2 Illumination of mice

For illumination, 6 to 8 week old mice were transferred from EPIC to the mouse room HPL F15. Here, they were kept for up to several weeks in open cages in a mouse incubator (UniProtect incubator from Bioscape, Castrop-Rauxel, Germany) with a 12h light-dark cycle and food and water *ad libitum*. During the light period, mice were illuminated for up to 6h every day by placing the cage into the lower shelf of a cupboard with a strip of light emitting diodes (LEDs) (Catalogue number 5119661 from Light & More, Forchtenberg, Germany) mounted on top of the lower shelf, facilitating illumination of the mice from the top. Control animals were placed into the upper shelf of the cupboard. Light intensities were measured with a Powermeter (LP1 from Sanwa, Tokyo, Japan) and were around 80µW/cm^2 (light) and 1.5µW/cm^2 (dark), compared to 25µW/cm^2 in the mouse incubator.

1.3 Excisional wounding

Mice at the age of 6 to 8 weeks were anaesthetised with a single intraperitoneal injection of ketamine (75µg/g) / xylazine (5µg/g) diluted in 0.9% (w/v) sodium chloride (NaCl) solution. One or two full-thickness excisional wounds of 5mm diameter were generated on either side of the dorsal midline on the back of the mice [131]. At different time points after injury, the mice were sacrificed using carbon dioxide (CO_2) and skin samples were harvested. When used for ribonucleic acid (RNA) or protein isolation, the skin samples were snap-frozen in liquid nitrogen, whereas when harvested for histology, they were stretched on a nitrocellulose membrane and fixed with 4% (w/v) paraformaldehyde (PFA) in phosphate-buffered saline (PBS).

1.4 Tape stripping

Six to 8 week old mice were anaesthetised with a single intraperitoneal injection of ketamine (75µg/g) / xylazine (5µg/g) diluted in 0.9% (w/v) NaCl solution. Afterwards, the epidermis on the back skin was removed with fabric tape (extra Power Perfect Gewebeband from Tesa, Hamburg, Germany) by sticking and removing a fresh tape with a size of ca. $1cm^2$ 5 to 25 times to the same area. Successful epidermis removal was confirmed visually by glossy appearance of the skin at the stripped area. At different time points after injury, the mice were sacrificed and skin samples were harvested. When used for RNA or protein isolation, the skin samples were snap-frozen in liquid nitrogen, however, when harvested for histology, they were stretched on a nitrocellulose membrane and fixed with 4% (w/v) PFA in PBS.

1.5 Preparation of tail explants

Mice at the age of 6 to 8 weeks were sacrificed using CO_2, their tails removed and the tail skin peeled off. The tail skin samples were cut into several pieces for different treatment conditions and digested with 0.25% (w/v) dispase in Dulbecco's modified eagle medium (DMEM) for 1h at 37°C while shaking at 60 rounds per minute (rpm). Afterwards, epidermis and dermis were separated using some forceps and the intact epidermal sheets were placed into 24-well plates (Greiner, Kremsmünster, Austria) containing DMEM with 2x Penicillin/Streptomycin solution.

Tail explants were cultivated for up to 48h before they were harvested for RNA or protein isolation.

1.6 Establishment of murine primary keratinocyte cultures

Primary keratinocytes were obtained from 3 to 5d old pups as described previously [132], but with few modifications. After decapitation and sterilisation by incubating the whole body for 1min in 70% (v/v) ethanol, the limbs were cut off and the tail was used as a genotyping sample. The skin at the belly was opened up and the whole trunk skin was peeled off. Then, the subcutaneous fat tissue was scraped off and the skin was placed with the dermis down into a 6-well plate (Greiner) containing 2ml 0.8% (w/v) trypsin in DMEM. After incubation for 1h at 37°C under continuous shaking at 60rpm, epidermis and dermis were separated using some forceps. The epidermis was placed into a Falcon tube (Greiner) containing 2ml 0.025% (w/v) DNase in DMEM + 10% (v/v) fetal bovine serum (FBS) and incubated for 30min at 37°C under continuous shaking at 60rpm. Afterwards, the cell pellet was resuspended in the supernatant and the single cells were separated by filtering the cell suspension through a 50µm cell strainer (Sysmex, Goerlitz, Germany). Then the cells were centrifuged for 5min at 500g, the cell pellet resuspended in keratinocyte growth medium and the cells seeded in 6-well plates, which were pre-coated with Collagen IV in PBS (2.5µg/cm^2). As a general rule, the obtained keratinocytes from one pup were distributed to 4 wells of a 6-well plate. They were cultivated for up to 1 week.

2. Cell culture

In general, cell culture experiments were conducted under sterile conditions in a SafeFAST Premium hood (FASTER, Cornaredo, Italy) using sterile plastic or autoclaved glass vessels and sterile solutions. The cells were cultivated at 37°C with 5% (v/v) CO_2 in a HERA cell culture incubator (Heraeus, Hanau, Germany). All cell lines were tested on a monthly basis for mycoplasma contamination using the PCR Mycoplasma Test Kit I/C (PromoCell) according to the manufacturer`s instructions.

2.1 Cell lines and cell types

Human embryonic kidney (HEK 293T) cells, human immortalised keratinocytes (HaCaT cells) as well as primary and immortalised murine keratinocytes were used for this study.

HEK 293T cells had been established by transfection of human embryonic kidney cells with fragments of adenovirus type 5 DNA, resulting in their transformation [133]. HEK 293T cells are exploited for a variety of biological questions due to their quick reproduction, easy maintenance and their extraordinarily high transfection efficiency [134].

HaCaT cells were established by Boukamp *et al.* by spontaneous immortalisation of primary human keratinocytes from the distant periphery of a melanoma on the back of a 62 year old male patient [135]. Although HaCaT cells harbour a *p53* mutation, they are able to undergo differentiation upon Ca^{2+} stimulation [136], as well as in three dimensional skin models and when transplanted onto nude mice [135]. Due to their versatility and uncomplicated cultivation conditions, HaCaT cells are widely used for the study of skin biology [137].

Primary murine keratinocytes were isolated as described above. For spontaneous immortalisation, they were passaged once before they underwent senescence and most of the cells died. After several months of cultivation, colonies of spontaneously immortalised keratinocytes regrew and could be cultivated infinitely [132].

2.2 Passaging of cells

To passage HEK cells, they were washed once with PBS, and trypsin-EDTA solution was added. In contrast, keratinocytes were washed for 10min with 1.3mM EDTA in PBS to reduce integrin binding to the surface before the cells were detached with trypsin. As soon as the cells were detached, trypsin was inhibited with DMEM + 10% (v/v) FBS and the cell suspension was transferred to a Falcon tube (Greiner). The cells were pelleted by centrifugation for 5min at 500g, the supernatant removed and the cells resuspended in the appropriate growth medium volume to dilute the cells for further cultivation or to seed them for experiments. HEK 293T and HaCaT cells were maintained in DMEM + 10% (v/v) FBS, whereas the murine keratinocytes were cultivated in keratinocyte growth medium. HEK cells were split up to 1:12, whereas HaCaT cells were split 1:8 at most, and murine keratinocytes not more than 1:4.

For seeding a certain number of cells for an experiment, the cells were counted using a Neubauer counting chamber (Hecht Assistent, Sondheim, Germany). For this purpose, 20µl of the cell suspension obtained after centrifugation were pre-diluted, if necessary, and mixed 1:1 with Trypan blue solution and a drop added to each side of the counting chamber. Then the cells in four squares of the chamber were counted and the cell concentration calculated according to the formula:

$$\frac{sum\ of\ counted\ cells}{counted\ squares\ \times chamber\ factor\ \times pre-dilution\ factor} cells/ml$$

$$= \frac{sum\ of\ counted\ cells}{4\ \times 10.000\ \times x} cells/ml$$

2.3 Cryopreservation of cells

To freeze cells, they were passaged as described before. However, instead of resuspending the cell pellet after centrifugation in the growth medium, cells were resuspended in 10% (v/v) dimethyl sulfoxide (DMSO) in FBS. Afterwards the cell suspension was aliquoted in 1.8ml cryotubes (Nunc, ThermoFisher Scientific) and frozen at -80°C using a CoolCell cooling chamber (Corning, New York, USA). In general, the cells harvested from a T75 flask were resuspended in 1.5ml and 500µl aliquots were made. After several hours of slow freezing, the aliquots were transferred to liquid nitrogen for long-term storage.

For thawing, the cells in a vial were thawed and immediately resuspended in 10ml DMEM + 10% (v/v) FBS. After centrifugation for 5min at 500g, the cell pellet was resuspended in fresh DMEM + 10% (v/v) FBS and the cells were plated. After 24h of cultivation, medium was exchanged again to remove all traces of DMSO from the culture.

2.4 Generation of lentivirus particles and lentiviral transduction

For lentivirus production, HEK 293T cells were seeded on p15 plates (Greiner) and, when they reached a confluency of ca. 60%, transfected using Lipofectamine 2000. For this purpose, 18µg of each lentiviral packaging plasmid psPAX2 (Addgene number 12260) and pCMV-VSV-G (Addgene number 8454) were mixed with 36µg of the plasmid harbouring the gene for OptoR2 or the empty plasmid for vector control cells. The plasmids were diluted in 9ml Opti-MEM reduced serum medium and added dropwise to a solution containing 80µl Lipofectamine 2000 diluted in 9ml OptiMEM medium. The transfection mix was incubated for 25min at RT in the dark. Meanwhile, the HEK 293T cells were washed once with PBS and 7ml OptiMEM medium were added to the plate. The transfection mix was added dropwise and the cells were cultivated overnight. After ca. 16h, the medium was changed to DMEM + 10% (v/v) FBS and the cells were cultivated for further 48h before the virus-containing medium was harvested.

Therefore, the medium was collected from the transfected cells and centrifuged for 5min at 500g to remove cell debris. Afterwards, the virus-containing medium was filtered through a 0.45µm filter with a polyethersulfone (PES) membrane (Sarstedt, Nümbrecht, Germany) and snap-frozen in 1ml aliquots in liquid nitrogen before the samples were stored at -80°C.

Afterwards, HEK cells and keratinocytes were lentivirally transduced by cultivating the cells for 48h with lentivirus-containing medium diluted ca. 1:10 in the respective growth medium. Then, the lentivirus-containing medium was removed and the cells were exposed to puromycin or G418 at concentrations, which were toxic for cells not harbouring a resistance gene. The optimal concentration had been determined by serial dilution beforehand. For selection of HEK cells and immortalised murine keratinocytes, which harbour a plasmid allowing constitutive expression of OptoR2 combined with a puromycin resistance cassette, 1.5µg/ml puromycin was used. HaCaT cells containing a doxycycline (Dox)-inducible transgene and a G418 resistance gene were selected with 1mg/ml G418. In addition to the OptoR2 harbouring cells and the respective vector control cells, also a control without lentivirus transduction was put under

selection pressure. After few weeks, colonies of positive clones formed and were further cultivated.

2.5 Starvation and illumination experiment

To deprive the cells from growth factors, HEK and HaCaT cells were starved by washing the cells twice with PBS and then changing the medium to DMEM without FBS. For the HaCaT cells harbouring the Dox-inducible construct, 50ng/ml Dox or the same amount of DMSO were added to the starvation medium. Murine primary and immortalised keratinocytes were washed twice with PBS as well, and then their medium was changed to keratinocyte starvation medium. The cells were cultivated under starvation conditions for 16h (HEK 293T cells) or 24h (keratinocytes), respectively.

Afterwards, the cells were treated with 10ng/ml growth factors (FGF7, FGF10, FGF1, EGF) or with blue light for different time periods, depending on the assay. For short-term continuous illumination (up to 3h), cell plates were put underneath a layer of LEDs (Catalogue number 5119661 from Light & More, Forchtenberg, Germany), which had been mounted on top of the shelf in the incubator. For long-term illumination, a light chamber for three 6-well plates (Greiner) with one LED for each well was custom-built. In this light-chamber, each 6-well plate could be illuminated separately and the illumination times were controlled using an Arduino UNO board (Arduino, Somerville, USA). For most experiments, one plate was illuminated using 1min on / 15min off cycles, one plate was illuminated using 1min on / 60min off cycles and one plate was continuously illuminated. The code for the control of the Arduino board can be found in the Appendix. The respective dark control cells were put onto another shelf of the same incubator, covered with black boxes to shade them from the blue light. Light intensities were measured with a Powermeter (LP1 from Sanwa, Tokyo, Japan) and were around 27µW/cm^2 and 0.2µW/cm^2 in the light and in the dark, respectively.

2.6 MTT assay

As readout for the cell number, for example during survival assays after prolonged cultivation under starvation and other stress conditions, a MTT assay was performed. Thereby, the yellow coloured thiazolyl blue tetrazolium bromide (MTT) is reduced to purple formazan by

metabolically active cells. MTT was dissolved to a concentration of 5mg/ml in PBS and added to the culture medium at 17% (v/v) (e.g. 150µl MTT solution to 750µl medium for a 12-well). Afterwards, the cells were incubated for 30min with the MTT solution, before the supernatant was removed and the cells were lysed in MTT lysis buffer containing 0.33% (v/v) hydrochloric acid (HCl) in isopropanol (e.g. 225µl MTT lysis buffer for a 12-well). The plates were incubated for 10min at RT while shaking, before the lysis solution was diluted 1:1 with ddH_2O. Then the diluted lysis solution was transferred to a 96-well plate (Greiner) and its absorption at 590nm was measured using a GloMax Discover Spectrometer (Promega, Madison, USA).

2.7 Scratch assay

To quantify cellular migration, scratch assays were performed in 6-well plates (Greiner). Therefore, three horizontal lines were drawn on the bottom of each well of a 6-well plate, which was pre-coated with collagen IV in PBS (2.5µg/cm^2) to facilitate migration. Afterwards, the cells were seeded and cultivated until they reached full confluency and were densely packed. After starvation, 2µg/ml mitomycin C were diluted in starvation media and the cells were cultivated with the mitomycin C-containing medium for 2h to irreversibly block proliferation and exclude its influence on scratch closure. Afterwards, a vertical scratch was induced in the cell culture plate with a 200µl pipet tip, forming a right angle with the drawn lines. To achieve a homogeneous scratch, pressure and scratching speed is decisive. Afterwards the wells were shaken, washed once with PBS and shaken again to remove detached cell sheets and single cells from the scratch. Then, starvation or treatment media were added, before the 0h pictures were taken above and below the intersection of the scratch with the drawn lines. This way, the corresponding pictures were taken exactly at the same location throughout the different time points. Then, the scratch-wounded cells were cultivated for up to 8 days with medium changes every two to three days, and pictures were taken every 24h. They were analysed by measuring the open scratch area at every time point using ImageJ, either manually or with the MRI wound healing tool (https://github.com/MontpellierRessourcesImagerie/imagej_macros_and_scripts/wiki/Wound-Healing-Tool, accessed 25th May 2020).

2.8 Chelation of FBS

For the murine keratinocyte culture, FBS was chelated to remove Ca^{2+} ions and thereby prevent the keratinocytes from differentiating prematurely. For this purpose, 200g Chelex 100 chelating resin were resuspended in 2l PBS and the pH of the solution was adjusted with HCl to 7.4. Afterwards, the Chelex was filtered through a folded filter paper, washed with 1l ddH_2O and immediately added to 500ml of freshly thawed FBS. The FBS was stirred slowly for 1h at RT or, for convenience, overnight at 4°C. Then the PBS was sterile filtered (Stericup Quick Release system from Merck, Darmstadt, Germany) and 40ml aliquots were frozen.

To regenerate the Chelex, it was transferred from the filter into a glass bottle, incubated with 800ml 1M HCl for 30min at RT while stirring slowly and again filtered through a folded filter paper. Then it was resuspended in 800ml 1M sodium hydroxide (NaOH) for 30min at RT while stirring slowly, before it was filtered again through a folded filter paper. It was resuspended in 400ml ddH_2O, autoclaved and stored at 4°C.

3. Cell stains

3.1 Crystal violet cell stain

As a preliminary readout for cell number, and therefore cellular proliferation and survival, a crystal violet cell stain following the clonogenic assay protocol was performed [138]. Therefore, the cells were washed once with PBS and fixed and stained by incubation with 6% (v/v) glutaraldehyde and 0.5% (w/v) crystal violet in ddH_2O for 30min at RT. Then, the wells were rinsed with tap water and dried at RT until they could be scanned.

3.2 Immunofluorescence staining of cells

For the general immunofluorescence staining protocol with different antibodies, the cells were seeded on sterile cover slips in 12-well plates (Greiner) and cultivated until they reached the desired confluency (e.g. for Ki67 ca. 50%, for OptoR2 and other markers ca. 70%). Then they were washed once with PBS and fixed with 4% (w/v) PFA in PBS for 20min at RT. After washing again once with PBS, the plate could be stored at 4°C or the staining was continued.

The PBS was aspirated and the cells were incubated with 0.5% (v/v) Triton X-100 in PBS for 5min at RT to permeabilise the cell membranes. After washing twice for 2min with PBS, the cells were incubated with blocking solution for 1h at RT while shaking. Meanwhile, the primary antibody was diluted in blocking solution (standard dilution: 1:100), and the wells were afterwards incubated with the primary antibody solution for 1h at RT under continuous shaking. Secondary antibody control cells were incubated with the blocking solution without primary antibody. Cells were then washed thrice for 5min with PBS under continuous shaking, before the secondary antibody (standard dilution: 1:200) together with Hoechst 33342 (1:3.000) was diluted in 0.05% (v/v) Triton X-100 in PBS. The cells were incubated with this solution for 1h at RT while shaking in the dark. The secondary antibodies recognise the constant antibody part that is characteristic for the host species of the primary antibody and are coupled with a fluorophore, which is light-sensitive. After the incubation, the cells were washed thrice for 10min with PBS while shaking, post-fixed with 1% (w/v) PFA in PBS for 5min at RT, washed again with PBS and the coverslips mounted to microscope slides with ProLong Gold Antifade Mountant (ThermoFisher, Waltham, USA). The slides were stored at 4°C in the dark.

3.3 BrdU staining

To determine the fraction of cells in the culture that go through the S-phase of the cell cycle, the cells that had been seeded on cover slips were treated for ca. 4h with 100µM 5'-bromo-2'-deoxyuridine (BrdU) in PBS. The incubation time was adjusted depending on the conditions and the proliferation status of the cells. Then the cells were fixed with 4% (w/v) PFA in PBS for 20min at RT. After washing the cells once with PBS, their DNA was denatured by incubating them with 0.1% (v/v) Triton X-100 in 2M HCl solution for 30min at RT under continuous shaking. Then the pH in the cells was neutralised with 0.1M sodium borate pH 8.5 for 5min at RT and the cells were blocked with 1% (w/v) bovine serum albumin (BSA) in PBS for 30min at RT under continuous shaking. Afterwards the cells were incubated with the primary antibody diluted 1:500 in the blocking solution overnight at 4°C while shaking in the dark.

The day after, the cells were washed thrice 5min with PBS, before the secondary antibody (standard dilution: 1:200) together with Hoechst 33342 (1:3.000) was diluted in 0.05% (v/v) Triton X-100 in PBS. The cells were incubated with this solution for 1h at RT under continuous shaking in the dark. The primary antibody for BrdU is already coupled to a fluorophore. Nevertheless, a secondary antibody was used to amplify the signal. After the incubation, the cells were washed thrice for 10min with PBS, post-fixed with 1% (w/v) PFA in PBS for 5min at RT, washed again with PBS, and the coverslips were mounted on microscope slides using ProLong Gold Antifade Mountant (ThermoFisher). The slides were stored at 4°C in the dark.

3.4 Staining for flow cytometry

Cells were stained for flow cytometry to quantify the number of cells that were positive for any given marker. For this purpose, the cells were detached from the plate with trypsin as described for passaging, but after centrifugation, the cell pellet was resuspended in PBS to wash the cells. Then the cells were pelleted again by centrifugation for 5min at 500g and the cell pellet was resuspended in 100µl 2% (w/v) PFA in PBS for fixation. The fixed cell suspension was transferred to a well of a 96-well plate (Greiner) and incubated for 20min at RT. Then, the plate was centrifuged for 5min at 300g and 4°C (identical to the following centrifugation steps during

the procedure). Afterwards, the supernatant was decanted and 200µl PBS were added. For convenience, the plate could be stored at 4°C or the staining procedure was continued.

The cells were pelleted by centrifugation, the supernatant was decanted and the cells were resuspended in 200µl staining buffer containing 0.1% (w/v) saponin in PBS. Then the plate was incubated for 5min at RT, before the cells were pelleted again by centrifugation. The primary antibody was diluted in staining buffer (standard dilution 1:1.000), added to the respective wells after decanting the supernatant and incubated for 1h at 4°C. Secondary antibody control cells were left with the staining solution without primary antibody. Afterwards, the cells were washed thrice by pelleting them by centrifugation, decanting the supernatant and resuspending the pellet in 200µl staining buffer. Then, the secondary antibody was diluted in staining buffer (standard dilution 1:400). The cell pellet supernatant was decanted and the cells were incubated with the secondary antibody solution for 1h at 4°C in the dark. Afterwards, three washing steps with 200µl staining buffer each were performed as described previously. Then, the cells were resuspended in 100µl PBS and stored at 4°C until they were analysed in a flow cytometer (BD LSR Fortessa from BD Biosciences, Franklin Lakes, USA).

3.5 Cell cycle analysis by flow cytometry

To analyse the distribution of the cells in the different phases of the cell cycle, they were stained with propidium iodide (PI) and then analysed by flow cytometry. For this purpose, the cells were detached by trypsinisation as described for passaging, but after centrifugation, the cell pellet was resuspended in ice-cold PBS. The cells were centrifuged for 5min at 500g and 4°C and the cell pellet was carefully resuspended in ice-cold 70% (v/v) ethanol by adding it dropwise while vortexing gently to ensure equal fixation of all cells and minimise cell clumping. Then, the cells were incubated at -20°C overnight or, for convenience, at least for 3h.

Afterwards, the cells were centrifuged for 10min at 400g and 4°C and resuspended in ice-cold PBS for washing. Then, they were centrifuged again for 10min at 400g and 4°C, before the supernatant was removed and the pellet was resuspended in staining solution. The cells were stained for 1h at RT in the dark and stored for up to 48h at 4°C until they were analysed with the flow cytometer (BD LSR Fortessa from BD Biosciences).

3.6 Microscopy

Photomicrographs of the fluorescently labelled cells were taken using an Axiovert microscope (Carl Zeiss, Oberkochen, Germany) equipped with a Axiocam 506 mono camera (Carl Zeiss) at 10x, 20x and 63x magnification. Additionally, photomicrographs of some cells were taken with a confocal microscope (Leica SP8 from Leica, Wetzlar, Germany) at 63x magnification.

4. Histological stains

4.1 Tissue processing for paraffin sections

Skin samples that had been fixed with 4% (w/v) PFA in PBS overnight at 4°C were embedded in paraffin using the spin tissue processor (Microm STP120 from ThermoFisher Scientific, Waltham, USA) with the following program.

Solution	Time	Temperature
0.9% (w/v) NaCl	30min	RT
30% (v/v) ethanol / 0.9% (w/v) NaCl	30min	RT
50% (v/v) ethanol / 0.9% (w/v) NaCl	30min	RT
70% (v/v) ethanol / 0.9% (w/v) NaCl	30min	RT
90% (v/v) ethanol / 0.9% (w/v) NaCl	30min	RT
96% (v/v) ethanol / 0.9% (w/v) NaCl	30min	RT
Ethanol	60min	RT
Ethanol	30min	RT
Xylene	30min	RT
Xylene	30min	RT
Paraffin	2.5h	60°C
Paraffin	5h	60°C
Store in paraffin at 60°C		

After embedding the samples in paraffin, they were cut at 7µm with a microtome (Microm HM 355S, ThermoFisher Scientific), attached to microscopy slides and stored at 4°C. Prior to staining, the samples were dewaxed and rehydrated manually following these steps:

Solution	Time
Xylene	10min
Xylene	10min
Ethanol	1min
96% (v/v) ethanol / ddH_2O	1min
80% (v/v) ethanol / ddH_2O	1min
70% (v/v) ethanol / ddH_2O	1min
50% (v/v) ethanol / ddH_2O	1min
ddH_2O	3min

4.2 H&E stain

The Hematoxylin and Eosin (H&E) stain is the most widely used staining method in histology and pathology because it allows a general overview of the tissue architecture [139]. Hematoxylin stains acidic components of the cell, such as the nucleus, in blue, whereas eosin stains basic components like the protein-rich cytoplasm and ECM components in red.

For this stain, PFA-fixed and paraffin-embedded tissue samples were rehydrated and stained manually following these steps:

Cycles	Solution	Time
1x	Mayer's Hematoxylin solution	3min
3x	ddH_2O	10sec
1x	Scott water	30sec
1x	ddH_2O	10sec
1x	70% (v/v) ethanol / ddH_2O	10sec
1x	Eosin solution	1min
2x	80% (v/v) ethanol / ddH_2O	10sec
2x	95% (v/v) ethanol / ddH_2O	10sec
2x	ethanol	10sec
2x	Xylene	10min
Mount with Eukitt and air-dry the slides		

4.3 Herovici's stain

Herovici's staining procedure is very useful for excisional wound healing studies focusing on the ECM deposition. It stains thick mature collagen fibrils in purple, whereas filamentous newly deposited collagen is stained in light blue and the cytoplasm areas appear in yellow [140].

For this stain, PFA-fixed and paraffin-embedded tissue samples were rehydrated and stained following these steps:

Cycles	Solution	Time
1x	Solution A	5min
1x	Running tap water (rinse)	2min
1x	Solution B	5min
1x	Running tap water (rinse)	2min

1x	Solution C	2min
1x	Solution D	2min
1x	Running tap water (rinse)	2min
1x	Solution E	2min
1x	Solution F	2min
1x	Solution G	2min
2x	Ethanol	1min
2x	Xylene	2min
Mount with Eukitt and air-dry the slides		

4.4 Masson-Goldner Trichrome stain

The Masson Trichrome stain is a three-coloured staining method as well, which stains cytoplasm and keratins in red, collagen and ECM components in blue and cell nuclei in black [141].

For this stain, PFA-fixed and paraffin-embedded tissue samples were rehydrated and stained following these steps:

Cycles	**Solution**	**Time**	**Temperature**
1x	Bouin's solution	1h	60°C
1x	ddH_2O	10sec	60°C
2x	ddH_2O	10sec	RT
1x	Weigert's Hematoxylin	10min	RT
2x	Tap water	10sec	RT
1x	ddH_2O	10sec	RT
1x	BSAF solution	10min	RT
2x	ddH_2O	10sec	RT
1x	PMPT solution	5min	RT
1x	Aniline blue solution	5min	RT
2x	ddH_2O	10sec	RT
1x	Acetic acid	2min	RT
3x	Tap water	10sec	RT
2x	96% (v/v) ethanol / ddH_2O	10sec	RT
2x	Ethanol	10sec	RT
2x	Xylene	10min	RT
Mount with Eukitt and air-dry the slides			

4.5 Immunohistochemistry staining of tissue sections

To immunohistochemically label proteins such as Ki67 or immune cell markers in tissues, PFA-fixed and paraffin-embedded tissue sections were rehydrated and treated with 0.33% (v/v) hydrogen peroxide (H_2O_2) in methanol for 40min. After washing the slides twice for 10min with PBS, the slides were boiled in 10mM sodium citrate pH 6 for 1h at 95°C. Afterwards the slides were washed again twice for 5min with PBS and the sections were encircled using Super^{HT} PAP pen mini (Biotium, Hayward, USA). The sections were blocked for 1h at RT with 12% (w/v) BSA in PBS. Afterwards, they were incubated with the primary antibody diluted in the blocking solution overnight at 4°C in a humid chamber (standard dilution 1:100).

After washing the slides thrice for 10min with PBS, the sections were incubated with the secondary antibody diluted in PBS for 45min at RT (standard dilution: 1.200). Then, the slides were washed again thrice for 5min with PBS, before incubation in the VECTASTAIN® Elite® ABC Kit (Maravai Life Sciences, San Diego, USA) Peroxidase solution, which had been prepared according to the manufacturer's instructions, for 20min at RT. Afterwards the slides were again washed thrice for 5min with PBS. Then, the DAB Kit (Maravai Life Sciences) solution, which had been prepared following the manufacturer's instructions, was added to the sections and left until the brown staining appeared. The reaction was stopped immediately by submersing the slides in tap water. Afterwards, the sections were counterstained with hematoxylin as described for the H&E staining procedure. For this purpose, the slides were stained for 3min with hematoxylin, washed thrice for 10sec with ddH_2O and stained with Scott water for 30sec. Afterwards the slides were washed in ddH_2O, mounted with Mowiol and air-dried.

4.6 Immunofluorescence staining of tissue sections

To fluorescently label proteins such as OptoR2 or keratins in tissue samples, PFA-fixed and paraffin-embedded tissue sections were rehydrated and treated as explained for immunohistochemistry with 0.33% (v/v) H_2O_2 in methanol for 40min. After washing the slides twice for 10min with PBS, they were boiled in 10mM sodium citrate pH 6 for 1h at 95°C. Afterwards the slides were washed again twice for 5min with PBS and the sections were encircled using Super^{HT} PAP pen mini (Biotium). The sections were blocked for 1h at RT with

12% (w/v) BSA in PBS. Afterwards, they were incubated with the primary antibody diluted in the blocking solution overnight at 4°C in a humid chamber (standard dilution 1:100).

After washing the slides thrice for 10min with PBS, the sections were incubated with the secondary antibody diluted in PBS for 1h at RT (standard dilution 1:200). The secondary antibodies recognise the constant antibody part that is characteristic for the host species of the primary antibody and are coupled with a fluorophore, which is light-sensitive. After the incubation, the plates were washed thrice for 10min with PBS under continuous shaking, post-fixed with 1% (w/v) PFA in PBS for 5min at RT, washed again with PBS, and the sections were mounted with ProLong Gold Antifade Mountant (ThermoFisher Scientific). The slides were stored at 4°C in the dark.

4.7 Microscopy

Photomicrographs of the histologically stained tissue sections were taken using the light microscope (Axioskop 2 from Carl Zeiss) equipped with a Axiocam 512 color camera (Carl Zeiss) at 2.5x, 10x and 20x magnification. Photomicrographs of the fluorescently labelled sections were taken using the Axiovert microscope (Carl Zeiss) equipped with a Axiocam 506 mono camera (Carl Zeiss) at 10x, 20x and 63x magnification.

5. DNA methods

5.1 KAPA PCR for genotyping

The KAPA PCR using the KAPA2G genotyping mix was used for genotyping PCRs as well as for cloning procedures as described below.

For the genotyping PCR, 0.5µl of tissue lysate was used as DNA source and added to 8µl of KAPA2G genotyping mix, 6µl ddH_2O, and 1µl primer mix (10µM, forward and reverse). The reaction mix was covered with a drop of mineral oil. The PCR reaction was performed in a Peqstar Thermocycler (Axonlab, Baden, Switzerland) using the PCR programs specified below.

PCR program for Cre, FGFR1, FGFR2, OptoR2

Cycles	Time	Temperature
1x	5min	95°C
33x	35sec	95°C
	35sec	60°C
	50sec	72°C
1x	10min	72°C
Store at 8°C		

PCR program for FGFR3

Cycles	Time	Temperature
1x	3min	95°C
30x	30sec	94°C
	30sec	62°C
	30sec	72°C
1x	10min	72°C
Store at 8°C		

5.2 Agarose gel

To analyse the size of the amplified fragments in the PCR product or during the cloning procedure, 10µl of the genotyping PCR product, the complete cloning PCR product or ca. 1µg digested DNA was loaded on a 1-2% (w/v) agarose gel in SBA buffer supplemented with 1µg/ml ethidium bromide. Additionally, 6µl of GeneRuler DNA ladder was used as loading control. After running the gel for ca. 15min at 300V, the bands were visualized using a UV light chamber (BioRad, Hercules, USA).

5.3 Measurement of the concentration of nucleic acids by Nanodrop

DNA as well as RNA concentrations were extrapolated by measuring the sample's absorption at 260nm using a Nanodrop spectrophotometer (ND-1000 from ThermoFisher Scientific), assuming these approximations:

$$OD_{260} = 1 \approx 50\mu g \text{ DNA or } 40\mu g \text{ RNA /ml}$$

The ratio of absorption at 260nm and 280nm was used as indicator for the purity of the nucleic acid solution, with the optimum value of 1.8 for DNA and 2.0 for RNA.

5.4 Molecular cloning using restriction enzymes

To insert the OptoR2 under the control of the K14 promoter, the OptoR2 transgene was transferred from the original pcDNA-based plasmid, which we received from our collaborators, to a pHR2 plasmid with the K14 promoter already present (Sabine Werner, ETH Zürich).

For this purpose, the target plasmid was digested with Hind *III* and Sma *I* restriction enzymes using a 1:1 mixture of CutSmart and NEB buffer 2.1 for 1h at RT and then for 1h at 37°C following the manufacturer's directions. The OptoR2 transgene was amplified with a KAPA PCR using 0.2µl of the original plasmid (381_OptoR2 2µg/µl) as DNA source. The PCR reaction was performed in a Peqstar Thermocycler (Axonlab) using the PCR program specified below.

Cycles	Time	Temperature
1x	3min	95°C
20x	30sec	95°C
	30sec	56°C
	60sec	72°C
1x	10min	72°C
Store at 4°C		

Then, the PCR product was run on a 1.5% (w/v) agarose gel, excised and purified with the NucleoSpin Gel and PCR Clean up Kit (Macherey-Nagel), before it was digested with Hind *III* in NEB buffer 2.1 for 2h at 37°C according to the manufacturer's instructions. Afterwards, both the digested vector as well as the insert were run on a 1% (w/v) agarose gel and purified again.

The insert was phosphorylated using T4 polynucleotide kinase (PNK) and the vector was dephosphorylated with recombinant shrimp alkaline phosphatase (rSAP), both for 2h at 37°C as recommended by the manufacturer. The DNA fragments were then purified again with the NucleoSpin Gel and PCR Clean up Kit. Plasmid and insert were mixed in a ratio of 2:1 in the T4 ligation reaction supplemented with 25mM adenosine triphosphate (ATP) and incubated overnight at 16°C. After transformation and growth of the chemically competent XL1 blue *Escherichia (E.) coli* colonies in Luria-Bertani (LB) medium supplemented with the respective antibiotic, cultures were tested by colony PCR using the KAPA2G system with 1µl bacterial culture as DNA source. The PCR reaction was performed in a Peqstar Thermocycler (Axonlab) using the PCR program specified below.

Cycles	**Time**	**Temperature**
1x	10min	95°C
20x	30sec	95°C
	30sec	60°C
	15sec	72°C
1x	10min	72°C
Store at 4°C		

Afterwards, the PCR products were run on a 2% (w/v) agarose gel, positive clones were selected and their plasmids purified using the NucleoSpin Plasmid Kit (Macherey-Nagel) according to the manufacturer's instructions. Successful insertion of the mutation-free transgene was confirmed by sequencing the whole sequence of the transgene using OptoR2 sequencing primers (Microsynth, Balgach, Switzerland). Plasmids from positive clones were purified from a 250ml bacterial culture using the Plasmid Plus Maxi Kit (Qiagen, Venlo, The Netherlands) following the manufacturer's instructions. 500µl of the bacterial culture were mixed with 500µl 50% (v/v) glycerol in ddH_2O and kept at -80°C.

For pronuclear injection of the transgene and its promoter, 50 µg of the product plasmid was linearised using Pci *I* and Pvu *I*-HF in NEB buffer 3.1 for 6h at 37°C, before running the digested vector on a 1% (w/v) agarose gel. The corresponding band was cut out and purified using the NucleoSpin Gel and PCR Clean up Kit. The product was eluted using the microinjection buffer supplied by Thomas Hennek from the animal facility EPIC.

5.5 Molecular cloning using Topoisomerase Ligation and Gateway strategy

To clone the OptoR2 transgene into the plasmid that allows Dox-inducible expression of transgenes, it was first amplified in a PCR reaction using the Phusion High-Fidelity DNA polymerase Kit with primers with a 4 basepair (bp) overhang (CACC). For this purpose, 5µl 4xHF buffer, 0.5µl 10mM deoxynucleoside triphosphates (dNTPs), 2.5µl primer mix (10µM, forward and reverse), 0.75µl DMSO and 0.5µl Phusion Polymerase were mixed with 1µg DNA of the original plasmid and the reaction filled up with ddH_2O to 20µl. The PCR reaction was performed in a Peqstar Thermocycler (Axonlab) using the PCR program specified below.

Cycles	Time	Temperature
1x	30sec	98°C
30x	10sec	98°C
	30sec	60°C
	75sec	72°C
1x	10min	72°C
Store at 4°C		

After adding 6x DNA loading dye, the complete PCR product was run on a 1% (w/v) agarose gel. The corresponding band (1980bp) was excised, purified with the NucleoSpin Gel and PCR Clean up Kit (Macherey-Nagel), and the DNA concentration was measured with the Nanodrop spectrophotometer (ThermoFisher Scientific).

Then, the topoisomerase-gated ligation was performed using the pENTR™/D-TOPO™ Cloning Kit (ThermoFisher Scientific) with 5-10ng DNA as input according to the manufacturer's instructions, except for incubation time. We chose overnight instead of 5min incubation at RT because we experienced higher success rates under these conditions.

Afterwards the ligation product was transformed into OneShot chemically competent *E. coli*, which were also supplied with the pENTR™/D-TOPO™ Cloning Kit, again following the manufacturer's instructions. After growing the bacteria in LB medium with the respective antibiotics and performing a colony PCR as described before, the PCR product was run on a 2% (w/v) agarose gel. Positive clones were selected and their plasmids were purified using the NucleoSpin Plasmid Kit according to the manufacturer's instructions. Successful insertion was confirmed by sequencing using the standard M13 forward and reverse primers (Microsynth).

Plasmids from positive clones were purified from a 250ml bacterial culture using the Plasmid Plus Maxi Kit (Qiagen) following the manufacturer's directions and 500µl of the bacterial culture were mixed with 500µl 50% (v/v) glycerol in ddH_2O and kept at -80°C.

Afterwards, the transgene was transferred from the pENTR plasmid to the pInducer20 plasmid (Addgene number 44012) using the Gateway cloning strategy provided with the Gateway™ LR Clonase™ II Enzyme mix (ThermoFisher Scientific) according to the manufacturer's instructions. After transformation of OneShot *E. coli* with the product, transgene insertion was again confirmed with a colony PCR before purifying the plasmid using the Plasmid Plus Maxi Kit and utilising the product to generate lentiviral particles for transduction.

5.6 Isolation of genomic DNA (HotShot)

For measuring the replication of Herpes simplex virus 1 (HSV-1), a HotShot lysis protocol, which had been described previously [142], was modified and applied [143]. For this purpose, cells on a 6-well plate (Greiner) or tail explants were lysed in 200µl alkaline lysis buffer, scraped off and transferred to a tube (Eppendorf, Hamburg, Germany). After incubating them for 30min at 95°C, 200µl neutralisation buffer were added and the samples were centrifuged for 10min at 17.000g. Then the supernatant was transferred to a new tube and the DNA concentration was measured using a Nanodrop spectrophotometer (ThermoFisher Scientific).

5.7 Analysis of viral DNA by qPCR

To analyse the viral DNA content, a quantitative PCR (qPCR) for the viral gene encoding glycoprotein B was performed, using human β-actin as loading control. For this purpose, 200ng genomic DNA were mixed with 3µl ddH_2O, 5.5µl LightCycler SYBR Green and 0.5µl primer mix (10µM, forward and reverse). The PCR reaction was performed in a qPCR thermocycler (LightCycler 480 II; Roche, Basel, Switzerland) using the PCR program specified below.

Cycles	Time	Temperature
1x	10min	95°C
45x	10sec	95°C
	30sec	58°C

	20sec	72°C
1x	5sec	95°C
1x	1min	65°C
1x	Slow heat	95°C
Store at 40°C		

6. RNA methods

In general, experiments with RNA were conducted using sterile plastic or autoclaved glass vessels. Additionally, all solutions were prepared using ddH_2O, which was pre-treated with 0.1% (v/v) diethyl pyrocarbonate (DEPC) to block RNases. For this purpose, the DEPC-treated water was stirred overnight at RT, and then autoclaved to remove the DEPC. Additionally, bench and pipettes were wiped with RNaseZAP™ before working with RNA to remove RNases.

6.1 Isolation of RNA from tissue

To isolate RNA from tissue samples, such as wounds, skin samples or tail explants, self-made Trizol reagent was used. For each sample, a round-bottom tube (Greiner) containing 1ml Trizol reagent was prepared and stored on ice. The samples that had been stored at -80°C were transferred first into liquid nitrogen for storage during the procedure and then one by one transferred into the tube with Trizol reagent and immediately homogenised using an Ultra-Turrax T25 homogenizer (Janke & Kunkel, IKA Labortechnik, Staufen im Breisgau, Germany). The samples were not allowed to thaw before homogenisation to avoid the activation of RNases, and were stored on ice afterwards until all samples had been homogenised.

Then, all samples were transferred to tubes (Eppendorf) and placed for 5min at RT before 200µl chloroform were added. The samples were mixed thoroughly by vortexing (Vortex Genie 2, Scientific Industries, Bohemia, USA) and incubated for another 10min at RT. Then they were centrifuged for 15min at 17.000g and 4°C to allow the separation of the different phases, and the upper phase (ca. 500µl) containing the RNA was carefully transferred to a new tube. This step was repeated: 200µl chloroform were added and the samples were vortexed thoroughly and incubated for 10min at RT. Afterwards they were centrifuged again for 15min at 17.000g and 4°C and the upper phase was carefully transferred to a new tube. 200µl isopropanol were added to the supernatant, and the liquid was mixed by pipetting up and down and incubated for 10min at RT. For convenience, this step could be also performed overnight at -20°C.

Afterwards, the samples were centrifuged for 8min at 15.000g and 4°C to form an RNA pellet. The supernatant was removed and the pellet was washed twice with 1ml 70% (v/v) ethanol in DEPC water. After pipetting up and down, the samples were centrifuged for 5min at 5.400g and

4°C and the supernatant was removed. In the last step, all supernatant was carefully removed and the RNA was dried carefully at 60°C until the RNA edges became transparent. Then the RNA was dissolved in 25µl nuclease-free ddH_2O for 5min at 60°C before it was put on ice. RNA concentrations were measured with the Nanodrop spectrophotometer (ThermoFisher Scientific) and RNA samples were stored at -80°C.

6.2 Isolation of RNA from cells

For isolation of RNA from cells, they were washed with PBS. Lysis and RNA isolation were performed using the Mini Total RNA Kit (IBI Scientific, Dubuque, USA) according to the manufacturer's instructions. The samples were eluted with 20µl nuclease-free ddH_2O and then put on ice. RNA concentrations were measured using the Nanodrop spectrophotometer (ThermoFisher Scientific) and the samples were stored at -80°C.

6.3 Reverse transcription

RNA was reverse transcribed using the iScript system (BioRad). For this purpose, 1µg RNA was mixed with 4µl RT buffer and 1µl reverse transcriptase and filled up to 20µl with nuclease-free ddH_2O. Afterwards the reverse transcription reaction was performed in a Peqstar thermocycler (Axonlab) using the following program:

Time	**Temperature**
5min	25°C
70min	42°C
15min	70°C
Store at 4°C	

Then the newly generated complementary DNA (cDNA) was diluted 1:10 in nuclease-free ddH_2O and stored at -20°C.

6.4 Analysis of the RNA content by qPCR

To analyse the relative RNA content, qPCR for different target genes was performed and compared to the signal of housekeeping genes (mouse: *Rps29*, human: *RPL27*). For this purpose, 5.5µl LightCycler SYBR Green were mixed with 0.5µl primer mix (10µM, forward and reverse) and 5µl of the reverse transcriptase product. Each reaction was set up in duplicates and the qPCR was performed in a qPCR Thermocycler (LightCycler 480 II; Roche) using the PCR program specified below:

Cycles	Time	Temperature
1x	10min	95°C
50x	10sec	95°C
	20sec	60°C
	20sec	72°C
1x	5sec	95°C
1x	1min	65°C
1x	Slow heat	95°C
Store at 40°C		

7. Protein methods

7.1 Preparation of protein lysates from tissue

For the preparation of protein lysates from tissue samples, such as wounds, skin samples or tail explants, ca. 2.5ml T-Per lysis buffer were used for 400mg of tissue. For each sample, a round-bottom tube (Greiner) containing T-Per lysis buffer was prepared and stored on ice. The samples, which had been stored at -80°C, were transferred first into liquid nitrogen for storage during the procedure and then one by one transferred into the tube with T-Per lysis buffer and immediately homogenised using the Ultra-Turrax T25 homogenizer (IKA Labortechnik). The samples were not allowed to thaw before and were stored on ice afterwards until all samples were been homogenised. Then the samples were subjected to sonication using 25 bursts of 500ms at amplitude 50 with an U200S control sonicator (IKA Labortechnik) on ice in a 4°C room. Afterwards, the samples were centrifuged for 1h at 3.200g and 4°C and the supernatant was carefully transferred to new tubes (Eppendorf). The samples were centrifuged for 5min at 8.000g and 4°C before the supernatant was again transferred to a new tube. The samples were stored on ice or at -20°C until their protein concentration was measured using a bicinchoninic acid (BCA) assay. They were mixed 1:1 with 2x sample buffer containing 20mM dithiothreitol (DTT) for subsequent Western blot analysis.

7.2 Preparation of protein lysates from cultured cells

For preparation of protein lysates from cultured cells, 2x sample buffer was diluted to 1x and heated to 95°C. After washing the cells with PBS, the hot 1x sample buffer was added to the plate (e.g. 200µl sample buffer for each well of a 6-well plate) and the cells were detached by scraping them off the surface while the plate was placed on the heat block as well. Afterwards the cell lysate was transferred to tubes (Eppendorf) which had also been pre-heated to 95°C and the samples were boiled for 10 more minutes at 95°C. Then the samples were centrifuged for 1min at 17.000g and stored at -20°C.

7.3 Nuclear-cytoplasmic fractionation of cells

To separate cell nuclei from the cytoplasm, cells were washed twice with ice-cold PBS. Afterwards they were lysed in ice-cold NP-40 lysis buffer (e.g. 350µl lysis buffer for each well of a 6-well plate) and detached by scraping them off the surface. This and all following steps were performed on ice. Afterwards the lysate was transferred to a tube (Eppendorf) and 50µl lysate were stored in a second tube as sample of the total lysate. Then the samples were centrifuged for 3min at 17.000g and 4°C and 50µl of supernatant was stored in a third tube as sample of the cytoplasmic fraction. The rest of the supernatant was removed and the nuclear pellet washed two to four times by adding 800µl NP-40 lysis buffer, vortexing, centrifuging for 3min at 17.000g and 4°C and removing the supernatant again, until the pellet seemed transparent. 2x sample buffer was diluted to 1x, and 10mM DTT with a pipet tip of bromophenol blue were added to the 1x sample buffer as well as to undiluted 2x sample buffer, to which 20mM DTT with bromophenol blue were added. Then the nuclear pellet was resuspended in 70µl 1x sample buffer with 10mM DTT, while 50µl 2x sample buffer with 20mM DTT were added to the total and cytoplasmic fractions. After boiling the samples for 10min at 95°C, they were stored at -20°C. After this procedure, the protein concentration was not measured by BCA, but was assumed to be ca. 1µg/µl.

7.4 Immunoprecipitation

To identify binding partners of the OptoR2, immunoprecipitation (IP) was performed using an antibody recognizing its HA tag. For this purpose, the cells were washed once with PBS and then scraped off in ice-cold PBS (e.g. 500µl for a p10 plate). The cells were transferred to a tube (Eppendorf) and the residual cells were removed from the plate by rinsing it again with 500µl ice-cold PBS. The combined cells were pelleted by centrifugation for 5min at 500g and 4°C, lysed in 500µl ice-cold IP buffer by incubating them for 10min on ice and afterwards the lysate was cleared by centrifugation for 10min at 16.000g and 4°C. In the meantime, 25µl anti-HA magnetic bead suspension (ThermoFisher Scientific) per sample was prepared by washing the beads three times with 500µl IP buffer. For this purpose, the IP buffer was added and the beads were resuspended by pipetting up and down using a pipet tip, from which the narrow end of the tip had been cut off. Afterwards the tube was put on a magnetic rack and the supernatant was aspirated. After the lysate had been cleared by centrifugation, 50µl of the sample was stored

as input lysate sample and the magnetic beads, which had been resuspended in a small volume of IP buffer, were added to the lysate. The IP was performed for 1h at RT while rotating. Afterwards, 50µl of the supernatant were removed and stored as unbound supernatant sample. The beads were washed thrice with 500µl TBS with 0.05% (v/v) Tween 20 and once with 500µl ddH_2O. After removing all supernatant, 100µl 1x sample buffer with 10mM DTT were added to the beads and 50µl 2x sample buffer with 20mM DTT were added to the input and supernatant samples taken during the procedure. All samples were boiled for 10min at 95°C and centrifuged for 1min at 17.000g before the supernatant of the bead eluate was transferred to new tubes. The samples were stored at -20°C. After this procedure, the protein concentration was not measured by BCA, but was assumed to be ca. 1µg/µl.

7.5 Measurement of the protein concentration using BCA assay

The protein concentration was determined using the BCA assay kit (ThermoFisher Scientific) following the manufacturer's instructions. Samples were pre-diluted 1:20 in ddH_2O, the assay was performed, and the absorption of the samples was measured at 562nm using a GloMax Microplate Reader (Promega). Afterwards the samples were diluted to 1µg/µl using 1x sample buffer and with 10mM DTT (end concentration) with bromophenol blue.

7.6 Western blot

First, 1.5mm polyacrylamide gels with 15 wells were prepared, each consisting of a separation gel, which was overlaid by a stacking gel using the Mini-PROTEAN® system (BioRad). After the gels had become solid, they were inserted into a Mini-PROTEAN® Tetra cell (BioRad) and submersed into SDS running buffer. The combs were removed and the gels were loaded with 5µl PageRuler Plus pre-stained protein ladder, and 20µg of the protein samples diluted in 1x sample buffer with 10mM DTT and bromophenol blue. Unused wells were loaded with 20µl 1x sample buffer. The gels were first run at 40V to concentrate the sample and after 15min, the voltage was increased to 80-120V for ca. 2h to separate the proteins, both at RT.

Afterwards, proteins were transferred from the gel to a Protran™ nitrocellulose membrane (GE Healthcare, Chicago, USA). For this purpose, the gel was removed from the running chamber and placed into a stack with a sponge, three 3mm Whatman papers (VWR, Radnor, USA), the

gel, the activated nitrocellulose membrane, three more Whatman papers and another sponge, while fully submersed in transfer buffer to avoid air bubbles. The stack was inserted into a Mini-PROTEAN® Tetra Electrophoresis System (BioRad), whereby the gel faced the cathode to allow transfer of the negatively charged proteins to the nitrocellulose membrane by attraction to the anode. The transfer was performed at 300mA per chamber for 2h at 4°C.

After the transfer, the stacks were disassembled and the membranes stained with Ponceau S by incubating them for 5min with the Ponceau S solution while shaking at RT. Excess colour was removed by washing the membranes with tap water and equal loading in all the lanes was confirmed. Afterwards the membranes were cut according to the molecular weight of the proteins of interest and incubated with the blocking solution for 1h at RT under continuous shaking. Membranes used for detection of total proteins were blocked with 5% (w/v) skim milk powder in Tris-buffered saline with Tween 20 (TBS-T), membranes used for detection of phosphorylated residues were blocked with 5% (w/v) BSA in TBS-T. Following blocking, primary antibodies against the protein of interest or phosphorylated residues of interest were diluted in 5% (w/v) BSA in TBS-T (standard dilution 1:1.000) and the membranes were incubated overnight with the primary antibody solutions at 4°C under continuous shaking.

Then, the membranes were washed thrice for 5min with TBS-T and the secondary antibodies, which recognise the constant antibody part characteristic for the host species of the primary antibody and are coupled with horseradish peroxidase (HRP), were diluted 1:5.000 in 5% (w/v) skim milk powder in TBS-T. The membranes were incubated for 1h at RT with the secondary antibody solution under continuous shaking. Afterwards, the membranes were again washed thrice for 10min with TBS-T before the signal was developed using WesternBright Sirius HRP substrate and the FUSION SOLO 6S chemiluminescence imaging system (Witec, Ulm, Germany).

7.7 ELISA for phospho-ERK1/2 and total ERK1/2

For the quantitative determination of the phospho-ERK1/2 signal in relation to the total ERK1/2 signal, the enzyme-linked immunosorbent assay (ELISA) Kit from Enzo Life Sciences was used according to the manufacturer's instructions. Briefly, the cells were lysed in radioimmunoprecipitation assay (RIPA) buffer provided by the kit. The lysates were added to the purchased wells with the antibody bound, and a sandwich-ELISA was performed.

Afterwards, the signal was developed using a colorimetric reaction and measured by determining the absorption at 450nm using a GloMax Microplate Reader (Promega).

8. Analysis and statistics

8.1 qPCR analysis

qPCR data were analysed using the double delta cycle threshold (CT) method. For this purpose, the cycle at which the DNA amplification reaches a certain threshold was determined for each sample. Then, the CT for the target gene was subtracted from the CT of the housekeeping gene for each condition (delta CT). Afterwards, delta CT for the experimental conditions were subtracted from the control condition (delta delta CT). Therefore, the values are presented in relation to the control condition [144].

8.2 Statistical analysis

Statistical analysis was performed using the Prism 8 software (GraphPad Software Inc., San Diego, USA). Quantitative data are presented as mean ± standard error mean (SEM). Unless stated otherwise, significance was calculated using Mann-Whitney-U test. * $p \leq 0.05$; ** $p \leq 0.01$; *** $p \leq 0.001$; **** $p \leq 0.0001$ [145].

References

131 **Thorey, I. S., Roth, J., Regenbogen, J., Halle, J.-P., Bittner, M., Vogl, T., Kaesler, S., Bugnon, P., Reitmaier, B. & Durka, S. (2001)** *The Ca2+-binding proteins S100A8 and S100A9 are encoded by novel injury-regulated genes*. Journal of Biological Chemistry 276, 35818-35825.

132 **Braun, S., Hanselmann, C., Gassmann, M. G., auf dem Keller, U., Born-Berclaz, C., Chan, K., Kan, Y. W. & Werner, S. (2002)** *Nrf2 transcription factor, a novel target of keratinocyte growth factor action which regulates gene expression and inflammation in the healing skin wound*. Molecular and Cellular Biology 22, 5492-5505.

133 **Graham, F. L., Smiley, J., Russell, W. C. & Nairn, R. (1977)** *Characteristics of a human cell line transformed by DNA from human adenovirus type 5*. Journal of General Virology 36, 59-72.

134 **Thomas, P. & Smart, T. G. (2005)** *HEK293 cell line: A vehicle for the expression of recombinant proteins*. Journal of Pharmacological and Toxicological Methods 51, 187-200.

135 **Boukamp, P., Petrussevska, R. T., Breitkreutz, D., Hornung, J., Markham, A. & Fusenig, N. E. (1988)** *Normal keratinization in a spontaneously immortalized aneuploid human keratinocyte cell line*. The Journal of Cell Biology 106, 761-771.

136 **Seo, E.-Y., Piao, Y.-J., Kim, J.-S., Suhr, K.-B., Park, J.-K. & Lee, J.-H. (2002)** *Identification of calcium-induced genes in HaCaT keratinocytes by polymerase chain reaction-based subtractive hybridization*. Archives of Dermatological Research 294, 411-418.

137 **Wilson, V. G.** in *Epidermal Cells: Methods and Protocols* (ed Kursad Turksen) 33-41 (Springer New York, 2014).

138 **Franken, N. A., Rodermond, H. M., Stap, J., Haveman, J. & van Bree, C. (2006)** *Clonogenic assay of cells in vitro*. Nature Protocols 1, 2315-2319.

139 **Wittekind, D. (2003)** *Traditional staining for routine diagnostic pathology including the role of tannic acid. 1. Value and limitations of the hematoxylin-eosin stain*. Biotechnic & Histochemistry 78, 261-270.

140 **Lillie, R., Tracy, R., Pizzolato, P., Donaldson, P. & Reynolds, C. (1980)** *Differential staining of collagen types in paraffin sections: A color change in degraded forms*. Virchows Archiv A 386, 153-159.

141 **Goldner, J. (1938)** *A modification of the Masson trichrome technique for routine laboratory purposes*. The American Journal of Pathology 14, 237-243.

142 **Truett, G. E., Heeger, P., Mynatt, R. L., Truett, A. A., Walker, J. A. & Warman, M. L. (2000)** *Preparation of PCR-quality mouse genomic DNA with hot sodium hydroxide and tris (HotSHOT)*. BioTechniques 29, 52-54.

143 **Strittmatter, G. E., Sand, J., Sauter, M., Seyffert, M., Steigerwald, R., Fraefel, C., Smola, S., French, L. E. & Beer, H.-D. (2016)** *IFN-γ primes keratinocytes for HSV-1–induced inflammasome activation*. Journal of Investigative Dermatology 136, 610-620.

144 **Zhang, J. D., Ruschhaupt, M. & Biczok, R.** (2010).

145 **Motulsky, H. (2007)** *Prism 5 Statistics Guide*. GraphPad Software.

4 Results

1. Optogenetic activation of FGFR2

Submitted as:

Rauschendorfer, T. *et al.* *Acute and chronic effects of a light-activated FGF receptor in keratinocytes in vitro and in mice.* Manuscript submitted.

My contribution:

- Cloning of the OptoR2 transgene (Figure 1A)
- Establishment of OptoR2 in HEK 293T cells (Figure 1B-G; Figure 1C, F and G performed by the master student Irina Heggli under my supervision)
- Investigation of OptoR2 signaling in HEK 293T cells (Supplementary Figure 1)
- Characterisation of OptoR2 downregulation in murine primary and immortalised keratinocytes (Figure 2; Figure 2B, C and D performed by the master student Selina Gurri under my supervision)
- Testing of OptoR2 in additional mouse and cell lines (Supplementary Figure 2; Supplementary Figure 2B performed by the master student Selina Gurri under my supervision)
- Investigation of tumour formation phenotype (Figure 3)
- Establishment of OptoR2 in HaCaT cells (Figure 4; generation of the inducible expression system and the cell lines performed by the master student Selina Gurri under my supervision)
- Investigation of consequences of long-term illumination on target gene expression and migration (Figure 5) and on OptoR2 expression (Supplementary Figure 5)
- Management of the mouse lines
- Design of the figures and writing of the manuscript

Acute and chronic effects of a light-activated FGF receptor in keratinocytes *in vitro* and in mice

Theresa Rauschendorfer[1], Selina Gurri[1], Irina Heggli[1], Luigi Maddaluno[1], Michael Meyer, [1] Alvaro Ingles-Prieto[2], Harald Janovjak[3,4*] and Sabine Werner[1*]

[1]Institute of Molecular Health Sciences, Department of Biology, ETH Zurich, Otto-Stern-Weg 7, 8093 Zurich, Switzerland

[2]CeMM Research Center for Molecular Medicine of the Austrian Academy of Sciences, 1090 Vienna, Austria

[3]Australian Regenerative Medicine Institute (ARMI), Faculty of Medicine, Nursing and Health Sciences, Monash University, Clayton, VIC, Australia

[4]European Molecular Biology Laboratory Australia (EMBL Australia), Monash University, Clayton, VIC 3800, Australia

*Correspondence: Prof. Dr. Sabine Werner and Prof. Dr. Harald Janovjak

Institute of Molecular Health Sciences

Otto-Stern-Weg 7, 8093 Zurich, Switzerland

Phone: +41 44 633 3941

sabine.werner@biol.ethz.ch, harald.janovjak@monash.edu

Abstract

Fibroblast growth factors (FGFs) and their high affinity receptors (FGFRs) play key roles in development, tissue repair and disease. Since FGFRs bind overlapping sets of ligands, their individual functions cannot be determined using ligand stimulation. Here, we generated a light-activated FGFR2 variant (OptoR2) to selectively activate signaling by the major FGFR in keratinocytes. Illumination of OptoR2-expressing HEK 293T cells activated FGFR signaling with remarkable temporal precision and promoted migration and proliferation. In murine and human keratinocytes, OptoR2 activation rapidly induced the classical FGFR signaling pathways and expression of FGF target genes. Surprisingly, multi-level counter-regulation occurred in keratinocytes *in vitro* and in transgenic mice *in vivo*, including OptoR2 down-regulation and loss of responsiveness to light activation. These results demonstrate unexpected cell type-specific limitations of optogenetic FGFRs in long-term *in vitro* and *in vivo* settings and highlight the complex consequences of transferring non-neuronal optogenetic cell signaling tools into their relevant cellular contexts.

1.1 Introduction

FGFs are evolutionary highly conserved signaling molecules and comprise a group of 22 structurally related proteins. Most of them signal through four tyrosine kinase receptors (FGFR1-4). FGFRs orchestrate migration, proliferation, differentiation and survival of multiple cell types and, therefore, they play crucial roles in development, homeostasis, repair and disease of a variety of tissues [45, 48, 57-60]. The biological output of FGF signaling depends on the type of FGF and FGFR, on the cell type and on the presence of heparan sulphate proteoglycans on the cell surface, which are required for FGF receptor binding and activation [45, 47, 48, 70]. For example, FGF7 and FGF10 both activate the "b" splice variant of FGFR2 (FGFR2b), but FGF7 induced receptor degradation and cell proliferation in HeLa cells, whereas FGF10 treatment induced receptor recycling and cell migration [71]. Little is known on how different cellular responses can be activated by stimulation of the same receptor with different FGFs or by stimulation of different receptors with the same ligand. Additionally, there are unsolved issues regarding possible unique or synergistic effects of different types of FGFRs. This is particularly relevant for cells, which express multiple FGF receptors, such as keratinocytes of the skin. These cells express FGFR1-3, with FGFR2 being the most relevant receptor for epidermal function and FGFR1 and FGFR3 serving as a “back-up” [65, 66]. Activation of these receptors in keratinocytes is of crucial importance for the maintenance of epidermal barrier function and wound healing, and mice lacking FGFR1 and FGFR2 in keratinocytes develop a phenotype resembling the inflammatory skin disease Atopic Dermatitis [65] and also show a severe defect in wound re-epithelialization [66].

To specifically test the contributions of an individual FGFR to a cellular outcome, it is necessary to selectively activate this receptor in a precise manner both in space and time. This is generally not possible using the ligands, because first, they do not offer spatial and temporal precision, and second, most FGFs are promiscuous and bind to different FGFRs with different affinities [57]. A promising alternative approach is optogenetics, where photoactivatable protein domains are used to tightly control and manipulate cellular signaling networks [72-74, 93-95, 99, 101, 108, 115]. FGFRs were among the first optogenetic tools developed specifically to manipulate cellular signaling pathways and cell behaviour [128, 129]. Initially, two different versions of a light-regulated FGFR1 were generated and characterized. One version takes advantage of aureochrome light-oxygen-voltage (LOV) domains for receptor homodimerisation, and illumination of this modified FGFR1 activated the canonical intracellular signaling cascades and induced proliferation, migration and *in vitro* capillary formation of endothelial cells [128].

The other receptor system uses cryptochrome 2 (CRY2) homo-interaction to induce receptor clustering. Light-induced stimulation of these receptors allowed activation of downstream signaling pathways, cytoskeletal reorganisation, alterations in cell polarity and directed cell migration [129]. Further modifications of FGFR1 rendered it sensitive to red light [146, 147], induced membrane recruitment of the receptor [148] or of a photo-domain [107], or resulted in receptor inactivation upon illumination [130, 149]. However, optogenetic FGFR activation was never extended past FGFR1. Furthermore, light-activated FGFRs and light-activated receptors or signaling proteins in general have not been deployed *in vivo* in transgenic rodents, which would allow precise timing of FGFR activation in a tissue-specific manner if the transgene is driven by specific promoters. Therefore, important open questions exist in the context of transferring this and also other optogenetic cell signaling technology to relevant biological contexts: 1) are light-activated signaling receptors applicable in transgenic animals, e.g. can required expression levels be reached [150, 151]? 2) What are potential negative consequences and how do these depend on cell type and strategy? Whilst studies with virally-delivered and recombinase-enabled optogenetic actuators [152] or bacterial cyclic nucleotide producing enzymes [153, 154] or experiments in transgenic invertebrate models [155-159] have shown promising results, the general feasibility of non-neuronal optogenetics in transgenic rodents remains to be demonstrated.

Due to the important function of FGF receptors, in particular of FGFR2, in keratinocytes, we generated a version of FGFR2 that can be activated by blue light instead of its natural ligand (named OptoR2). We show that activation of OptoR2 with blue light robustly activates signaling and induces migration and proliferation in human embryonic kidney (HEK) 293T cells and also in murine and human keratinocytes. However, down-regulation of the receptor was observed in keratinocytes, suggesting that long-term activation of OptoR2, even at a low level, is deleterious for these cells. These results unravel advantages, but also some limitations of optogenetics for the analysis of growth factor signaling.

1.2 Materials and Methods

1.2.1 Recombinant proteins, antibodies and primers

The following recombinant proteins were used: Murine EGF (E4127, Sigma, St Louis, MO), human FGF7 (100-19, PeproTech, Rocky Hill, NJ) and human FGF10 (100-26, PeproTech). Standard chemicals were from Sigma or Merck, Darmstadt, Germany.

The following primary antibodies were used:

Antigen	**Host**	**Dilution**	**Application**	**Catalogue no.**	**Manufacturer**
AKT	rabbit	1:1.000	Western blot	9272	Cell Signaling Technologies, Danvers, MA
AKT (phospho T308)	rabbit	1:1.000	Western blot	9275	Cell Signaling Technologies
AKT (phospho S473)	rabbit	1:1.000	Western blot	3787	Cell Signaling Technologies
CD31	rat	1:100	Immunofluorescence	553370	BD Biosciences, Franklin Lakes, NJ
E-Cadherin	mouse	1:100	Immunofluorescence	610181	BD Biosciences
ERK	rabbit	1:1.000	Western Blot	9102	Cell Signaling Technologies
ERK (phospho T202/Y204)	rabbit	1:100	Immunofluorescence	9101	Cell Signaling Technologies
		1:1.000	Western blot		
FRS2α (phospho Y196)	rabbit	1:1.000	Western blot	3864	Cell Signaling Technologies
FRS2α (phospho Y436)	rabbit	1:1.000	Western blot	3861	Cell Signaling Technologies
GAPDH	mouse	1:5.000	Western blot	5G4cc	HyTest, Turku, Finland
HA (OptoR2)	rabbit	1:100	Immunofluorescence	3724	Cell Signaling Technologies
		1:1.000	Western blot		
Ki67	rabbit	1:500	Immunohistochemistry Immunofluorescence	ab16667	Abcam, Cambridge, UK
p38	rabbit	1:1.000	Western blot	9212	Cell Signaling Technologies
p38 (phospho T180/Y182)	rabbit	1:1.000	Western blot	9211	Cell Signaling Technologies

The following secondary antibodies were used:

Antigen species	coupled with	Dilution	Application	Catalogue no.	Manufacturer
mouse	Cy2	1:200	Immunofluorescence	115-225-003	Jackson ImmunoResearch, West Grove, PA
mouse	HRP	1:5.000	Western blot	W4021	Promega, Madison, WI
rabbit	biotin	1:500	Immunohistochemistry	111-065-003	Jackson ImmunoResearch
rabbit	Cy2	1:200	Immunofluorescence	111-225-144	Jackson ImmunoResearch
rabbit	Cy3	1:200	Immunofluorescence	111-165-003	Jackson ImmunoResearch
rabbit	HRP	1:5.000	Western blot	W4011	Promega
rat	Cy3	1:200	Immunofluorescence	712-165-153	Jackson ImmunoResearch

The following primers were used:

Gene	Sequence	Application
DUSP6 (human)	5'-GTT CTA CCT GGA AGG TGG CT-3' 5'-AGT CCG TTG CAC TAT TGG GG-3'	qRT-PCR
FGFR2 (human)	5'-AGC TGG GGT CGT TTC ATC TG-3' 5'-TTG GTT GGT GGC TCT TCT GG-3'	qRT-PCR
HBEGF (human)	5'-TTA GTC ATG CCC AAC TTC ACT TT-3' 5'-ATC GTG GGG CTT CTC ATG TTT-3'	qRT-PCR
OptoR2	5'-TGA CCA GCA GCT TGG CAT AA-3' 5'-GCT CTG CAA ATG GCA CAA CA-3'	Genotyping PCR
	5'-GCT CTG CAA ATG GCA CAA CA-3' 5'-TGA CCA GCA GCT TGG CAT AA-3'	qRT-PCR
RPL27 (human)	5'-TCA CCT AAT GCC CAC AAG GTA-3' 5'-CCA CTT GTT CTT GCC TGT CTT-3'	qRT-PCR
Rps29 (mouse)	5'-GGT CAC CAG CAG CTC TAC TG-3' 5'-GTC CAA CTT AAT GAA GCC TAT GTC C-3'	qRT-PCR
VEGF (human)	Hs_VEGFA_6_SG, QuantiTect Primer Assay (QT01682072)	qRT-PCR

1.2.2 Generation of OptoR2

The transgene encoding OptoR2 was generated by restriction digest and ligation. For this purpose, the intracellular domain (ICD) of human FGFR2 was tagged N-terminally with a myristoylation domain for membrane anchorage and fused with aureochrome LOV domain from *Vaucheria frigida*, tagged at the C-terminus with a hemagglutinin (HA) epitope. In the

utilized region, mouse FGFR2 exhibits 92% sequence identity to human FGFR2, and the murine and human receptors can fully substitute each other's function [48].

1.2.3 Mice

The transgenic mouse line was generated by inserting the OptoR2-transgene under the control of the K14-promoter into C57BL/6 mouse oocytes by microinjection. After implanting the embryos into foster mice and delivery, their offspring was genotyped. Transgenic animals were used to establish three independent mouse lines, of which two exhibited undetectable transgene expression levels (Figure 2 - figure supplement 1A). Mice were kept under specific pathogen-free (SPF) conditions according to federal guidelines with food and water *ad libitum* and a 12 h light-dark cycle. All mouse experiments were approved by the local veterinary authorities of Zurich, Switzerland (Kantonales Veterinäramt der Stadt Zürich, Switzerland). Mice with a single skin tumour that reached 1 cm diameter, with more than one tumour with 0.5 mm diameter or with tumours at a burdening body site were sacrificed according to animal welfare regulations.

For genotyping, skin obtained upon ear clipping was digested with proteinase K (A3830, AppliChem, Darmstadt, Germany) and then used for the genotyping polymerase chain reaction (PCR). The genotyping mix contains 0.5 µl tissue lysate, 8 µl KAPA2G genotyping mix (KK5620, Roche, Basel, Switzerland), 6 µl ddH_2O and 1 µl primer mix (10 µM). The PCR reaction was performed according to the protocol below and the samples were analysed in a 2% agarose gel in SBA buffer containing 20 mM NaOH and 80.8 mM boric acid in water.

Cycles	**Time**	**Temperature**
1x	5 min	95°C
33x	35 sec	95°C
	35 sec	60°C
	50 sec	72°C
1x	10 min	72°C
Store at 8°C		

1.2.4 Establishment of murine primary keratinocyte cultures

Primary keratinocytes were obtained from 3- to 5-day old pups as described previously [132], with few modifications. The pups were sacrificed and the whole trunk skin was peeled off. After scraping off the subcutaneous fat tissue, the skin was incubated with 0.8% (w/v) trypsin (27250-018, Thermo Fisher Scientific, Waltham, MA) in Dulbecco's modified eagle medium (DMEM) (Merck) for 1 h at 37°C. Afterwards, the epidermis was separated from the dermis and incubated for 30 min at 37°C with 0.025% (w/v) DNase (DN25, Sigma) in DMEM + 10% (v/v) FBS (A3160802, LOT 2166297, Thermo Fisher Scientific). The cell pellet was resuspended in keratinocyte growth medium [132] and the cells seeded in cell culture dishes pre-coated with collagen IV (C7521, Sigma) in PBS (2.5 µg/cm^2). They were cultivated for up to 1 week.

1.2.5 Cell culture

Human embryonic kidney T (HEK 293T) cells (Sigma), low passage human immortalised keratinocytes (HaCaT cells) [135] (kindly provided by Prof. P. Boukamp, Düsseldorf, Germany) as well as primary and spontaneously immortalised murine keratinocytes were used. They were cultivated in DMEM + 10% FBS (HEK 293T and HaCaT) or keratinocyte growth medium as described in [132] (primary and immortalised murine keratinocytes) and passaged twice weekly. All cell lines were routinely screened for mycoplasma and found negative.

For the generation of stable cell lines, lentivirus particles were generated in HEK cells. Cells were transiently transfected with a pcDNA-based plasmid (V79020, Thermo Fisher Scientific) or a pInducer plasmid (Addgene, Watertown, MA; no. 44012) harbouring the *OptoR2* transgene or empty vector as a control, together with the packaging plasmids psPAX2 (Addgene no. 12260) and pCMV-VSV-G (Addgene no. 8454) using Lipofectamine 2000 Transfection reagent (11668030, Thermo Fisher Scientific). After virus production for 48 h, the supernatant was collected, cleared by filtration through a 0.45 µm filter and stored at -80°C. Target cells were transduced by incubating them for 48 h with the lentivirus supernatant diluted 1:10 in DMEM + 10% FBS and selected with 1.5 µg/ml puromycin (P8833, Sigma) (HEK 293T with pcDNA plasmid) or 1 mg/ml G418 (11811031, Thermo Fisher Scientific) (HaCaT with pInducer plasmid).

1.2.6 Starvation and illumination

HEK and HaCaT cells were starved by washing twice with PBS and changing the medium to DMEM without FBS. For the HaCaT cells harbouring the doxycycline (Dox)-inducible construct, 50 ng/ml Dox (D1822, Sigma) or the same amount of dimethyl sulfoxide (DMSO) (1.02952, Merck) were added. Murine primary and immortalised keratinocytes were washed twice with PBS, and their medium was changed to defined keratinocyte serum-free medium (10744019, Thermo Fisher Scientific) without supplements, but with penicillin/streptomycin (P0781, Merck) and 4.2 pg/ml cholera toxin (C8052, Sigma). The cells were cultivated under starvation conditions for 16 h (HEK 293T) or 24 h (keratinocytes), respectively.

Afterwards, they were treated with 10 ng/ml FGF7, FGF10 or EGF or illuminated with blue light for different time periods. For short-term continuous illumination (up to 3 h), cell plates were put underneath a layer of light emitting diodes (LEDs) (5119661, Light & More, Forchtenberg, Germany), while for long-term illumination, a light chamber for three 6-well plates (Greiner, Kremsmünster, Austria) with one LED for each well was custom-built using an Arduino UNO board (Arduino, Somerville, MA). The plates were illuminated using "1 min on / 15 min off" or "1 min on / 60 min off" cycles or using continuous illumination. The respective dark control cells were covered and kept in the same incubator. Light intensities were measured with a Powermeter (LP1 from Sanwa, Tokyo, Japan) and were around 27 $\mu W/cm^2$ and 0.2 $\mu W/cm^2$ in the light and in the dark, respectively.

1.2.7 Scratch assay

Cells were cultivated on dishes pre-coated with collagen IV in PBS (2.5 $\mu g/cm^2$) until they reached full confluency, starved as described before and treated for 2 h with 2 µg/ml mitomycin C (M4287, Sigma) to block proliferation. Afterwards, a scratch was induced with a pipet tip and the cells were washed with PBS before starvation or treatment media were added. Pictures were taken at the same spot every 24 h for 72 h. They were analysed manually or with the MRI wound healing tool (https://github.com/MontpellierRessourcesImagerie/imagej_macros_and_scripts/wiki/Wound-Healing-Tool, accessed 25th May 2020).

1.2.8 RNA isolation and qRT-PCR

Cells were washed with PBS before extracting their RNA with the Mini Total RNA Kit (IBI Scientific, Dubuque, IA) according to the manufacturer's instructions. One µg RNA was used

for reverse transcription in a reaction volume of 20 µl with the iScript cDNA synthesis kit (1708890, BioRad, Hercules, CA). The product was diluted 1:10 in water, and 5 µl cDNA were mixed with 5.5 µl LightCycler SYBR green (04887352001, Roche) and 0.5 µl primer mix (10 µM). The qPCR reaction was performed according to the program specified below, and data were analysed using the double delta cycle threshold (CT) method.

Cycles	Time	Temperature
1x	10 min	95°C
50x	10 sec	95°C
	20 sec	60°C
	20 sec	72°C
1x	5 sec	95°C
1x	1 min	65°C
1x	Slow heat	95°C
Store at 40°C		

1.2.9 Preparation of protein lysates and Western blot

Cells were washed with PBS and lysed in lysis buffer containing 240 mM Tris-HCl pH 6.8, 280 mM SDS and 40% (v/v) glycerol, heated to 95°C. After heating the samples for 10 min at 95°C and short centrifugation, their protein concentration was determined using the BCA Protein assay kit (23225, Thermo Fisher Scientific) and a GloMax Microplate Reader (Promega, Madison, MA). Afterwards, the samples were diluted to 1 µg/µl using lysis buffer with a final concentration of 10 mM DTT and bromophenol blue.

Samples of 20 µg protein were separated by SDS-PAGE and transferred to Protran™ nitrocellulose membranes (GE Healthcare, Chicago, IL). For probing with phospho-antibodies, membranes were blocked for 1 h with 5% (w/v) bovine serum albumin (BSA) (P06-1391100, PAN Biotech, Aidenbach, Germany) in Tris-buffered saline with Tween 20 (TBS-T) containing 25 mM Tris base, 137 mM NaCl, 2.7 mM KCl and 0.1% (v/v) Tween 20, pH adjusted to 8.0, while the membranes for incubation with non-phospho antibodies were blocked for 1 h with 5% (w/v) skim milk powder (150141000000, Rapilait, Basel, Switzerland) in TBS-T. They were then incubated with the primary antibody diluted in 5% (w/v) BSA in TBS-T overnight at 4°C, washed thrice for 5 min with TBS-T, incubated for 1 h with the secondary antibody diluted in 5% (w/v) skim milk powder in TBS-T and washed thrice for 10 min with TBS-T. Signals

were developed using WesternBright Sirius HRP substrate (K-12043, Advansta, San Jose, CA) and the FUSION SOLO 6S chemiluminescence imaging system (Witec, Ulm, Germany).

1.2.10 Immunofluorescence staining of cells

Cells were cultivated on cover slips, washed with PBS and fixed for 20 min with 4% (w/v) paraformaldehyde (PFA) (P6148, Sigma) in PBS. After washing with PBS, they were permeabilised for 5 min with 0.5% (v/v) Triton X-100 in PBS and washed twice with PBS. Epitopes were blocked for 1 h with 2% (w/v) BSA and 0.05% (v/v) Triton X-100 in PBS. Then, the cells were incubated for 1 h with the primary antibodies diluted in the blocking solution, washed thrice for 5 min with PBS and incubated for 1 h with the secondary antibodies and Hoechst 33342 (1:3.000) diluted in 0.05% (v/v) Triton X-100 in PBS. After washing thrice for 10 min with PBS, they were post-fixed for 5 min with 1% (w/v) PFA in PBS, washed with PBS and mounted with ProLong Gold Antifade Mountant (Thermo Fisher Scientific). Photomicrographs were taken with an Axiovert microscope (Carl Zeiss, Oberkochen, Germany) equipped with a Axiocam 506 mono camera (Carl Zeiss) at 10x and 20x magnification or with a confocal microscope (Leica SP8 from Leica, Wetzlar, Germany) at 63x magnification.

1.2.11 H&E staining of tissue sections

Samples from normal skin or skin tumours were fixed with 4% (w/v) PFA in PBS overnight at 4°C and then gradually dehydrated using an increasing ethanol gradient before embedding in paraffin (39601006, Leica Biosystems). Sections (7 µm) were dewaxed and rehydrated with a decreasing ethanol gradient, before staining them with hematoxylin and eosin (H&E).

Cycles	**Solution**	**Time**
1x	Mayer's Hematoxylin solution	3 min
3x	ddH_2O	10 sec
1x	Scott water	30 sec
1x	ddH_2O	10 sec
1x	70% (v/v) ethanol / ddH_2O	10 sec
1x	Eosin solution	1 min
2x	80% (v/v) ethanol / ddH_2O	10 sec
2x	95% (v/v) ethanol / ddH_2O	10 sec
2x	ethanol	10 sec
2x	Xylene	10 min

Mount with Eukitt and air-dry the slides

1.2.12 Immunofluorescence and immunohistochemistry staining of tissue sections

PFA-fixed and paraffin-embedded tissue sections were rehydrated and treated for 40 min with 0.33% (v/v) H_2O_2 in methanol. After washing the sections twice for 10 min with PBS, antigens were unmasked in 10 mM sodium citrate pH 6 (71405, Fluka, St Louis, MO) for 1 h at 95°C. After washing twice for 10 min with PBS, sections were blocked for 1 h with 12% (w/v) BSA in PBS and incubated overnight at 4°C with the primary antibodies diluted in blocking solution.

For immunofluorescence, the sections were then washed twice for 10 min with PBS, incubated for 1 h with the secondary antibodies diluted in PBS, before washing them thrice for 10 min with PBS. They were post-fixed for 5 min with 1% (w/v) PFA in PBS, washed with PBS and mounted with ProLong Gold Antifade Mountant (Thermo Fisher Scientific). Photomicrographs were taken with an Axiovert microscope (Carl Zeiss, Oberkochen, Germany) equipped with a Axiocam 506 mono camera (Carl Zeiss) at 10x magnification.

For immunohistochemistry, sections were washed thrice for 10 min with PBS, incubated for 45 min with the secondary antibody diluted in PBS, before washing them thrice for 5 min with PBS. Afterwards they were incubated with the VECTASTAIN® Elite® ABC Kit Peroxidase solution (PK-4000, Maravai Life Sciences, San Diego, CA), washed again thrice for 5 min with PBS, before diaminobenzidine Kit solution (SK-4100, Maravai Life Sciences) was added until the brown staining was visible. The reaction was stopped by submersing the slides in tap water. Sections were counterstained with hematoxylin and mounted with Mowiol (81381, Sigma). Photomicrographs were taken using a light microscope (Axioskop 2, Carl Zeiss) equipped with a Axiocam 512 color camera (Carl Zeiss) at 2.5x,10x and 20x magnification.

1.2.13 Statistical analysis

Statistical analysis was performed using the Prism 8 software (GraphPad Software Inc., San Diego, CA). Quantitative data are presented as mean ± standard error of the mean (SEM). Significance was calculated using Mann-Whitney-U test. * $p \leq 0.05$; ** $p \leq 0.01$; *** $p \leq 0.001$; **** $p \leq 0.0001$.

1.3 Results

1.3.1 Establishment of light-induced FGFR2 activation in HEK 293T cells

We established an optogenetic approach to selectively activate FGFR2 in keratinocytes. For this purpose, a hemagglutinin (HA) epitope-tagged aureochrome LOV domain was fused C-terminally to the intracellular part of FGFR2. The extracellular ligand binding domains were removed, and the receptor was anchored to the cell membrane using a myristoylation signal (Figure 1A). The same approach was successfully used to generate the OptoFGFR1 and other light-activated receptor tyrosine kinases [128, 160]. Consequently, OptoR2 is not responsive to its natural ligands, but only to optogenetic stimulation by blue light.

HEK 293T cells, which stably and constitutively express OptoR2, responded to 15 min blue light illumination with phosphorylation/activation of ERK1/2. The level of ERK1/2 activation was comparable to the level achieved with epidermal growth factor (EGF) (Figure 1B). By contrast, vector-transfected control (ctrl) and OptoR2-expressing HEK 293T cells only responded weakly to FGF7 and FGF10, the canonical ligands of the FGFR2b splice variant that is highly expressed in keratinocytes. This is consistent with qRT-PCR data, which showed that endogenous FGFR2 is only weakly expressed in HEK 293T cells compared to immortalized human keratinocytes (HaCaT cells) (Figure 1 – figure supplement 1A). As expected, illumination of ctrl cells had no effect on ERK1/2 activation (Figure 1B). Immunofluorescence staining for pERK1/2 confirmed this result and demonstrated that blue light robustly activated ERK1/2 (Figure 1C).

Using light emitting diodes (LEDs) we found that OptoR2 was activated by blue light ($\lambda \sim 450$ nm) and also by white LEDs that emitted light of a continuous spectrum. As expected, OptoR2 was not activated by red light ($\lambda \sim 700$ nm) (Figure 1C), consistent with the activation characteristics of flavin mononucleotide, the ubiquitously present light-sensitive co-factor of LOV domains. Light activation of OptoR2 was very rapid, as a one second illumination pulse with blue light was sufficient to induce ERK1/2 phosphorylation. For maximum signal amplitude, however, 30 seconds of illumination were necessary (Figure 1D). These findings highlight the remarkable temporal precision that can be achieved with optogenetics.

Activation of OptoR2 also resulted in phosphorylation of the scaffold protein FGFR substrate (FRS) 2α (Y436), while other signaling molecules that are frequently activated by FGFRs, such as AKT and p38, were neither activated by OptoR2 nor by FGFR2 in the transfected HEK 293T

cells (Figure 1 – figure supplement 1B). The kinetics of ERK1/2 activation by OptoR2 was comparable to the activation of FGFR2 by its natural ligand FGF7, albeit of greater intensity (Figure 1 – figure supplement 1C).

Importantly, activation of OptoR2 was capable to affect cell behaviour. In scratch wounding assays, HEK 293T cells expressing OptoR2 migrated significantly faster within 48 h in the light than in the dark, while FGF7 and FGF10 had only a weak or no effect in this assay, respectively (Figure 1F). OptoR2-HEK 293T cells also proliferated significantly more when exposed to blue light for 1 h or 24 h, with the longer exposure being more efficient and stronger than the effect achieved with FGF7 and FGF10 or even with fetal bovine serum (FBS) (Figure 1G). Of note, minimal residual (i.e. in the dark) signaling activity was observed (e.g. Figures 1B and Figure 1 - figure supplement 1B, C), rendering OptoR2 a highly efficient optogenetic tool.

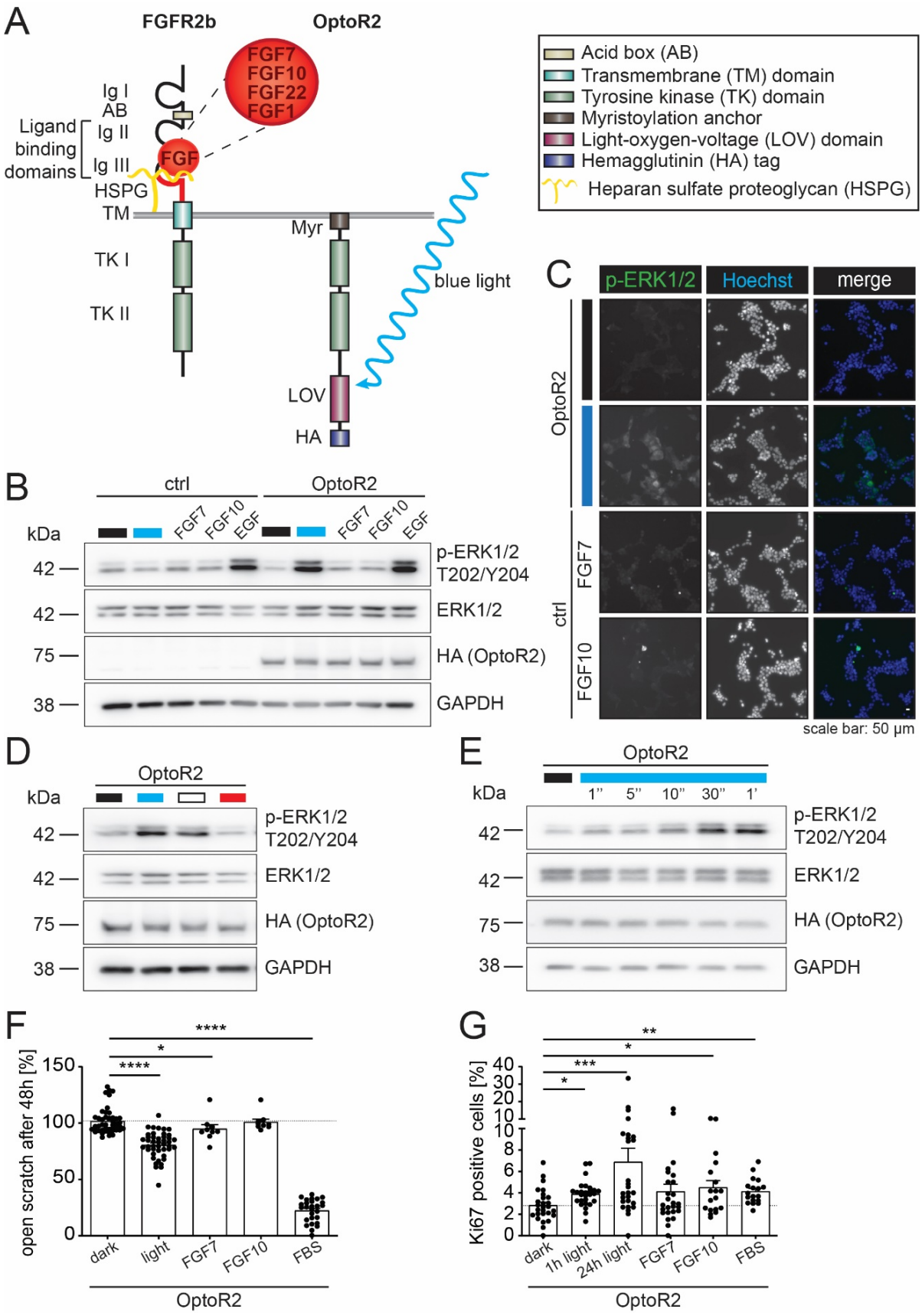

Figure 1: OptoR2 is functional in HEK 293T cells.

(**A**) Schematic representation of endogenous FGFR2b and OptoR2 with their different domains. AB: Acid box, HSPG: heparan sulphate proteoglycan (HSPG); HA: Hemagglutinin epitope, Ig: Immunoglobulin-like domain; LOV: Light-oxygen-voltage domain; Myr: Myristoylation signal, TK; Tyrosine kinase domains TM: Transmembrane domain. OptoR2 is activated by illumination-induced dimerisation via the intracellular LOV domains.

(**B, C**) HEK 293T cells constitutively expressing OptoR2 and vector-transduced control cells (ctrl) were serum-starved for 16 h. Subsequently, they were left untreated (black bar), or illuminated for 15 min with blue light (blue bar), or treated for 15 min with FGF7, FGF10 or EGF (10 ng/ml). Protein lysates were analysed by Western blot for phospho-ERK1/2 (p-ERK T202/Y204), total ERK1/2, HA (OptoR2) and GAPDH (loading control) (B), and fixed cells were analysed by immunofluorescence staining for p-ERK1/2 (T202/Y204, green). Nuclei were counterstained with Hoechst 33342 (blue) (C) Note that the single channels are shown in black and white and the colours are only shown in the merge. Scale bar: 50 μm.

(**D, E**) OptoR2 HEK 293T cells were serum-starved for 16 h and then illuminated for 15 min with light of different wavelengths (D) or illuminated for 1 sec to 1 min with blue light (E). For (E) lysates were prepared 2 min after the onset of illumination. They were analysed by Western blot for p-ERK (T202/Y204), total ERK1/2, HA (OptoR2) and GAPDH.

(**F**) OptoR2-transduced HEK 293T cells were cultured in medium with 0.5% FBS for 16 h, subjected to scratch wounding, and illuminated with blue light, or treated with FGF7, FGF10 (10 ng/ml) or 10% FBS. The area of open scratch was measured manually in pictures taken at the same spot at 0 h and 48 h and is indicated in the bar graph as percentage of control (0 h).

(**G**) OptoR2-transduced HEK 293T cells were serum-starved for 16 h and then illuminated for either 1 h or 24 h or treated with FGF7, FGF10 (10 ng/ml) or 10% FBS for 24 h. At the 24 h time point they were analysed by immunofluorescence staining for Ki67, and nuclei were counterstained with Hoechst 33342. The number of Ki67-positive and total cells was counted manually and the percentage of positive cells is shown.

Data information: Scatter plots show mean ± SEM. (B), (D), (E): Representative of 4 experiments. (C): Representative pictures of 2 experiments. (F): N = 9-45 from 3 experiments. (G): N = 18-27 from 2 experiments. * $P \leq 0.05$, ** $P \leq 0.01$, *** $P \leq 0.001$, **** $P \leq 0.0001$ (Mann-Whitney U-test).

1.3.2 OptoR2 is functional in primary and immortalized murine keratinocytes, but undergoes down-regulation

We next generated transgenic mice expressing OptoR2 under the control of the keratin 14 (K14) promoter, which targets expression of transgenes to basal keratinocytes of the epidermis and outer root sheath keratinocytes of the hair follicles [14]. Three independent transgenic mouse lines were obtained, but only primary keratinocytes from one mouse line expressed the transgene at significant levels (transgenic mouse line 1; Figure 2A), while transgene expression was not detectable or extremely low in the other lines (transgenic mouse lines 2 and 3; Figure 2 – figure supplement 2A). Keratinocytes, which expressed the transgene, responded to 15 min

blue light as well as to FGF7 treatment with phosphorylation of ERK1/2, whilst cells from wild-type pups (ctrl) did not respond to light (Figure 2A). No residual signaling activity of the receptor was observed in the absence of light. These results demonstrate the success of the transgenic targeting strategy employing an endogenous promoter. However, we found individual differences in the OptoR2 expression level between cells from different pups of one litter. Furthermore, freshly isolated primary keratinocytes from the progeny of mouse line 1 (1.5 years or 3 generations later) no longer responded in the same experimental setting (Figure 2A). This is most likely the consequence of a strong downregulation of OptoR2, which was observed both at the mRNA and at the protein level (Figure 2B, left and right panel).

To validate this finding in another model, we examined spontaneously immortalized keratinocytes obtained from cells of the first generation of mice. While these cells showed robust ERK1/2 activation in response to blue light shortly after immortalization, continuous passaging and cultivation for 6 months also in this case completely abolished their light response (Figure 2C). Importantly, both illumination or treatment with FGF7 or FGF10 strongly stimulated cell migration at the beginning of the cultivation period, but only FGFs induced migration 6 months later, while light had no effect (Figure 2D). An additional OptoR2 cell line also lost the light responsiveness (Figure 2 – figure supplement 2B).

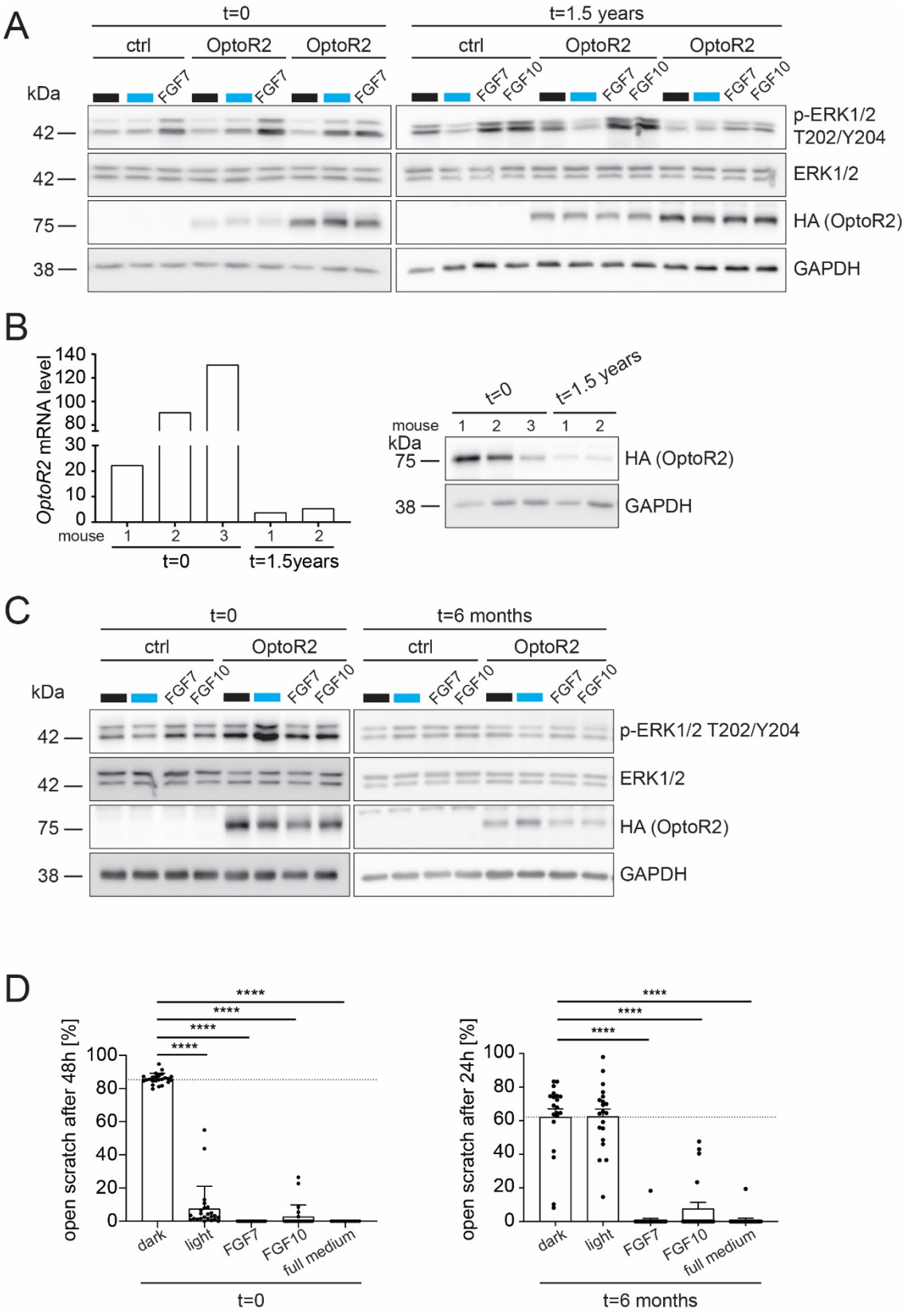

Figure 2: OptoR2 expression is functional in murine keratinocytes, but down-regulated over time.

(**A, B**) Primary keratinocytes were isolated from one new-born ctrl and two OptoR2 mice (transgenic mouse line 1) in the direct offspring of the founder mice as well as 1.5 years (3 generations) later. They were serum-starved for 24 h and illuminated with blue light or treated with FGF7 or FGF10 (10 ng/ml)

for 15 min. Protein lysates were analysed by Western blot for p-ERK1/2 (T202/Y204), ERK1/2, HA (OptoR2) and GAPDH. Note that different exposure times were used for the HA blots in the left and right panels (A). RNA from different batches of untreated primary keratinocytes was analysed by qRT-PCR for expression of *OptoR2* relative to *Rps29*, and protein lysates were analysed by Western blot for HA (OptoR2) and GAPDH (B).

(**C**, **D**) Spontaneously immortalized keratinocytes from K14-OptoR2 mice and a wild-type littermate (ctrl) were serum-starved for 24 h and illuminated with blue light or treated with FGF7 or FGF10 (10 ng/ml) for 15 min, both at the beginning of the cultivation period (t = 0) as well as after extended cultivation and passaging (t = 6 months). Protein lysates were analysed by Western blot for p-ERK1/2 (T202/Y204), total ERK1/2, HA (OptoR2) and GAPDH (C). Alternatively, confluent and serum-starved cells were subjected to scratch wounding and illuminated with blue light or treated with FGF7, FGF10 (10 ng/ml) or full keratinocyte growth medium (D). The area of open scratch was measured manually in pictures taken at the same spot at 0 h and 24 h or 48 h and is shown as percentage of control (0 h) in the bar graph.

Data information: Scatter plots show mean ± SEM. (A) Representative of 4 experiments. t = 0: N = 4 mice per genotype. t = 1.5 years: N = 12-18 mice per genotype. (B) Ctrl littermate expression level was set to 1. One experiment. N = 2-3 mice per genotype. (C) Representative of two experiments with 3 cell lines. (D) t = 0: N = 24 from 2 experiments. t = 6 months: N = 20 from 3 experiments. **** ≤ 0.0001 (Mann-Whitney U-test).

1.3.3 Expression of OptoR2 induces skin tumour formation

Along with the changes in the primary and immortalized cells generated from the mouse line, we also noticed changes in the adult mice of this colony. In the early generations, a high percentage of the transgenic mice, in particular males, developed epithelial skin tumours at light-exposed sites (back, face) at the age of 6-12 weeks (Figure 3A, left upper panel). Histologically, these tumours were highly keratinised and showed invasive growth and strong cell proliferation as revealed by Ki67 staining (Figure 3A, upper right and lower left panels). This strong phenotype prevented us from performing *in vivo* illumination experiments, and the mice were sacrificed according to animal welfare regulations at an early stage of tumour development. Membrane staining for OptoR2 was readily detected in the tumour cells (Figure 3A, lower right panel), whereas the expression level of OptoR2 in the normal back skin was below the detection limit. The upregulation of OptoR2 in the tumours is consistent with the strong activity of the K14 promoter in hyperproliferative epithelia [14]. These findings suggest that the continuous weak activation of OptoR2, which occurs under normal housing conditions, results in tumour formation over time that is further driven by strong activity of the employed promoter in keratinocytic tumour tissue. Correlating with our *in vitro* findings, the tumour incidence strongly declined in the following generations in mice of both genders (Figure 3B).

This supports the hypothesis that continuous OptoR2 expression/activation induces counter-regulatory mechanisms both *in vitro* and *in vivo*.

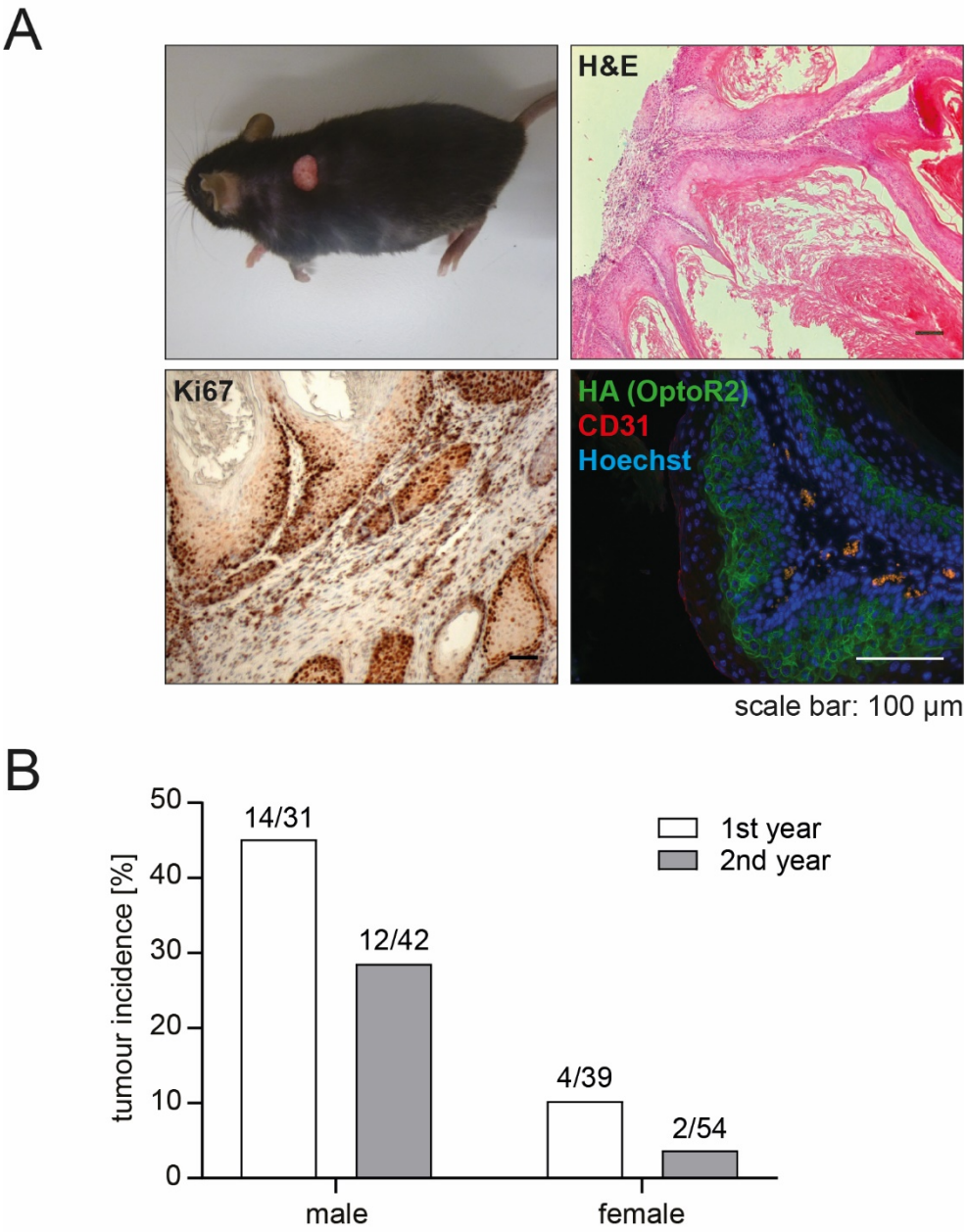

Figure 3: OptoR2 expression in keratinocytes of transgenic mice induces skin tumour formation, which declines over time.

(**A**) Left upper panel: Photograph of an adult K14-OptoR2 mouse with a skin tumour on the upper back. Other panels: Representative photomicrographs from skin tumour sections stained with hematoxylin & eosin, immunostained for Ki67 (immunohistochemistry) and counterstained with hematoxylin, or immunostained (immunofluorescence) for HA (OptoR2; green) and the endothelial cell marker CD31 (red). Nuclei were and counterstained with Hoechst 33342 (blue). Scale bar: 100 µm.

(**B**) Tumour incidence in adult K14-OptoR2 mice of both genders during the first and second year after generation of the mouse line.

Data information: (A): Representative pictures of N = 11 mice. (B): Number of mice with tumors and of total mice is indicated in the graph.

1.3.4 OptoR2 activation by light mimics signaling by endogenous FGFR2 in human keratinocytes

To avoid the counter-regulation observed in the constitutive expression system in keratinocytes, we generated HaCaT cells expressing OptoR2 under the control of a doxycycline (Dox)-inducible promoter using a lentiviral transduction system. Twenty-four hours after Dox addition, OptoR2 was efficiently expressed, and the cells responded to 15 min blue light illumination or exposure to FGF7 or FGF10 with phosphorylation of ERK1/2 (Figure 4A). OptoR2 was present at the plasma membrane and co-localized with E-cadherin, a plasma membrane marker (Figure 4B).

The kinetics of ERK1/2 activation by light was comparable to the activation of endogenous FGFR2b by FGF7 and FGF10: ERK1/2 was phosphorylated already after 5 min of illumination or FGF treatment, followed by a continuous decrease in the levels of phosphorylated ERK1/2 within 2 h (Figure 4C). Given the significance of temporal dynamics for the outcome of signaling [71, 119], this finding is crucial for the successful application of OptoR2. Furthermore, FRS2α as well as other downstream effectors, including AKT and p38, were phosphorylated upon illumination of OptoR2-expressing cells or treatment with FGFs (Figure 4D). We also observed no obvious activation of signaling in the dark in this cell line (e.g. Figure 4A-D).

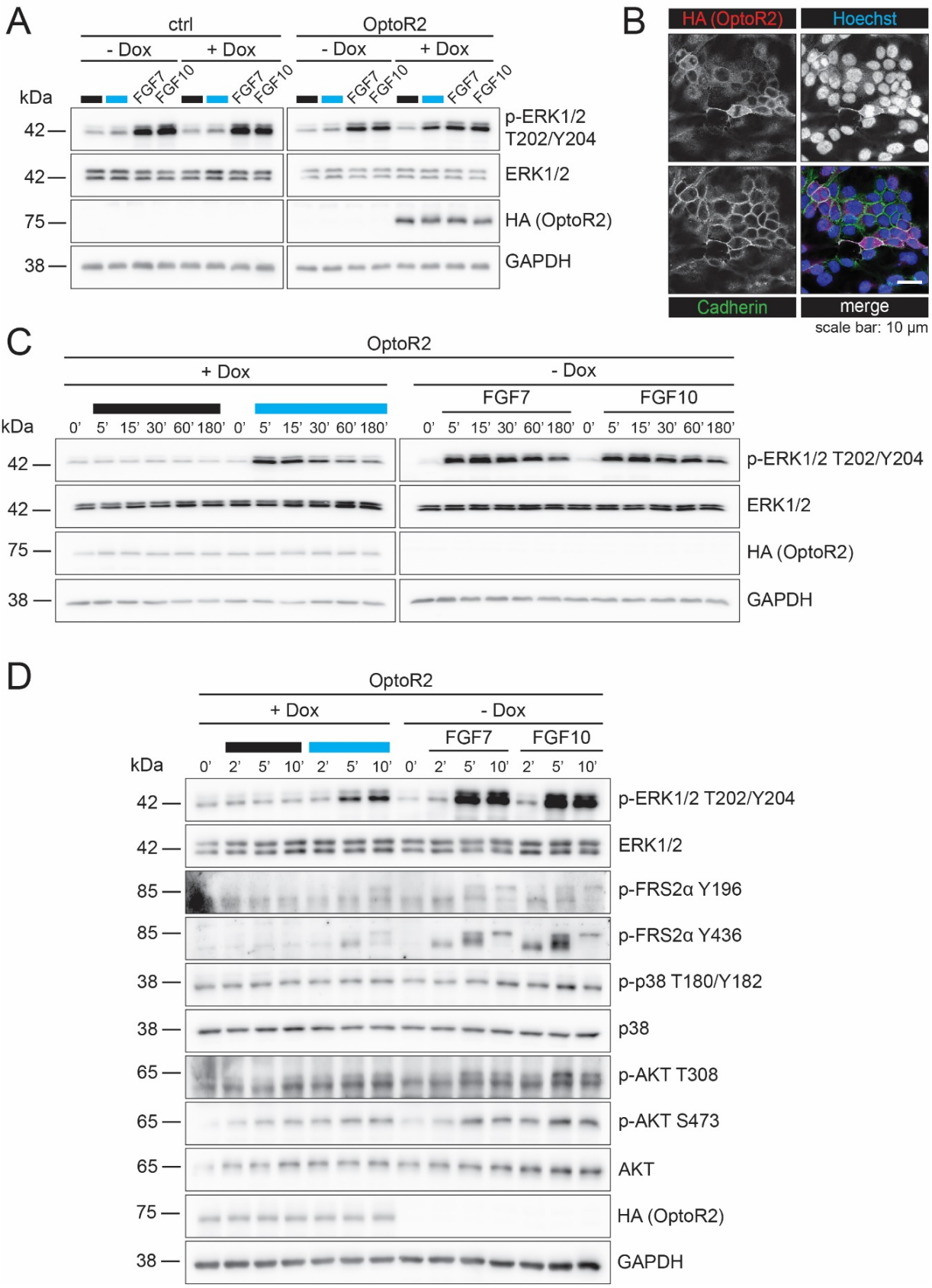

Figure 4: Activation of inducibly expressed OptoR2 in human keratinocytes mimics FGFR2 signaling.

(**A**) OptoR2- and vector-transduced (ctrl) HaCaT cells were serum-starved and treated with 50 ng/ml Dox or DMSO (vehicle) for 24 h. Afterwards, they were illuminated or treated with FGF7 or FGF10 (10 ng/ml) for 15 min. Protein lysates were analysed by Western blot for p-ERK1/2 (T202/Y204), total ERK1/2, HA (OptoR2) and GAPDH.

(**B**) OptoR2-transduced HaCaT cells were serum-starved, treated with 50 ng/ml Dox for 24 h and analysed by immunofluorescence staining for OptoR2 (using an HA antibody) and E-cadherin. Nuclei were counterstained with Hoechst 33342 (blue). Note that the single channels are shown in black and white and the colours are only shown in the merge. Scale bar: 10 μm.

(**C**) OptoR2-transduced HaCaT cells were serum-starved, treated with 50 ng/ml Dox or DMSO for 24 h, and then illuminated with blue light or treated with FGF7 or FGF10 (10 ng/ml) for 5, 15, 30, 60 or 180 min. Protein lysates were analysed by Western blot for p-ERK1/2 (T202/Y204), total ERK1/2, HA (OptoR2) and GAPDH.

(**D**) OptoR2-transduced HaCaT cells were serum-starved, treated with 50 ng/ml Dox or DMSO for 24 h, and then illuminated or treated with FGF7 or FGF10 (10 ng/ml) for 2, 5, or 10 min. Protein lysates were analysed by Western blot for p-ERK1/2 (T202/Y204), total ERK1/2, p-FRS2α (Y196 and Y436), p-p38 (T180/Y182), total p38, p-AKT (T308 and S473), total AKT, HA (OptoR2) and GAPDH.

Data information: (A): Representative of 6 experiments. (B): Representative confocal pictures of 2 experiments. (C): Representative of 2 experiments. (D) Representative of 6 experiments.

1.3.5 Illumination of OptoR2-expressing keratinocytes activates FGF target gene expression and induces migration

Alongside with activation of the major FGFR intracellular signaling pathways, illumination of the OptoR2-expressing HaCaT cells also activated the expression of known FGFR target genes in keratinocytes, including dual-specific phosphatase (*DUSP*) 6, heparin binding EGF like growth factor (*HBEGF*) and vascular endothelial growth factor (*VEGF*) [161-163]. Their mRNA levels significantly increased after 6 h of stimulation with FGF7, FGF10 or continuous illumination with blue light (Figure 5A). Remarkably, dim light (~ 30 $\mu W/cm^2$) was sufficient for OptoR2 activation. This light intensity is lower than the intensity required to activate many other optogenetic tools, for example mW/cm^2 in the case of engineered ion-conducting opsins [150, 151], demonstrating the high sensitivity of OptoR2. Further reduced light doses through intermittent light pulsing with "1 min on / 15 min off" (1/15) or "1 min on / 60 min off" (1/60) cycles, which were introduced to prevent possible negative feedback mechanisms of receptor downregulation over extended illumination periods, were not sufficient to influence the expression of these genes.

The migratory capacity of HaCaT cells in the scratch wounding assay was generally rather weak, even upon stimulation with FGF7 or FGF10. Nevertheless, there was a mild increase in

migration upon exposure to continuous or 1/60 intermittent light (Figure 5B and Figure 5 - figure supplement 5A). The rather weak effect might be a consequence of receptor down-regulation. Indeed, after 3 h of continuous illumination, OptoR2 protein levels were slightly reduced and after 24 h, the recombinant protein was almost undetectable. OptoR2 mRNA also declined with similar kinetics, and this correlated with a reduction in DUSP6 mRNA levels after the initial strong increase, while expression of housekeeping genes was not affected (Figure 5C and Figure 5 – figure supplement 5B and C). There was no overgrowth of OptoR2-negative cells during this period, since no obvious cell death and little proliferation were detected. Rather, OptoR2 was lost in the cells by continuous illumination for several hours. Taken together, short-term OptoR2 activation robustly induced canonical FGFR signaling and consequent changes in gene expression and cell function in keratinocytes, while long-term consequences could not be studied in this cell type due to unexpected counter-regulations.

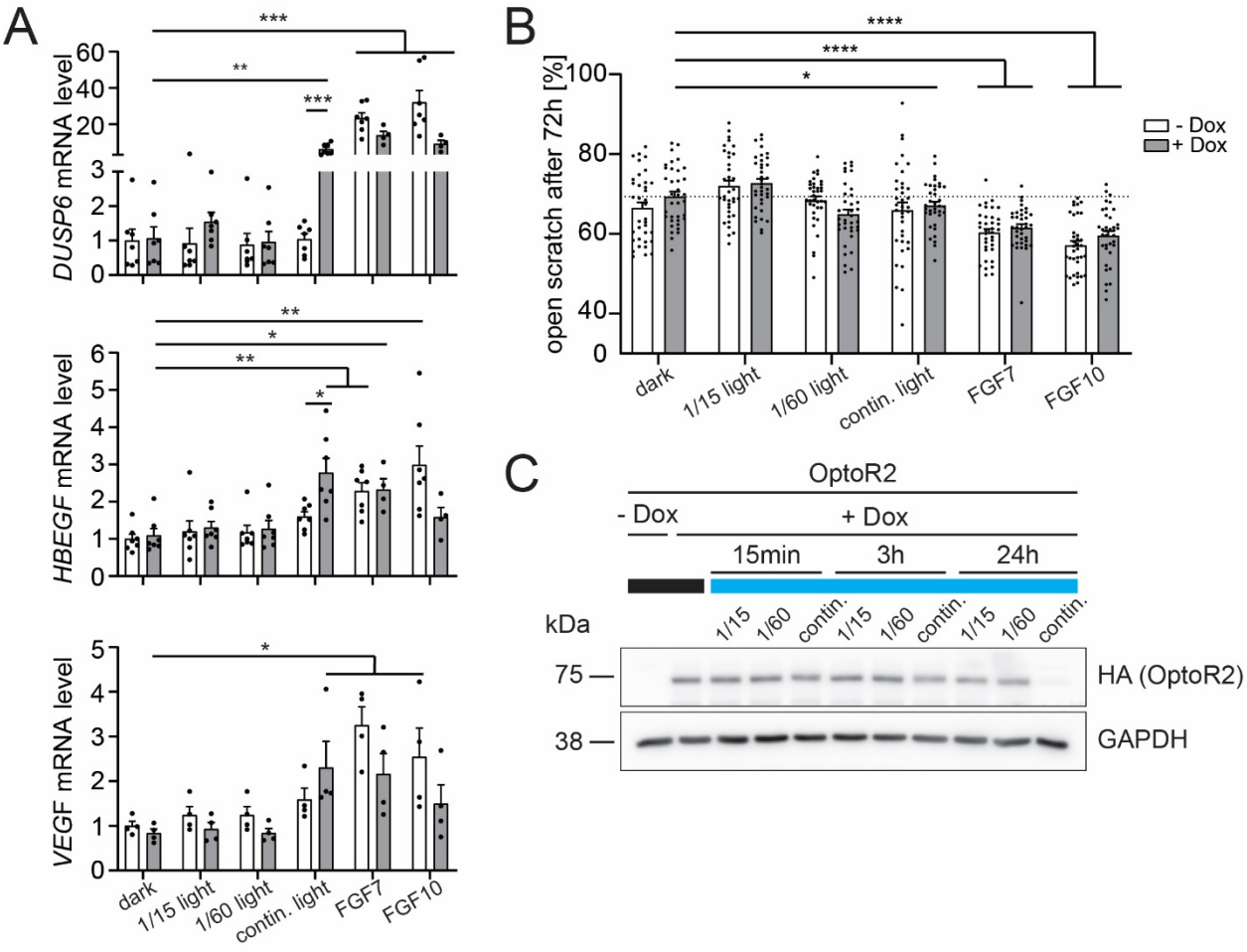

Figure 5: Activation of OptoR2 in human keratinocytes induces expression of FGF target genes and promotes cell migration

(A) OptoR2-transduced HaCaT cells were serum-starved, treated with 50 ng/ml Dox or DMSO for 24 h and then illuminated with blue light (three different illumination schemes; 1 min on / 15 min off (1/15),

1 min on / 60 min off (1/60) cycles), continuous illumination) or treated with FGF7 or FGF10 (10 ng/ml) for 6 h. RNA samples were analysed by qRT-PCR for *DUSP6*, *HBEGF* and *VEGF* relative to *RPL27*.

(B) OptoR2 HaCaT cells were serum-starved, treated with 50 ng/ml Dox or vehicle for 24 h and subjected to scratch wounding. Immediately after scratching, cells were illuminated using three different illumination schemes or incubated with 10 ng/ml FGF7 or FGF10. The area of open scratch was measured with the "MRI wound healing tool" in ImageJ or manually in pictures taken at the same spot at 0 h and 72 h and is shown as percentage of ctrl (0 h) in the bar graph.

(C) OptoR2 HaCaT cells were serum-starved, treated with 50 ng/ml Dox or DMSO for 24 h, and then illuminated for 15 min, 3 h or 24 h using three different illumination schemes. Protein lysates were analysed by Western blot for HA (OptoR2) and GAPDH.

Data information: Scatter plots show mean ± SEM. (A): "dark – Dox" expression level was set to 1. N = 4-7 from 2-5 experiments. (B): N = 36 from 2 experiments. (C): Representative of 3 experiments. * $P \leq 0.05$, ** $P \leq 0.01$, *** $P \leq 0.001$, **** ≤ 0.0001 (Mann-Whitney U-test).

1.4 Discussion

We used optogenetics to selectively activate the major FGFR in keratinocytes within its natural cellular context *in vitro* and in transgenic mice *in vivo*. Optogenetic experiments in rodent models most commonly employ viral gene delivery paired with cell type-specific expression or implantation of engineered light-sensitive cells. An ongoing challenge is to transfer the many powerful optogenetic methods from the cell systems in which they were developed, in our case HEK 293T cells, to relevant primary cell types and *in vivo* contexts. Whilst this was successful for cell signaling methods in transgenic invertebrates, prominently *Drosophila* [156-158], as well as for a selection of microbial neuron-targeted ion conducting opsins [150, 151] and bacterial cyclic nucleotide producing enzymes [153, 154], demonstration of non-neuronal optogenetics using transgenic rodents is lacking to the best of our knowledge. Therefore, we generated a transgenic mouse model in which the expression of OptoR2 is driven by a keratinocyte-specific promoter. Despite the highly robust function of the method *prime facie*, expression in the native cell type *in vitro* and *in vivo* revealed a series of undesired consequences that will be informative for future studies in the field. First, despite functional expression from the cell type-specific promoter, we found a gradual loss of the receptor in keratinocytes obtained from transgenic mice. This loss highlights one possible response mechanism of a native cell type to chronic activation of an endogenous but engineered receptor. Second, we found that light-exposed tissues in the transgenic animals exhibited tumour growth, which may at least in part be driven by a positive feedback loop involving a promoter that is active in hyperproliferative keratinocytes. This result also proposes the use of cages with colour filtering properties to study optogenetic systems in light-exposed tissues, since reduction of ambient light in animal colonies is not compatible with animal welfare regulations in many countries. Third, these findings further indicate that the severity of undesired cellular outcomes is likely dependent on the cell type and the genetic strategy. Overall, further optimization of optogenetic approaches for the activation of growth factor signaling will be important and should be tailored to the type of receptor and the target cell.

In spite of the limitations discovered in this work, a major strength of our approach is the rapid and highly specific activation of FGFR2 signaling. The kinetics of ERK1/2 activation in keratinocytes was similar to the kinetics observed in response to FGF7 and FGF10. In addition, all canonical FGFR signaling pathways were activated in these cells by OptoR2, resulting in the activation of classical FGFR target genes. These results suggest that OptoR2 strongly mimics the effect of the endogenous ligands. Therefore, it is highly suitable to study the early

responses to FGFR activation with robust function and minimal residual activity in its natural cellular context. It will also allow the combined use of OptoR2 and other light-activatable receptors (e.g. OptoR1, see above) to study individual, overlapping or synergistic activities of different FGFRs or other receptor tyrosine kinases, and the identification of signaling molecules and target genes, which are activated by individual receptors.

However, in all keratinocyte systems that we established, we noticed a decrease in OptoR2 levels and/or a loss of light responsiveness over time, which limits the use of OptoR2 to study FGF-regulated alterations in keratinocyte behaviour in long-term experiments. Overall, these data suggest that mild, but chronic FGFR signaling negatively affects keratinocyte viability or plating efficiency. This would result in selection of cells/mice, which have down-regulated the receptor. We did not observe significant cell death of the OptoR2-expressing keratinocytes at a given time point, but even apoptosis of a small percentage of cells may result in progressive overgrowth by keratinocytes that have down-regulated the receptor. It is also possible that the differentiation of OptoR2-expressing keratinocytes is enhanced. This hypothesis is supported by the delayed keratinocyte differentiation in mice expressing a dominant-negative FGFR in suprabasal keratinocytes [62], the induction of early and late keratinocyte differentiation in HaCaT cells by overexpression of FGFR2b and stimulation with FGF7 [164, 165], and the strong keratinization of the tumours that formed in OptoR2 mice (this study). Although we did not observe a strong effect of OptoR2 expression on keratinocyte differentiation markers in pilot *in vitro* experiments, a continuous mild effect on differentiation may lead to the loss of some differentiated cells upon passaging.

Finally, it will be interesting to address the mechanisms underlying the loss of OptoR2 expression or responsiveness in keratinocytes. In the mice and upon long-term culture of cell lines, this may involve epigenetic mechanisms, which are well known to silence transgene expression in different mouse lines and can be tackled, for example, by targeted demethylation [166-168]. In addition to loss of transgene expression, negative feedback regulation may occur in response to OptoR2 activation, e.g. via activation of endogenous signaling inhibitors [5, 35]. However, this does not explain the rapid loss of the receptor that occurred after continuous illumination of OptoR2-expressing HaCaT keratinocytes, even when an inducible expression system was used. Therefore, active receptor down-regulation is likely to occur as previously suggested for wound keratinocytes, where high levels of FGF7 are present [169]. At the protein level, this is achieved by receptor ubiquitination and subsequent internalisation, frequently followed by proteasomal degradation [48, 71]. Down-regulation of FGFR2 mRNA by FGFR

activation has also been observed in fibroblasts and did not involve reduced transcription of the gene [170]. Therefore, mRNA decay is a more likely mechanism, which may occur in response to FGFR kinase activation and/or continuous light exposure. Our newly developed OptoR2 could be an important tool to address the mechanisms of receptor down-regulation at the RNA and protein levels in the future.

Taken together, our study identified major strengths, but also limitations of optogenetic FGFR activation, which should be taken into consideration in future *in vitro* and *in vivo* studies.

Acknowledgements

We thank Connor Richterich and Patricia Reinert, ETH Zurich, for invaluable experimental help, Manuela Pérez Berlanga, University Zurich, for help with the confocal imaging, Lukas Fischer for help with electrical engineering, Thomas Hennek, Sol Taguinod and Dr. Stephan Sonntag, EPIC Phenomics Center, ETH Zürich, for the generation (oocyte injection) and maintenance of the K14-OptoR2 mice, and Dr. Petra Boukamp, Leibniz Institute, Düsseldorf, Germany, for early passage HaCaT keratinocytes.

This work was supported by the ETH Zurich (grant ETH-06 15-1 to S.W. and L.M.), the Swiss National Science Foundation (grant 31003A_169204 and 31003B-189364 to S.W), and a Marie Curie postdoctoral fellowship from the European Union (to L. M).

Author contributions

T.R., S.G., and I.H. performed experiments and analysed the data. L.M. and M.M. helped with the design of the study. A.IP. provided the OptoR2 transgene. S.W. designed the study and wrote the manuscript together with T.R. and H.J., and provided the funding. All authors made important suggestions to the manuscript.

Disclosure

The authors have no competing interests.

Supplementary figures

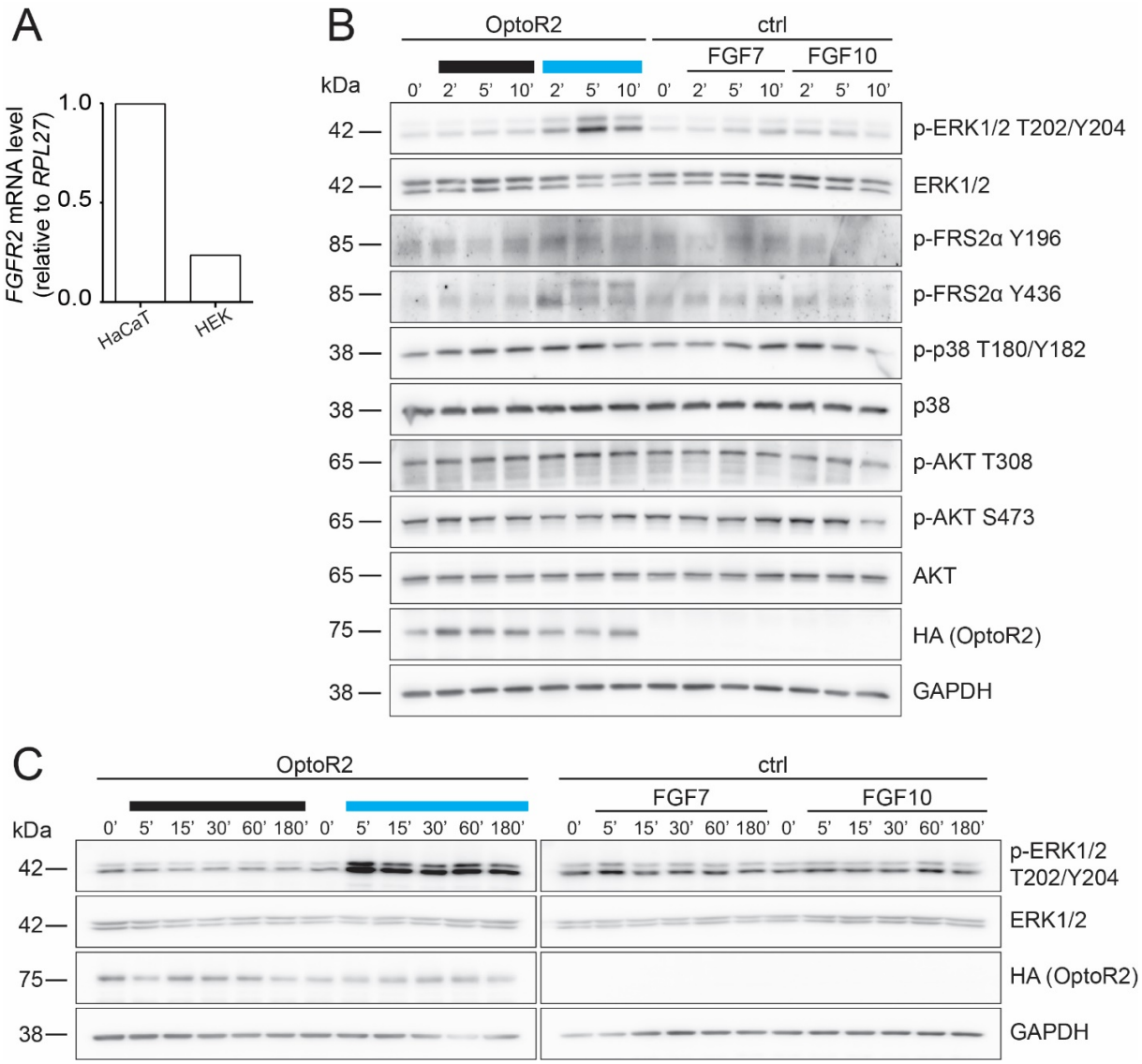

Supplement to Figure 1: Blue light activates FGFR signaling pathways in OptoR2-expressing HEK 293T cells.

(**A**): RNA samples from vector-transfected HEK 293T and HaCaT cells were analysed by qRT-PCR for *FGFR2* relative to *RPL27*. Expression levels in HaCaT cells were set to 1.

(**B**) Ctrl and OptoR2-transduced HEK 293T cells were serum-starved for 16 h and then illuminated with blue light or incubated with FGF7 or FGF10 (10 ng/ml) for 2, 5 or 10 min. Protein lysates were analysed by Western blot for p-ERK1/2 (T202/Y204), total ERK1/2, p-FRS2α (Y196 and Y436), p-p38 (T180/Y182), total p38, p-AKT (T308 and S473), total AKT, HA (OptoR2) and GAPDH.

(**C**) After serum-starvation for 16 h, OptoR2 and ctrl HEK 293T cells were illuminated with blue light or incubated with FGF7 or FGF10 (10 ng/ml) for 5, 15, 30, 60 or 180 min. Protein lysates were analysed by Western blot for p-ERK1/2 (T202/Y204), total ERK1/2, HA (OptoR2) and GAPDH.

Data information: (A): Expression level in HaCaT cells was set to 1. One experiment, duplicate determination. (B): Representative of 2 experiments. (C): Representative of 4 experiments.

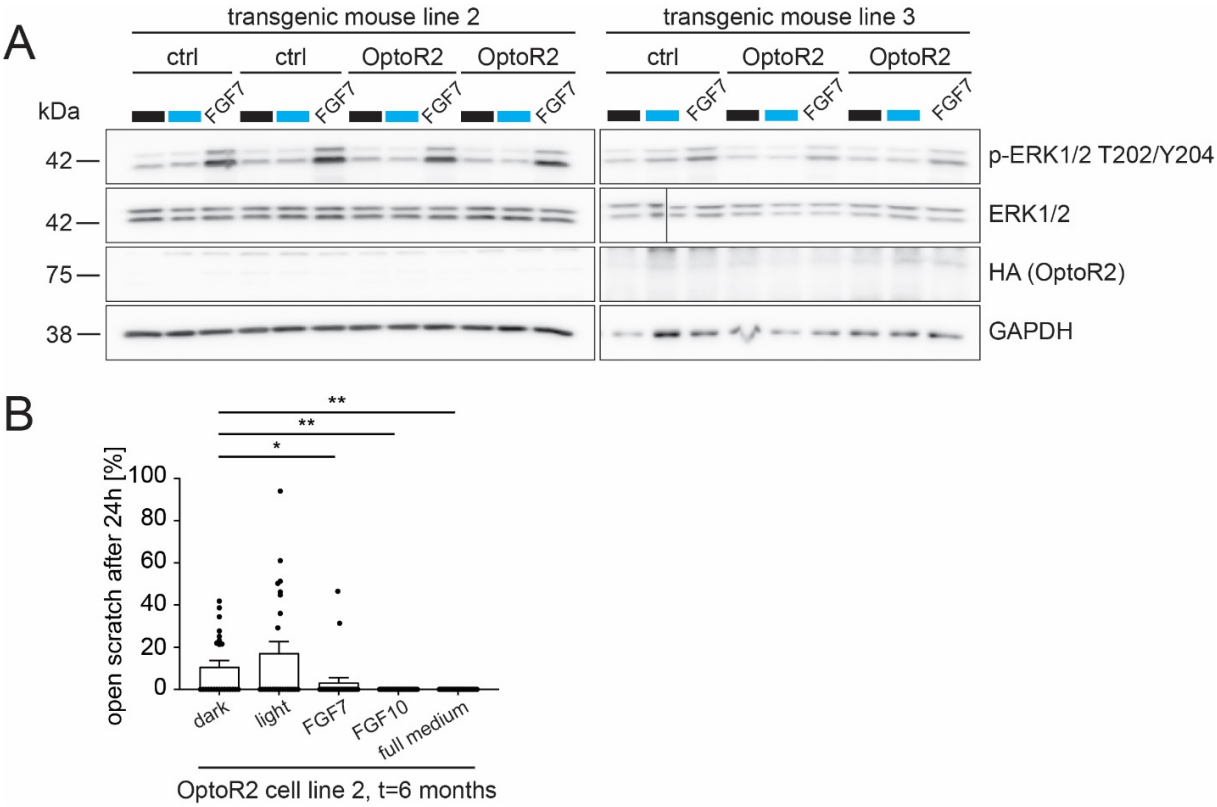

Supplement to Figure 2: Illumination of cells with low OptoR2 expression or after long cultivation time does not activate signaling or promote migration.

(**A**) Primary keratinocytes from new-born ctrl and OptoR2 mice (transgenic mouse lines 2 and 3, two different batches each) were serum-starved for 24 h and illuminated with blue light or treated with FGF7 or FGF10 (10 ng/ml) for 15 min. Protein lysates were analysed by Western blot for p-ERK1/2 (T202/Y204), ERK1/2, HA (OptoR2) and GAPDH.

(**B**) Confluent immortalized murine keratinocytes from K14-OptoR2 mice were serum-starved for 24 h, subjected to scratch wounding and illuminated with blue light or treated with FGF7, FGF10 (10 ng/ml) or full keratinocyte growth medium. The area of open scratch was measured with the "MRI wound healing tool" in ImageJ or manually in pictures taken at the same spot at 0 h and 24 h and is shown as percentage of ctrl (dark) in the bar graph.

Data information: Scatter plots show mean ± SEM. (A) Representative of 3 experiments. Transgenic mouse line 2: N = 3 mice per genotype. Transgenic mouse line 3: N = 6-8 mice per genotype. (B) OptoR2 cell line 2: N = 24 from one experiment. * $P \leq 0.05$, ** $P \leq 0.01$ (Mann-Whitney U-test).

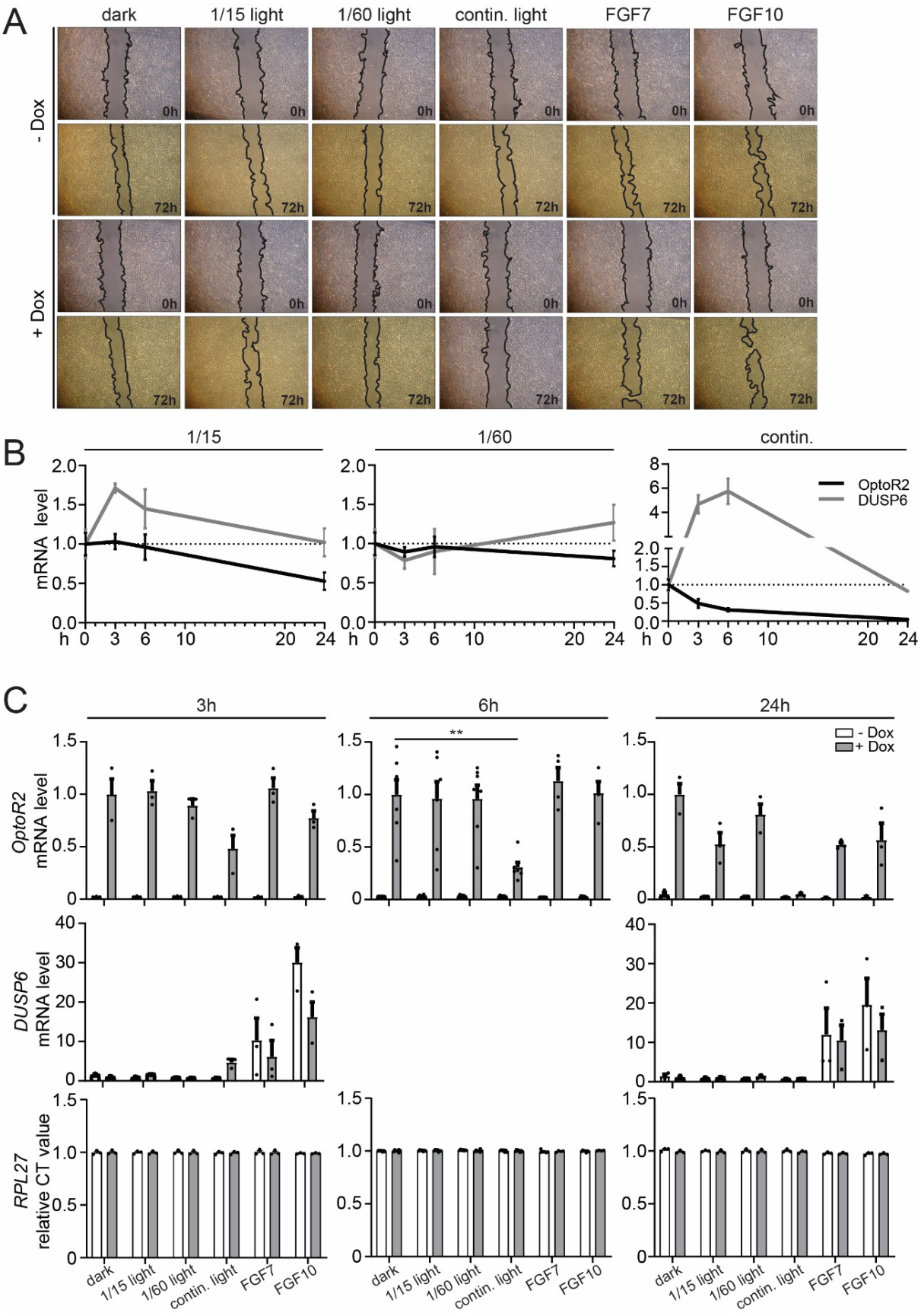

Supplement to Figure 5: Activation of OptoR2 in HaCaT cells promotes migration and FGF target gene expression, but also OptoR2 down-regulation.

(**A**) Representative pictures of the scratch wounding experiment shown in Figure 5B.

(**B, C**) OptoR2-transduced HaCaT cells were serum-starved and treated with 50 ng/ml Dox for 24 h and then illuminated with blue light (three different illumination schemes) for 3, 6 or 24 h (B, C) or treated with FGF7 or FGF10 (C). RNA samples were analysed for expression of *OptoR2* and *DUSP6* relative to *RPL27* by qRT-PCR with the respective "dark + Dox" values at the different time points set to 1. Shown in (B) are the mean ± SEM mRNA levels of stimulated cells after illumination for different periods based on the results shown as bar graphs in Figure 5A (*DUSP6* after 6 h) and figure 5 - figure supplement 1C (*DUSP6* after 3 and 24 h, *OptoR2* all time points). CT values for the housekeeping gene *RPL27*, which was used for normalization, is shown in (C), bottom panel.

Data information: (A): Representative pictures of 2 experiments. (B, C): "dark + Dox" expression level was set to 1. N = 3-7 from 3-5 experiments. ** $P \leq 0.01$ (Mann-Whitney U-test).

References

14 **Fuchs, E. (1993)** *Epidermal differentiation and keratin gene expression*. Journal of Cell Science 17, 197-208.

45 **Beenken, A. & Mohammadi, M. (2009)** *The FGF family: Biology, pathophysiology and therapy*. Nature Reviews Drug Discovery 8, 235-253.

47 **Makarenkova, H. P., Hoffman, M. P., Beenken, A., Eliseenkova, A. V., Meech, R., Tsau, C., Patel, V. N., Lang, R. A. & Mohammadi, M. (2009)** *Differential interactions of FGFs with heparan sulfate control gradient formation and branching morphogenesis*. Science Signaling 2, ra55.

48 **Ornitz, D. M. & Itoh, N. (2015)** *The fibroblast growth factor signaling pathway*. Wiley Interdisciplinary Reviews: Developmental Biology 4, 215-266.

57 **Mason, I. (2007)** *Initiation to end point: The multiple roles of fibroblast growth factors in neural development*. Nature Reviews Neuroscience 8, 583-596.

58 **Turner, N. & Grose, R. (2010)** *Fibroblast growth factor signalling: From development to cancer*. Nature Reviews Cancer 10, 116-129.

59 **Coutu, D. L. & Galipeau, J. (2011)** *Roles of FGF signaling in stem cell self-renewal, senescence and aging*. Aging 3, 920-933.

60 **Fearon, A. E., Gould, C. R. & Grose, R. P. (2013)** *FGFR signalling in women's cancers*. International Journal of Biochemistry & Cell Biology 45, 2832-2842.

62 **Werner, S., Weinberg, W., Liao, X., Peters, K., Blessing, M., Yuspa, S., Weiner, R. & Williams, L. (1993)** *Targeted expression of a dominant-negative FGF receptor mutant in the epidermis of transgenic mice reveals a role of FGF in keratinocyte organization and differentiation*. The EMBO Journal 12, 2635-2643.

65 **Yang, J., Meyer, M., Muller, A. K., Bohm, F., Grose, R., Dauwalder, T., Verrey, F., Kopf, M., Partanen, J., Bloch, W., Ornitz, D. M. & Werner, S. (2010)** *Fibroblast growth factor receptors 1 and 2 in keratinocytes control the epidermal barrier and cutaneous homeostasis*. Journal of Cell Biology 188, 935-952.

66 **Meyer, M., Muller, A. K., Yang, J., Moik, D., Ponzio, G., Ornitz, D. M., Grose, R. & Werner, S. (2012)** *FGF receptors 1 and 2 are key regulators of keratinocyte migration in vitro and in wounded skin*. Journal of Cell Science 125, 5690-5701.

70 **Dailey, L., Ambrosetti, D., Mansukhani, A. & Basilico, C. (2005)** *Mechanisms underlying differential responses to FGF signaling*. Cytokine & Growth Factor Reviews 16, 233-247.

71 **Francavilla, C., Rigbolt, K. T., Emdal, K. B., Carraro, G., Vernet, E., Bekker-Jensen, D. B., Streicher, W., Wikstrom, M., Sundstrom, M., Bellusci, S., Cavallaro, U., Blagoev, B. & Olsen, J. V. (2013)** *Functional proteomics defines the molecular switch underlying FGF receptor trafficking and cellular outputs*. Molecular Cell 51, 707-722.

72 **Tischer, D. & Weiner, O. D. (2014)** *Illuminating cell signalling with optogenetic tools*. Nature Reviews Molecular Cell Biology 15, 551-558.

73 **Zhang, K. & Cui, B. (2015)** *Optogenetic control of intracellular signaling pathways*. Trends in Biotechnology 33, 92-100.

74 **Kwon, E. & Heo, W. D. (2020)** *Optogenetic tools for dissecting complex intracellular signaling pathways*. Biochemical and Biophysical Research Communications 527, 331-336.

93 **Gorostiza, P. & Isacoff, E. Y. (2008)** *Optical switches for remote and noninvasive control of cell signaling*. Science 322, 395-399.

94 **Airan, R. D., Thompson, K. R., Fenno, L. E., Bernstein, H. & Deisseroth, K. (2009)** *Temporally precise in vivo control of intracellular signalling*. Nature 458, 1025-1029.

95 **Bacchus, W. & Fussenegger, M. (2012)** *The use of light for engineered control and reprogramming of cellular functions*. Current Opinion in Biotechnology 23, 695-702.

99 **Kushibiki, T., Okawa, S., Hirasawa, T. & Ishihara, M. (2014)** *Optogenetics: Novel tools for controlling mammalian cell functions with light*. International Journal of Photoenergy 2014, 1-10.

101 **Rogers, K. W. & Muller, P. (2020)** *Optogenetic approaches to investigate spatiotemporal signaling during development*. Current Topics in Developmental Biology 137, 37-77.

107 **Bugaj, L. J., Choksi, A. T., Mesuda, C. K., Kane, R. S. & Schaffer, D. V. (2013)** *Optogenetic protein clustering and signaling activation in mammalian cells*. Nature Methods 10, 249-252.

108 **Pudasaini, A., El-Arab, K. K. & Zoltowski, B. D. (2015)** *LOV-based optogenetic devices: Light-driven modules to impart photoregulated control of cellular signaling*. Frontiers in Molecular Biosciences 2, 18.

115 **Toettcher, J. E., Voigt, C. A., Weiner, O. D. & Lim, W. A. (2011)** *The promise of optogenetics in cell biology: Interrogating molecular circuits in space and time*. Nature Methods 8, 35-38.

119 **Zhang, K., Duan, L., Ong, Q., Lin, Z., Varman, P. M., Sung, K. & Cui, B. (2014)** *Light-mediated kinetic control reveals the temporal effect of the Raf/MEK/ERK pathway in PC12 cell neurite outgrowth*. PLoS One 9, e92917.

128 **Grusch, M., Schelch, K., Riedler, R., Reichhart, E., Differ, C., Berger, W., Ingles-Prieto, A. & Janovjak, H. (2014)** *Spatio-temporally precise activation of engineered receptor tyrosine kinases by light*. The EMBO Journal 33, 1713-1726.

129 **Kim, N., Kim, J. M., Lee, M., Kim, C. Y., Chang, K.-Y. & Heo, W. D. (2014)** *Spatiotemporal control of fibroblast growth factor receptor signals by blue light*. Chemistry & Biology 21, 903-912.

130 **Kainrath, S., Stadler, M., Reichhart, E., Distel, M. & Janovjak, H. (2017)** *Green-light-induced inactivation of receptor signaling using cobalamin-binding domains*. Angewandte Chemie International Edition 56, 4608-4611.

132 **Braun, S., Hanselmann, C., Gassmann, M. G., auf dem Keller, U., Born-Berclaz, C., Chan, K., Kan, Y. W. & Werner, S. (2002)** *Nrf2 transcription factor, a novel target of keratinocyte growth factor action which regulates gene expression and inflammation in the healing skin wound*. Molecular and Cellular Biology 22, 5492-5505.

135 **Boukamp, P., Petrussevska, R. T., Breitkreutz, D., Hornung, J., Markham, A. & Fusenig, N. E. (1988)** *Normal keratinization in a spontaneously immortalized aneuploid human keratinocyte cell line*. The Journal of Cell Biology 106, 761-771.

146 **Reichhart, E., Ingles-Prieto, A., Tichy, A. M., McKenzie, C. & Janovjak, H. (2016)** *A phytochrome sensory domain permits receptor activation by red light*. Angewandte Chemie International Edition 55, 6339-6342.

147 **Leopold, A. V., Pletnev, S. & Verkhusha, V. V. (2020)** *Bacterial phytochrome as a scaffold for engineering of receptor tyrosine kinases controlled with near-infrared light*. Journal of Molecular Biology 432, 3749-3760.

148 **Krishnamurthy, V. V., Fu, J., Oh, T. J., Khamo, J., Yang, J. & Zhang, K. (2020)** *A generalizable optogenetic strategy to regulate receptor tyrosine kinases during vertebrate embryonic development*. Journal of Molecular Biology 432, 3149-3158.

149 **Kainrath, S. & Janovjak, H. (2020)** *Design and application of light-regulated receptor tyrosine kinases*. Methods in Molecular Biology 2173, 233-246.

150 **Zeng, H. & Madisen, L. (2012)** *Mouse transgenic approaches in optogenetics*. Progress in Brain Research 196, 193-213.

151 **Ting, J. T. & Feng, G. (2013)** *Development of transgenic animals for optogenetic manipulation of mammalian nervous system function: progress and prospects for behavioral neuroscience*. Behavioural Brain Research 255, 3-18.

152 **Nectow, A. R. & Nestler, E. J. (2020)** *Viral tools for neuroscience*. Nature Reviews Neuroscience 21, 669-681.

153 **Jansen, V., Alvarez, L., Balbach, M., Strünker, T., Hegemann, P., Kaupp, U. B. & Wachten, D. (2015)** *Controlling fertilization and cAMP signaling in sperm by optogenetics*. eLife 4.

154 **Luyben, T. T., Rai, J., Li, H., Georgiou, J., Avila, A., Zhen, M., Collingridge, G. L., Tominaga, T. & Okamoto, K. (2020)** *Optogenetic manipulation of postsynaptic cAMP using a novel transgenic mouse line enables synaptic plasticity and enhances depolarization following tetanic stimulation in the hippocampal dentate gyrus*. Frontiers in Neural Circuits 14, 24.

155 **Husson, S. J., Gottschalk, A. & Leifer, A. M. (2013)** *Optogenetic manipulation of neural activity in C. elegans: From synapse to circuits and behaviour*. Biology of the Cell 105, 235-250.

156 **Guglielmi, G., Barry, J. D., Huber, W. & De Renzis, S. (2015)** *An optogenetic method to modulate cell contractility during tissue morphogenesis*. Developmental Cell 35, 646-660.

157 **Johnson, H. E., Goyal, Y., Pannucci, N. L., Schüpbach, T., Shvartsman, S. Y. & Toettcher, J. E. (2017)** *The spatiotemporal limits of developmental Erk signaling*. Developmental Cell 40, 185-192.

158 **Bunnag, N., Tan, Q. H., Kaur, P., Ramamoorthy, A., Sung, I. C. H., Lusk, J. & Tolwinski, N. S. (2020)** *An optogenetic method to study signal transduction in intestinal stem cell homeostasis*. Journal of Molecular Biology 432, 3159-3176.

159 **Tsukada, Y. & Mori, I. (2021)** *Optogenetics in Caenorhabditis elegans*. Advances in Experimental Medicine and Biology 1293, 321-334.

160 **Welm, B. E., Freeman, K. W., Chen, M., Contreras, A., Spencer, D. M. & Rosen, J. M. (2002)** *Inducible dimerization of FGFR1: Development of a mouse model to analyze progressive transformation of the mammary gland*. Journal of Cell Biology 157, 703-714.

161 **Frank, S., Hübner, G., Breier, G., Longaker, M. T., Greenhalgh, D. G. & Werner, S. (1995)** *Regulation of vascular endothelial growth factor expression in cultured keratinocytes. Implications for normal and impaired wound healing*. Journal of Biological Chemistry 270, 12607-12613.

162 **Li, C., Scott, D. A., Hatch, E., Tian, X. & Mansour, S. L. (2007)** *Dusp6 (Mkp3) is a negative feedback regulator of FGF-stimulated ERK signaling during mouse development*. Development 134, 167-176.

163 **Maddaluno, L., Urwyler, C., Rauschendorfer, T., Meyer, M., Stefanova, D., Spörri, R., Wietecha, M., Ferrarese, L., Stoycheva, D., Bender, D., Li, N., Strittmatter, G., Nasirujjaman, K., Beer, H. D., Staeheli, P., Hildt, E., Oxenius, A. & Werner, S. (2020)** *Antagonism of interferon signaling by fibroblast growth factors promotes viral replication*. EMBO Molecular Medicine 12, e11793.

164 **Belleudi, F., Purpura, V. & Torrisi, M. R. (2011)** *The receptor tyrosine kinase FGFR2b/KGFR controls early differentiation of human keratinocytes*. PLoS One 6, e24194.

165 **Rosato, B., Ranieri, D., Nanni, M., Torrisi, M. R. & Belleudi, F. (2018)** *Role of FGFR2b expression and signaling in keratinocyte differentiation: Sequential involvement of PKCδ and PKCα*. Cell Death & Disease 9, 565.

166 **Calero-Nieto, F. J., Bert, A. G. & Cockerill, P. N. (2010)** *Transcription-dependent silencing of inducible convergent transgenes in transgenic mice*. Epigenetics & Chromatin 3, 3.

167 **Blewitt, M. & Whitelaw, E. (2013)** *The use of mouse models to study epigenetics*. Cold Spring Harbor Perspectives in Biology 5, a017939.

168 **Gödecke, N., Zha, L., Spencer, S., Behme, S., Riemer, P., Rehli, M., Hauser, H. & Wirth, D. (2017)** *Controlled re-activation of epigenetically silenced Tet promoter-driven transgene expression by targeted demethylation*. Nucleic Acids Research 45, e147.

169 **Marchese, C., Chedid, M., Dirsch, O. R., Csaky, K. G., Santanelli, F., Latini, C., LaRochelle, W. J., Torrisi, M. R. & Aaronson, S. A. (1995)** *Modulation of keratinocyte growth factor and its receptor in reepithelializing human skin*. Journal of Experimental Medicine 182, 1369-1376.

170 **Ali, J., Mansukhani, A. & Basilico, C. (1995)** *Fibroblast growth factor receptors 1 and 2 are differentially regulated in murine embryonal carcinoma cells and in response to fibroblast growth factor-4*. Journal of Cellular Physiology 165, 438-448.

2. FGF, interferon and antiviral defence

Published as:

Maddaluno, L. *et al.* (2020) *Antagonism of interferon signaling by fibroblast growth factors promotes viral replication*. EMBO Molecular Medicine 12, e11793.

DOI: 10.15252/emmm.201911793

My contribution:

- Confirmation of ISG up-regulation in freshly isolated primary K5-R1/R2 mouse keratinocytes (Figure 1D)
- Confirmation of ISG up-regulation in primary K5-R1/R2 mouse keratinocytes (Figure 1E)
- Confirmation of ISG down-regulation in IFNAR KO primary mouse keratinocytes (Figure 2D, 2 out of 4 experiments)
- Signaling analysis after FGF7 and IFNα treatment in HaCaT cells (Figure 3C)
- Signaling analysis after FGF7 and Poly(I:C) treatment in HaCaT cells (Figure 4B)
- Signaling analysis after HSV-1 infection and FGF7 treatment (Figure 6E, Western blot for p-STAT1 Y701, STAT1, GAPDH, p-STAT2 Y690, STAT2, IRF1, p-IRF3 S396, IRF3 and GAPDH)
- Analysis of HSV-1 infection with FGFR inhibitor treatment (Figure 7B, 3 out of 4 experiments)
- Manuscript editing

Antagonism of interferon signaling by fibroblast growth factors promotes viral replication

Luigi Maddaluno[1*#], Corinne Urwyler[1*], Theresa Rauschendorfer[1*], Michael Meyer[1], Debora Stefanova[1], Roman Spörri[2], Mateusz Wietecha[1], Luca Ferrarese[1], Diana Stoycheva[2], Daniela Bender[3], Nick Li[1,4], Gerhard Strittmatter[4], Khondokar Nasirujjaman[1,5], Hans-Dietmar Beer[4], Peter Staeheli[6,7], Eberhard Hildt[3], Annette Oxenius[2], and Sabine Werner[1#]

*Joint first authors

[1]Institute of Molecular Health Sciences, Department of Biology, ETH Zurich, 8093 Zurich, Switzerland

[2]Institute of Microbiology, Department of Biology, ETH Zurich, 8093 Zurich, Switzerland

[3]Department of Virology, Paul-Ehrlich-Institute, D-63225 Langen, Germany

[4]Department of Dermatology, University Hospital of Zurich, 8091 Zurich, Switzerland

[5]Department of Genetic Engineering and Biotechnology, University of Rajshahi, 6205 Rajshahi, Bangladesh

[6]Institute of Virology, University Hospital Freiburg, and [7]Faculty of Medicine, University of Freiburg, 79104 Freiburg, Germany

[#]Corresponding authors: Prof. Dr. Sabine Werner and Dr. Luigi Maddaluno

Institute of Molecular Health Sciences

Otto-Stern-Weg 7, 8093 Zurich, Switzerland

Phone: +41 44 633 3941

E-mail: sabine.werner@biol.ethz.ch; luigi.maddaluno@gmail.com

The paper explained

Problem

Viral infections are a major threat to human health. Combating such infections and prevention of a pandemic requires the development of vaccines, but also of efficient therapeutics. Unfortunately, many therapeutics are virus-specific and/or have high toxicity. Therefore, the development of novel approaches for the treatment of viral infections is essential.

Results

We identified a previously uncharacterized role of fibroblast growth factors (FGFs) in antiviral defence. FGFs efficiently suppress the interferon response and thus the expression of major antiviral genes and proteins under basal conditions and in response to interferon treatment or viral infections, while FGF receptor inhibition has the opposite effect.

Impact

Our study suggests the use of FGF receptor inhibitors for the treatment of viral infections. This is a promising approach, since such inhibitors are already in clinical trials for the treatment of different types of cancers and are relatively well tolerated. Due to the wide-spread activities of FGFs and interferons, it will also be important to study the relevance of their unexpected cross-talk described in this study in various other human diseases as well as in tissue repair.

Supporting information is available at EMBO Molecular Medicine online.

Graphical abstract

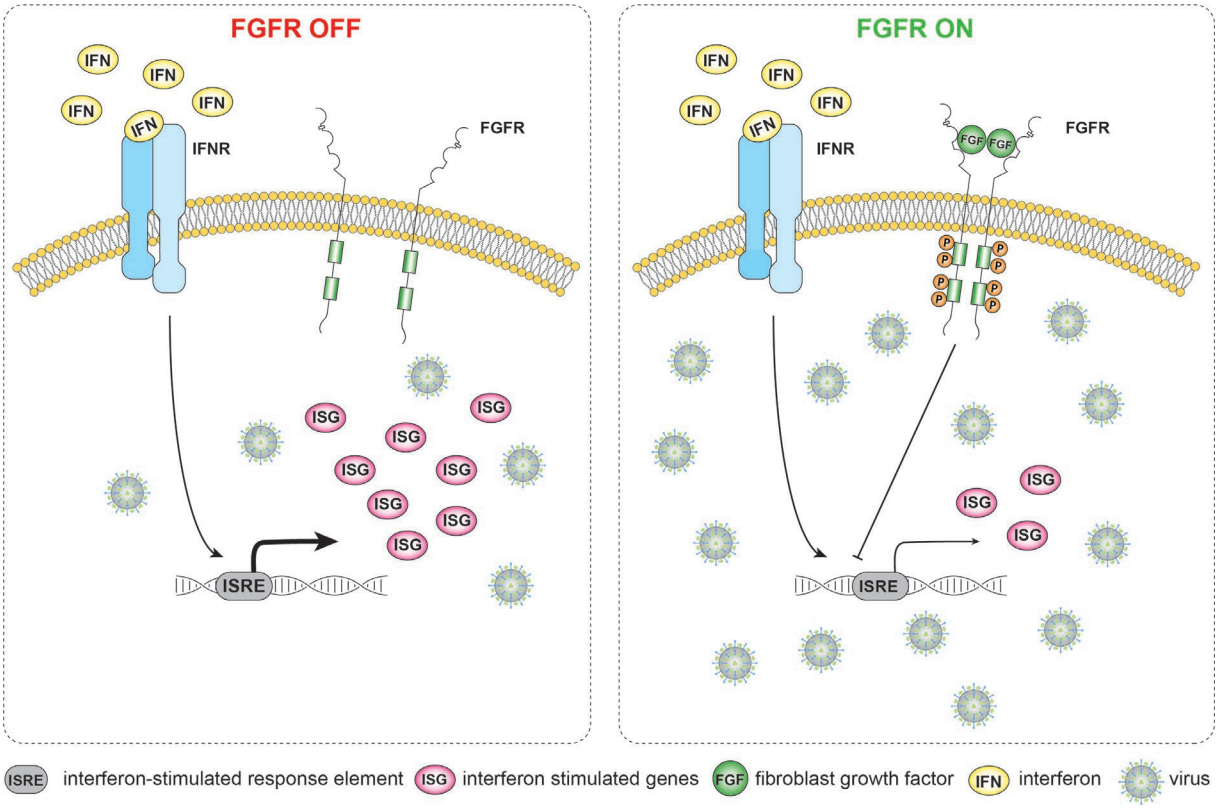

Abstract

Fibroblast growth factors (FGFs) play key roles in the pathogenesis of different human diseases, but the cross-talk between FGFs and other cytokines remains largely unexplored. We identified an unexpected antagonistic effect of FGFs on the interferon (IFN) signaling pathway. Genetic or pharmacological inhibition of FGF receptor signaling in keratinocytes promoted the expression of interferon-stimulated genes (ISG) and proteins *in vitro* and *in vivo*. Conversely, FGF7 or FGF10 treatment of keratinocytes suppressed ISG expression under homeostatic conditions and in response to IFN or poly(I:C) treatment. FGF-mediated ISG suppression was independent of IFN receptors, occurred at the transcriptional level and required FGF receptor kinase and proteasomal activity. It is not restricted to keratinocytes and functionally relevant, since FGFs promoted the replication of herpes simplex virus I (HSV-1), lymphocytic choriomeningitis virus and Zika virus. Most importantly, inhibition of FGFR signaling blocked HSV-1 replication in cultured human keratinocytes and in mice. These results suggest the use of FGFR kinase inhibitors for the treatment of viral infections.

Key words: FGF, FGF receptor, Herpes simplex virus, Interferon, Zika virus

2.1 Introduction

Fibroblast growth factors (FGFs), which comprise a family of 22 proteins, are master regulators of development and tissue repair, and abnormalities in FGF signaling are involved in the pathogenesis of major human diseases, including developmental and inflammatory diseases and cancer [45, 48]. Most FGFs signal through one or more of four receptor tyrosine kinases, designated FGF receptor (FGFR)1 to FGFR4. Additional complexity is achieved by alternative splicing, resulting in the production of FGFR splice variants with different ligand binding specificities [48]. Expression of most FGFs is low under homeostatic conditions, but induced upon injury to various tissues and organs, which is essential for efficient tissue repair and regeneration [42]. Therefore, recombinant FGFs are clinically used for the promotion of tissue repair, such as cutaneous wound healing, and for the protection of tissues from different types of damage [171, 172]. On the other hand, enhanced expression of FGFs or FGFRs and/or abnormal FGFR signaling is frequently observed in cancer, and FGFR inhibitors are therefore in clinical trials for the treatment of various malignancies [173]. Given these important activities of FGFs, it is paramount to identify the mechanisms of action of FGFs, the responsible target genes, and the cross-talk between FGFs and other growth factors and cytokines.

To study FGF function in the skin, we previously generated mice lacking FGFR1, FGFR2 or both receptors in keratinocytes of the epidermis and hair follicles. These mice develop a progressive inflammatory skin disease with features resembling atopic dermatitis in humans, which results at least in part from a defect in the epidermal barrier [65]. However, the epidermal and immune phenotype only develops around 3 weeks after birth and therefore, young mice are ideally suited for the identification of direct targets of FGF signaling in the epidermis.

Here we show that expression of various ISGs is suppressed by FGFs in keratinocytes and correlates with enhanced replication of different types of viruses. These results identify FGF receptor inhibitors as promising compounds for antiviral therapies.

2.2 Materials and Methods

2.2.1 Antibodies, recombinant proteins and chemical inhibitors

The following recombinant proteins and chemical inhibitors were used: Human FGF7 (100-19, PeproTech Inc., Rocky Hill, NJ or R&D Systems, Minneapolis, MN), human FGF10 (100-26, PeproTech Inc.), human FGF2 (100-18, PeproTech Inc.), human IFN-α (300-02AA, PeproTech Inc.), FGFR1/2/3 inhibitors AZD4547 (S2801, Selleckchem, Houston, TX) and BGJ398 (NVP-BGJ398; S2183, Selleckchem), PI3K inhibitor LY294002 (InvivoGen, San Diego, CA), AKT1/2 inhibitor A6730 (A6730, Sigma, Munich, Germany), Mek1/2 inhibitor U0126 (662005, Calbiochem, San Diego, CA), PLCγ inhibitor U73122 (1278, Tocris, Bristol, UK), and proteasome inhibitors MG132 (S2619 Selleckchem), bortezomib (PS-341) (S1013, Selleckchem) and epoxomicin (E3652, Sigma).

2.2.2 Genetically modified mice and infection of mice with HSV-1

K5-R1/R2 and control mice (mice with floxed *fgfr1/fgfr2* alleles, but without Cre, or K5-Cre mice with wild-type *fgfr* alleles) in C57BL/6 genetic background and mice lacking IFNAR1 or both IFNAR1 and IFNLR1 in C57BL/6 genetic background were described previously [65, 174, 175]. They were maintained under specific pathogen-free conditions and received food and water *ad libitum*. For HSV-1 infection, female mice at the age of 8-10 weeks were shaved, and 24 h later each mouse received 4 subcutaneous injections of 50 µl HSV-1 (MOI = 10) on the flank. 48 h later, they were sacrificed and the amount of *ICP0* DNA in the injected skin was determined using primers 5'-ATA AGT TAG CCC TGG CCC CGA-3' and 5'-GCT GCG TCT CGC TCC G-3'. *ICP0* DNA levels were normalized to the host *Tbx15* DNA (primers: 5'-TCC CCC TTC TCT TGT GTC AG-3' and 5'-CGG AAG CAA GTC TCA GAT CC-3') [176]. For the establishment of primary keratinocytes, we used neonatal mice at P3 from both genders. Mouse maintenance and all animal experiments were performed according to Swiss Law and approved after in-depth review and approval by the local veterinary authorities of Zurich, Switzerland (Kantonales Veterinäramt Zürich).

2.2.3 Separation of dermis from epidermis of mouse back skin

Separation of epidermis from dermis was achieved either by heat shock treatment (30 sec at 55-60°C followed by 1 min at 4°C, both in PBS), by incubation for 50-60 min at 37°C in 0.143%

dispase (17105-041, Life Technologies, Carlsbad, CA) in DMEM or by incubation in 0.8% trypsin (27250-018, Life Technologies)/DMEM for 15-30 min at 37°C. For dispase and trypsin treatment the subcutaneous fat was gently scraped off with a scalpel prior to incubation.

2.2.4 Immunofluorescence analysis of skin sections and cultured cells

Frozen mouse back skin sections were fixed with cold methanol, and unspecific binding sites were blocked with PBS containing 2% bovine serum albumin (BSA) (Sigma)/1% fish skin gelatin (Sigma)/0.05% Triton X-100 (Carl Roth GmbH, Karlsruhe, Germany) for 2 h at room temperature. Samples were then incubated overnight at 4°C with the primary antibodies diluted in the same buffer. After three washes with PBS-T (1×PBS/0.1% Tween 20 (Carl Roth GmbH)), slides were incubated at room temperature for 4 h with secondary antibodies and DAPI (4',6-diamidino-2-phenylindole dihydrochloride) (Sigma) as counter-stain, washed with PBS-T again and mounted with Mowiol (Hoechst, Frankfurt, Germany). Stained sections were photographed using a Leica SP1-2 confocal microscope equipped with a 63×0.6–1.32 NA (Iris) PL Apo Oil objective. Data acquisition was performed using Leica Confocal Software (Leica, Wetzlar, Germany). For immunofluorescence analysis of cultured cells, cells were washed in PBS and then either fixed for 5 min with cold methanol for staining with antibodies against ZO-1 and IRF7, or with 4% paraformaldehyde (PFA) (Sigma) for 20 min at RT for Glyc-D staining. PFA-fixed cells were then incubated for 10 min with 0.5% Triton X-100 in PBS. After 1 h blocking in PBS containing 2% BSA, cells were stained with primary antibodies for 1 h in the same blocking buffer. After three washes with PBS, cells were incubated with secondary antibodies and DAPI. Stained cells were photographed using a Zeiss Imager.A1 microscope equipped with an Axiocam MRm camera and EC Plan-Neofluar objectives (10×/0.3, 20×/0.5). For data acquisition we used the Axiovision 4.6 software (all from Carl Zeiss Inc., Jena, Germany). The Glyc-D positive area was quantified by digital pixel measurements using ImageJ software. Antibodies used for immunofluorescence staining are listed in Appendix Table S1.

2.2.5 RNA isolation and qRT-PCR

Total RNA from the epidermis of mice or from total skin was isolated with Trizol followed by purification with the RNeasy Mini Kit, including on-column DNase treatment (Qiagen, Hilden, Germany). Total RNA from cultured cells was extracted directly with the RNeasy Mini Kit. cDNA was synthesized using the iScript kit (Bio-Rad Laboratories, Berkeley, CA). Relative

gene expression was determined using the Roche LightCycler 480 SYBR Green system (Roche, Rotkreuz, Switzerland). Expression of the genes encoding ribosomal protein L29 (*Rpl29*) or ribosomal protein lateral stalk subunit P0 (*RPLP0*) was used for normalization of expression levels of murine or human genes, respectively, unless otherwise indicated in the figure legends. Primers used for qRT-PCR are listed in Appendix Table S2.

2.2.6 Gene expression profiling and bioinformatic analysis

Epidermis from nine K5-R1/R2 and nine control mice at P18 was separated from the dermis and immediately frozen in liquid nitrogen. Samples from three mice per genotype were pooled and subjected to Affymetrix microarray hybridization (N=3 pools per genotype) [177]. Genes, which were significantly and more than 1.5 log2 (fold change) regulated in K5-R1/R2 compared with control mice were entered into EnrichR to discover functional enrichments of the FGF-regulated genes [178]. Tables referring to Gene Ontology (GO) Biological Process 2017b and Reactome 2016 were downloaded. Lists of significantly upregulated genes, ISGs and original tables from functional enrichments can be found in Dataset EV1.

2.2.7 Cell culture

Primary keratinocytes were isolated from neonatal mice [65] and cultured for 3 days in defined keratinocyte serum-free medium (dK-SFM) (Invitrogen, Carlsbad, CA) supplemented with 10 ng/ml EGF, 10^{-10} M cholera toxin and 100 U/ml penicillin/100 µg/ml streptomycin (Sigma). Plates were coated with collagen IV (Sigma) prior to seeding the cells.

Human primary foreskin keratinocytes were established from foreskin [143]. Foreskin samples had been obtained upon informed written consent of the parents and upon approval by the local ethical committee (KEK-ZH-Nr. 2015-0198) and according to the Declaration of Helsinki Principles. They were cultured in CnT-Prime Epithelial Cell Culture Medium (CELLnTEC, Bern, Switzerland) and used for experiments between passages 3 and 5.

HaCaT keratinocytes [135] were obtained from the owner, Prof. P. Boukamp, German Cancer Research Center Heidelberg, and Caco-2 colon cancer cells were from Sigma. Both cell lines were cultured in DMEM (Sigma) supplemented with 10% FCS (Thermo Fisher Scientific, Waltham, MA).

For treatment of cells with FGF7, FGF10, FGF2 (Peprotech; 10 ng/ml, unless otherwise indicated in the legends), IFN-α (Peprotech, 500-1000 U/ml) or poly(I:C) (Sigma, 5 µg/ml,

unless otherwise indicated in the legends), cells were grown to confluency, starved overnight in serum-free medium, and treated for different time periods. In some experiments, cells were pre-incubated with different inhibitors or vehicle (DMSO) for 2-3 h at 37°C, prior to treatment with FGF7.

2.2.8 Cell transfection and luciferase assay

Transient transfection of HaCaT cells was performed with a TK-Renilla luciferase expression vector and the pGL4.45 [*luc2P*/ISRE/Hygro] reporter vector (Promega, Fitchburg, WI), the latter containing five copies of an ISRE that drives transcription of the luciferase reporter gene. Cells were seeded into 24-well plates, cultured for 24 h, and transfected using Xfect™ (Takara, Kusatsu, Japan). Subsequently, cells were starved in serum-free medium overnight, then treated with FGF7 (10 ng/ml) for 20 h, lysed and assayed with a dual-luciferase assay system (Promega) according to the manufacturer's instructions. Relative light units were measured in a GloMax Discover Microplate (Promega). Firefly luciferase activity was normalized to Renilla luciferase activity (transfection control).

2.2.9 Preparation of protein lysates and Western blot

Cells were harvested in T-PER tissue protein extraction reagent (Pierce, Rockford, IL) containing Complete Protease Inhibitor Cocktail (Roche). Lysates were cleared by centrifugation (13,000 rpm, 30 min, 4°C), snap frozen, and stored at -80°C. The protein concentration was determined using the BCA Protein assay (Pierce). Proteins were separated by SDS-PAGE and transferred onto nitrocellulose membranes. Membranes were incubated with primary antibodies and, subsequently, antibody-bound proteins were detected with horseradish peroxidase-coupled antibodies against goat-IgG (Sigma), rabbit-IgG, or mouse IgG (all from Promega). Antibodies used for Western blot analysis are listed in Appendix Table S1.

2.2.10 HSV-1 production and cell infection

HSV-1 was produced as described [143]. Subconfluent keratinocytes were starved overnight in serum-free medium and then incubated with HSV-1 (MOI = 0.5) in the presence or absence of FGF7, FGF10 or FGF2. Where indicated, infection was preceded by treatment with AZD4547 (Selleckchem, 1 μM), BGJ398 (Selleckchem, 3.5 μM) or DMSO (vehicle) for 3 h before treatment with FGF7. Infected cells were then cultured for 10-16 h before the assessment of

viral load. Alternatively, subconfluent HaCaT cells were infected in DMEM/5% FCS with HSV-1 (MOI=0.5) in the presence or absence of AZD4547 and/or BGJ398 and used for the analysis of viral load 14 h later.

2.2.11 Preparation of genomic and viral DNA from HSV-1 infected cells

Genomic and viral DNA were obtained from infected cells as previously described [143]. Samples were used for quantitative PCR to measure HSV-1 virus load. Primers for amplification of the human β-actin DNA (5'-TAC TCC TGC TTG CTG ATC CAC-3' and 5'-TGT GTG GGG AGC TGT CAC AT-3') and the viral glycoprotein B (*Glyc-B*) DNA (5'-CGC ATC AAG ACC ACC TCC TC-3' and 5'-GCT CGC ACC ACG CGA-3') were used.

2.2.12 Analysis of HSV-1 viral titers

Viral titers were measured using plaque assay. Infected cells were scraped in 500 µl DMEM and lysed by single freeze-thawing. 24-well plates with Vero cells were infected at 37°C for 2 h with serial 10-fold dilutions of the cell lysate. After infection, the lysate was removed and the cells were washed twice with PBS and overlaid with DMEM containing 0.7% agarose. Two days later, the cells were fixed and stained overnight with a solution containing 0.2% crystal violet, 11% formaldehyde, 2% ethanol and 2% paraformaldehyde. The next day the plates were washed with water. Plaques were counted and plaque forming units (PFUs) were calculated taking into consideration the dilution factor.

2.2.13 *Ex vivo* HSV-1 infection

HSV-1 infection of mouse tail epidermis was previously described [179]. Briefly, skin was prepared from the tails of three-months-old mice. The epidermis was separated from the dermis by dispase treatment (5 mg/ml). After floating the epidermal sheets on serum-free DMEM overnight, they were incubated with HSV-1 alone (MOI = 2) or in combination with FGF7 (10 ng/ml) for 48 h and subsequently fixed in 4% PFA for 1 h at RT. Tissues were incubated in blocking solution (PBS 2% BSA/1% fish skin gelatin/0.05% Triton X-100) for 2 h at RT and stained overnight at 4°C with an anti-Glyc-D antibody. After three washes in PBS, epidermal sheets were incubated for 4 h with AF555-conjugated anti-mouse IgG and DAPI diluted in PBS/0.05% Triton X-100 at RT and mounted with their basal side on top of a specimen slide using Mowiol.

2.2.14 LCMV infection and flow cytometric analysis

Subconfluent HaCaT cells were serum-starved overnight and incubated overnight at 37°C with LCMV (MOI 0.05 and 0.2). Cells were detached from the 12-well plate using 1% trypsin and fixed/permeabilized in 500 µl 2× FACS Lyse (Becton Dickinson, Franklin Lakes, NJ) with 0.05% Tween 20 for 10 min at room temperature. After washing, intracellular staining was performed for 30 min at room temperature using the LCMV nucleoprotein-specific antibody VL-4. After washing, they were resuspended in PBS/1% PFA. Flow cytometric analysis was performed using an LSRII flow cytometer (Becton Dickinson). Raw data were analysed using FlowJo software (Tree Star Inc, Ashland, OR).

2.2.15 ZIKV infection

HaCaT cells were seeded on a four-well tissue chamber on a PCA slide (5x 10^4/chamber). After overnight serum starvation, cells were infected with the ZIKV strains Uganda (strain 976) (MOI = 0.1) (kindly provided by the European Virus Archive goes Global (EVAg) project) or French-Polynesia (PF13/251013-18) (MOI = 20). 2 h post infection cells were treated with 20 ng/ml FGF7 or left untreated. Culture medium +/- FGF7 was changed every day. 48 h post-infection cells were either analysed by immunofluorescence using a Flavivirus group-specific antibody (4G2) detecting the ZIKV envelope protein (ZIKV- Env) or harvested and analysed for ZIKV expression levels by qRT-PCR relative to human *RPL27* (ZIKV primers: 5`-AGA TCC CGG CTG AAA CAC TG-3`; 5`-TTG CAA GGT CCA TCT GTC CC-3`).

Alternatively, HaCaT cells were seeded in six-well plates. After overnight serum starvation, confluent cells were infected with the ZIKV strain French-Polynesia (PF13/251013-18) (MOI = 20) in the presence or absence of FGF7 (20 ng/ml). 72 h post-infection cells were analysed for *OAS1* and *MxA* expression levels by qRT-PCR relative to *RPL27*.

2.2.16 Statistical analysis

For all experiments the sample size was estimated based on previous experience. There was no exclusion of any animal or data point. Analysis of stained skin sections or epidermal sheets was performed blinded by the investigators. Group allocation of the mutant mice could not be performed blinded, because the phenotype of the K5-R1/R2 mice is obvious macroscopically and histologically. Experiments were performed at least twice and the number of replicate experiments is indicated in the figure legends.

Statistical analysis was performed using the PRISM software (Graph Pad Software Inc., San Diego, CA). Mann–Whitney U test for non-Gaussian distribution or t-test with Welsh correction were used for experiments examining differences between two groups. For comparison of more than two groups, we used Brown-Forsythe test to verify equal variance between groups, followed by two-way ANOVA and Tukey's multiple comparisons post-hoc tests.

2.2.17 Data availability

The microarray data have been deposited in NCBI's Gene Expression Omnibus and are accessible via the following link:

https://www.ncbi.nlm.nih.gov/geo/query/acc.cgi?acc=GSE111274.

All original Western blots and other original data (including exact P-values) are available in Dataset EV2.

2.3 Results

2.3.1 Inhibition of FGFR signaling promotes expression of IFN-stimulated genes in keratinocytes

To identify FGF targets in the epidermis, we performed microarray analysis of epidermal RNA from mice lacking FGFR1 and FGFR2 in keratinocytes (K5-R1/R2 mice) and control mice without Cre recombinase [65] at postnatal day 18 (P18) and thus prior to the development of skin inflammation and epidermal thickening. Functional enrichment analysis of the differentially regulated genes (log2(f.c.) > 1.5, $p < 0.05$) identified enriched ontologies and pathways that reflect the epidermal abnormalities of K5-R1/R2 mice and the loss of hair follicles and associated melanocytes (Table 1A and B). Remarkably, the top hits are genes characteristic for the "Type I Interferon Response" (Table 1A and B and Dataset EV1), and at least 15% (11/63) of the genes that were upregulated in K5-R1/R2 epidermis compared with controls (log2(f.c.) > 1.5, $p < 0.05$), in particular the majority of the most strongly regulated genes, are classical IFN-stimulated genes (ISGs) (Table 1C). Upregulation of ISGs was confirmed by qRT-PCR analysis of epidermal RNA from adult mice for some of the genes identified in the microarray and for additional ISGs, including IFN response factor 7 (*Irf7*), radical S-adenosyl methionine domain containing 2 (*Rsad2*), 2'-5'-oligoadenylate synthetase-like 2 (*Oasl2*), IFN-induced protein with tetratricopeptide repeats 1 (*Ifit1*), signal transducer and activator of transcription 1 (*Stat1*), and *Stat2* (Fig 1A). Upregulation of some ISGs was already significant at day 5 after birth (P5) and very robust at P9 (Fig 1B) and thus prior to the development of the barrier defect and associated cutaneous abnormalities and concomitant with the complete deletion of the *Fgfr1* and *Fgfr2* genes [65, 180].

Elevated expression of IRF7 in the epidermis of adult K5-R1/R2 mice was confirmed by strong immunostaining in the nuclei of basal and suprabasal keratinocytes of the mutant mice (Fig 1C, red dots indicated by arrows). The nuclear localization of IRF7, which together with IRF3 and NF-κB controls the expression of interferons type I (IFN-α and -β) and type III (IFN-λ), hints at enhanced production of IFNs in the epidermis of FGFR1/R2-deficient mice. Indeed, *Ifnb* and *Ifnl3* expression was significantly increased in freshly isolated, non-cultured keratinocytes from the epidermis of K5-R1/R2 mice, concomitantly with all tested ISGs. This was already seen at P7 and thus preceding the increase in immune cells (Fig 1D).

Upregulation of ISG expression is a cell-autonomous effect, since it was also observed in cultured primary keratinocytes from neonate K5-R1/R2 mice (Fig 1E). However, it was less pronounced compared with non-cultured, freshly isolated keratinocytes (P7), suggesting that IFNs produced by immune cells *in vivo* potentiate this effect. An effect of Cre recombinase on ISG expression was excluded, since the expression levels of these genes were similar in primary keratinocytes isolated from the epidermis of wild-type and K5-Cre mice (Fig 1F). Upregulation of ISG expression in the absence of FGFR1 and FGFR2 was confirmed at the protein level for IRF1, IRF7 and IRF9 by Western blot analysis of total and in particular of nuclear lysates of spontaneously immortalized keratinocytes from K5-R1/R2 mice (Fig 1G). The important role of FGFR signaling in the suppression of ISG expression was confirmed when human immortalized keratinocytes (HaCaT cells) were treated for 48h with the FGFR kinase inhibitor BGJ398 [181] in the presence of serum, which contains low levels of FGFs. FGFR inhibition promoted expression of ISGs, including *RSAD2* and interferon-stimulated gene 15 (*ISG15*) (Fig 1H).

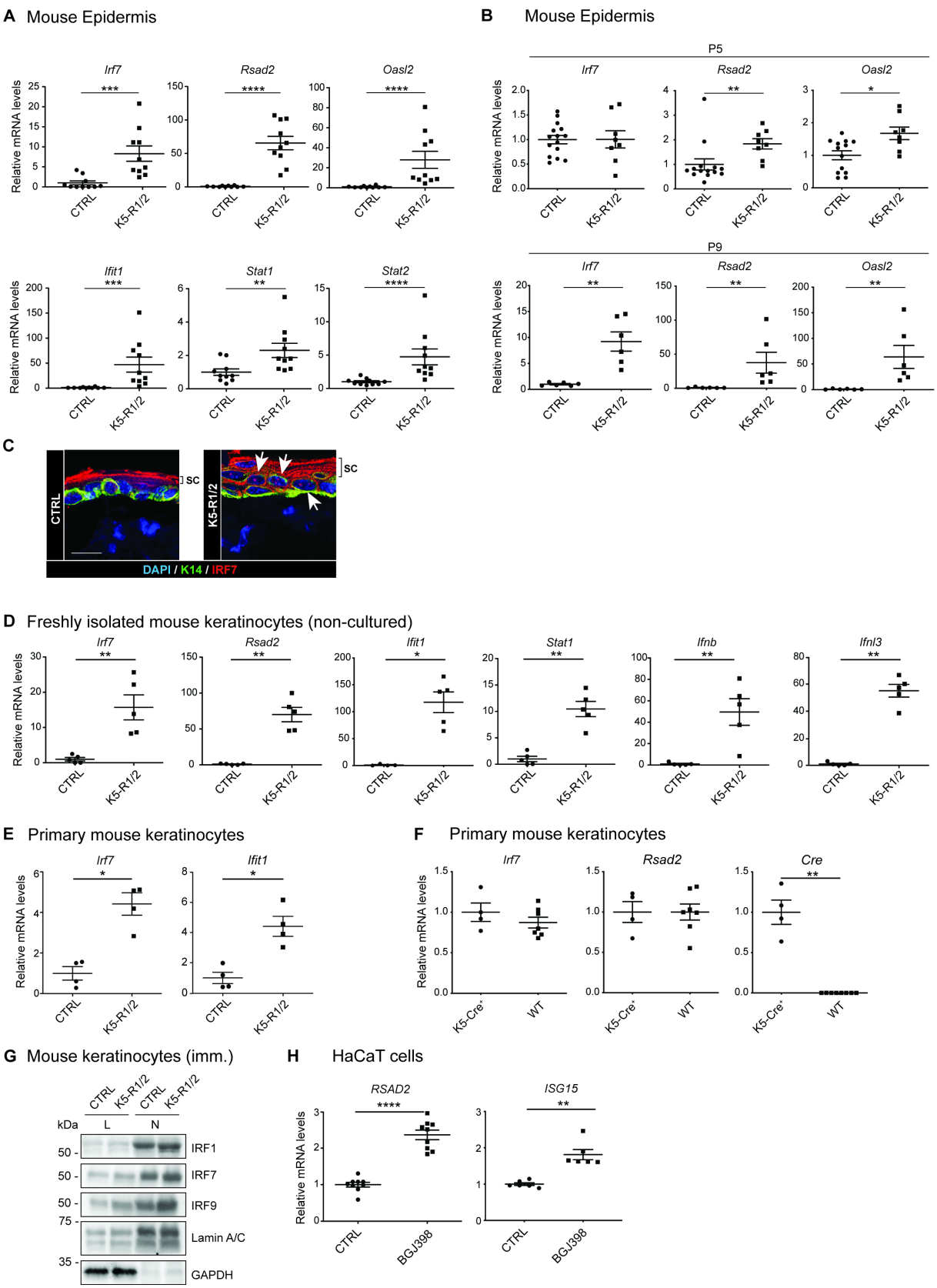

Fig 1: Inhibition of FGFR signaling in keratinocytes promotes IFN and ISG expression.

(**A,B**) qRT-PCR for different ISGs relative to *Rps29* using epidermal RNA from 8 week-old (A) or 5 day- or 9 day-old (B) K5-R1/R2 and control (CTRL) mice.

(**C**) Confocal microscopy images of epidermal sheets from back skin of K5-R1/R2 and CTRL mice stained for IRF7 and K14, counterstained with DAPI. Arrows denote nuclear IRF7 (red) in basal and suprabasal keratinocytes of K5-R1/R2 mice. The strong red staining of the *stratum corneum* (sc) is unspecific background and is more pronounced in K5-R1/R2 mice due to the increased thickness of this layer.

(D) qRT-PCR for different ISGs, *Ifnb,* and *Ifnl3* relative to *Rps29* using RNA from freshly isolated, non-cultured keratinocytes of K5-R1/R2 and control (CTRL) mice at P7.

(**E**) qRT-PCR for ISGs relative to *Rps29* using RNA from primary keratinocytes of neonatal CTRL and K5-R1/R2 mice.

(F) qRT-PCR for ISGs and Cre relative to *Rps29* using RNA from primary keratinocytes of neonatal K5-Cre and wild-type (WT) mice.

(**G**) Western blot analysis of total (L) and nuclear (N) lysates from immortalized (imm.) keratinocytes of CTRL and K5-R1/R2 mice for IRF1, IRF7, IRF9, Lamin A/C (nuclear marker, loading control) and GAPDH (cytosolic marker, loading control).

(**H**) qRT-PCR for *RSAD2* and *ISG15* relative to RPLP0 using RNA from HaCaT keratinocytes treated for 48 h with the FGFR inhibitor BGJ398 (3.5 μM) or vehicle in the presence of serum.

Data information: Scatter plots show mean +/- S.E.M. Mean expression levels in CTRL mice or cell cultures were set to 1, and mRNA levels relative to this value are shown. In (F) expression levels in K5-Cre mice were set to 1. A: N=10 mice per genotype, B: N=6-14 mice per genotype. C: Representative images of two experiments. Magnification bar: 20 μm. D: N=5 mice per genotype. E, F: N=4-7 cultures (each from a different mouse) per genotype. G: Representative of three experiments. H: N=6-9 per treatment group. * $P \leq 0.05$, ** $P \leq 0.01$, *** $P \leq 0.001$, **** $P \leq 0.0001$ (Mann-Whitney U test). Exact P-values are provided in Dataset EV2.

2.3.2 FGFs suppress ISG expression in keratinocytes and intestinal epithelial cells

To further determine if FGF signaling directly regulates ISG expression, we treated primary murine keratinocytes with FGF7, a major ligand of the FGFR2 splice variant expressed on keratinocytes (FGFR2b) [48]. Like many other cell types [182], mouse keratinocytes show a tonic expression of various ISGs. Treatment of these cells with FGF7 for only 3-6 h suppressed the tonic expression of all ISGs that we tested (Fig 2A). This was verified with HaCaT keratinocytes at the mRNA level for ISGs, which were also regulated in mouse keratinocytes and which have a human orthologue with similar function (Fig. 1 and Table 1C) and also for additional ISGs that we tested with the human cells. In HaCaT cells, FGF7 suppressed, for example, the expression of *IRF7*, *RSAD2* and *IRF1* (Fig. 2B; Fig EV1A) and of suppressor of cytokine signaling 1 and 3 (*SOCS1* and *SOCS3*) (Fig EV1A), which are ISG products and involved in negative regulation of IFN signaling [183, 184]. FGF10, which also activates FGFR2b and in addition FGFR1b [48], had a similar effect (Fig 2B and Fig EV1A). The effect

of FGF7 was verified at the protein level for IRF1 and IRF9 (Fig 2C, see also Fig. 3C). By contrast, IRF3 expression was not suppressed by FGF7 at the mRNA or protein level (Fig EV1A and Fig 2C). The efficiency of FGF7 and FGF10 treatment in these experiments was validated by analysis of the expression of dual-specific phosphatase 6 (*DUSP6*), a classical FGF target gene that is strongly upregulated in response to FGFs [162] (Fig EV1A).

The suppressive effect of FGF7 on ISG expression and the concomitant increase in *DUSP6* expression was also observed with the Caco-2 colon cancer cell line, which is responsive to FGF7 [185]. While *IRF7* expression was not regulated by FGF7 in these cells, there was a significant FGF7-induced reduction of the mRNA levels of IFIT1, ISG15 and also of the pattern recognition receptor RIG-I (retinoic acid inducible gene I (encoded by the *DDX58* gene)), which upon ligand binding promotes IFN expression [186] (Fig EV1B). RSAD2 mRNA was not detectable in these cells.

The effect of FGF7 on ISG expression was dependent on the FGFR kinase activity, since it was largely inhibited in primary mouse keratinocytes or human HaCaT keratinocytes upon treatment with the FGFR kinase inhibitors AZD4547 [187] or BGJ398 [181] (Fig EV2A and B). Blockade of the major FGFR signaling pathways, the phosphatidylinositide 3-kinase (PI3K)/AKT and MEK1/2-ERK1/2 pathways mildly, but non-significantly, reduced the effect of FGF7 on the expression of some ISGs in HaCaT keratinocytes, while other ISGs were not affected (Fig EV2C). Importantly, however, combined treatment with MEK1/2 and PI3K inhibitors partially or completely blocked the effect of FGF7 (Fig EV2C). By contrast, we did not observe an effect of phospholipase Cγ inhibition (Fig EV2D). Verification of the activity of the inhibitors is shown in Appendix Figure S1.

In contrast to ISGs, IFN expression is hardly detectable in keratinocytes under normal culture conditions and therefore it is unlikely that a further reduction in IFN protein levels contributes to the effect of FGF7. Furthermore, expression of *SOCS1* and *SOCS3,* which inhibit IFN signaling by competing with STATs for receptor binding and by suppression of JAK activity [188], was even down-regulated by FGF7 or FGF10 (Fig EV1A). Rather, the rapid suppression of the expression level of several ISGs suggests that FGF7 regulates ISGs independent of IFN receptors. To test this possibility, we treated primary keratinocytes from mice lacking the IFN-α and -β receptor (IFNAR) or double knockout mice deficient in IFNAR and the IFN-λ receptor (IFNLR) with FGF7. As expected, expression levels of ISGs were significantly lower in knockout compared to wild-type cells (Fig 2D), but still detectable (Cp values around 27.5 in the cells from double knockout mice). Nevertheless, the FGF7-induced suppression of ISG

expression was still observed in the absence of these receptors (Fig 2E). These findings strongly suggest that FGF7 signaling directly affects the transcription of ISGs. Consistent with this assumption, FGF7 suppressed the basal expression level of a luciferase reporter gene driven by five interferon-stimulated response elements (ISRE) in HaCaT cells (Fig 2F). Since the effect of FGF7 is rapid, it may be the consequence of FGF7-mediated degradation of a protein required for efficient ISG transcription. Indeed, the effect of FGF7 was abolished in the presence of the proteasome inhibitors MG132, epoxomicin or bortezomib (Fig 2G and H and Appendix Fig S2A). The activity of the proteasome inhibitors was verified by Western blot analysis of the nuclear factor erythroid 2-related factor 2 (NRF2) transcription factor, which is rapidly degraded by the proteasome under normal conditions [189] (Appendix Fig. S2B).

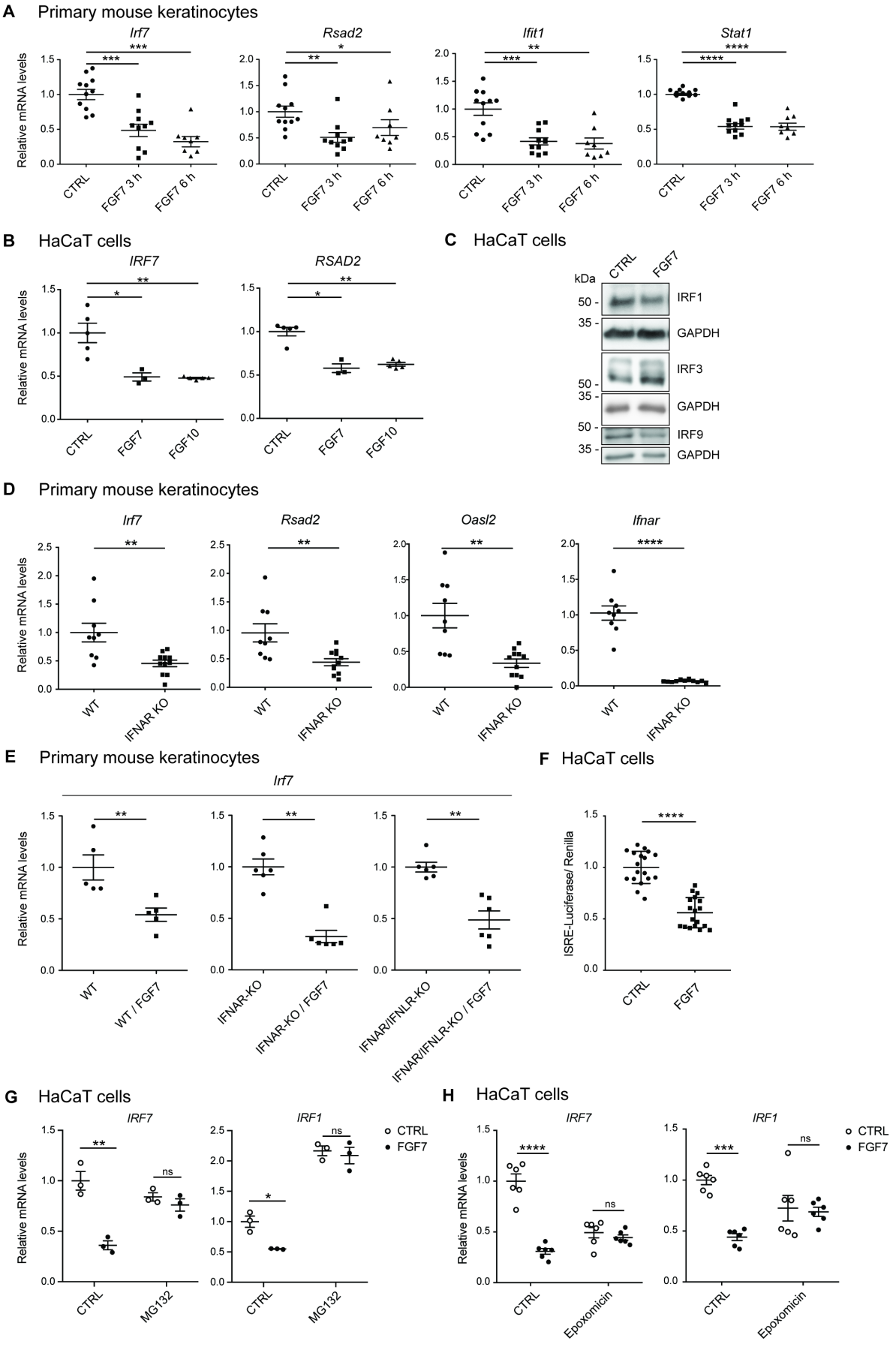

Fig 2: FGF7 and FGF10 suppress the IFN response in keratinocytes.

(**A**) Growth factor-starved primary keratinocytes from WT mice were treated for 3 or 6 h with FGF7 (10 ng/ml) or vehicle (CTRL). RNA samples were analysed by qRT-PCR for the indicated ISGs relative to *Rps29*.

(B) Serum-starved HaCaT keratinocytes were treated for 6 h with FGF7 or FGF10 (each 10 ng/ml). RNA samples were analysed by qRT-PCR for IRF7 and RSAD2 relative to RPLP0.

(C) Serum-starved HaCaT keratinocytes were treated for 16 h with FGF7 (10 ng/ml). Protein lysates were analysed by Western blot for IRF1, IRF3, IRF9 and GAPDH.

(D) RNA samples from untreated, serum-starved primary keratinocytes from WT and Ifnrar1-KO mice were analysed by qRT-PCR for Irf7, Rsad2, Oasl2 and Ifnar1 relative to Rps29.

(E) Growth factor-starved primary keratinocytes from neonatal WT, Ifnar1-KO or Ifnar1/Ifnlr1-KO mice were treated for 24 h with FGF7 (10 ng/ml). RNA samples were analysed by qRT-PCR for Irf7 relative to *Rps29.*

(F) HaCaT keratinocytes were transiently transfected with an ISRE-Luciferase reporter construct and starved 24 h after transfection for 9 h. They were then incubated in the presence or absence of FGF7 (10 ng/ml) for 20 h. Lysates were analysed using a DualGlo Luciferase Assay.

(**G, H**) HaCaT keratinocytes were pre-treated for 2 h with the proteasome inhibitors MG132 (10 μm) (G) or epoxomicin (100 nM) (H), followed by a 20h treatment with FGF7 (10 ng/ml) or vehicle. RNA samples were analysed by qRT-PCR for *IRF7* and *IRF1* relative to RPLP0.

Data information: Scatter plots show mean +/- S.E.M. Mean expression levels in CTRL cell cultures (not treated with FGF7 or any inhibitor) were set to 1. In (D) and in the left panel of (E) expression levels in wt cells were set to 1, while expression levels in untreated IFN receptor knockout cells were set to 1 in the middle and right panel of (E). A: N=8-11 cultures (each from a different mouse) from four experiments. B: N=3-5 from one experiment. C: Representative of 3 experiments. D, E: N=5-11 cultures (each from a different mouse) from two experiments. The results with Ifnar1-KO mice were reproduced in two additional experiments. F: N=16-18 from 4 experiments. G: Representative of four experiments, N=3 per treatment group for each experiment. H: N=6 per treatment group from two experiments. ns: non-significant, * $P \leq 0.05$, ** $P \leq 0.01$, *** $P \leq 0.001$, **** $P \leq 0.0001$ (Mann-Whitney U test (A, B, D, E, F, H) or t-test for assessment of FGF7 effect (G), with Welch correction for *IRF1*. Exact P-values are shown in Dataset EV2.

2.3.3 FGF7 suppresses IFN-induced ISG expression

We tested next whether FGF7 also suppresses the response of keratinocytes to exogenous IFNs. Indeed, the IFN-α-induced upregulation of ISG expression in HaCaT cells was at least in part suppressed by FGF7 (Fig 3A). FGF7 exerted this effect in a dose-dependent manner and was effective in the range between 1 and 10 ng/ml (Fig 3B).

Western blot analysis showed strong suppression of IRF1 protein levels by FGF7 (12 h treatment) in the presence or absence of IFN-α. However, levels of total and phosphorylated STAT1 (Y701 and S727) and of RSAD2 were not affected, possibly because of a longer half-

life of these proteins. IRF9 protein levels were down-regulated by FGF7 in the absence, but not in the presence of IFN-α (Fig. 3C).

The suppressive effect of FGF7 on the basal and IFN-α-induced ISG expression was verified with primary human keratinocytes (Fig 3D). We only used cells from two donors in this experiment, but the values were very similar among them.

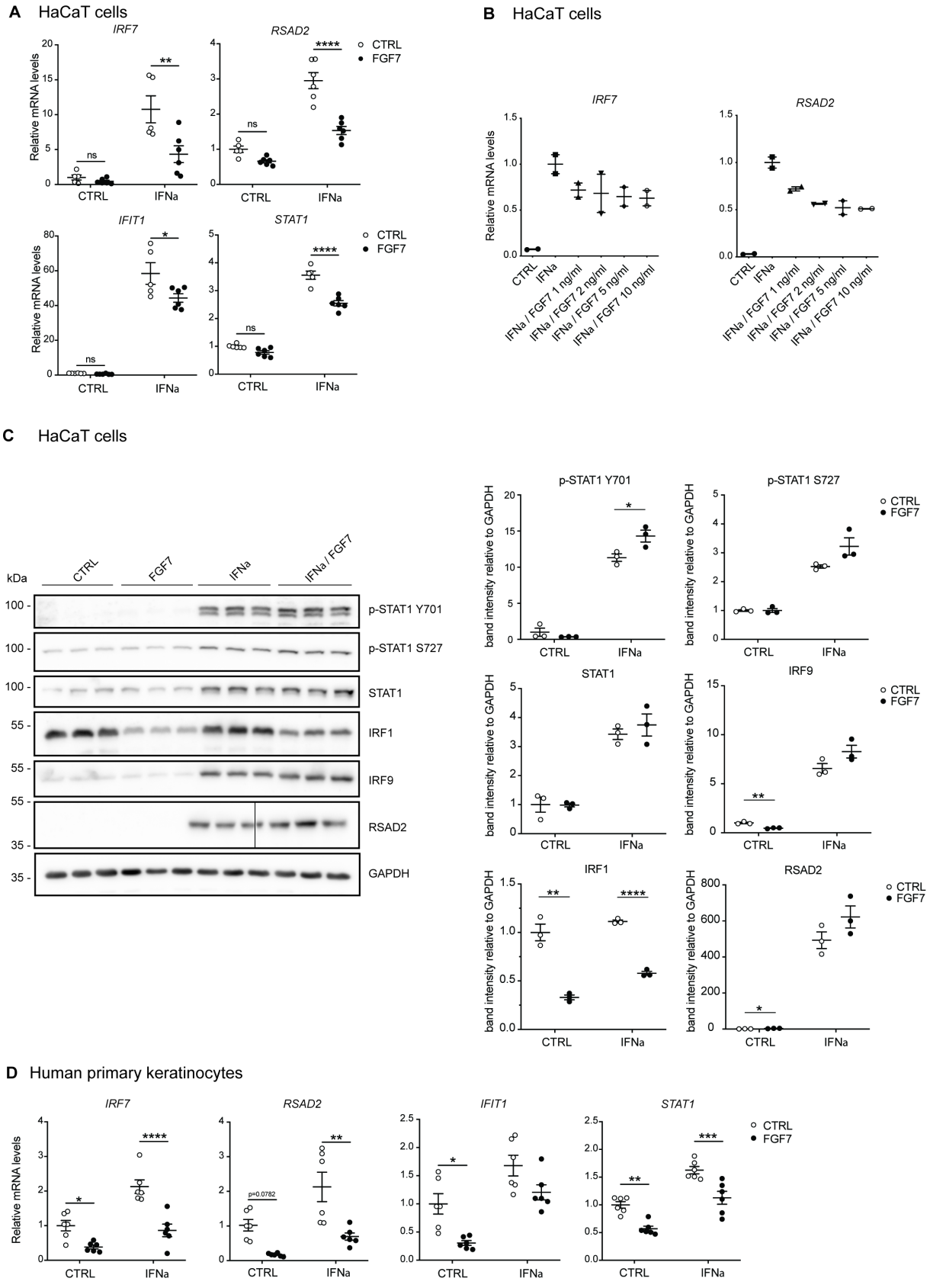

Fig 3: FGF7 suppresses IFN-induced ISG expression.

(A-C) Serum-starved HaCaT keratinocytes were treated with FGF7 (10 ng/ml (A, C) or different concentrations as indicated (B) and/or IFN-α (500-1000 U/ml) for 12-16 h. RNA was analysed by qRT-

PCR for ISGs relative to RPLP0 (A, B) and protein samples by Western blot for total and pSTAT1 (Y701 and S727), IRF1, IRF9 and RSAD2 and GAPDH (C). The vertical line in the RSAD2 blot indicates a place where the gel was broken. Densitometric quantification of the different blots (N=3) is shown on the right.

(**D**) Human primary keratinocytes were starved and treated for 12 h with FGF7 (10 ng/ml) and/or IFN-α (1000 U/ml). RNA samples were analysed by qRT-PCR for ISGs relative to RPLP0**.**

Data information: Scatter plots show mean +/- S.E.M. Mean expression levels in CTRL cell cultures were set to 1. A: N=5-6 from two independent experiments. B: N=2-3 from one experiment. C: Representative blot from two experiments. The intensities of the bands were used for the quantification (N=3). D: N=6 replicates from two experiments with cells from two donors. ns: non-significant, * $P \leq 0.05$, ** $P \leq 0.01$, *** $P \leq 0.001$, **** $P \leq 0.0001$ (2-way ANOVA with Tukey's multiple comparisons test (A, D) or t test with Welch correction for assessment of FGF7 effect (C)). Exact P-values are shown in Dataset EV2.

2.3.4 FGF7 suppresses poly(I:C)-induced ISG and IFN expression

ISGs encode various proteins that control IFN production, such as the transcription factors IRF7 and IRF1 [190, 191], and different proteins involved in nucleic acid sensing [192]. Therefore, we tested if FGF signaling also suppresses IFN expression. Indeed, when HaCaT cells were treated with poly(I:C), which induces IFN expression by binding to toll-like receptor 3 (TLR3) [193], expression of *IFNB* and of *IFNL1* was strongly induced. This was accompanied by a strong increase in the expression of *IRF7*, *RSAD2, IRF1, CGAS, TLR3* and *DDX58* (Fig 4A). The poly(I:C)-induced increase in the expression of *IFNB*, *IFNL1*, *IRF7*, *RSAD2*, *IRF1* and *DDX58* was significantly suppressed by FGF7 (Fig 4A), demonstrating that FGF signaling not only interferes with the IFN response, but also with the expression of IFNs. The poly(I:C)-induced increase in TLR3 mRNA levels was also mildly, although non-significantly reduced by FGF7, while cyclic GMP-AMP synthase (*CGAS*) expression was not affected (Fig 4A). The effect of FGF7 was confirmed at the protein level for total and phosphorylated STAT1 (Y701 and S727), and for phosphorylated STAT2 (Y690), reflecting the suppression of IFN production (Fig 4B and quantification in Fig EV3). As shown before (Fig. 2C and 3C), IRF1 and IRF9 expression was suppressed by FGF7 in the basal state, but this was overruled at this time point by the strong effect of poly(I:C) (Fig. 4B and quantification in Fig EV3).

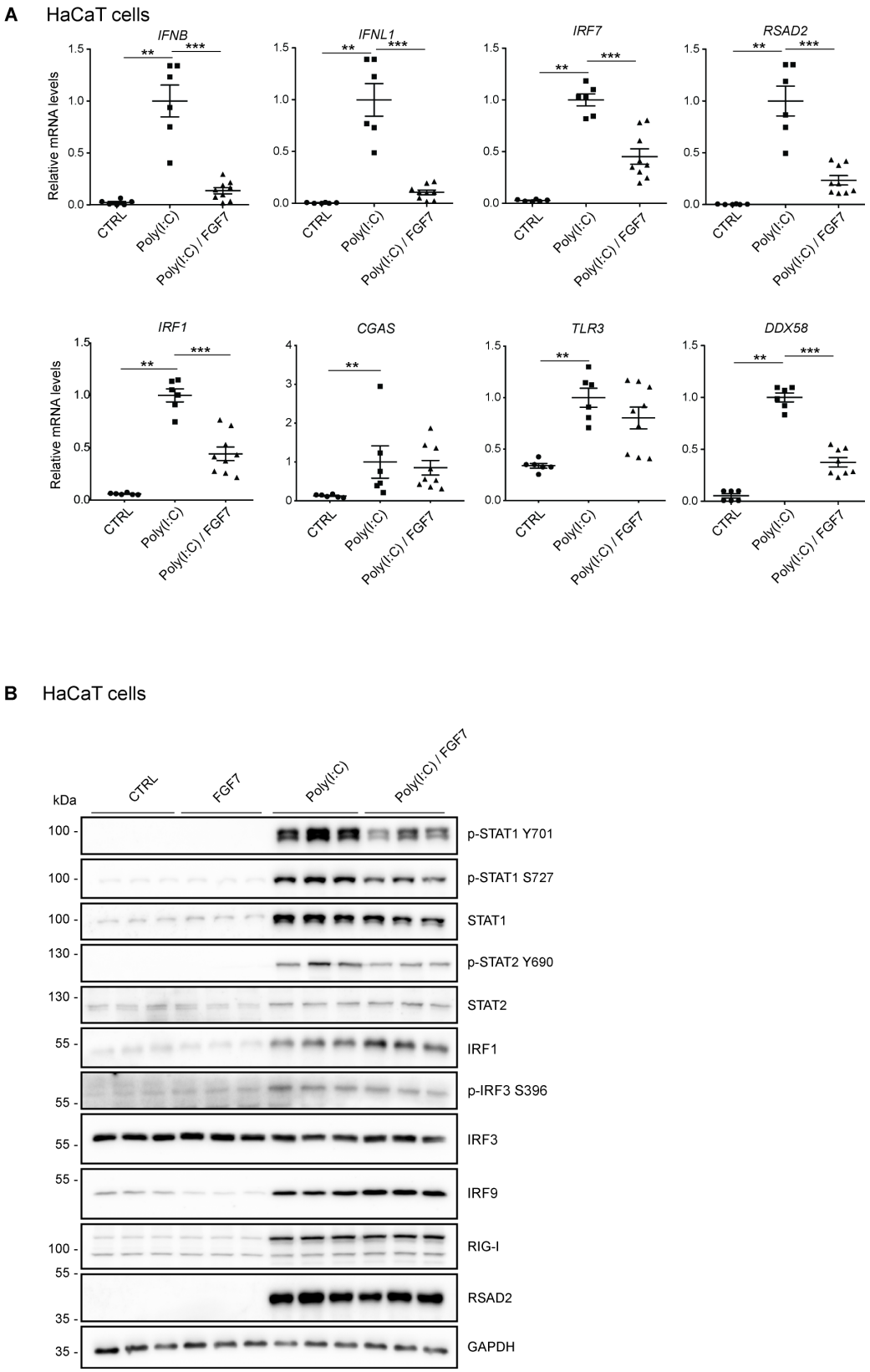

Fig 4: FGF7 suppresses poly(I:C)-induced IFN and ISG expression.

(**A**) Serum-starved HaCaT cells were treated for 24 h with poly(I:C) (5 µg/ml) in the presence or absence of FGF7 (10 ng/ml). RNA samples were analysed by qRT-PCR for *IFNL1*, *IFNB*, *RSAD2*, *IRF1*, *IRF7*, *CGAS, TLR3 or DDX58,* relative to RPLP0.

(**B**) Serum-starved HaCaT cells were treated for 18 h with poly(I:C) (5 μg/ml) in the presence or absence of FGF7 (10 ng/ml). Protein lysates were analysed by Western blot for total and pSTAT1 (Y701 and S727), total and pSTAT2 (Y690), IRF1, IRF3, pIRF3 (S396), IRF9, RIG-1, RSAD2 and GAPDH.

Data information: Scatter plots show mean +/- S.E.M. Mean expression levels in cell cultures treated with poly(I:C) only were set to 1, since IFN mRNA levels in non-treated cells are hardly detectable. A: N=6-9 from two experiments. B: Representative blot from two experiments. Quantification of the bands is shown in Figure EV3. ** $P \leq 0.01$, *** $P \leq 0.001$ (2-way ANOVA with Tukey's multiple comparisons test). Exact P-values are shown in Dataset EV2.

2.3.5 FGF signaling promotes replication of Herpes Simplex Virus type 1 (HSV-1) in keratinocytes

The potent effect of FGF signaling on IFN and ISG repression raised the intriguing possibility that modulation of FGF signaling may affect viral infection. Since human keratinocytes are the first entry sites for HSV-1 [194], we used this pathogen to address this question. Indeed, FGF7 boosted the production of viral glycoprotein B (*Glyc-B*) DNA and of glycoprotein D (Glyc-D) protein after HSV-1 infection of HaCaT keratinocytes, while IFN-α had the opposite effect (Fig 5A and B). 48 h after infection, HSV-1 infected cells had fused, but were still attached. In the presence of FGF7, however, most infected cells were detached (Fig 5C). The effect of FGF7 on HSV-1 viral load was dose-dependent (Fig 5D) and was also observed with human primary keratinocytes from two different donors (Fig 5E). It is most likely mediated via the FGFR2b splice variant on keratinocytes, since the high affinity ligands of this receptor, FGF7 and FGF10, strongly elevated Glyc-D DNA and protein levels, whereas FGF2, which binds to FGFR2b with much lower affinity [50], had only a weak effect (Fig 5F). When we infected epidermal sheets from mouse tail skin *ex vivo* with HSV-1 in serum-free medium, the virus preferentially infected cells of the hair follicles as indicated by follicular staining for Glyc-D (Fig 5G, middle panel). FGF7 treatment resulted in a much larger Glyc-D-positive area, and virus-infected cells were seen throughout the interfollicular epidermis (Fig 5G, right panel). Promotion of HSV-1 infection of cultured keratinocytes by FGF7 was even observed in the presence of IFN-α (Fig 5H). There was still a considerable elevation in viral DNA levels even when FGF7 was added 4 h after addition of HSV-1 and after removal of the virus (Fig 5I). While this result does not exclude an effect on viral entry, it suggests that FGF7 mainly promotes viral replication. Consistent with this assumption, expression of nectin-1 (*NECT1*), which is required for HSV-1 entry into keratinocytes [194, 195], was even slightly down-regulated by FGF7 (Fig 5J).

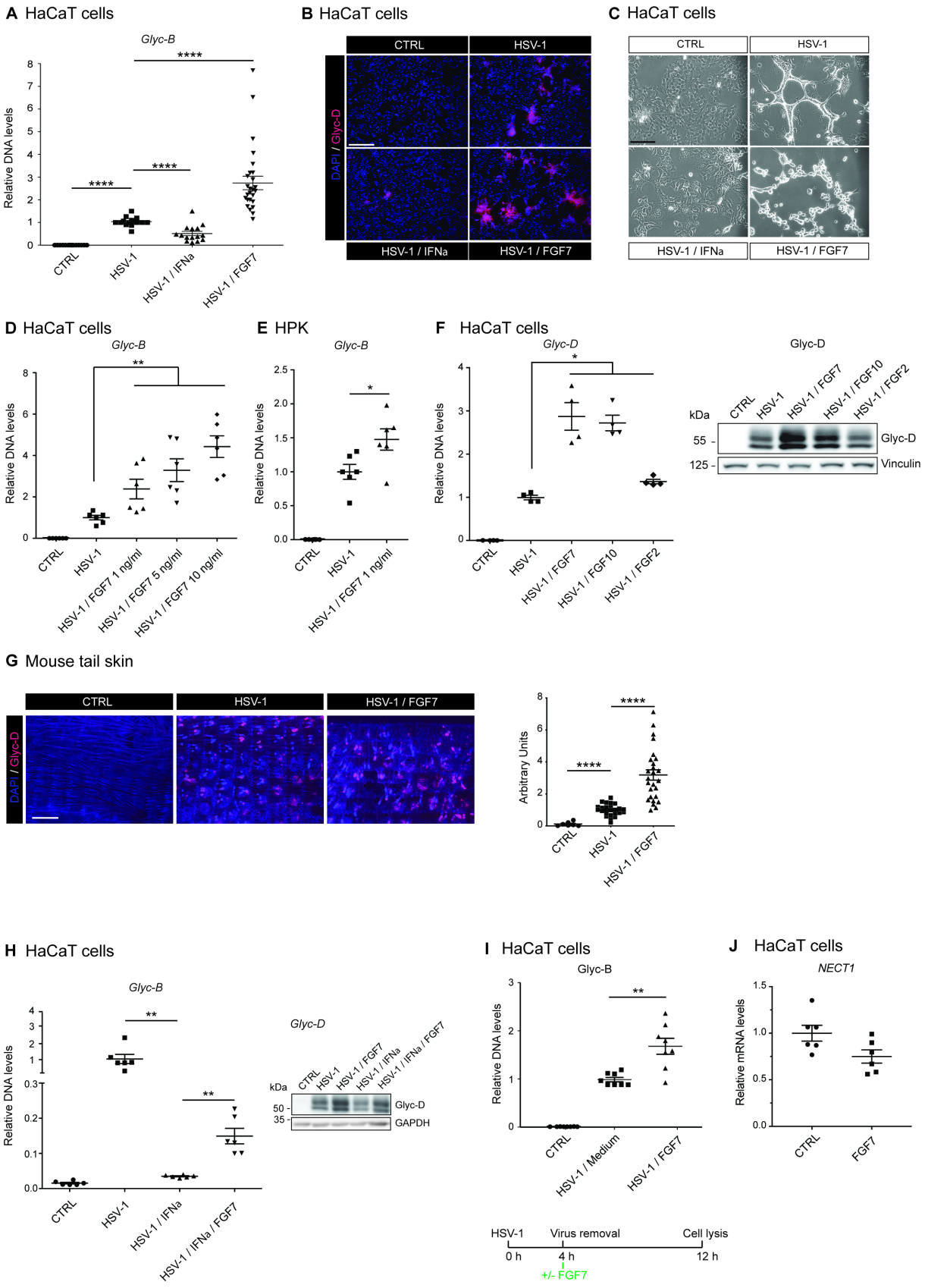

Fig 5: FGF7 promotes HSV-1 replication in human keratinocytes.

(**A-C**) Serum-starved HaCaT cells were infected with HSV-1 (MOI=0.5) in the presence or absence of FGF7 (10 ng/ml) or IFN-α (1000 U/ml). Viral load was determined 24 h post infection (hpi) by qPCR

for the HSV-1 *Glyc-B* gene relative to the human β-actin gene (*ACTB*) (A) or by HSV-1 Glyc-D immunofluorescence (red) and DAPI counterstaining (blue) (B). (C) Transmission microscopy images of HaCaT cells 48 h post infection (hpi).

(**D, E**) Serum-starved HaCaT cells (D) or human primary keratinocytes (HPK, from two donors) (E) were infected with HSV-1 (MOI=0.5) in the presence or absence of FGF7 at the indicated concentrations. Virus load was determined by qPCR for HSV-1 *Glyc-B* relative to *ACTB* 24 hpi.

(**F**) Serum-starved HaCaT cells were infected with HSV-1 (MOI=0.5) in the presence or absence of FGF7, FGF10 or FGF2 (10 ng/ml). DNA samples were analysed by qPCR for *Glyc-D* DNA relative to *ACTB* and protein lysates were analysed by Western blot for Glyc-D and vinculin 10 hpi.

(**G**) Epidermal sheets from tail skin, infected *ex vivo* with HSV-1 (MOI = 2) +/- FGF7 (10 ng/ml), were stained 48 hpi for Glyc-D (red) using DAPI as counterstain (blue). The infected area (red staining) was measured using Image J software. Data are expressed as A.U. = arbitrary unit. Background staining of hairs was subtracted manually.

(**H**) Serum-starved HaCaT cells were infected with HSV-1 in the presence or absence of FGF7 (10 ng/ml) or IFN-α (1000 U/ml). Viral load was determined 24 hpi by qPCR for the HSV-1 *Glyc-B* gene relative to *ACTB* or by Western blot for the viral protein Glyc-D and GAPDH.

(**I**) Serum-starved HaCaT cells were infected with HSV-1 (MOI = 0.5). Four hours hpi, infected cells were washed and incubated in fresh serum-free medium containing FGF7 (10 ng/ml). Viral load was measured 8 h later by qPCR for *Glyc-B* relative to *ACTB*.

(**J**) Serum-starved HaCaT keratinocytes were treated for 6 h with FGF7 (10 ng/ml). RNA samples were analysed by qRT-PCR for *NECT1* (encoding nectin-1) relative to *RPLP0*.

Data information: Scatter plots show mean +/- S.E.M. In (A), and (D-I) mean viral DNA levels or stained area in HSV-1-infected, but non-treated cells were set to 1. In (J) mean expression levels in CTRL cell cultures were set to 1. A: N=16-24 from four independent experiments. B, C: Representative pictures are shown. D: N=6 from one experiment. E: N=6 from two experiments and two donors. F: N=4 from two experiments. The Western blot is a representative of two experiments. G: N=16-24 measured areas from 8 mice from 4 experiments. H (scatter plot): N=6 from two experiments. The Western blot is a representative of two experiments. I: N=8 mice from two experiments. J: N=6 from 2 experiments. * $P \leq 0.05$, ** $P \leq 0.01$, **** $P \leq 0.0001$ (Mann-Whitney U test). Exact P-values are shown in Dataset EV2. Magnification bars: 200 μm (B) or 80 μm (C) and 800 μm (G).

We next treated keratinocytes with FGF7 at different time points after HSV-1 infection (Fig. 6A). FGF7 suppressed ISG expression and caused a robust increase in HSV-1 DNA when added together with the virus or 2-4 h post infection (Fig 6B and C) and was thus present for 8-12 h. However, when FGF7 was added 8 h post infection, suppression of ISG expression and promotion of viral replication was no longer observed (Fig 6C). Importantly, Glyc-B DNA levels negatively correlated with the mRNA levels of ISGs and of IFNL2 (Fig 6B-D). This inverse correlation was also seen at the protein level: High levels of the HSV-1 Glyc-D protein correlated with reduced levels of RSAD2, IRF7, IRF9, STAT2, and IRF1, while there was no correlation with STAT1 and IRF3. In addition, Glyc-D levels inversely correlated with levels

of phosphorylated STAT1 and STAT2 (Fig 6E). These findings strongly suggest that the FGF7-mediated suppression of ISG and also of IFN expression contributes to the promotion of viral replication.

2.3.6 FGF signaling promotes replication of RNA viruses

The FGF7 effect was not restricted to the DNA virus HSV-1, but it also promoted replication of the RNA virus lymphocytic choriomeningitis virus (LCMV). Expression levels of LCMV nucleoprotein (NP) were strongly elevated in the presence of FGF7, while IFN-α had the opposite effect (Fig 6F).

Next, HaCaT cells were infected with two strains of the human pathogen Zika virus (ZIKV), which naturally gains access to the body via mosquito bites and can infect cells of the skin, including keratinocytes [196]. The number of cells expressing the ZIKV envelope protein (ZIKV-ENV) was higher in FGF7-treated compared to mock-treated cells (Fig 6G). qRT-PCR analysis of ZIKV RNA demonstrated that FGF7 was also effective when added 2 h after infection (Fig 6H). Consistent with the important role of ISGs in the effect of FGF7, *MxA* (human myxovirus resistance protein) and *OAS1* (2'-5'-oligoadenylate synthase 1), two ISGs that are highly expressed during infection by viruses of the *Flaviviridae* family [197], were upregulated during ZIKV infection, and FGF7 antagonized this effect (Fig 6I and J).

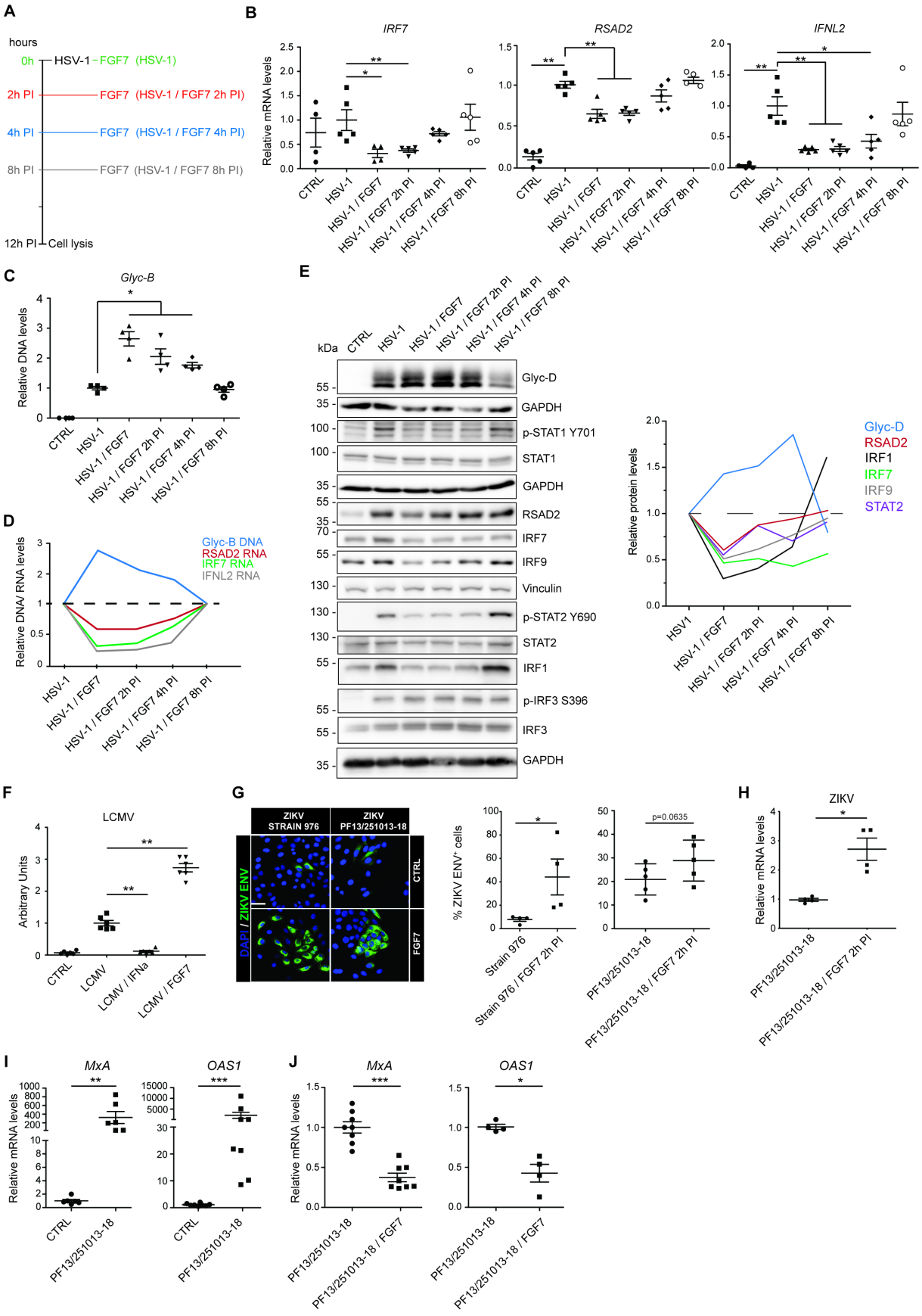

Fig 6: FGF7 suppresses virus-induced ISG expression and stimulates replication of different viruses in keratinocytes.

(**A-E**) Serum-starved HaCaT cells were infected with HSV-1 (MOI=0.5) +/- FGF7 (10 ng/ml), added at the indicated time points (A). 12 h after infection, RNA samples were analysed by qRT-PCR for *RSAD2*, *IRF7* and *IFNL2* relative to *RPLP0* (B), DNA samples were analysed by qPCR for *Glyc-B* DNA relative to *ACTB* (C), and protein lysates were analysed by Western blot for Glyc-D, total and phosphorylated STAT1 (Y701), STAT2 and IRF3, for IRF1, IRF7, IRF9 and RSAD2 and for GAPDH or vinculin (loading controls) (E). Quantification of the Glyc-D, RSAD2, IRF1, IRF7, IRF9 and STAT2 band intensity relative to GAPDH is shown on the right hand side. (D) shows mean *Glyc-B* DNA and RSAD2, IRF7 and IFNL2 mRNA levels (based on results shown in Fig. 6B and C) in virus-infected cells treated for different periods with FGF7.

(**F**) HaCaT cells were infected with LCMV in the presence or absence of FGF7 (10 ng/ml) or IFN-α (1000 U/ml) and analysed for LCMV nucleoprotein (NP) by flow cytometry 24 hpi. Arbitrary units are shown.

(**G, H**) HaCaT cells were infected with ZIKV strains 976 (Uganda isolate) (MOI = 0.1) or PF13/251013-18 (French Polynesia isolate) (MOI = 20) and treated 2 hpi with FGF7 (20 ng/ml) or vehicle (CTRL). Immunofluorescence staining for the ZIKV envelope protein and quantification of the percentage of cells expressing the ZIKV envelope protein (G) and qRT-PCR analysis of RNA samples for ZIKV RNA (H) 48 hpi is shown.

(**I, J**) HaCaT cells were infected with the ZIKV PF13/251013-18 (MOI = 20) in the presence or absence of FGF7 (20 ng/ml). RNA samples were analysed by qRT-PCR for *OAS1* and *MxA* relative to *RPLP0* 72 hpi.

Data information: Scatter plots show mean +/- S.E.M. In (B-H and J) results obtained with virus-infected, but non-treated cells were set to 1; in (I) mean expression levels in non-infected cell cultures were set to 1. B: N=4-5 from 2 experiments. C: N=4 from 2 experiments. E: Representative blots of two experiments. F: N=5-6 from two experiments. G, H: N=4 from one experiment. I, J: N=4-8 from two experiments. Magnification bar in (G): 40 μm. * $P \leq 0.05$, ** $P \leq 0.01$, *** $P \leq 0.001$ (Mann-Whitney U test). Exact P-values are provided in Dataset EV2.

2.3.7 Inhibition of FGFR signaling is an antiviral strategy

Finally, we determined whether FGFR inhibitors have antiviral activity. As expected, the FGF7-induced promotion of viral replication in serum-starved keratinocytes was suppressed by the FGFR kinase inhibitors AZD4547 and BGJ398 as determined by analysis of *Glyc-B* DNA and Glyc-D protein levels 24 h after HSV-1 infection (Fig 7A). In the presence of serum, which contains FGFs, HSV-1 infection was effectively suppressed by treatment with these inhibitors alone or in combination as demonstrated by analysis of *Glyc-B* DNA levels or viral titers (Fig 7B and C). Since both inhibitors are highly selective for FGFR1-3, these findings strongly suggest that FGFR inhibition is sufficient to suppress viral replication in serum-containing medium, although a minor contribution of other kinases that are inefficiently inhibited by AZD4547 and BGJ398 cannot be excluded.

Finally, we examined the effects of loss of FGFR signaling on HSV-1 replication *in vivo*. 48 h after subcutaneous inoculation of HSV-1 into wild-type mice [198], we observed a mild, but significantly increased expression of *Fgf7* (Fig 7D). Notably, the viral load was significantly lower in K5-R1/R2 compared with control mice 48 h after cutaneous HSV-1 infection as revealed by PCR analysis of the DNA encoding the immediate-early protein ICP0 (Fig 7E).

Taken together, these results highlight the biological relevance of the FGF-mediated regulation of ISG expression and the antiviral activity of FGFR kinase inhibition.

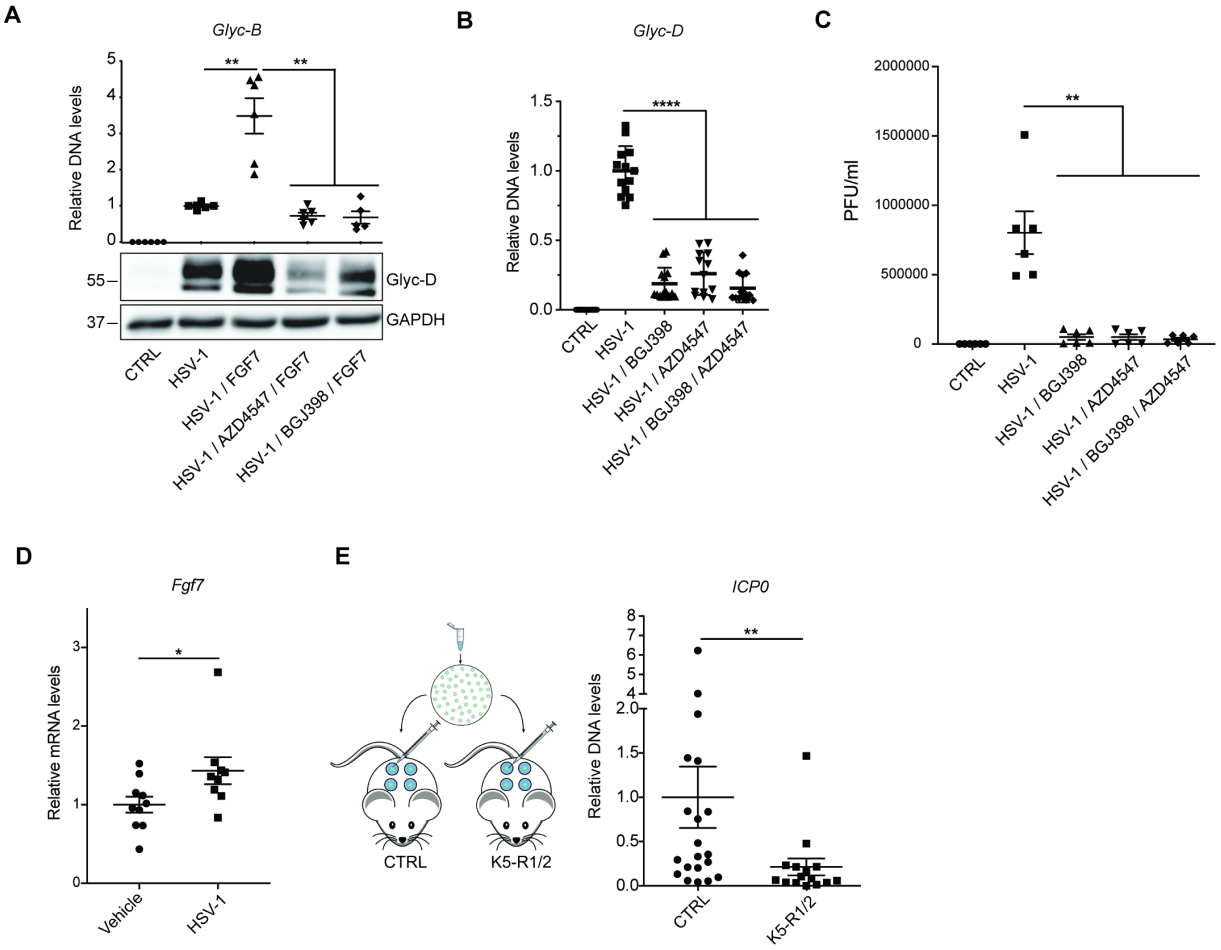

Fig 7: Inhibition of FGFR signaling blocks HSV-1 replication.

(**A**) Serum-starved HaCaT cells were infected with HSV-1 (MOI = 0.5) in the presence or absence of FGF7 (10 ng/ml) and the FGFR kinase inhibitors AZD4547 (1 μM) or BGJ398 (3.5 μM). DNA and protein lysates were analysed by qPCR for *Glyc-B* relative to *ACTB* or by Western blot for Glyc-D and GAPDH, respectively, 16 hpi.

(**B, C**) HaCaT cells were cultured in DMEM/10% FCS (B) or DMEM/5% FCS (C) and infected with HSV-1 (MOI=0.5) in the presence or absence of AZD45347 (1 μM) and/or BGJ398 (3.5 μM). Viral load was determined by qPCR for *Glyc-D* relative to *ACTB* (B) or by measurement of viral titers (plaque forming units (PFU)) 14 hpi (C).

(**D, E**) Adult C57BL/6 wild-type (D) or K5-R1/R2 mice and respective controls (E) were infected subcutaneously with HSV-1 (MOI = 10). RNA from infected skin was analysed by qRT-PCR for *Fgf7* relative to *Rps29* (D) and DNA was analysed by qPCR for *ICP0*, normalized to the host gene *Tbx15* 48 hpi (E).

Data information: Scatter plots show mean +/- S.E.M. In (A, B) mean viral DNA levels in HSV-1-infected, but non-treated cells were set to 1. In (C) absolute PFU/ml cell lysate is shown. In (D) mean expression in non-infected mice (vehicle-injected) were set to 1, and in (E) mean *ICP0* DNA levels in Ctrl mice were set to 1. A: N=5-6 from two experiments. B: N=12-13 from 4 experiments. C: N=6 from two experiments. D: N=9-10 infected mouse skin spots from two experiments. F: N=20-24 infected mouse skin spots from two experiments. * $P \leq 0.05$, ** $P \leq 0.01$, **** $P \leq 0.0001$ (Mann-Whitney U test). Exact P-values are provided in Dataset EV2.

2.4 Discussion

We identified an unexpected role of FGFR signaling in antiviral defence, which is mediated at least in part via control of the cellular IFN response. FGFs exert their early effect on ISG expression at the transcriptional level and in an FGFR kinase-dependent, but IFN receptor-independent manner. This conclusion is based on the findings that 1) FGF7 and FGF10 suppressed ISG expression already within 3-6 h, 2) the FGF-mediated suppression of ISG expression was still observed in the absence of the receptors for type I and type III IFNs, 3) expression of *SOCS1* and *SOCS3*, which encode inhibitors of the IFN receptor signaling complex, was not upregulated by FGF7, and 4) FGF7 suppressed the expression of an ISRE reporter gene. The effect of FGF7 is likely to involve proteasomal degradation of a protein required for ISG expression, since it was abolished in the presence of different proteasome inhibitors. Our results further suggest an involvement of a combination of the MEK1/2-ERK1/2 and PI3K-AKT pathways in the FGF7-mediated ISG regulation. A role of MEK/ERK signaling is consistent with the induction of a type I IFN response in human keratinocytes by MEK inhibitors [199] and with the down-regulation of the IFN-induced antiviral response by activated Ras in fibroblasts [200].

The ISREs present in the promoters of ISGs are recognition sites for the IFN-stimulated gene factor 3 (ISGF3), a complex of IRF9, pSTAT1 and pSTAT2 [201]. ISREs also have an embedded IRF response element (IRE) [184], and ISREs and/or IREs are present in the promoters of ISGs [188]. Through binding to ISREs and IREs, different IRFs, including IRF9, IRF1 and IRF7, regulate ISG expression [191, 202]. Since IRF and also STAT1/2 levels are frequently regulated by ubiquitination and subsequent proteasomal degradation [203-205] and since inhibition of the proteasome blocked the effect of FGF7 on ISG expression, IRFs and STATs are candidate targets of the rapid effect of FGF7. Future biochemical/proteomics studies will be required to characterize the ISRE/IRE-bound proteins in the presence or absence of FGF7 or FGFR inhibitors to further elucidate the molecular mechanism of this pathway.

The two-to-three-fold down-regulation of the expression of various ISGs within a few hours of FGF7 stimulation is likely to be sustained, since some ISGs encode positive regulators of ISGs, such as STAT1, STAT2 and several IRFs [201]. In particular the effect of FGF7 on IRF7, but also on IRF1, which was shown to regulate IFN expression [206], also provides a likely explanation for the FGF-mediated impairment of IFN expression in response to poly(I:C) or viruses. This is likely to be potentiated by the FGF-mediated suppression of ISGs that encode proteins involved in pathogen sensing and subsequent induction of IFN expression.

IFNs and ISGs are known for their multiple activities in the control of cell proliferation, apoptosis, cancer inhibition and immunomodulation [207, 208]. Thus, the results presented in this study may have widespread positive or negative consequences *in vivo*. It remains to be determined whether the increased expression of ISGs contributes to the atopic dermatitis-like phenotype that develops in K5-R1/R2 mice. This is, however, not very likely, since ISGs were already upregulated prior to the development of the phenotype and even before the excessive infiltration of the skin by immune cells.

By contrast, the effect of FGFs on IFN and ISG expression correlated with a strong suppression of the antiviral defence, a key function of IFNs. FGF7 mainly promoted viral replication, although an effect on viral entry cannot be excluded due to the inhibitory effect of ISGs on different stages of the viral life cycle [209]. It has been suggested that HSV-1 enters cells via FGF receptors [210]. However, this cannot explain the effect that we observed, since FGF7 enhanced the viral load, while the entry of HSV-1 via an FGFR was inhibited by recombinant FGF [210]. In addition, our results suggest that the effect of FGFs on HSV-1 infection is not mediated via nectin-1 expression. This is further supported by the finding that FGF7 also inhibited replication of the RNA viruses ZIKV and LCMV. Rather, the effect on different viruses is consistent with the broad antiviral activities of ISGs [211].

Interestingly, FGF7 expression is upregulated in wounded/inflamed skin [212] and also in response to cutaneous HSV-1 infection (this study). This may promote viral replication at the site of injury/inflammation through suppression of ISG expression. Therefore, the beneficial effect of increased FGF7 expression, which includes promotion of tissue repair and protection from physical and chemical insults [42, 213], may come with a risk of enhanced viral infections.

The results of our work are likely of medical relevance, since they suggest the use of FGFR inhibitors for the control of viral infections in humans. Such an approach would most likely not be confined to the skin. Consistent with this assumption, FGF2 promoted hepatitis C virion production in hepatoma cells [214] and Zika virus infection of human fetal astrocytes [215]. Furthermore, FGF7 or FGF2 suppressed the expression of some ISGs in human lung epithelial cells [216], colon cancer cells (this study) or in human astrocytes, respectively [215]. However, the use of FGFR inhibitors as an antiviral strategy will require a precise timing of the treatment, since they may affect tissue healing. Indeed, inhibition of FGFR signaling impeded the repair of mouse lungs after influenza virus infection [217]. Besides timing, the affected cell type and its FGFR expression pattern is likely to be relevant. Thus, a subset of FGFs, which mainly activate FGFR3, inhibited infection of different types of cancer cells with Vesicular Stomatitis

Virus or Coxsackie Virus through an as yet unidentified mechanism that is independent of ISG regulation [218]. Therefore, it will be important to determine whether certain cancer cells, amongst which many show deregulated FGFR signaling [173], may not be protected from viruses by FGFR inhibitors, but rather become more susceptible. Furthermore, other effects of FGFs on the viral life cycle need to be considered as recently shown for Dengue Virus, where inhibition of FGFR4 decreased viral replication, but increased the infectivity of the resulting virions [219].

In spite of these open questions, the prospect of using FGFR inhibition as an antiviral strategy is promising, since FGFR kinase inhibitors, FGFR neutralizing antibodies or FGF ligand traps are in clinical trials for the treatment of different types of cancers and are generally well tolerated [54, 173]. Obviously, such a novel indication for FGFR inhibitors will require intensive studies regarding dosing, mode of application, efficacy against different viruses and side effects in virus-infected patients. Nevertheless, the effort seems to be justified given the limited options for the treatment of viral infections, of which some have a high mortality rate or for which vaccines are not yet available, such as SARS-CoV-2. Virostatic agents, which interfere with the viral life cycle, are frequently employed. However, they are most often virus-specific and thus susceptible to viral variation, and they often exhibit high toxicity. Thus, improved strategies are urgently needed, and FGFR inhibition is a fundamentally different approach.

Acknowledgments

We thank Stefanie Trautweiler, ETH Zurich, for experimental help, Drs. Andrii Kuklin, ETH Zurich, Gian Paolo Dotto, University of Lausanne, Cord Brakebusch, University of Copenhagen and Dagmar Moersdorf, University of Cologne, for helpful suggestions, Drs. Juha Partanen, University of Helsinki, and David Ornitz, Washington University St. Louis, for the *Fgfr1* and *Fgfr2* floxed mice, respectively, Dr. Petra Boukamp, German Cancer Research Center Heidelberg, for early passage HaCaT keratinocytes, and Dr. Didier Musso, Research and Diagnosis Laboratory, Institute Louis Marlade, Papeete, Tahiti, for ZIKV Polynesia strain PF 13/251013-18.

This work was supported by the Swiss National Science Foundation (grants 31003A_169204 and 31003B-189364 to S.W), the ETH Zurich (grant ETH-06 15-1 to S.W. and L.M.), a Marie Curie postdoctoral fellowship from the European Union (to L. M.), a Swiss Government Excellence Postdoctoral Scholarship (to K. N.) and the European Union Horizon 2020 research and innovation program (grant agreement No 653316; "European Virus Archive goes Global (EVAg) project") that provided the ZIKV strain Uganda (strain 976).

Author contributions

LM designed the study together with SW. LM, CU, TR, MM, LF, DR, RS, DS, DB, NL, GS, KN, H-DB performed experiments and analysed data, MW performed the bioinformatics analysis, LM and CU made the figures, PS provided IFN receptor knockout mice, EH supervised the Zika virus experiments, AO supervised the LCMV and *in vivo* HSV-1 experiments. SW designed the study together with LM, supervised the work and provided the funding. All authors made important comments to the manuscript.

Conflict of interest

L.M., M.M. and S.W. have filed a patent for the use of FGFR inhibitors in antiviral defence (Filing No. EP3308786A1). There are no additional competing interests of any of the authors.

Tables

Table 1: Type I interferon signaling is the top regulated pathway in the epidermis of K5-R1/R2 mice.

A: GeneOntology (GO) Biological Process 2017b.

Index	Name	P-value	Adj. p-value
1	Negative regulation of single stranded viral RNA replication via double stranded DNA intermediate (GO:0045869)	0.000008	0.001836
2	Negative regulation of viral genome replication (GO:0045071)	0.000006	0.001836
3	Negative regulation by host of viral genome replication (GO:0044828)	0.000015	0.002497
4	Melanin biosynthetic process from tyrosine (GO:0006583)	0.000000	0.000315
5	Skin epidermis development (GO:0098773)	0.000171	0.006386
6	Defence response to fungus (GO:0050832)	0.000379	0.006386
7	Antifungal innate immune response (GO:0061760)	0.000379	0.006386
8	Defence response to fungus, incompatible interaction (GO:0009817)	0.000379	0.006386
9	Neutrophil mediated killing of fungus (GO:0070947)	0.000379	0.006386
10	Negative regulation of single stranded viral RNA replication via double stranded DNA intermediate (GO:0045869)	0.000008	0.001836

B: Reactome 2016.

Index	Name	P-value	Adj. p-value
1	Interferon alpha/beta signaling_Homo sapiens_R-HSA-909733	0.000017	0.001495
2	Interferon Signaling_Homo sapiens_R-HSA-913531	0.000870	0.039131
3	Glutathione conjugation_Homo sapiens_R-HSA-156590	0.003484	0.104528
4	Antiviral mechanism by IFN-stimulated genes_Homo sapiens_R-HSA-1169410	0.011532	0.207580
5	ISG15 antiviral mechanism-Homo sapiens_R-HSA-1169408	0.011532	0.207580

C: ISGs that are upregulated (log2(f.c.) > 1.5, $p < 0.05$) in the epidermis of K5-R1/R2 mice at P18 (microarray data).

Gene Symbol	Description	Gene ID	Affy Probe ID	Log2 (f.c.)	P-value
Rtp4	Receptor transporter protein 4	67775	1418580_at	2.841	0.003
Rsad2	Radical S-adenosyl methionine domain containing 2	58185	1421009_at	2.824	0.007
Il1f8	Interleukin 1 family, member 8	69677	1425715_at	2.652	0.014
Ifit1	Interferon-induced protein with tetratricopeptide repeats 1	15957	1450783_at	2.649	0.014
Rsad2	Radical S-adenosyl methionine domain containing 2	58185	1436058_at	2.589	0.021
Ifi27l2a	Interferon, alpha-inducible protein 27 like 2A	76933	1426278_at	2.506	0.021
Ifi44	Interferon-induced protein 44	99899	1423555_a_at	2.493	0.004
Isg15	ISG15 ubiquitin-like modifier	100038882	1431591_s_at	2.027	0.009
Rsad2	Radical S-adenosyl methionine domain containing 2	58185	1421008_at	1.931	0.009
Oas1d	2'-5'-oligoadenylate synthetase 1D	100535	1416847_s_at	1.879	0.039
Defb3	Defensin beta 3	27358	1421806_at	1.56	0.044

Extended data

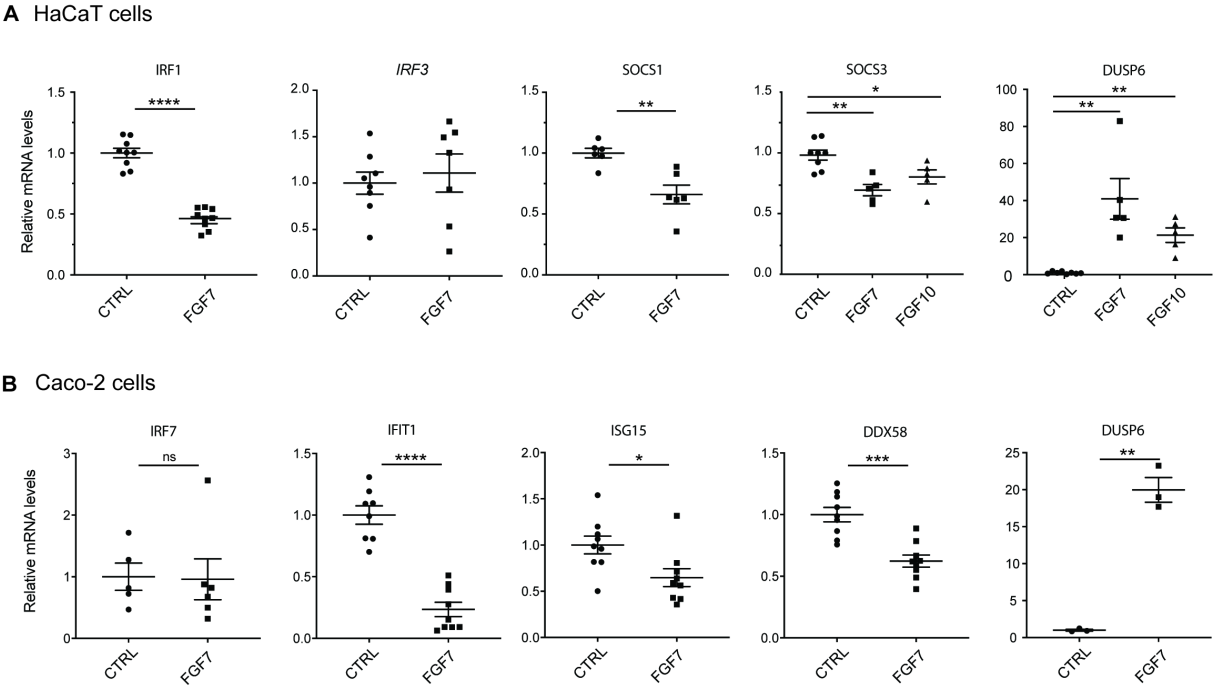

Fig EV1: FGF signaling suppresses ISG expression in HaCaT keratinocytes and Caco-2 colon cancer cells.

(A) Serum-starved HaCaT keratinocytes were treated for 16 h with FGF7 or FGF10 (10 ng/ml each). RNA samples were analysed by qRT-PCR for IRF1, IRF3, SOCS1, SOCS3 and DUSP6 relative to RPLP0.

(**B**) Serum-starved Caco-2 cells were treated for 6 h with FGF7 (10 ng/ml). RNA samples were analysed by qRT-PCR for *IRF7*, *IFIT1*, *ISG15*, *DDX58* or *DUSP6* relative to *RPLP0*.

Data information: Scatter plots show mean +/- S.E.M. Mean expression levels in CTRL cell cultures were set to 1. A: N=5-9 from 2-3 experiments, B: N=5-8 from 3 experiments for ISGs, N=3 from 1 experiment for DUSP6. ns: non-significant, * $P \leq 0.05$, ** $P \leq 0.01$, *** $P \leq 0.001$, **** $P \leq 0.0001$ (Mann-Whitney U test). Exact P-Values are provided in Dataset EV2.

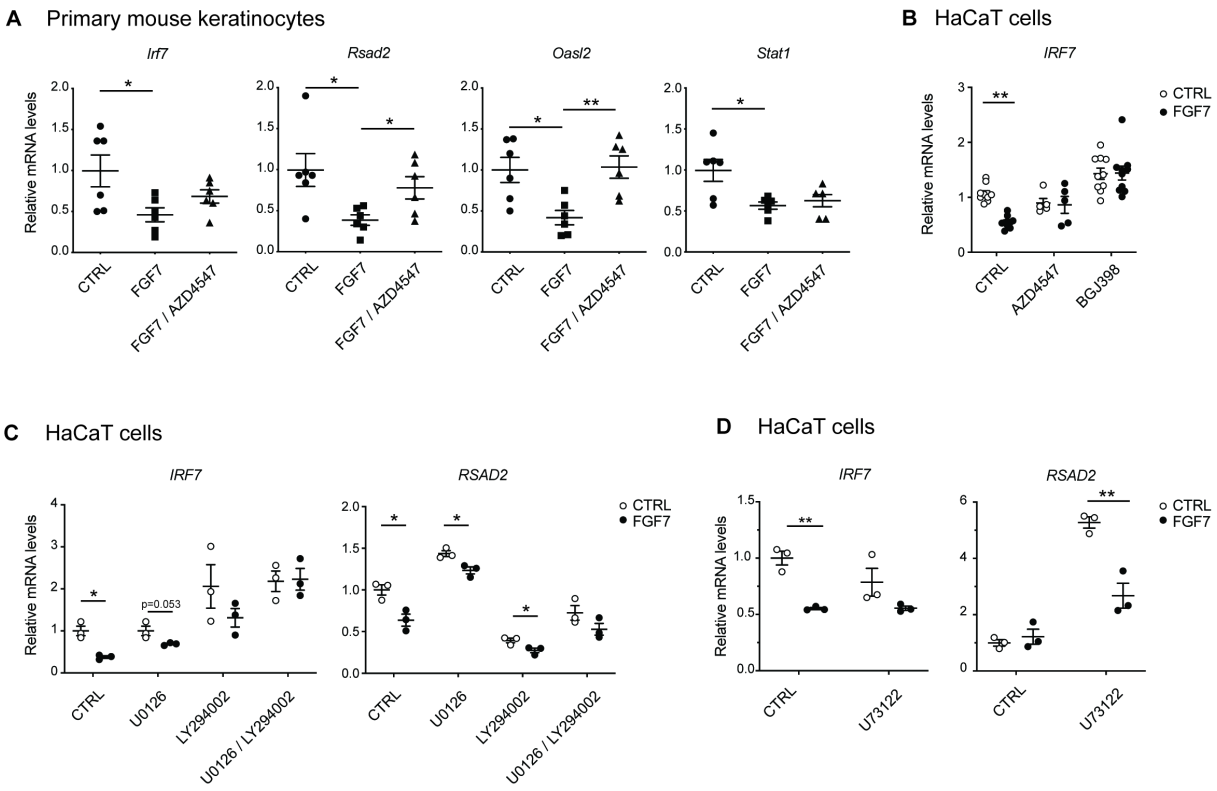

Fig EV2: FGF7 suppresses ISG expression in keratinocytes via FGFR-mediated MEK1/2-ERK1/2 and PI3K-AKT signaling.

(**A**) Growth factor-starved primary mouse keratinocytes were treated for 6 h with FGF7 (10 ng/ml) in the presence of absence of the FGFR kinase inhibitor AZD4547 (1 μM) (added 3 h prior to FGF7). RNA samples were analysed by qRT-PCR for expression of *Irf7*, *Rsad2*, *Oasl2* and *Stat1* relative to *Rps29*.

(**B**) Serum-starved HaCaT cells were treated for 6 h with FGF7 (10 ng/ml) in the absence or presence of the FGFR kinase inhibitors AZD4547 (1 μM) or BGJ398 (3.5 μM) (added 2 h prior to FGF7) and analysed by qRT-PCR for *IRF*7 relative to *RPLP0*.

(**C**, **D**) Serum-starved HaCaT keratinocytes were treated for 6 h with FGF7 (10 ng/ml) in the absence or presence of the PI3K inhibitor LY294002 (5 μM) and/or the MEK1/2 inhibitor U0126 (10 μM) (C) or the PLCγ inhibitor U73122 (5 μM) (D) (added 2 h prior to FGF7) and analysed by qRT-PCR for *IRF*7 and *RSAD2* relative to *RPLP0*.

Data information: Scatter plots show mean +/- S.E.M. Mean expression levels in CTRL cell cultures were set to 1. A: N=5-6 from 2 experiments, B: N=5-10 from 4 experiments. C, D; Representative experiments from at least two independent experiments are shown, N=3 per experiment. * $P \leq 0.05$, ** $P \leq 0.01$ (Mann-Whitney U test (A, B) and t-test with Welch correction for assessment of FGF7 effect (C, D). Exact P-values are provided in Dataset EV2.

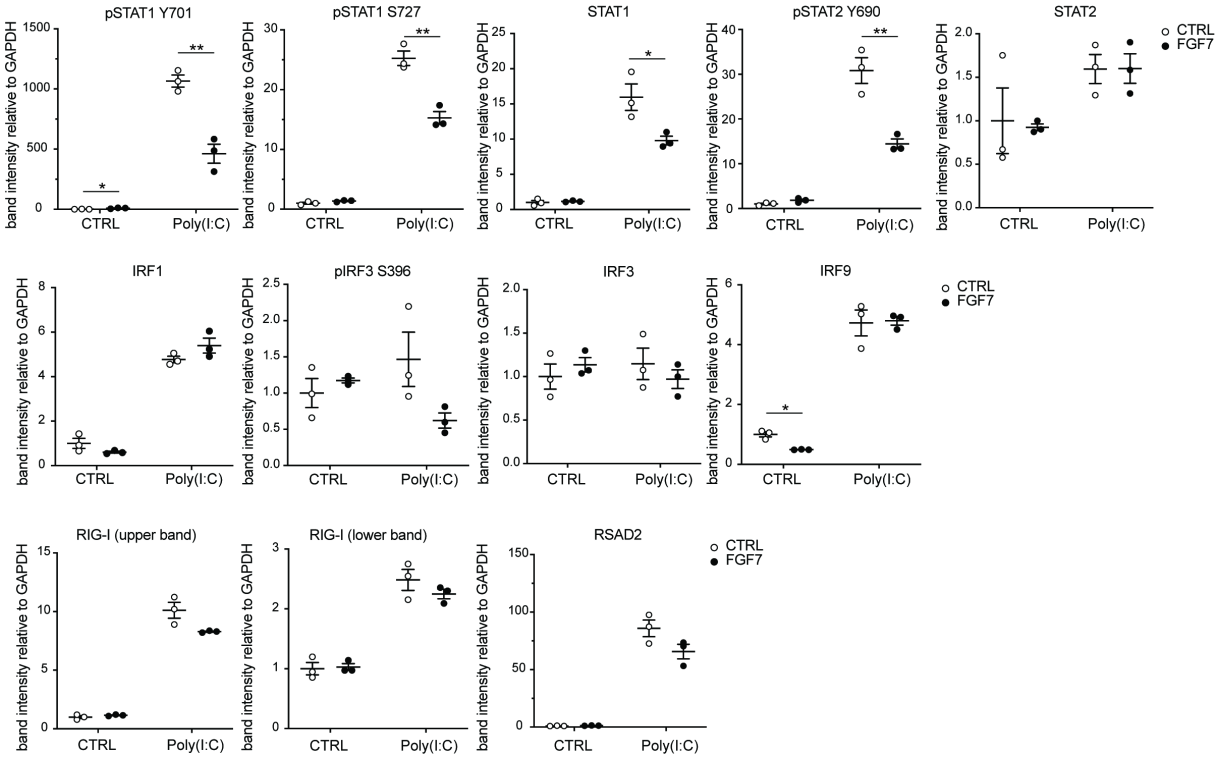

Fig EV3: FGF7 suppresses ISG expression and poly(I:C)-induced STAT1 and STAT2 activation.

Quantification of the Western blot data shown in Fig 4B. Band intensities (based on densitometry) were normalized to the intensities of the GAPDH bands. Scatter plots show mean +/- S.E.M (N=3). Mean band intensity in the CTRL cell cultures was set to 1. * $P \leq 0.05$, ** $P \leq 0.01$ (t-test with Welch correction for assessment of FGF7 effect). Exact P-values are provided in Dataset EV2.

Appendix

Appendix figures

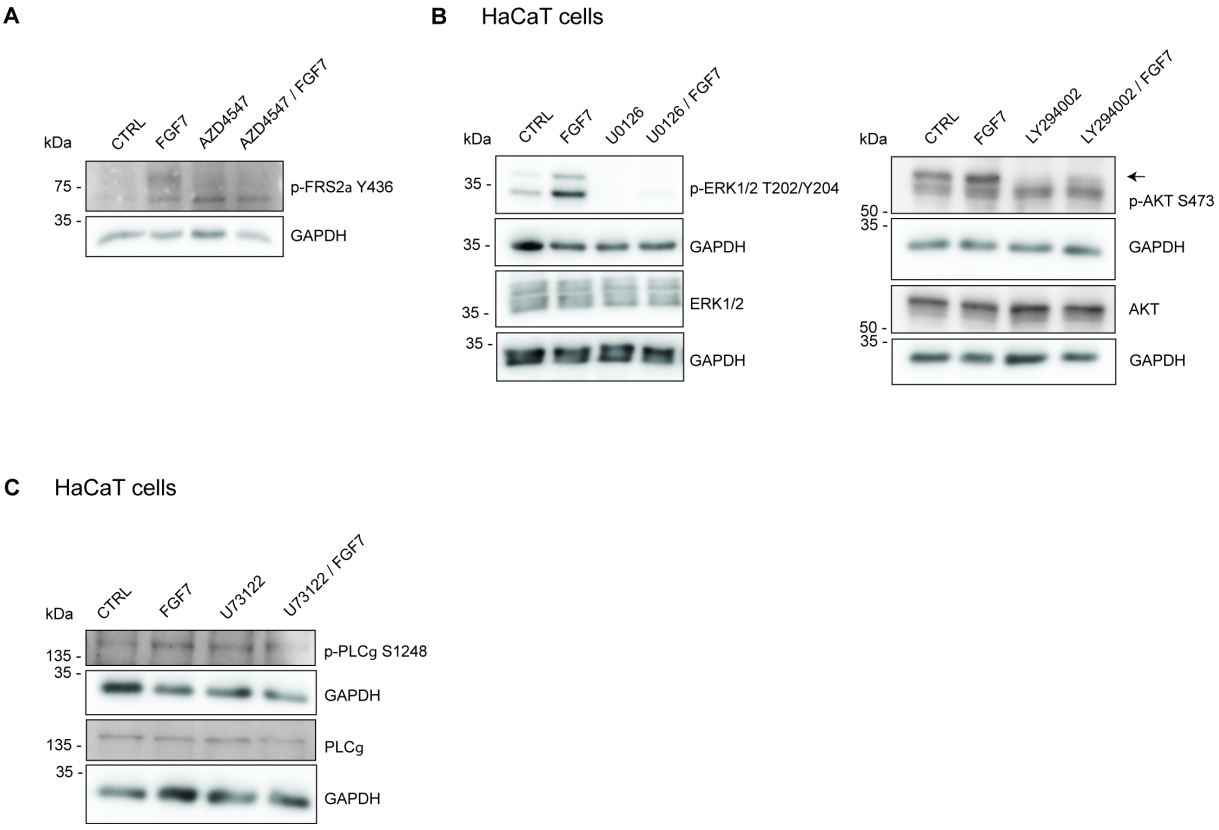

Appendix Fig S1: Verification of the efficiency of different inhibitors of FGFR signaling proteins.

(A-C) Serum-starved HaCaT keratinocytes were pre-treated with the FGFR inhibitor AZD4547 (1 µM) (A), the MEK1/MEK2 inhibitor U0126 (10 µM) (B, left panel), the PI3K inhibitor LY294002 (5 µM) (B, right panel), or the PLCγ inhibitor U73122 (5 µM) (C) or vehicle and then incubated with FGF7 for 15 min. Cell lysates were analysed by Western blot for total and phosphorylated FRS2a (A), pERK1/2 and AKT (B), pPLCγ (C) and GAPDH (loading control).

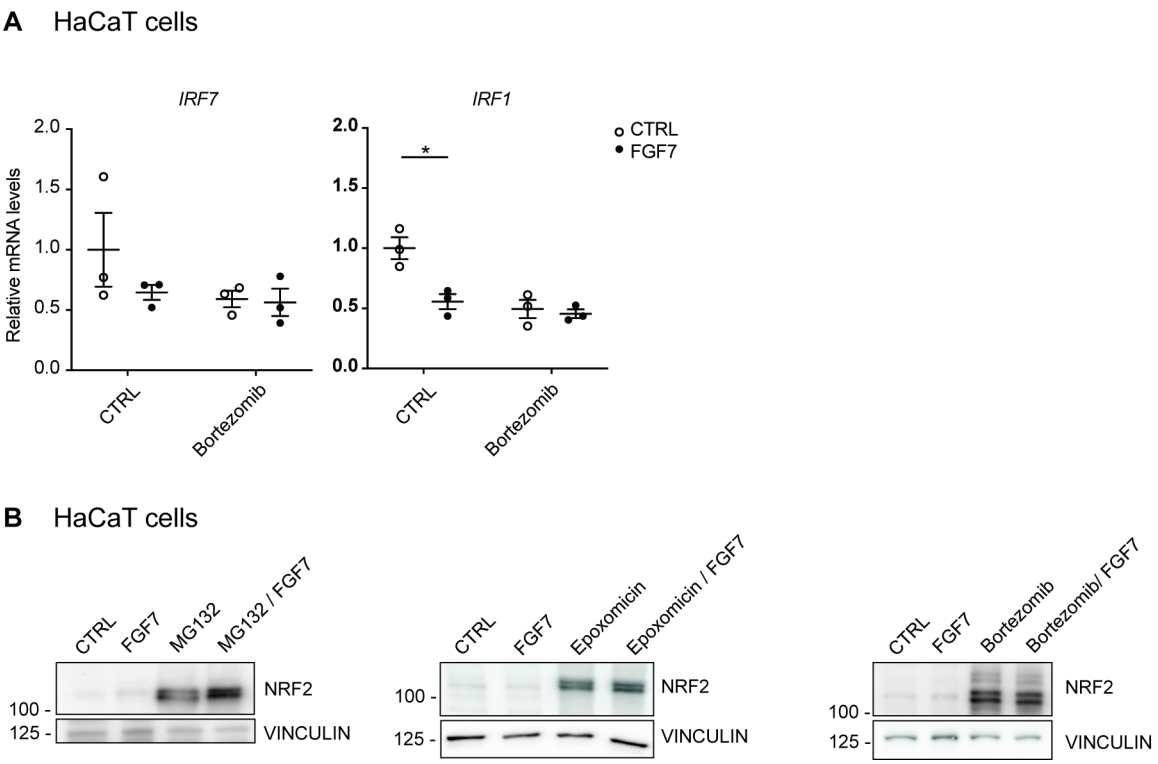

Appendix Fig. S2: Proteasome inhibition abolishes the effect of FGF7 on ISG expression.

(A) HaCaT keratinocytes were pre-treated for 2 h with the proteasome inhibitor bortezomib (10 μM), followed by a 6 h treatment with FGF7 (10 ng/ml) or vehicle. RNA samples were analysed by qRT-PCR for *IRF7* and *IRF1* relative to *RPLP0*.

(B) To test the efficiency of the proteasome inhibitors used for the experiments shown in Fig. 2G, H and Appendix Fig. S2A, HaCaT keratinocytes were treated as described in the legends of these figures and analysed by Western blot for expression of NRF2 and vinculin (loading control).

Data information: Scatter plots show mean +/- S.E.M. Mean expression levels in CTRL cell cultures was set to 1, and mRNA levels relative to this value are shown. N=3 per treatment group from one experiment. *** $P \leq 0.001$ (Mann-Whitney U test).

Appendix tables

Appendix Table S1: Antibodies used for Western blot and/or immunostaining.

Antigen	Cat. No.	Dilution	Company/Source
IRF1	8478	1:1.000	Cell Signaling, Danvers, MA
IRF3	11904	1:1.000	Cell Signaling
Phospho-IRF3	4947	1:1.000	Cell Signaling
IRF7	Sc-9083	1:400	Santa Cruz, Santa Cruz, CA
IRF7	4920	1:1.000	Cell Signaling
RSAD2	13996	1:1.000	Cell Signaling
IRF9	76684	1:1.000	Cell Signaling
Lamin A/C	4777	1:2.000	Cell Signaling
Phospho-STAT1 (Y701)	9167	1:1.000	Cell Signaling
Phospho-STAT1 (S727)	8826	1:1.000	Cell Signaling
STAT1	610115	1:500	BD Biosciences, San José, CA
RSAD2	13996	1:1.000	Cell Signaling
Phospho-STAT2 (Y690)	88410	1:1.000	Cell Signaling
STAT2	4594	1:1.000	Cell Signaling
Glyceraldehyde 3 -phosphate dehydrogenase (GAPDH)	5G4	1:10.000	HyTest, Turku, Finland
Zona Occludens 1 (ZO.1)	339100	1:500	Invitrogen, Carlsbad, CA
Keratin 14 (K14)	PRB-155P	1:1.000	Biolegend, San Diego, CA
Vinculin	v4505	1:2.000	Sigma; Munich Germany
Flavivirus group antigen antibody (clone D1-4G2-4-15)	MAB10216	1:400	Merck-Millipore, Darmstadt, Germany
Herpes Simplex Virus 1 (HSV-1) glycoprotein D (Glyc-D)	ab27586 and ab6507	1:1.000	Abcam, Cambridge, UK
LCMV nucleoprotein (clone VL-4)		1:400	Kindly provided by Prof. Rolf Zinkernagel, Zurich, Switzerland
AF555-conjugated anti-mouse IgG	A-21422	1:400	Thermo Fisher
AF555-conjugated anti-rabbit IgG	A-21428	1:400	Thermo Fisher
AF488-conjugated anti-mouse IgG	A-11001	1:400	Thermo Fisher

Appendix Table S2: Primers used for qRT-PCR

Primers used for mouse samples:

Target gene	Sequence
Ifit1	5`-AGC AAC CAT GGG AGA GAA TGC-3`
	5`-CT TTC AGG TGC CTC ACG TA-3
Irf7	5`-AGC TTG GAT CTA CTG TGC GC-3`
	5`-GGG TTC CTC GTA AAC ACG GT-3`
Oasl2	5`-TGC CTG GGA GAG AAT CGA AG-3`
	5`-AGC CTC CCT TCA CCA CCT TA-3`
Rps29	5`-GGT CAC CAG CAG CTC TAC TG-3`
	5`-GTC CAA CTT AAT GAA GCC TAT GTC C-3`
Stat1	5`-GGA TCG CTT GCC CAA CTC T-3`
	5`-GCA GAG CTG AAA CGA CCT AGA-3`
Rsad2	5`-GGA GGT GGT GCA GGG ATT AC-3`
	5`-GGA AAA CCT TCC AGC GCA CA-3`
Stat2	5`-CTT TTG CAA GCG AGA GAG CC-3`
	5`-TGA AGC GCA GTA GGA AGG TG-3`
Ifnb	5`-CTG GCT TCC ATC ATG AAC AA-3`
	5` -CAT TTC CGA ATG TTC GTC CT-3`
Ifnl3	5`-GGT TGG AGG TGA CAG AGT-3`
	5`-AAG GGT GCC ATC GAG AAG-3`
Fgf7	5`-CCT TTG ATT GCC ACA ATT CC-3`
	5`-CAA ACG GCT ACG AGT GTG AA-3`
Cre	5`-CGA CCA GGT TCG TTC ACT CA-3`
	5`-CGA GTT GAT AGC TGG CTG GT-3`

Primers used for human samples:

Target gene	Sequence
DUSP6	5`-GTT CTA CCT GGA AGG TGG CT-3`
	5`-AGT CCG TTG CAC TAT TGG GG-3`
IFIT1	5`-AGC TTA CAC CAT TGG CTG CT-3`
	5`-CCA TTT GTA CTC ATG GTT GCT GT-3`
IRF1	5`-CTC TGA AGC TAC AAC AGA TGA G-3`
	5`-GTA GAC TCA GCC CAA TAT CCC-3`
IRF3	5`-TCG TGA TGG TCA AGG TTG T-3`
	5`-AGG TCC ACA GTA TTC TCC AG-3`
IRF7	5`-AGC TGT GCT GGC GAG AAG-3`
	5`-CTC TCC AGG AGC CTT GGT TG-3`
OAS2	5`-GGG CTA TTT CCA GAC AAC GC-3`
	5`-GAA AAC CAG GCC TGT GAT CTT GG-3`
ISG15	5`-ACT CAT CTT TGC CAG TAC AGG AG-3`
	5`-CAG CAT CTT CAC CGT CAG GTC-3`
NECT1	5`-CTA CCA CAT GGA CCG CTT CAA G-3`
	5`-CTT TGC AGG TGA GCT TCA CGT C-3`
RPLP0	5`-CCA CAT TGT CTG CTC CCA CA-3`
	5`-GAA GAC AGG GCG ACC TGG AA-3`

RSAD2	5`-GCT GCT AGC TAC CAA GAG GAG-3`
	5`-ATC TTC TCC ATA CCA GCT TCC-3`
STAT1	5`-AAA GGA AGC ACC AGA GCC AAT-3`
	5`-TCC GAG ACA CCT CGT CAA AC-3`
STAT2	5`-GGA TCC TAC CCA GTT GGC TG-3`
	5`-GAG GGT GTC TTC CCT TTG GC-3`
OAS1	5`-TTC CTC CCT GCC ATT CAT CC-3`
	5`-TCC AGA AAC CCT CGA TTG TGA-3`
MxA	5`-ACC TAC AGC TGG CTC CTG AA-3`
	5`-GCA CTC AAG TCG TCA GTC CA-3`
DDX58	5`-ATC CCA GTG TAT GAA CAG CAG-3`
	5`-GCC TGT AAC TCT ATA CCC ATG TC-3`
CGAS	5`-GGG AGC CCT GCT GTA ACA CTT CTT AT-3`
	5`-CCT TTG CAT GCT TGG GTA CAA GGT-3`
TLR3	5`-TGG TTG GGC CAC CTA GAA GTA-3`
	5`-TCT CCA TTC CTG GCC TGT G-3`
IFNB	5`-TGG GAG GAT TCT GCA TTA CC -3`
	5`-CAG CAT CTG CTG GTT GAA GA -3`
IFNL1	5`-GGT GAC TTT GGT GCT AGG-3`
	5`-TGA GTG ACT CTT CCA AGG -3`
RPL27	5`-AAA GCT GTC ATC GTG AAG AAC-3`
	5`-GCT GCT ACT TTG CGG GGG TAG-3`
SOCS1	5`-GGA ACT GCT TTT TCG CCC TTA -3`
	5`-AGC AGC TCG AAG AGG CAG TC-3`
SOCS3	5`-GGC CAC TCT TCA GCA TCT C-3`
	5`-ATC GTA CTG GTC CAG GAA CTC-3`

References

42 **Maddaluno, L., Urwyler, C. & Werner, S. (2017)** *Fibroblast growth factors: Key players in regeneration and tissue repair*. Development 144, 4047-4060.

45 **Beenken, A. & Mohammadi, M. (2009)** *The FGF family: Biology, pathophysiology and therapy*. Nature Reviews Drug Discovery 8, 235-253.

48 **Ornitz, D. M. & Itoh, N. (2015)** *The fibroblast growth factor signaling pathway*. Wiley Interdisciplinary Reviews: Developmental Biology 4, 215-266.

50 **Zhang, X., Ibrahimi, O. A., Olsen, S. K., Umemori, H., Mohammadi, M. & Ornitz, D. M. (2006)** *Receptor specificity of the fibroblast growth factor family. The complete mammalian FGF family*. Journal of Biological Chemistry 281, 15694-15700.

54 **Touat, M., Ileana, E., Postel-Vinay, S., André, F. & Soria, J.-C. (2015)** *Targeting FGFR Signaling in Cancer*. Clinical Cancer Research 21, 2684-2694.

65 **Yang, J., Meyer, M., Muller, A. K., Bohm, F., Grose, R., Dauwalder, T., Verrey, F., Kopf, M., Partanen, J., Bloch, W., Ornitz, D. M. & Werner, S. (2010)** *Fibroblast growth factor receptors 1 and 2 in keratinocytes control the epidermal barrier and cutaneous homeostasis*. Journal of Cell Biology 188, 935-952.

135 **Boukamp, P., Petrussevska, R. T., Breitkreutz, D., Hornung, J., Markham, A. & Fusenig, N. E. (1988)** *Normal keratinization in a spontaneously immortalized aneuploid human keratinocyte cell line*. The Journal of Cell Biology 106, 761-771.

143 **Strittmatter, G. E., Sand, J., Sauter, M., Seyffert, M., Steigerwald, R., Fraefel, C., Smola, S., French, L. E. & Beer, H.-D. (2016)** *IFN-γ primes keratinocytes for HSV-1–induced inflammasome activation*. Journal of Investigative Dermatology 136, 610-620.

162 **Li, C., Scott, D. A., Hatch, E., Tian, X. & Mansour, S. L. (2007)** *Dusp6 (Mkp3) is a negative feedback regulator of FGF-stimulated ERK signaling during mouse development*. Development 134, 167-176.

171 **Nunes, Q. M., Li, Y., Sun, C., Kinnunen, T. K. & Fernig, D. G. (2016)** *Fibroblast growth factors as tissue repair and regeneration therapeutics*. PeerJ 4, e1535.

172 **Zhang, J. & Li, Y. (2016)** *Therapeutic uses of FGFs*. Seminars in Cell & Developmental Biology 53, 144-154.

173 **Tanner, Y. & Grose, R. P. (2016)** *Dysregulated FGF signalling in neoplastic disorders*. Seminars in Cell and Developmental Biology 53, 126-135.

174 **Ank, N., Iversen, M. B., Bartholdy, C., Staeheli, P., Hartmann, R., Jensen, U. B., Dagnaes-Hansen, F., Thomsen, A. R., Chen, Z., Haugen, H., Klucher, K. &**

Paludan, S. R. (2008) *An important role for type III interferon (IFN-lambda/IL-28) in TLR-induced antiviral activity*. Journal of Immunology 180, 2474-2485.

175 **Mordstein, M., Kochs, G., Dumoutier, L., Renauld, J. C., Paludan, S. R., Klucher, K. & Staeheli, P. (2008)** *Interferon-lambda contributes to innate immunity of mice against influenza A virus but not against hepatotropic viruses*. PLoS Pathogens 4, e1000151.

176 **Mohn, F., Weber, M., Schubeler, D. & Roloff, T. C. (2009)** *Methylated DNA immunoprecipitation (MeDIP)*. Methods in Molecular Biology 507, 55-64.

177 **Beyer, T. A., Xu, W., Teupser, D., auf dem Keller, U., Bugnon, P., Hildt, E., Thiery, J., Kan, Y. W. & Werner, S. (2008)** *Impaired liver regeneration in Nrf2 knockout mice: Role of ROS-mediated insulin/IGF-1 resistance*. The EMBO Journal 27, 212-223.

178 **Kuleshov, M. V., Jones, M. R., Rouillard, A. D., Fernandez, N. F., Duan, Q., Wang, Z., Koplev, S., Jenkins, S. L., Jagodnik, K. M., Lachmann, A., McDermott, M. G., Monteiro, C. D., Gundersen, G. W. & Ma'ayan, A. (2016)** *Enrichr: A comprehensive gene set enrichment analysis web server 2016 update*. Nucleic Acids Research 44, W90-97.

179 **Rahn, E., Thier, K., Petermann, P. & Knebel-Mörsdorf, D. (2015)** *Ex vivo infection of murine epidermis with Herpes simplex virus type 1*. Journal of Visualized Experiments, e53046.

180 **Sulcova, J., Maddaluno, L., Meyer, M. & Werner, S. (2015)** *Accumulation and activation of epidermal γδ T cells in a mouse model of chronic dermatitis is not required for the inflammatory phenotype*. European Journal of Immunology 45, 2517-2528.

181 **Guagnano, V., Furet, P., Spanka, C., Bordas, V., Le Douget, M., Stamm, C., Brueggen, J., Jensen, M. R., Schnell, C., Schmid, H., Wartmann, M., Berghausen, J., Drueckes, P., Zimmerlin, A., Bussiere, D., Murray, J. & Graus Porta, D. (2011)** *Discovery of 3-(2,6-dichloro-3,5-dimethoxy-phenyl)-1-{6-[4-(4-ethyl-piperazin-1-yl)-phenylamin o]-pyrimidin-4-yl}-1-methyl-urea (NVP-BGJ398), a potent and selective inhibitor of the fibroblast growth factor receptor family of receptor tyrosine kinase*. Journal of Medicinal Chemistry 54, 7066-7083.

182 **Gough, D. J., Messina, N. L., Clarke, C. J., Johnstone, R. W. & Levy, D. E. (2012)** *Constitutive type I interferon modulates homeostatic balance through tonic signaling*. Immunity 36, 166-174.

183 **Blumer, T., Coto-Llerena, M., Duong, F. H. T. & Heim, M. H. (2017)** *SOCS1 is an inducible negative regulator of interferon lambda (IFN-lambda)-induced gene expression in vivo*. Journal of Biological Chemistry 292, 17928-17938.

184 **Michalska, A., Blaszczyk, K., Wesoly, J. & Bluyssen, H. A. R. (2018)** *A positive feedback amplifier circuit that regulates interferon (IFN)-stimulated gene expression and controls type I and type II IFN responses*. Frontiers in Immunology 9, 1135.

185 **Visco, V., Bava, F. A., d'Alessandro, F., Cavallini, M., Ziparo, V. & Torrisi, M. R. (2009)** *Human colon fibroblasts induce differentiation and proliferation of intestinal epithelial cells through the direct paracrine action of keratinocyte growth factor*. Journal of Cellular Physiology 220, 204-213.

186 **Bruns, A. M. & Horvath, C. M. (2014)** *Antiviral RNA recognition and assembly by RLR family innate immune sensors*. Cytokine & Growth Factor Reviews 25, 507-512.

187 **Gavine, P. R., Mooney, L., Kilgour, E., Thomas, A. P., Al-Kadhimi, K., Beck, S., Rooney, C., Coleman, T., Baker, D., Mellor, M. J., Brooks, A. N. & Klinowska, T. (2012)** *AZD4547: An orally bioavailable, potent, and selective inhibitor of the fibroblast growth factor receptor tyrosine kinase family*. Cancer Research 72, 2045-2056.

188 **Ivashkiv, L. B. & Donlin, L. T. (2014)** *Regulation of type I interferon responses*. Nature Reviews Immunology 14, 36-49.

189 **Villeneuve, N. F., Lau, A. & Zhang, D. D. (2010)** *Regulation of the Nrf2-Keap1 antioxidant response by the ubiquitin proteasome system: An insight into cullin-ring ubiquitin ligases*. Antioxidants & Redox Signaling 13, 1699-1712.

190 **Honda, K., Yanai, H., Negishi, H., Asagiri, M., Sato, M., Mizutani, T., Shimada, N., Ohba, Y., Takaoka, A., Yoshida, N. & Taniguchi, T. (2005)** *IRF-7 is the master regulator of type-I interferon-dependent immune responses*. Nature 434, 772-777.

191 **Panda, D., Gjinaj, E., Bachu, M., Squire, E., Novatt, H., Ozato, K. & Rabin, R. L. (2019)** *IRF1 maintains optimal constitutive expression of antiviral genes and regulates the early antiviral response*. Frontiers in Immunology 10, 1019.

192 **Shaw, A. E., Hughes, J., Gu, Q., Behdenna, A., Singer, J. B., Dennis, T., Orton, R. J., Varela, M., Gifford, R. J., Wilson, S. J. & Palmarini, M. (2017)** *Fundamental properties of the mammalian innate immune system revealed by multispecies comparison of type I interferon responses*. PLoS Biology 15, e2004086.

193 **Alexopoulou, L., Holt, A. C., Medzhitov, R. & Flavell, R. A. (2001)** *Recognition of double-stranded RNA and activation of NF-kappaB by Toll-like receptor 3*. Nature 413, 732-738.

194 **Petermann, P., Thier, K., Rahn, E., Rixon, F. J., Bloch, W., Ozcelik, S., Krummenacher, C., Barron, M. J., Dixon, M. J., Scheu, S., Pfeffer, K. & Knebel-Morsdorf, D. (2015)** *Entry mechanisms of herpes simplex virus 1 into murine epidermis: Involvement of nectin-1 and herpesvirus entry mediator as cellular receptors*. Journal of Virology 89, 262-274.

195 **Sayers, C. L. & Elliott, G. (2016)** *Herpes simplex virus 1 enters human keratinocytes by a nectin-1-dependent, rapid plasma membrane fusion pathway that functions at low temperature*. Journal of Virology 90, 10379-10389.

196 **Hamel, R., Dejarnac, O., Wichit, S., Ekchariyawat, P., Neyret, A., Luplertlop, N., Perera-Lecoin, M., Surasombatpattana, P., Talignani, L., Thomas, F., Cao-Lormeau, V. M., Choumet, V., Briant, L., Despres, P., Amara, A., Yssel, H. & Misse, D. (2015)** *Biology of zika virus infection in human skin cells*. Journal of Virology 89, 8880-8896.

197 **Zhu, X., He, Z., Hu, Y., Wen, W., Lin, C., Yu, J., Pan, J., Li, R., Deng, H., Liao, S., Yuan, J., Wu, J., Li, J. & Li, M. (2014)** *MicroRNA-30e* suppresses dengue virus replication by promoting NF-kappaB-dependent IFN production*. PLoS Neglected Tropical Diseases 8, e3088.

198 **Aoki, R., Kawamura, T., Goshima, F., Ogawa, Y., Nakae, S., Nakao, A., Moriishi, K., Nishiyama, Y. & Shimada, S. (2013)** *Mast cells play a key role in host defense against herpes simplex virus infection through TNF-alpha and IL-6 production*. Journal of Investigative Dermatology 133, 2170-2179.

199 **Lulli, D., Carbone, M. L. & Pastore, S. (2017)** *The MEK inhibitors trametinib and cobimetinib induce a type I interferon response in human keratinocytes*. International Journal of Molecular Sciences 18.

200 **Battcock, S. M., Collier, T. W., Zu, D. & Hirasawa, K. (2006)** *Negative regulation of the alpha interferon-induced antiviral response by the Ras/Raf/MEK pathway*. Journal of Virology 80, 4422-4430.

201 **Darnell, J. E., Jr., Kerr, I. M. & Stark, G. R. (1994)** *Jak-STAT pathways and transcriptional activation in response to IFNs and other extracellular signaling proteins*. Science 264, 1415-1421.

202 **Leviyang, S., Strawn, N. & Griva, I. (2019)** *Regulation of interferon stimulated gene expression levels at homeostasis*. Cytokine 126, 154870.

203 **Nakagawa, K. & Yokosawa, H. (2000)** *Degradation of transcription factor IRF-1 by the ubiquitin-proteasome pathway. The C-terminal region governs the protein stability*. European Journal of Biochemistry 267, 1680-1686.

204 **Barro, M. & Patton, J. T. (2007)** *Rotavirus NSP1 inhibits expression of type I interferon by antagonizing the function of interferon regulatory factors IRF3, IRF5, and IRF7*. Journal of Virology 81, 4473-4481.

205 **Zhao, X., Zhu, H., Yu, J., Li, H., Ge, J. & Chen, W. (2016)** *c-Cbl-mediated ubiquitination of IRF3 negatively regulates IFN-beta production and cellular antiviral response*. Cell Signaling 28, 1683-1693.

206 **Fujita, T., Kimura, Y., Miyamoto, M., Barsoumian, E. L. & Taniguchi, T. (1989)** *Induction of endogenous IFN-alpha and IFN-beta genes by a regulatory transcription factor, IRF-1*. Nature 337, 270-272.

207 **Maher, S. G., Romero-Weaver, A. L., Scarzello, A. J. & Gamero, A. M. (2007)** *Interferon: cellular executioner or white knight?* Current Medicinal Chemistry 14, 1279-1289.

208 **Lasfar, A., Zloza, A., de la Torre, A. & Cohen-Solal, K. A. (2016)** *IFN-lambda: A new inducer of local immunity against cancer and infections*. Frontiers in Immunology 7, 598.

209 **Schneider, W. M., Chevillotte, M. D. & Rice, C. M. (2014)** *Interferon-stimulated genes: A complex web of host defenses*. Annual Reviews Immunology 32, 513-545.

210 **Kaner, R. J., Baird, A., Mansukhani, A., Basilico, C., Summers, B. D., Florkiewicz, R. Z. & Hajjar, D. P. (1990)** *Fibroblast growth factor receptor is a portal of cellular entry for herpes simplex virus type 1*. Science 248, 1410-1413.

211 **Schoggins, J. W. & Rice, C. M. (2011)** *Interferon-stimulated genes and their antiviral effector functions*. Current Opinion in Virology 1, 519-525.

212 **Werner, S., Peters, K. G., Longaker, M. T., Fuller-Pace, F., Banda, M. J. & Williams, L. T. (1992)** *Large induction of keratinocyte growth factor expression in the dermis during wound healing*. Proceedings of the National Academy of Sciences 89, 6896-6900.

213 **Finch, P. W. & Rubin, J. S. (2004)** *Keratinocyte growth factor/fibroblast growth factor 7, a homeostatic factor with therapeutic potential for epithelial protection and repair*. Advances in Cancer Research 91, 69-136.

214 **Van, N. D., Falk, C. S., Sandmann, L., Vondran, F. W., Helfritz, F., Wedemeyer, H., Manns, M. P., Ciesek, S. & von Hahn, T. (2016)** *Modulation of HCV reinfection after orthotopic liver transplantation by fibroblast growth factor-2 and other non-interferon mediators*. Gut 65, 1015-1023.

215 **Limonta, D., Jovel, J., Kumar, A., Lu, J., Hou, S., Airo, A. M., Lopez-Orozco, J., Wong, C. P., Saito, L., Branton, W., Wong, G. K.-S., Mason, A., Power, C. & Hobman, T. C. (2019)** *Fibroblast growth factor 2 enhances zika virus infection in human fetal brain*. The Journal of Infectious Diseases 220, 1377-1387.

216 **Prince, L. S., Karp, P. H., Moninger, T. O. & Welsh, M. J. (2001)** *KGF alters gene expression in human airway epithelia: Potential regulation of the inflammatory response*. Physiological Genomics 6, 81-89.

217 **Quantius, J., Schmoldt, C., Vazquez-Armendariz, A. I., Becker, C., El Agha, E., Wilhelm, J., Morty, R. E., Vadasz, I., Mayer, K., Gattenloehner, S., Fink, L.,**

Matrosovich, M., Li, X., Seeger, W., Lohmeyer, J., Bellusci, S. & Herold, S. (2016) *Influenza virus infects epithelial stem/progenitor cells of the distal lung: Impact on Fgfr2b-driven epithelial repair*. PLoS Pathogens 12, e1005544.

218 **van Asten, S. D., Raaben, M., Nota, B. & Spaapen, R. M. (2018)** *Secretome screening reveals fibroblast growth factors as novel inhibitors of viral replication*. Journal of Virology 92, e00260-00218.

219 **Cortese, M., Kumar, A., Matula, P., Kaderali, L., Scaturro, P., Erfle, H., Acosta, E. G., Buehler, S., Ruggieri, A., Chatel-Chaix, L., Rohr, K. & Bartenschlager, R. (2019)** *Reciprocal effects of fibroblast growth factor receptor signaling on dengue virus replication and virion production*. Cell Reports 27, 2579-2592.

3. FGF receptor triple knockout in skin

Published as:

Meyer, M. et al. (2019) *Mouse genetics identifies unique and overlapping functions of fibroblast growth factor receptors in keratinocytes.* Journal of Cellular and Molecular Medicine 24, 1774-1785.

DOI: 10.1111/jcmm.14871

My contribution:

- Verification of the knockout in the primary keratinocytes (Figure 1C)
- Analysis of proliferation after FGF1 stimulation (Figure 1D)
- Management of the mouse lines
- Manuscript editing

Mouse genetics identifies unique and overlapping functions of FGF receptors in keratinocytes

Michael Meyer[1], Maya Ben-Yehuda Greenwald[1], Theresa Rauschendorfer[1], Catharina Sänger[1], Marko Jukic[1], Haruka Iizuka[1], Fumimasa Kubo[1], Lin Chen[2], David M. Ornitz[3] and Sabine Werner[1]*

[1]Institute of Molecular Health Sciences, Department of Biology, ETH Zurich, 8093 Zurich, Switzerland

[2]Center of Bone Metabolism and Repair, Department of Rehabilitation Medicine, State Key Laboratory of Trauma, Burns and Combined injury, Trauma Center, Research Institute of Surgery, Daping Hospital, Third Military Medical University, Chongqing 400042, China;

[3]Department of Developmental Biology, Washington University School of Medicine, St. Louis, Missouri 63110

*Address for correspondence:

Prof. Dr. Sabine Werner
Institute of Molecular Health Sciences
Otto-Stern-Weg 7
8093 Zurich, Switzerland
Phone: +41 44 633 3941
Fax: +41 44 633 1174
E-mail: sabine.werner@biol.ethz.ch

Abstract

Fibroblast growth factors (FGFs) are key regulators of tissue development, homeostasis and repair, and abnormal FGF signaling is associated with various human diseases. In human and murine epidermis, FGF receptor 3 (FGFR3) activation causes benign skin tumors, but the consequences of FGFR3 deficiency in this tissue have not been determined. Here we show that FGFR3 in keratinocytes is dispensable for mouse skin development, homeostasis and wound repair. However, the defect in the epidermal barrier and the resulting inflammatory skin disease that develops in mice lacking FGFR1 and FGFR2 in keratinocytes were further aggravated upon additional loss of FGFR3. This caused fibroblast activation and fibrosis in the FGFR1/FGFR2 double knockout mice and even more in mice lacking all three FGFRs, revealing functional redundancy of FGFR3 with FGFR1 and FGFR2 for maintaining the epidermal barrier. Taken together, our study demonstrates that FGFR1, FGFR2 and FGFR3 act together to maintain epidermal integrity and cutaneous homeostasis, with FGFR2 being the dominant receptor.

Key words: Atopic dermatitis, Epidermal barrier, Epidermis, FGF, FGF receptor, Fibrosis, Skin

3.1 Introduction

Fibroblast growth factors (FGFs) are master regulators of development and tissue repair, and abnormal expression of FGFs or their receptors is associated with a wide variety of human diseases [42, 45, 48]. Most of the 22 members of the mammalian FGF family bind and activate four receptor tyrosine kinases, designated FGFR1 – FGFR4 [48], which exert distinct functions in different tissues and organs. In some cases, however, partially overlapping functions have been discovered as revealed by a stronger phenotype of double compared to single knockout mice. This was previously demonstrated in our laboratory for the skin through generation and characterization of mice lacking FGFR1 or FGFR2 or both receptors in keratinocytes [65]. While mice lacking only FGFR1 in this cell type are phenotypically normal, mice lacking FGFR2 in keratinocytes develop hair and sebaceous gland abnormalities and mild, although progressive skin inflammation [65, 220]. Interestingly, loss of both receptors resulted in a strong phenotype characterized by progressive loss of hair follicles and sebaceous glands and development of chronic skin inflammation [65, 180, 221]. This finding demonstrates that FGFR1 signaling is unmasked, probably through FGF10/FGF22 signaling to the b splice variant of FGFR1 [42, 65]. The phenotype of the double mutant mice (designated K5-R1/R2 mice) shows many similarities to the skin inflammation that occurs in patients with the chronic inflammatory skin disease atopic dermatitis (AD) [65, 180, 221, 222], which results from a defect in the epidermal barrier that is caused at least in part by decreased expression of major tight junction components that are under direct control of FGFR signaling in keratinocytes [65, 180, 221, 222]. We showed that different types of immune cells are attracted and/or activated upon establishment of the barrier defect, and growth factors and cytokines secreted by immune cells and fibroblasts caused keratinocyte hyperproliferation and epidermal thickening [65, 180, 221, 222]. Nevertheless, the double knockout mice have a normal life expectancy and the inflammatory phenotype remains surprisingly mild under non-challenged conditions. This suggested that other FGF receptors or receptors for different growth factors can compensate at least in part for the loss of FGFR1 and FGFR2 in keratinocytes. Since FGFR3, in particular the FGFR3b splice variant, is also expressed in the murine epidermis [62], we speculated that loss of this receptor in K5-R1/R2 mice would aggravate the phenotype. In addition, a phenotype in mice lacking only FGFR3 in keratinocytes was anticipated, since activating mutations in the *FGFR3* gene are the cause of the genetic skin disorder acanthosis nigricans and also induce seborrheic keratosis and epidermal nevi [223-226]. Here we show, however, that loss of FGFR3 in keratinocytes does not obviously affect skin morphogenesis, homeostasis or wound repair in

mice. Surprisingly, loss of all FGF receptors in keratinocytes is compatible with life, but the FGFR3 deficiency further aggravated some of the phenotypic abnormalities seen in K5-R1/R2 mice. Overall, these results identify FGFR2 as the major functional FGF receptor in keratinocytes, while FGFR1 and FGFR3 have a “back-up” function.

3.2 Materials and Methods

3.2.1 Mice

Mice lacking FGFR1 and FGFR2 in keratinocytes (K5-R1/R2 mice) were previously described [65, 66, 180, 221, 222]. To generate mice lacking a functional FGFR3 protein in keratinocytes, we mated mice with floxed *FGFR3* alleles [227] with K5-Cre mice [228]. Triple mutant mice were obtained by crossing females with floxed *FGFR3* alleles with K5-R1/R2 males (Figure 1A). The F1 generation was paired *inter se* until K5-R1/R2/R3 mice were obtained as described in Figure 1A. All K5-Cre mice used for breeding were males, since global deletion occurred with females [228]. Due to the difficult breeding scheme, each experiment included mice from different litters, but at least 1-2 mice from the same litter were used for a direct comparison in all experiments. All mice were in C57BL/6 genetic background. Control mice (ctrl) were mice with floxed *FGFR* alleles but without Cre recombinase or occasionally K5-Cre mice. They were housed under specific pathogen-free conditions and received food and water *ad libitum*. Mouse maintenance and all animal experiments had been approved by the veterinary authorities of Zurich, Switzerland (Kantonales Veterinäramt Zürich).

3.2.2 Establishment and culture of primary mouse keratinocytes

Keratinocytes were isolated from single mice as described previously [65] and cultured in defined keratinocyte serum-free medium (Invitrogen, Paisley, UK) supplemented with 10 ng/mL epidermal growth factor (EGF) and 10^{-10} M cholera toxin and 100 U/mL penicillin/100 µg/mL streptomycin (Sigma) in keratinocyte medium [229]. Plates were coated with collagen IV (2.5 g/cm^2) prior to seeding of the cells.

3.2.3 BrdU incorporation assay

Primary keratinocytes were incubated overnight in keratinocyte serum-free medium without EGF. BrdU (Sigma) was added to the cell culture medium at a final concentration of 100 µM followed by incubation for 4 h at 37ºC and 5% CO_2. Then, cells were washed with PBS and fixed with 4% paraformaldehyde for 30 min at RT. Afterwards, they were permeabilized and DNA was denatured using 0.1% Triton-X100 in 2M HCl for 30 min. Cells were then incubated in boric buffer (100 mM boric acid, 75 mM NaCl, 25 mM sodium tetraborate, pH 8.5) for neutralization for 5 min and blocked using 1% BSA for 30 min, followed by incubation with a

FITC-coupled anti-BrdU antibody (11202693001, Sigma) at 4°C overnight. Cells were then washed with PBS, and a Cy2-conjugated secondary antibody (1:500, Jackson ImmunoResearch Laboratories, Inc., West Grove, PA) was added to amplify the signal. Nuclei were counterstained with Hoechst 33342 (1:3000, Sigma).

3.2.4 Histology

Skin samples were fixed overnight with 4% paraformaldehyde (PFA) or 95% ethanol/1% acetic acid prior to paraffin embedding. Sections (7 µm) were stained with hematoxylin and eosin (H&E), or using the Herovici procedure [230]. Visualization of mast cells was carried out using toluidine blue staining [65]. Stained sections were analysed with an Axioskop 2 microscope equipped with a Plan-Neofluar objective (20x/0.5NA) and photographed with an Axiocam HRc camera (all from Carl Zeiss, Inc., Jena, Germany). The Axiovision 4.6 software (Carl Zeiss, Inc.) was used for acquisition of data. Data were analysed using ImageJ software. All analyses were performed blinded with regard to the genotype of the mice.

3.2.5 Immunohistochemistry and immunofluorescence analysis

Paraffin sections were dewaxed and rehydrated using a xylene/ethanol gradient followed by antigen retrieval using citrate buffer (10 mM citric acid, pH 6.0) at 95°C for 1 h and three washes with PBST (PBS, 0.1% Tween). Skin sections were then blocked with PBS containing 12% BSA for 1 h at RT, followed by incubation with the primary antibodies overnight at 4°C. Cryo-sections were fixed in 1-4% paraformaldehyde for 10 min at RT, washed for 2 x 5 min in PBS and blocked in 5% BSA for 1 h at room temperature, followed by incubation with the primary antibodies overnight at 4°C. For bright-field microscopy analysis, a biotin-conjugated secondary antibody, the Vectastain ABC kit (Vector Laboratories, Burlingame, CA) and the DAB peroxidase substrate kit (Vector Laboratories) were used for visualization. For immunofluorescence staining, slides were incubated at room temperature for 1 h with the Cy2- or Cy3-conjugated secondary antibodies (Jackson ImmunoResearch Laboratories, Inc., West Grove, PA) and counterstained with Hoechst 33342 (Sigma). The antibodies used are listed in Table 1.

Table 1. Antibodies used in immunohistochemistry or immunofluorescence

Antibody	Source	Identifier
Rabbit anti-Ki67	Abcam, Cambridge, UK	Cat#Ab15580; RRID:AB_443209

Biotinylated anti-rabbit IgG	Jackson ImmunoResearch	Cat#111-065-003; RRID:AB_2337959
Rabbit anti-keratin 6	BioLegend, San Diego, CA	Cat#PRB-169P-100; RRID:AB_10063923
Mouse anti-keratin 10	DAKO, Glostrup, Denmark	Cat#M7002
Rabbit anti-keratin 14	BAbCo, Richmond, CA	Cat#PRB-155P; RRID:AB_292096
Rabbit anti-loricrin	BioLegend	Cat#PRB-145P; RRID:AB_10064155
Rabbit anti-vimentin	Abcam	Cat#ab92547; RRID:AB_10562134
Anti-rabbit Cy3	Jackson ImmunoResearch	Cat#711-165-152; RRID:AB_2307443
Anti-mouse Cy3	Jackson ImmunoResearch	Cat#715-165-150; RRID:AB_2340813
Anti-rabbit Cy2	Jackson ImmunoResearch	Cat#111-225-003; RRID:AB_2307385

3.2.6 Analysis of transepidermal water loss (TEWL)

Mouse back skin was shaved one day before TEWL analysis. TEWL was determined using a Tewameter (Courage and Khazaka Electronic GmbH, Cologne, Germany) as described previously [180]. Twenty-five consecutive measurements were taken from four different places on the back on different days.

3.2.7 Isolation of RNA from mouse skin

Mice were sacrificed, shaved, and epidermis from mouse back skin was separated from the dermis after heat shock treatment (30 s at 60°C in PBS followed by 1 min at 4°C in PBS). Isolated epidermis and dermis were immediately frozen in liquid nitrogen. For RNA isolation we used Trizol® according to the manufacturer's instructions (Cat# 15596, Life Technologies, Carlsbad, CA).

3.2.8 Real-time RT-PCR

RNA was reverse transcribed using the iScript™ cDNA synthesis kit (Cat# 1708890, BioRad, Hercules, CA). Quantitative real-time RT-PCR (qRT-PCR) was performed as described in the manual of the Light Cycler 480 II (Roche, Rotkreuz, Switzerland). The reverse transcription product obtained from 25 ng RNA was used together with 5.5 µl of SYBR Green reaction mix including 0.45 µM forward and reverse primer mix. The reaction was performed in 50 cycles

(95°C for 10 min for initial denaturation; 95°C for 10 s, 60°C for 20 s and 72°C for 20 s for each cycle). Samples were analysed in duplicates. Data were quantified using second derivative maximum analysis and gene expression represented as relative to the mRNA encoding ribosomal protein S29 (*Rps29*).

The following primers were used:

Table 2. Real-time PCR primers

Target gene	Sequence
Cldn1	5'-CTTCTCTGGGATGGATCG-3'
	5'-GGGTTGCCTGCAAAGTACTGT-3'
Cldn3	5'-GCGGCTCTGCTCACCTTAGT-3'
	5'-GACGTAGTCCTTGCGGTCGTA-3'
Cldn8	5'-TCAGAATGCAGTGCAAGGTC-3'
	5'-AGCCGGTGATGAAGAAGATG-3'
FGFR1	5'-CAACCGTGTGACCAAAGTGG-3'
	5'-TCCGACAGGTCCTTCTCCG-3'
FGFR2	5'-ATCCCCCTGCGGAGACA-3'
	5'-GAGGACAGACGCGTTGTTATCC-3'
FGFR3 total (exon 2/3)	5'-GTG GCT GGA GCT ACT TCC GA-3'
	5'-ATC CTT AGC CCA GAC CGT GG-3'
FGFR3c (exon(7/8)	5'-ACT CAA GAC TGC AGG CGC TA-3'
	5'-GTC CTC AAA GGT GAC ATT GTG C-3'
FGFR4	5'-TTG GCC CTG TTG AGC ATC T-3'
	5'-GCC CTC TTT GTA CCA GTG ACG-3'
Fst	5'-AGGGAAAGTGTATCACAAAGT-3'
	5'-GAGTTGCAAGATCCAGAATG-3'
Il36b	5'-GCCTGTCATTCTTAGCTTGAT-3'
	5'-TGTCTACTTCCTTAAGCTGC-3'
Inhba	5'-GGA GAA CGG GTA TGT GGA GA-3'
	5'-ACA GGT CAC TGC CTT CCT TG-3'
Ocln	5'-TTG AAG TCC ACC TCC TTA CAG A-3'
	5'-CCG GAT AAA AAG AGT ACG CTG G-3'
Rps29	5'-GGTCACCAGCAGCTCTACTG-3'
	5'-GTCCAACTTAATGAAGCCTATGTCC-3'
S100a8	5'-GCCGTCTGAACTGGAGAAG-3'
	5'-GTGAGATGCCACACCCACTTT-3'
S100a9	5'-CGCAGCATAACCACCATCAT-3'
	5'-AAGATCAACTTTGCCATCAGC-3'
Tgfb1	5'-AGC CCG AAG CGG ACT ACT AT-3'
	5'-TCC ACA TGT TGC TCC ACA CT-3'
Tgfb3	5'-CTC TGG GTT CAG GGT GTT GT-3'
	5'-AAC CTG GAG GAG AAC TGC TG-3'
Cre	5'-AAC ATG CTT CAT CGT CGG-3'
	5'-TTC GGA TCA TCA GCT ACA CC-3'

3.2.9 Isolation of skin cells for flow cytometry

Mice were sacrificed, shaved, and the back skin was harvested. The subcutaneous fat was scraped off. Epidermis and dermis were separated using 0.25% dispase (Gibco, Zug, Switzerland) for 50 min at 37°C under continuous shaking. The epidermis was treated with 100 Kunitz units/ml DNase (Sigma) in RPMI supplemented with P/S, 10% FBS and 20 mM HEPES for 45 min at 37°C under continuous shaking. The dermis was cut into small pieces and treated with 0.25 mg/ml TL Liberase in RPMI supplemented with P/S and 20 mM HEPES for 1 h at 37°C under continuous shaking. Single cell suspensions were prepared by passing mixtures through 70 µm cell strainers, and cells were washed 3x with 1x PBS.

3.2.10 Flow cytometry

Unspecific binding sites were blocked using a CD16/CD32 antibody. Dead cells were stained with Zombie Aqua™ dye (BioLegend, San Diego, CA). The antibodies used for flow cytometry analysis are listed below. Stained cells were quantified using a BD Fortessa machine and BD FACSDiva™ 6.0 software (both from BD Biosciences, San Jose, CA). FlowJo v10 software (FlowJo, Ashland, OR) was used for data analysis. Compensation was performed using single color controls. Compensation matrices were calculated using FlowJo v10 software and applied. Doublets and dead cells were excluded from the analysis. Fluorescence minus one (FMO) controls were used for gating analyses to distinguish positively from negatively staining cell populations.

Table 3. Antibodies used for flow cytometry analysis

Antigen	Clone	Fluorophor	Dilution	Source
Zombie Aqua	NA	Aqua	1:1.000	BioLegend
CD45	30-F11	PB	1:400	BioLegend
Fc block (CD 16/32)	2.4G2	NA	1:100	BD Biosciences
CD3	17A2	BV785	1:300	BioLegend
I-A/I-E	M5/114.15.2	PE	1:2.000	BD Biosciences
TCRδ	GL3	FITC	1:400	BD Biosciences

3.2.11 Statistical analysis

Statistical analysis was performed using PRISM software v5 (Graph Pad Software Inc., La Jolla, CA). Mann-Whitney U test was used for comparison between two different groups. * $P \leq 0.05$, ** $P \leq 0.01$, *** $P \leq 0.001$, **** $P \leq 0.0001$.

3.3 Results

3.3.1 FGF receptors 1, 2, and 3 are expressed in the epidermis and in cultured keratinocytes

To determine if the loss of FGFR1 and FGFR2 in keratinocytes can be partially compensated by other FGF receptors, we first analysed published data for *FGFR1, FGFR2, FGFR3* and *FGFR4* expression levels. RNA sequencing data of FACS-isolated cells from mouse skin at embryonic day 14.5 (E14.5) or postnatal day 5 (P5) [231] revealed low expression levels of *FGFR1* in the epidermis, while *FGFR3* was expressed at intermediate levels and *FGFR2* at high levels. *FGFR4* expression was not detectable in the embryonic or neonate epidermis (Supplementary Figure S1A, B). In addition, various FGF ligands are expressed in embryonic and neonate mouse skin, in particular *FGF2*, *FGF7*, *FGF10* and *FGF18* [231]. These data are consistent with single cell RNA sequencing data of cells from adult mouse epidermis [232]. The relatively high expression of *FGFR3* in the epidermis suggests that this type of receptor may function alone or redundantly with FGFR1 and FGFR2 in keratinocytes.

3.3.2 Loss of FGFR3 in keratinocytes does not affect epidermal homeostasis and wound healing

To determine the functional relevance of FGFR3 in keratinocytes, we generated mice lacking FGFR3 in keratinocytes (designated K5-R3 mice). Mice with floxed *FGFR3* alleles [227] were mated with transgenic mice expressing Cre recombinase in keratinocytes under control of the keratin 5 (K5) promoter [228] to generate K5-Cre, $Fgfr3^{f/f}$ mice (designated K5-R3 mice). K5-R3 mice were viable and fertile and did not reveal macroscopically visible or histological abnormalities in the skin (Supplementary Figure S2A, B). A quantitative analysis further showed that the thickness of the epidermis, the number of proliferating keratinocytes in the epidermis (Ki67-positive cells) and the dermal thickness were similar in K5-R3 and Ctrl mice (Supplementary Figure S2C-E). Remarkably, even the healing of full-thickness excisional wounds proceeded normally and there was no significant difference in wound closure or wound diameter (Supplementary Figure S2F).

3.3.3 Generation of mice lacking all FGF receptors in keratinocytes

We next determined if loss of FGFR3 aggravates the phenotype of mice lacking FGFR1 and FGFR2 in keratinocytes by generation of triple conditional knockout mice (K5-R1/R2/R3 mice; see breeding scheme in Figure 1A). K5-R1/R2/R3 mice were born with the expected Mendelian ratio. qRT-PCR analysis of RNA from isolated epidermis of K5-R1/R2/R3 mice confirmed the expression of Cre recombinase in the mutant mice and the efficient deletion of all three receptors (Figure 1B). The Cre-mediated deletion of the *Fgfr3* floxed alleles results in deletion of the IIIc exon and the exon encoding the transmembrane domain [227], and we confirmed the efficient deletion using primers that hybridize to this part of the mRNA (exons 7/8). The major FGFR3 splice variant in the skin, however, is FGFR3b, which differs from FGFR3c in the second half of the third immunoglobulin (Ig)-like domain and thus has different ligand binding specificities [233]. The *FGFR3* knockout mice may still express a truncated RNA including the exon IIIb coding sequences, which, however, cannot give rise to a functional receptor due to the lack of the transmembrane domain. However, we also observed an efficient down-regulation of FGFR3 mRNA in K5-R3 and K5-R1/R2/R3 mice using a primer hybridizing to exons 2/3, which should be present in such a truncated RNA. Therefore, such transcripts are most likely unstable. The efficient reduction in FGFR3 mRNA levels also suggests that keratinocytes are the predominant producers of this receptor in the epidermis and that the expression in epidermal immune cells is negligible.

Efficient deletion of all FGF receptors was confirmed with cultured primary keratinocytes from the different mutant mice (Figure 1C). The loss of *FGFR1*, *FGFR2* and *FGFR3* did not result in a compensatory upregulation of *FGFR4*, and the mRNA levels of this receptor remained below the detection limit in mice of all genotypes. Further, we did not detect a compensatory upregulation of *FGFR3* in K5-R1/R2 mice, but rather a reduced expression of this receptor (Figure 1B, C). Surprisingly, expression levels of *FGFR3* were highly variable in keratinocytes with wild-type *FGFR3* alleles (Figure 1B, C), but this did not correlate with obvious phenotypic differences.

The complete loss of FGFR signaling in cultured keratinocytes from K5-R1/R2/R3 mice was confirmed by proliferation studies with FGF1, which activates all FGFR variants [50]. While cells from control mice incorporated 5-bromo-2`-deoxyuridine (BrdU) in response to FGF1 and to epidermal growth factor (EGF) - used here as positive control -, keratinocytes from K5-R1/R2/R3 mice only responded to EGF (Figure 1D).

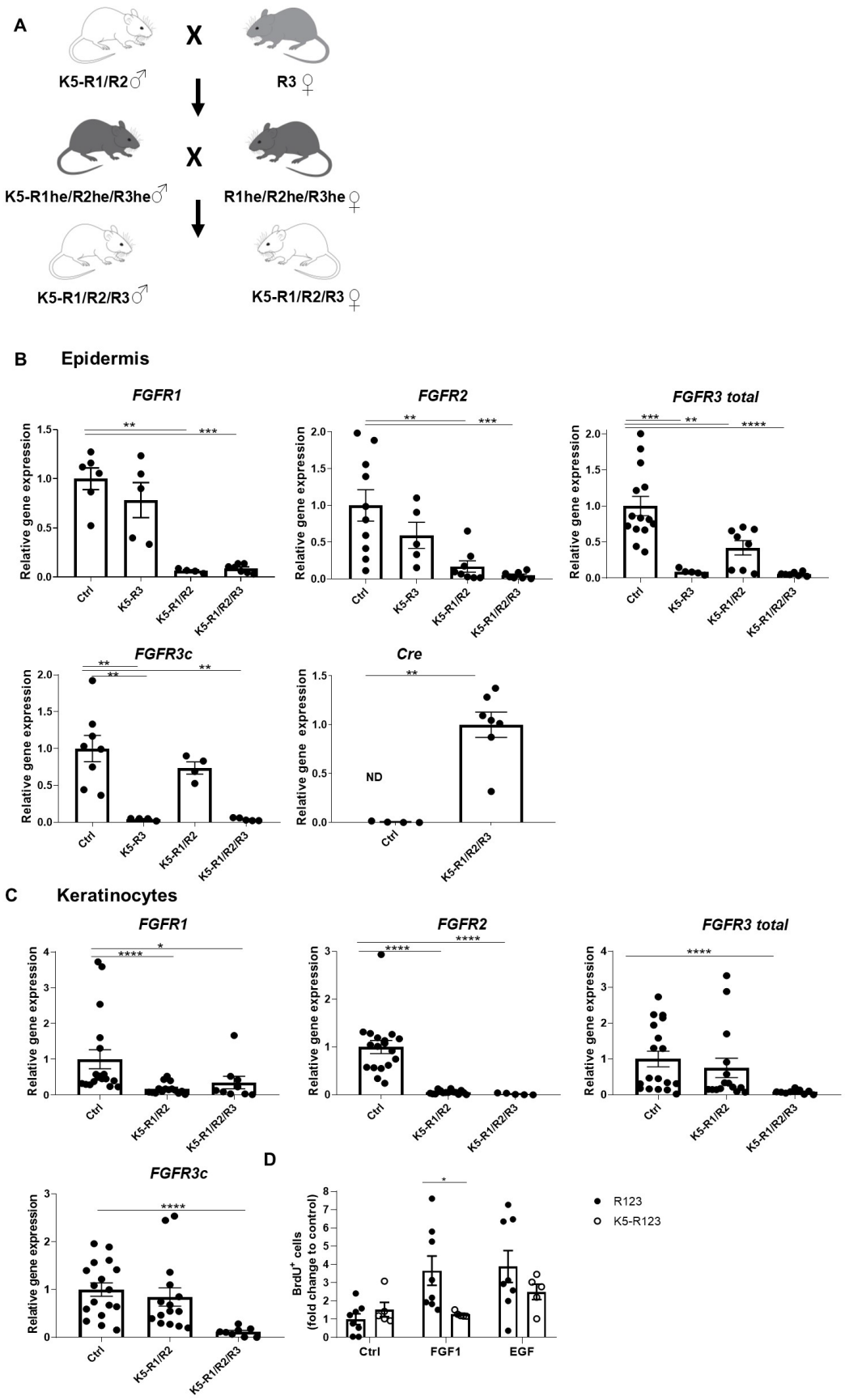

Figure 1: Verification of the *FGFR3* knockout in the mutant epidermis and in isolated primary keratinocytes.

(A) Breeding scheme for the generation of mice lacking FGFR1, FGFR2 and FGFR3 in keratinocytes (K5-R1/R2/R3 mice). He = heterozygous.

(**B**) qRT-PCR analysis of RNA samples from isolated epidermis of adult Ctrl, K5-R3, K5-R1/R2 and K5-R1/R2/R3 mice for *FGFR1*, *FGFR2*, *FGFR3* (all isoforms), *FGFR3c,* and *Cre* relative to *Rps29* as indicated.

(C) qRT-PCR analysis of RNA samples from primary keratinocytes derived from 3-day old Ctrl, K5-R1/R2 and K5-R1/R2/R3 mice for *FGFR1*, *FGFR2*, *FGFR3* (all isoforms), and *FGFR3c* relative to *Rps29* as indicated.

(D) Primary keratinocytes from K5-R1/R2/R3 or control mice were incubated overnight in keratinocyte serum-free medium without EGF and subsequently treated with 10 ng/ml FGF1 or EGF for 24 h and analysed for BrdU incorporation.

Bars indicate mean ± SE. N=4-11 per genotype. * $P \leq 0.05$, ** $P \leq 0.01$, *** $P \leq 0.001$, **** $P \leq 0.0001$. Mann-Whitney U test.

3.3.4 Loss of FGFR3 in keratinocytes does not aggravate the macroscopic and histological phenotype of K5-R1/R2 mice

K5-R1/R2/R3 mice were macroscopically similar to K5-R1/R2 mice, including the progressive hair loss and the small body size (Figure 2A). Furthermore, K5-R1/R2 and K5-R1/R2/R3 mice had a similar reduction in body weight compared to control mice (Figure 2B).

Histological analysis of the skin showed the characteristic phenotype of K5-R1/R2 mice with epidermal thickening [65]. Again, this was not obviously aggravated by the additional loss of FGFR3, and loss of FGFR3 alone did not affect the epidermal thickness (Figure 2C). In addition, keratinocyte proliferation and differentiation as revealed by Ki67 immunohistochemistry (Figure 2D) or immunofluorescence analyses for differentiation-specific proteins (Supplementary Figure S3), respectively, were similar in K5-R1/R2/R3 and K5-R1/R2 mice. As previously shown [65], K5-R1/R2 mice exhibited interfollicular expression of keratin 6 (K6), a sign for abnormal keratinocyte differentiation and enhanced proliferation [234]. This was also not further aggravated by the loss of FGFR3, and the other differentiation-specific keratins as well as the late differentiation marker loricrin were normally expressed in both the double and triple knockout mice (Supplementary Figure S3).

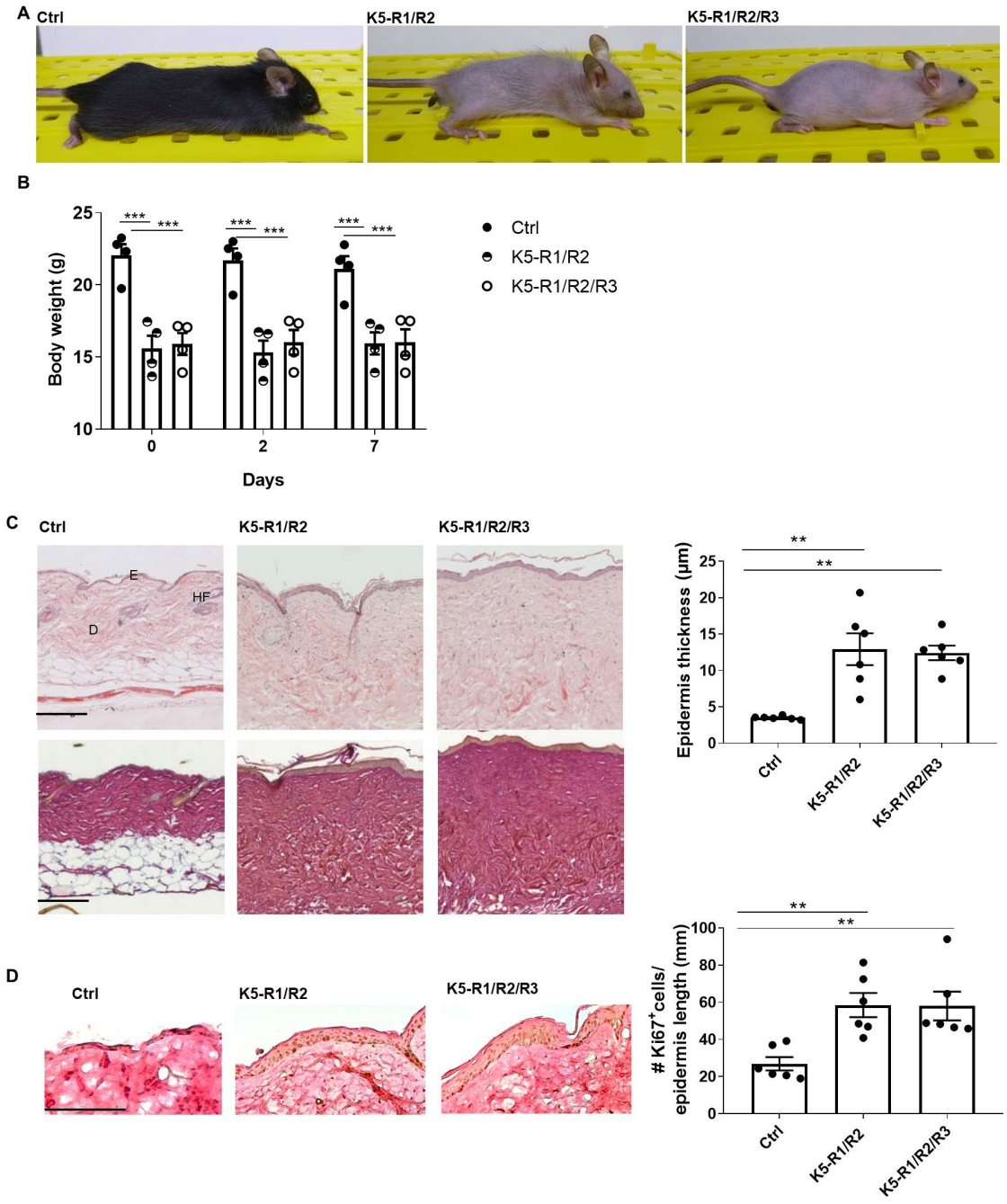

Figure 2: Loss of FGFR3 in keratinocytes does not aggravate the macroscopic phenotype of K5-R1/R2 mice.

(**A**) Representative photographs of K5-R1/R2/R3 mice and their control littermates lacking Cre recombinase, compared to K5-R1/R2 mice.

(**B**) Body weight of Ctrl, K5-R1/R2 and K5-R1/R2/R3 mice at the age of 12 weeks. N=4 per genotype.

(**C**) Representative photomicrographs of hematoxylin/eosin- (upper panel) and Herovici-stained (lower panel) paraffin sections from back skin of 9 months old mice and their control littermates (left panel) and quantification of epidermal thickness (right panel). Magnification bars: 100 µm. D: Dermis; E: Epidermis, HF: Hair follicles.

(**D**) Representative images of Ki67-stained paraffin sections from back skin of 9 months old mice and their control littermates (left panel) and quantification of Ki67-positive cells per length epidermis (right panel).

Magnification bars: 100 μm. D: Dermis; E: Epidermis, HF: Hair follicles. Bars indicate mean ± SE in all graphs. N=4-6 per genotype. ** $P \leq 0.01$, *** $P \leq 0.001$. Mann-Whitney U test.

3.3.5 Loss of FGFR3 further aggravates the epidermal barrier deficiency of K5-R1/R2 mice

A hallmark of the phenotype of K5-R1/R2 mice is the defect in epidermal barrier function, which results at least in part from reduced expression of tight junction proteins and which causes a chronic inflammatory skin disease [65, 180, 221, 222]. The transepidermal water loss (TEWL), which reflects the integrity of the inside-out barrier, was indeed significantly higher in K5-R1/R2/R3 compared to K5-R1/R2 mice (Figure 3A). This was associated with a mild, but non-significant reduction in the mRNA levels of the tight junction proteins claudin 1 (*Cldn1*) and occludin (*Ocln*), while *Cldn3* and *Cldn8* were expressed at equally low levels in mice of both genotypes (Figure 3B).

Flow cytometry analysis demonstrated that the number of total immune cells, Langerhans cells (MHCII-positive cells in the epidermis), and epidermal γδ T cells (dendritic epidermal T cells (DETC)) were equally low in control *vs*. K5-R3 mice (Figure 3C, and Supplementary Figure S4 for flow cytometry), and the number of toluidine blue-positive mast cells was even mildly reduced by the loss of FGFR3 (Figure 3D). These immune cells were analysed, because their numbers are strongly increased in K5-R1/R2 *vs.* control mice [65, 180, 221] (Figure 3C, D). With the exception of a significant increase in epidermal γδ T cells in K5-R1/R2/R3 *vs.* K5-R1/R2 mice, the additional loss of FGFR3 did not further affect the number of the other immune cell types (Figure 3C, D). Consistent with the similar number of immune cells in K5-R1/R2 and K5-R1/R2/R3 mice, the genes encoding the pro-inflammatory cytokines IL-36β (=IL1-F8) (*Il1f8*), S100A8 (*S100a8*) and S100A9 (*S100a9*) were expressed at similar levels in mice of both genotypes (Figure 3E).

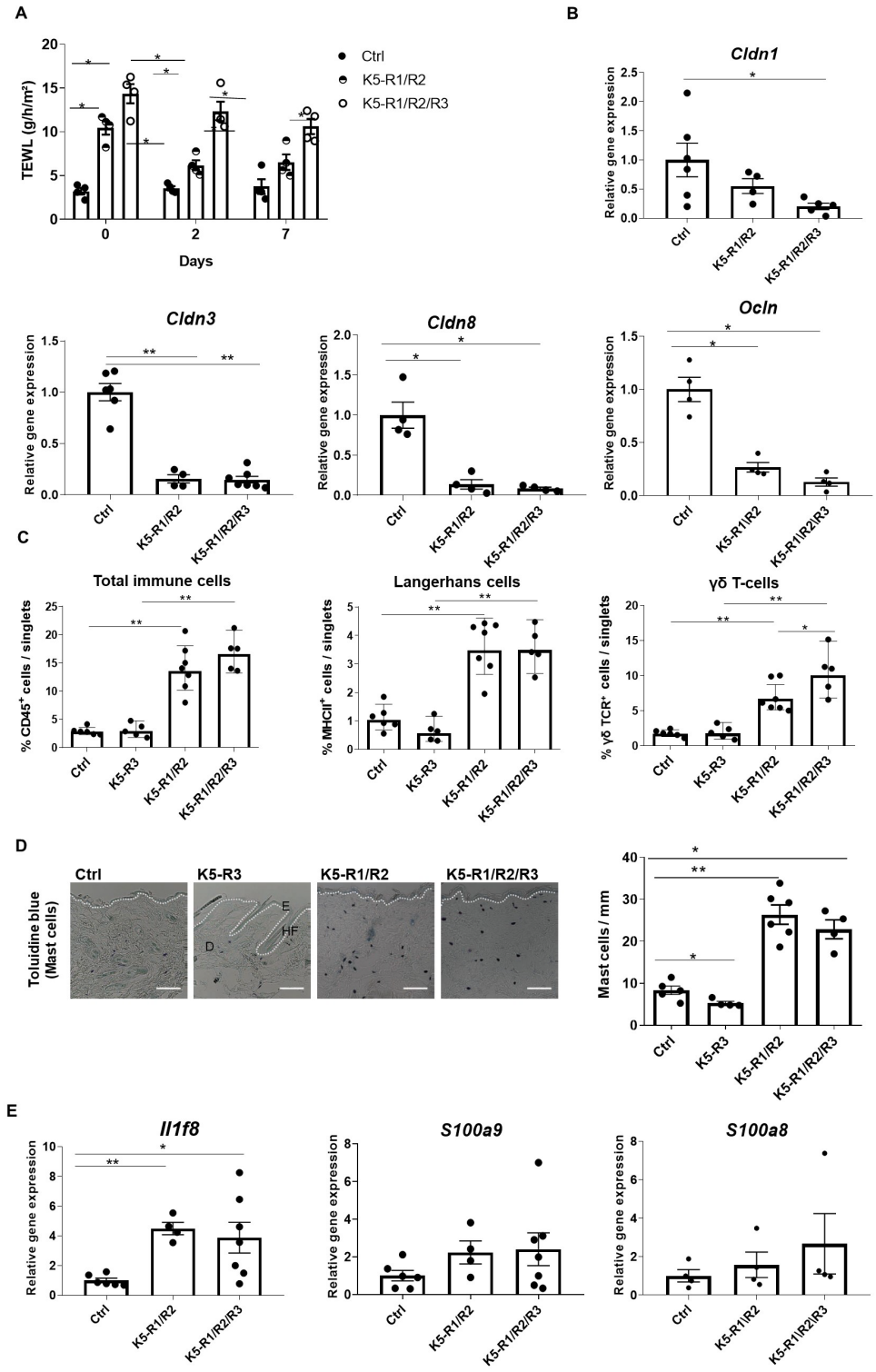

Figure 3: Loss of FGFR3 in keratinocytes mildly aggravates the barrier function defect of K5-R1/R2 mice.

(**A**) Transepidermal water loss (TEWL) on the back skin of 9 weeks old Ctrl, K5-R1/R2 and K5-R1/R2/R3 mice (in g/h/m^2). Measurements were repeated on the same mice 2 and 7 days later. N = 4 mice per genotype.

(**B**) qRT-PCR analysis of RNA samples from the epidermis of Ctrl, K5-R1/R2 and K5-R1/R2/R3 mice for *Cldn1* and *Cldn3* relative to *Rps29*. N = 4-6 per genotype.

(**C**) Flow cytometry analysis of dissociated epidermal cells from Ctrl, K5-R3, K5-R1/R2 and K5-R1/R2/R3 mice for quantification of total $CD45^+$ immune cells, MHCII-positive Langerhans cells and γδ T cells (DETCs). N=5-7 per genotype.

(**D**) Representative images of toluidine blue-stained paraffin sections from back skin and quantification of toluidine-blue stained mast cells / mm dermis. The dotted white line indicates the basement membrane. Magnification bars: 50 μm. D: Dermis, E: Epidermis, HF: Hair follicle.

(**E**) qRT-PCR analysis of RNA samples from the epidermis for *Il1f8, S100a8* and *S100a9* relative to *Rps29*. N = 4-6 per genotype.

Bars indicate mean ± SE in all graphs. * $P \leq 0.05$, ** $P \leq 0.01$. Mann-Whitney U test.

3.3.6 FGFR deficiency in the epidermis causes dermal fibrosis

An additional hallmark of the phenotype of K5-R1/R2 mice, which we had previously not characterized, is the development of skin fibrosis. This is reflected by the enhanced dermal thickness and the presence of a dense connective tissue characterized by high levels of collagen, which had replaced the adipose tissue (Figure 4A). The fibrotic phenotype was particularly pronounced in K5-R1/R2/R3 mice. There was a further significant increase in dermal thickness compared to K5-R1/R2 mice (Figure 4B). The percentage of dermal area that stained positive for vimentin was also higher in K5-R1/R2/R3 compared to K5-R1/R2 mice (Figure 4C), suggesting an increase in the number of mesenchymal cells in the dermis. Consistent with this finding, the number of dermal cells expressing the proliferation marker Ki67 was higher in K5-R1/R2 compared to control mice and further increased in K5-R1/R2/R3 mice (Fig. 4D).

Overall, these findings suggest that the defect in the epidermal barrier affects the fibroblast phenotype, possibly through release of pro-fibrotic factors. To test this possibility, we analysed the expression of *Tgfb1*, *Tgfb3*, *Inhba* and *Fst*, which give rise to the secreted factors TGF-β1, TGF-β3, activin A and the activin antagonist follistatin. While expression of the pro-fibrotic factors *Tgfb1, Tgfb3,* and *Inhba* was even moderately reduced in K5-R1/R2 and K5-R1/R2/R3 mice, *Fst* expression was strongly down-regulated in mice of both genotypes, indicating a potential increase in biologically active activin (Figure 4E).

Taken together, these results demonstrate that loss of FGFR1/R2 in keratinocytes causes skin fibrosis, which is further aggravated upon loss of FGFR3.

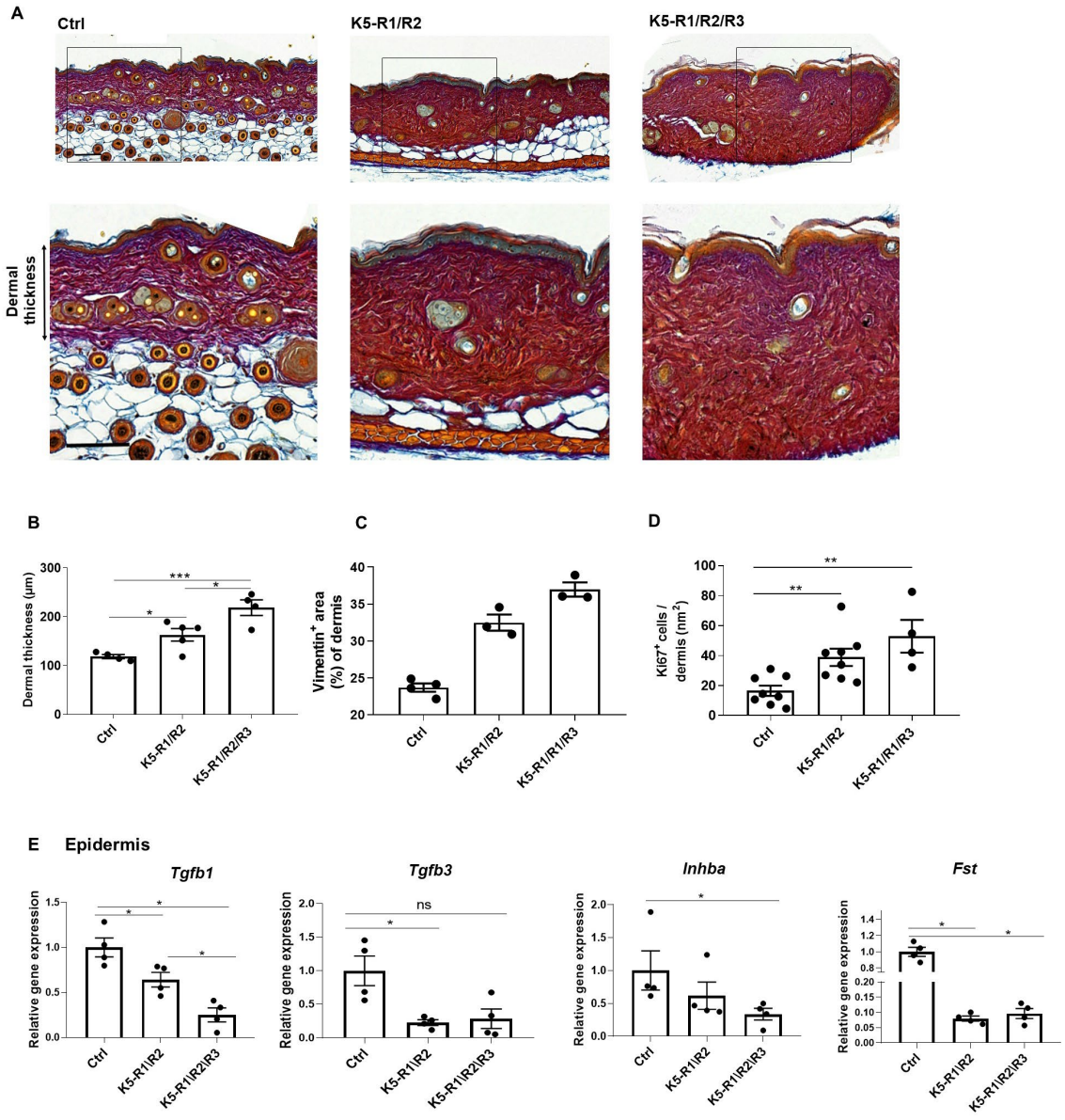

Figure 4: Loss of FGFR signaling in keratinocytes causes dermal fibrosis.

(A) Representative images of Herovici-stained sections of 3 months old Ctrl, K5-R1/R2 and K5-R1/R2/R3 mice. Magnification bars: 100 µm. Note the replacement of adipose tissue by fibrous tissue in the FGFR mutant mice. Squares indicate the area where the high magnification image was taken (lower panel).

(B) Quantification of dermal thickness in Ctrl, K5-R1/R2 and K5-R1/R2/R3 mice. N=4 per genotype.

(C) Quantification of the percentage of vimentin-positive skin area in Ctrl, K5-R1/R2 and K5-R1/R2/R3 mice. Epidermal area was excluded. N=3-4 per genotype.

(D) Quantification of Ki67-positive cells in the dermis and subcutis of Ctrl, K5-R1/R2 and K5-R1/R2/R3 mice. N=4-8 per genotype.

(E) qRT-PCR analysis of RNA samples from the epidermis of Ctrl, K5-R1/R2 and K5-R1/R2/R3 mice for *Tgfb1, Tgfb3, Inhba and Fst* relative to *Rps29*. N = 4 per genotype. Mean expression in Ctrl mice was set to 1.

Bars indicate mean ± SE in all graphs. * $P \leq 0.05$, ** $P \leq 0.01$, *** $P \leq 0.001$. Mann-Whitney U test.

3.4 Discussion

Epidermal FGFR signaling plays a key role in skin homeostasis, repair and disease, but the contribution of the individual FGF receptors to different skin functions have remained largely unknown. Here we show that FGFR2 is the major FGFR in the murine epidermis, while FGFR3 has only a minor supporting role. FGFR3 in keratinocytes is even dispensable for wound healing, in spite of its upregulation in wounded mouse skin [212]. This is surprising, since activating mutations in this type of receptor cause acanthosis nigricans, seborrheic keratosis and epidermal nevi [223-226]. However, our findings are consistent with data from human keratinocytes demonstrating that knock-down of FGFR3 does not affect normal keratinocyte growth *in vitro* [235], even though this receptor is strongly expressed in the human epidermis [236]. These results point to a minor role of wild-type FGFR3 in keratinocytes, at least under non-challenged conditions.

Keratinocytes mainly express the IIIb splice variants of all FGF receptors, including FGFR3 [233], and this type of receptor is rather poorly activated by most FGFs [50]. By contrast, FGFR2b is strongly activated by FGF7 and FGF10, which are highly expressed in the skin [212, 231, 237]. This provides a likely explanation for the particularly important role of FGFR2 *vs.* FGFR1 and FGFR3 in keratinocytes. This unique role of FGFR2 is also reflected by the skin abnormalities seen in mice lacking only this receptor in keratinocytes [65, 220], which are aggravated, however, upon additional deletion of FGFR1 [65].

Our results further demonstrate that the loss of one FGF receptor in keratinocytes can be partially compensated by the other FGF receptors. Thus, FGFR1, FGFR2 and FGFR3 act together to maintain epidermal integrity, although the individual contributions are different. Finally, we also show that loss of all FGF receptors in keratinocytes is compatible with life and with *in vitro* growth of keratinocytes. Therefore, other growth factor receptors are likely to compensate for the loss of FGFR signaling.

In spite of the keratinocyte-specific deletion of FGF receptors, dermal fibrosis was seen in K5-R1/R2 mice and was more severe in K5-R1/R2/R3 mice. This may well be a consequence of the increase in immune cells that occurs in K5-R1/R2 and also in K5-R1/R2/R3 mice. However, additional loss of either mast cells or γδ T cells, two immune cell populations that are strongly increased in K5-R1/R2 and in K5-R1/R2/R3 mice, did not affect the dermal or epidermal phenotype in K5-R1/R2 mice [180, 221]. These findings suggest that fibroblasts are activated as a consequence of the epidermal abnormalities. Consistent with this assumption, it has been

shown that a defect in the epidermal barrier results in upregulation of cytokines, such as S100A8, S100A9 and S100A12 [238-240], which in turn cause fibroblast activation and fibrosis. S100A8 and S100A9 are also upregulated in K5-R1/R2 [65, 222] and to a similar extent in K5-R1/R2/R3 mice, and these cytokines likely contribute to the dermal fibrosis. Furthermore, we show here that expression of follistatin is strongly down-regulated in the epidermis of K5-R1/R2 and K5-R1/R2/R3 *vs.* control mice, which is likely to result in higher levels of bioactive activin, a potent pro-fibrotic factor [241, 242]. Therefore, the epidermal abnormalities seen in our FGFR mutant mice and also in patients with Atopic Dermatitis are likely to contribute to the development of skin fibrosis. Thus, amelioration of the epidermal alterations and the resulting inflammation is of crucial importance for the prevention of fibroblast activation, and activation of FGFR signaling in keratinocytes may be a promising strategy to improve the epidermal barrier and even to prevent/ameliorate the resulting dermal fibrosis.

Acknowledgements

We thank Drs. Anna-Katharina Müller and Jitka Somandin, ETH Zurich, Switzerland, for invaluable experimental help, Dr. Juha Partanen, University of Helsinki, Finland, for the floxed *FGFR1* mice and Drs. Angel Ramirez and José Jorcano, CIEMAT, Madrid, Spain, for the K5-Cre mice. This work was supported by the Swiss National Science Foundation (310030_132884 and 31003A-169204/1 to S.W), the ETH Zurich (grant ETH-06 15-1 to S.W.) and a predoctoral fellowship from the Studienstiftung des Deutschen Volkes (to C.S).

Author contributions

M.M., M.BG, T.R., C.S. M.J., H.I. and F.K. performed experiments and analysed the data. L.C. provided floxed FGFR3 mice. D.O. provided floxed FGFR1/FGFR2/FGFR3 mice. S.W. designed the study together with M.M, wrote the manuscript and provided the funding. All authors made important suggestions to the manuscript.

Disclosure

The authors declare no competing interests.

Supplementary figures

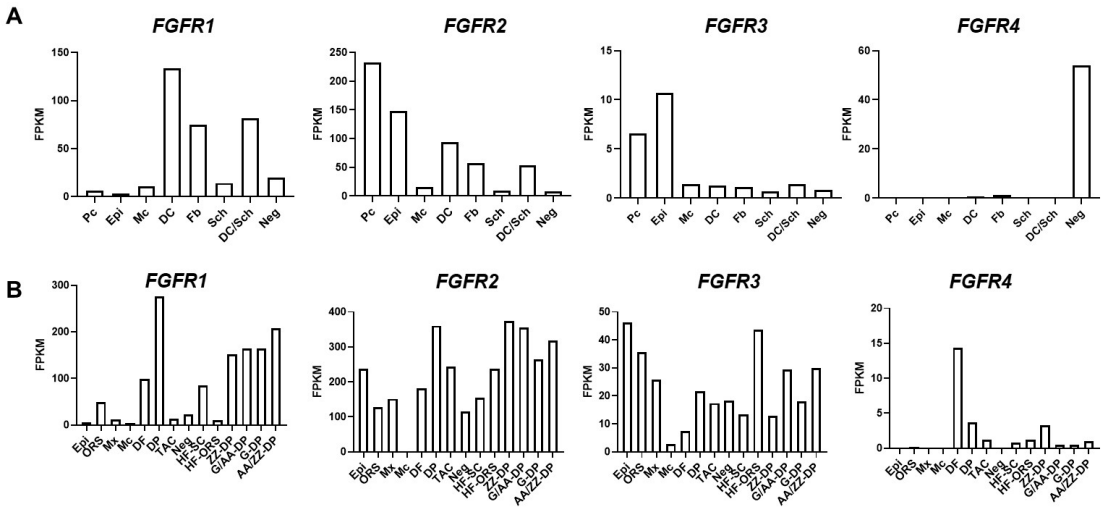

Supplementary Figure S1: Expression of FGF receptors in embryonic and neonatal mouse skin.

(**A, B**) RNA sequencing data of FACS-isolated cell populations from E14.5 (A) and P5 (B) mouse skin [231] showing low expression of *FGFR1*, intermediate expression of *FGFR3* and strong expression of *FGFR2*, but undetectable expression of *FGFR4* in the epidermis. Abbreviations A: FPKM: Fragments Per Kilobase Million; Pc: Placode; Epi: Epidermis; Mc: melanocytes; Dc: Dermal condensate; Fb: Fibroblast; Sch: Schwann cells; Neg: unlabelled dermal cells. Abbreviations B: Epi: Epidermis: ORS: Outer root sheath; Mx: Matrix; Mc: Melanocyte; DF: Dermal fibroblasts, DP: Dermal papilla; TAC: Transit amplifying cells; HF-SC: Hair follicle stem cells; HF-ORS: Hair follicle outer root sheath; ZZ-DP: Zigzag dermal papilla; G/AA-DP: Guard/Awl and Auchenne dermal papilla; G-DP: Guard dermal papilla; AA/ZZ-DP: Awl and Auchenne/Zigzag dermal papilla.

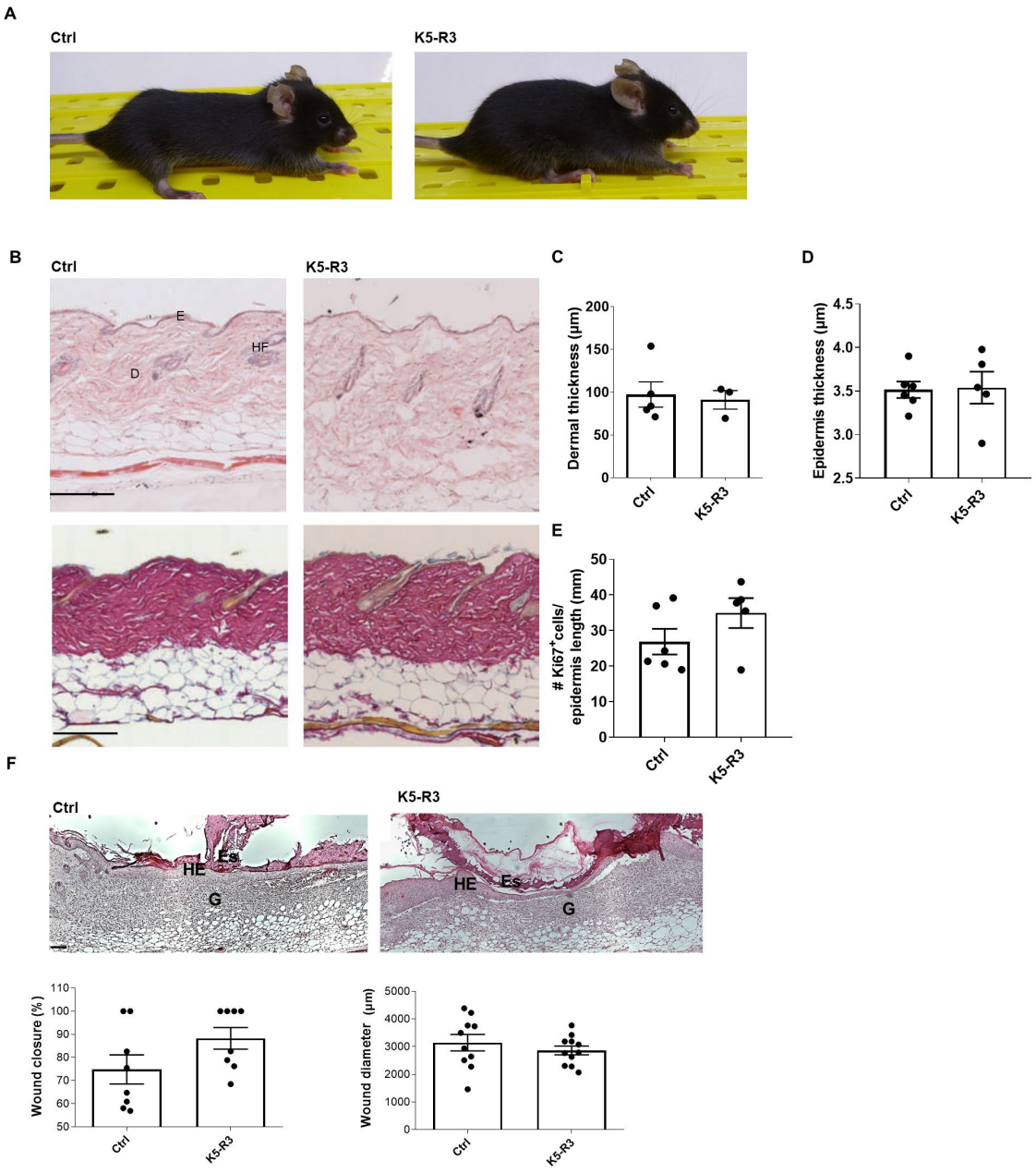

Supplementary Figure S2: Loss of FGFR3 in keratinocytes does not affect the macroscopic appearance of mice or skin homeostasis and repair.

(A) Representative photographs of K5-R3 mice and their control littermates lacking Cre recombinase (Ctrl).

(B) Representative photomicrographs of hematoxylin/eosin- and Masson trichrome-stained sections from non-wounded back skin. D: Dermis, E: Epidermis, HF: Hair follicle. Magnification bars: 100 µm.

(C-E) Quantification of epidermal thickness (C), keratinocyte proliferation in the epidermis (Ki67-positive cells per length epidermis) (D) and dermal thickness (E). N=5-6 per genotype.

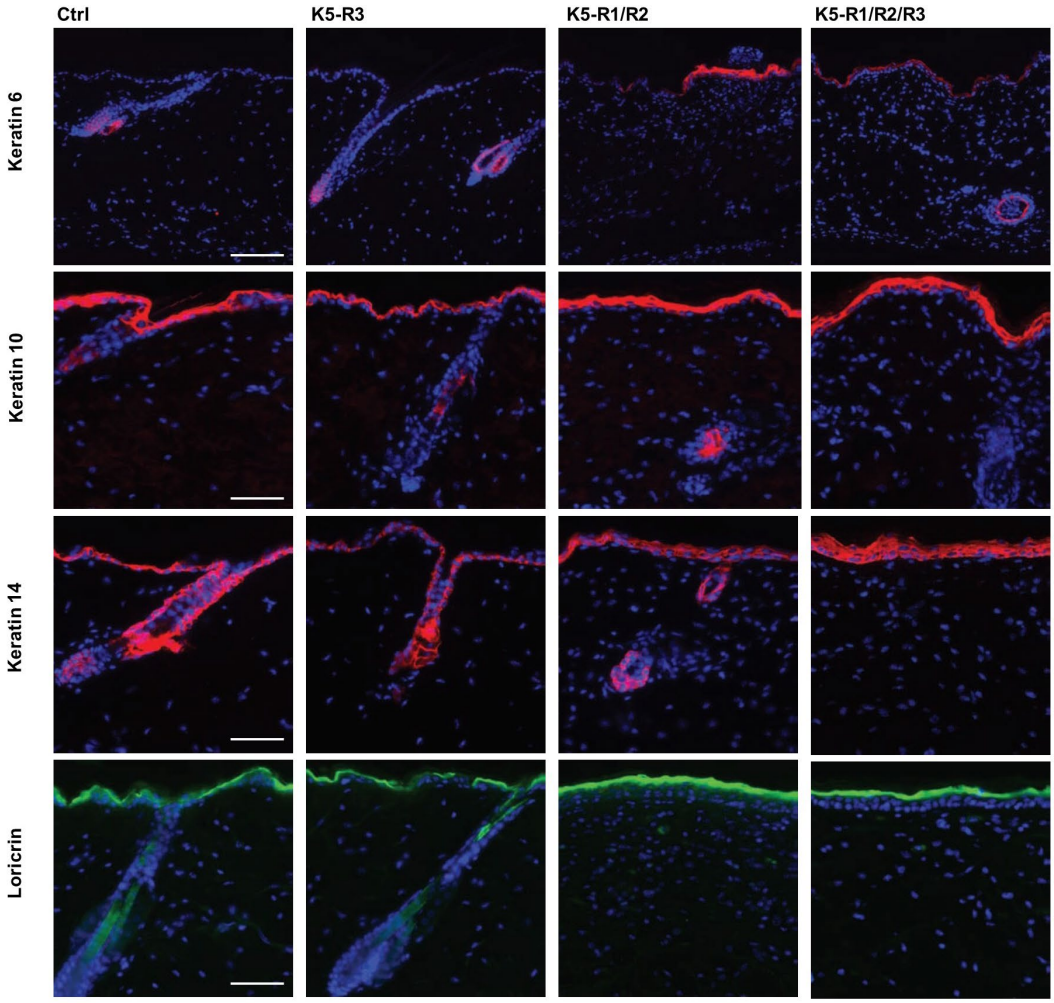

Supplementary Figure S3: Loss of FGFR3 in keratinocytes does not affect epidermal differentiation.

Representative photomicrographs of back skin sections from 2 months old Ctrl, K5-R3, K5-R1/R2 and K5-R1/R2/R3 mice stained with antibodies against keratins 6, 10 and 14 (red) or loricrin (green). Nuclei were counterstained with Hoechst (blue). Note the normal expression of keratin 10, keratin 14 and loricrin, but the interfollicular expression of keratin 6 in K5-R1/R2 and K5-R1/R2/R3 mice. Magnification bars: Keratin 6: 100 µm; keratin 10, keratin 14, loricrin: 50 µm.

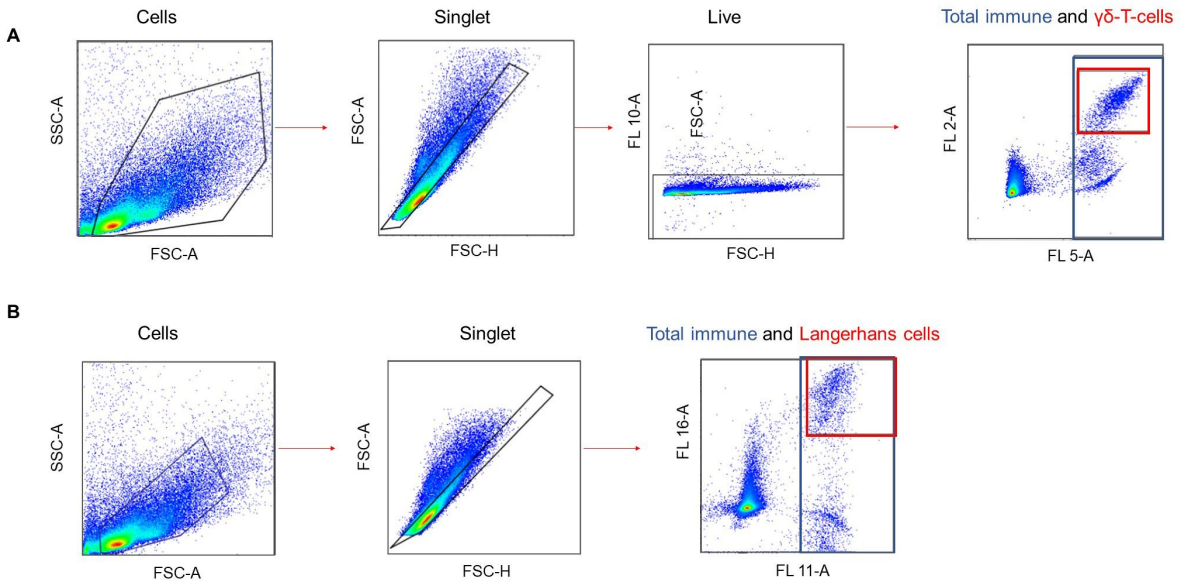

Supplementary Figure S4: Gating strategy for flow cytometry analysis of cutaneous immune cells.

(A) Gating strategy used for the quantification of γδ T cells (DETCs). Events from forward scatter (FSC) - side scatter (SSC) were gated, from which live cells and then singlets were selected to display total immune and γδ T cells (DETCs) on the last plot.

(B) Gating strategy used for the quantification of Langerhans cells. Events from FSC-SSC were gated, from which singlets were selected to display total immune and Langerhans on the last plot.

References

42 **Maddaluno, L., Urwyler, C. & Werner, S. (2017)** *Fibroblast growth factors: Key players in regeneration and tissue repair*. Development 144, 4047-4060.

45 **Beenken, A. & Mohammadi, M. (2009)** *The FGF family: Biology, pathophysiology and therapy*. Nature Reviews Drug Discovery 8, 235-253.

48 **Ornitz, D. M. & Itoh, N. (2015)** *The fibroblast growth factor signaling pathway*. Wiley Interdisciplinary Reviews: Developmental Biology 4, 215-266.

50 **Zhang, X., Ibrahimi, O. A., Olsen, S. K., Umemori, H., Mohammadi, M. & Ornitz, D. M. (2006)** *Receptor specificity of the fibroblast growth factor family. The complete mammalian FGF family*. Journal of Biological Chemistry 281, 15694-15700.

62 **Werner, S., Weinberg, W., Liao, X., Peters, K., Blessing, M., Yuspa, S., Weiner, R. & Williams, L. (1993)** *Targeted expression of a dominant-negative FGF receptor mutant in the epidermis of transgenic mice reveals a role of FGF in keratinocyte organization and differentiation*. The EMBO Journal 12, 2635-2643.

65 **Yang, J., Meyer, M., Muller, A. K., Bohm, F., Grose, R., Dauwalder, T., Verrey, F., Kopf, M., Partanen, J., Bloch, W., Ornitz, D. M. & Werner, S. (2010)** *Fibroblast growth factor receptors 1 and 2 in keratinocytes control the epidermal barrier and cutaneous homeostasis*. Journal of Cell Biology 188, 935-952.

66 **Meyer, M., Muller, A. K., Yang, J., Moik, D., Ponzio, G., Ornitz, D. M., Grose, R. & Werner, S. (2012)** *FGF receptors 1 and 2 are key regulators of keratinocyte migration in vitro and in wounded skin*. Journal of Cell Science 125, 5690-5701.

180 **Sulcova, J., Maddaluno, L., Meyer, M. & Werner, S. (2015)** *Accumulation and activation of epidermal γδ T cells in a mouse model of chronic dermatitis is not required for the inflammatory phenotype*. European Journal of Immunology 45, 2517-2528.

212 **Werner, S., Peters, K. G., Longaker, M. T., Fuller-Pace, F., Banda, M. J. & Williams, L. T. (1992)** *Large induction of keratinocyte growth factor expression in the dermis during wound healing*. Proceedings of the National Academy of Sciences 89, 6896-6900.

220 **Grose, R., Fantl, V., Werner, S., Chioni, A. M., Jarosz, M., Rudling, R., Cross, B., Hart, I. R. & Dickson, C. (2007)** *The role of fibroblast growth factor receptor 2b in skin homeostasis and cancer development*. The EMBO Journal 26, 1268-1278.

221 **Sulcova, J., Meyer, M., Guiducci, E., Feyerabend, T. B., Rodewald, H.-R. & Werner, S. (2015)** *Mast cells are dispensable in a genetic mouse model of chronic dermatitis*. American Journal of Pathology 185, 1575-1587.

222 **Seltmann, K., Meyer, M., Sulcova, J., Kockmann, T., Wehkamp, U., Weidinger, S., auf dem Keller, U. & Werner, S. (2018)** *Humidity-regulated CLCA2 protects the epidermis from hyperosmotic stress*. Science Translational Medicine 10, eaao4650.

223 **Meyers, G. A., Orlow, S. J., Munro, I. R., Przylepa, K. A. & Jabs, E. W. (1995)** *Fibroblast growth factor receptor 3 (FGFR3) transmembrane mutation in Crouzon syndrome with acanthosis nigricans*. Nature Genetics 11, 462.

224 **Wilkes, D., Rutland, P., Pulleyn, L., Reardon, W., Moss, C., Ellis, J., Winter, R. & Malcolm, S. (1996)** *A recurrent mutation, ala391glu, in the transmembrane region of FGFR3 causes Crouzon syndrome and acanthosis nigricans*. Journal of Medical Genetics 33, 744-748.

225 **Logie, A., Dunois-Larde, C., Rosty, C., Levrel, O., Blanche, M., Ribeiro, A., Gasc, J.-M., Jorcano, J., Werner, S. & Sastre-Garau, X. (2005)** *Activating mutations of the tyrosine kinase receptor FGFR3 are associated with benign skin tumors in mice and humans*. Human Molecular Genetics 14, 1153-1160.

226 **Hafner, C., van Oers, J. M., Vogt, T., Landthaler, M., Stoehr, R., Blaszyk, H., Hofstaedter, F., Zwarthoff, E. C. & Hartmann, A. (2006)** *Mosaicism of activating FGFR3 mutations in human skin causes epidermal nevi*. Journal of Clinical Investigation 116, 2201-2207.

227 **Su, N., Xu, X., Li, C., He, Q., Zhao, L., Li, C., Chen, S., Luo, F., Yi, L. & Du, X. (2010)** *Generation of Fgfr3 conditional knockout mice*. International Journal of Biological Sciences 6, 327.

228 **Ramirez, A., Page, A., Gandarillas, A., Zanet, J., Pibre, S., Vidal, M., Tusell, L., Genesca, A., Whitaker, D. A. & Melton, D. W. (2004)** *A keratin K5-Cre transgenic line appropriate for tissue-specific or generalized Cre-mediated recombination*. Genesis 39, 52-57.

229 **Chrostek, A., Wu, X., Quondamatteo, F., Hu, R., Sanecka, A., Niemann, C., Langbein, L., Haase, I. & Brakebusch, C. (2006)** *Rac1 is crucial for hair follicle integrity but is not essential for maintenance of the epidermis*. Molecular and Cellular Biology 26, 6957-6970.

230 **Herovici, C. (1963)** *Picropolychrome: Histological staining technic intended for the study of normal and pathological connective tissue*. Revue francaise d'etudes cliniques et biologiques 8, 88.

231 **Sennett, R., Wang, Z., Rezza, A., Grisanti, L., Roitershtein, N., Sicchio, C., Mok, K. W., Heitman, N. J., Clavel, C. & Ma'ayan, A. (2015)** *An integrated transcriptome atlas of embryonic hair follicle progenitors, their niche, and the developing skin*. Developmental Cell 34, 577-591.

232 **Joost, S., Zeisel, A., Jacob, T., Sun, X., La Manno, G., Lönnerberg, P., Linnarsson, S. & Kasper, M. (2016)** *Single-cell transcriptomics reveals that differentiation and spatial signatures shape epidermal and hair follicle heterogeneity*. Cell Systems 3, 221-237. e229.

233 **Chellaiah, A. T., McEwen, D. G., Werner, S., Xu, J. & Ornitz, D. M. (1994)** *Fibroblast growth factor receptor (FGFR) 3. Alternative splicing in immunoglobulin-like domain III creates a receptor highly specific for acidic FGF/FGF-1*. Journal of Biological Chemistry 269, 11620-11627.

234 **McGowan, K. & Coulombe, P. (1998)** *The wound repair-associated keratins 6, 16, and 17. Insights into the role of intermediate filaments in specifying keratinocyte cytoarchitecture*. Sub-cellular Biochemistry 31, 173-204.

235 **Duperret, E. K., Oh, S. J., McNeal, A., Prouty, S. M. & Ridky, T. W. (2014)** *Activating FGFR3 mutations cause mild hyperplasia in human skin, but are insufficient to drive benign or malignant skin tumors*. Cell Cycle 13, 1551-1559.

236 **Takenaka, H., Yasuno, H. & Kishimoto, S. (2002)** *Immunolocalization of fibroblast growth factor receptors in normal and wounded human skin*. Archives of Dermatological Research 294, 331-338.

237 **Beer, H.-D., Florence, C., Dammeier, J., McGuire, L., Werner, S. & Duan, D. R. (1997)** *Mouse fibroblast growth factor 10: cDNA cloning, protein characterization, and regulation of mRNA expression*. Oncogene 15, 2211.

238 **Xu, W., Hong, S. J., Zhong, A., Xie, P., Jia, S., Xie, Z., Zeitchek, M., Niknam-Bienia, S., Zhao, J. & Porterfield, D. M. (2015)** *Sodium channel Nax is a regulator in epithelial sodium homeostasis*. Science Translational Medicine 7, 312ra177-312ra177.

239 **Zhao, J., Zhong, A., Friedrich, E. E., Jia, S., Xie, P., Galiano, R. D., Mustoe, T. A. & Hong, S. J. (2017)** *S100A12 induced in the epidermis by reduced hydration activates dermal fibroblasts and causes dermal fibrosis*. Journal of Investigative Dermatology 137, 650-659.

240 **Zhong, A., Xu, W., Zhao, J., Xie, P., Jia, S., Sun, J., Galiano, R. D., Mustoe, T. A. & Hong, S. J. (2016)** *S100A8 and S100A9 are induced by decreased hydration in the epidermis and promote fibroblast activation and fibrosis in the dermis*. American Journal of Pathology 186, 109-122.

241 **Hedger, M. P. & de Kretser, D. M. (2013)** *The activins and their binding protein, follistatin — diagnostic and therapeutic targets in inflammatory disease and fibrosis*. Cytokine & Growth factor Reviews 24, 285-295.

242 **Werner, S. & Alzheimer, C. (2006)** *Roles of activin in tissue repair, fibrosis, and inflammatory disease*. Cytokine & Growth Factor Reviews 17, 157-171.

5 Conclusions and Outlook

My thesis investigated several aspects of FGF biology. The major part of my project focused on the development of an optogenetic approach to study FGF signaling in keratinocytes. In addition, my work identified novel and unexpected activities of FGFs in viral replication and provided first insights into the underlying mechanisms. Finally, I contributed to a study that identified FGFR2 as the major FGFR in keratinocytes and identified back-up functions of FGFR1 and FGFR3.

1. Optogenetic activation of FGFR2

To elucidate the role of FGFR signaling dynamics in keratinocytes and to identify the specific contribution of FGFR2 to FGF signaling and function in this cell type, we designed and successfully applied a light-regulated version of FGFR2 (OptoR2). Illumination of OptoR2 induced activation of FGFR signaling cascades, expression of FGF target genes as well as migration and proliferation of HEK 293T cells and keratinocytes. In both cell types, we observed a highly specific activation, which occurred at a remarkable temporal precision and was comparable to the activation achieved with endogenous ligands of FGFR2b, the major FGFR in keratinocytes. These results make OptoR2 a powerful tool to dissect signaling pathways, possibly also in combination with other light-activatable FGFRs like OptoR1 [128, 129]. The use of an OptoR1 and -R2 combination would allow us to determine if the combined activation of both receptors induces similar or different biological responses compared to activation of individual receptors, and to identify unique and overlapping FGFR1 and FGFR2 signaling pathways and target genes.

In spite of these promising results, when keratinocytes were illuminated for longer time periods to investigate effects on proliferation or migration, the blue light that we applied had only a very mild or no effect at all. A likely explanation is the down-regulation of OptoR2 and/or reduced responsiveness to OptoR2, which we found in all keratinocyte systems used. The reason and the mechanism behind this observation remain to be clarified – possible explanations will be discussed later. These effects underline the importance of carefully balancing the OptoR2 expression and the illumination intensity and duration in keratinocytes. This limits the

usefulness of this tool to study long-term effects of activation of growth factor signaling in keratinocytes and potentially other cell types. Possibilities to overcome these obstacles will also be addressed below.

1.1 Reduction in the cellular response to OptoR2 in keratinocytes

We observed a reduction in the cellular response to OptoR2 in all keratinocyte systems that we used: 1) in freshly isolated primary keratinocytes, the OptoR2 expression level decreased over the course of 3 mouse generations; 2) in immortalised murine keratinocytes, the OptoR2 responsiveness got lost over a cultivation time of 6 months; 3) in adult mice expressing OptoR2 in keratinocytes, their initial tumour formation phenotype decreased over the course of 2 years; and 4) in immortalised human keratinocytes inducibly expressing OptoR2, the expression was down-regulated both at the mRNA and protein level after 24 h of continuous illumination. Regardless of the system-specific differences, the outcome was the same: over time, keratinocytes carrying an OptoR2 transgene no longer responded to blue light.

It is likely that a mild activation of OptoR2 occurs when the cells are exposed to the room light upon passaging and in the skin of the transgenic mice, although we tried to reduce this exposure to a minimum. The resulting mild, but chronic FGFR signaling may well be deleterious for keratinocytes. Therefore, responsive mice/cells would be selected against, which would lead to overall down-regulation of the receptor responsiveness in the population.

1.1.1 Reason(s) for the progressive loss of OptoR2 expressing cells

There are several possible reasons for the loss of OptoR2 expressing/responsive keratinocytes, including phototoxic cell death, apoptosis or differentiation. Indeed, we observed some phototoxicity when we first illuminated keratinocytes with the custom-built light chamber for up to 3 days. Therefore, we determined the light intensity of the new light chamber in comparison to the illumination device used before. We measured ca. 30 $\mu W/cm^2$ for the short-term illumination device and ca. 200 $\mu W/cm^2$ for the new light chamber. Although phototoxicity is usually observed only at higher light doses [243], we reduced the light intensity in the new chamber by shielding the light with Whatman paper, which resulted in a light intensity of ca 30 $\mu W/cm^2$ also for the custom-built chamber. After this adaptation, we no longer observed visible phototoxic cell death during long-term illumination. Therefore, phototoxicity is obviously not the reason for the loss of OptoR2-expressing cells. This mechanism would also

not explain the selective loss of OptoR2-positive cells, since it is expected that all cells are equally affected.

Another possibility is the loss of OptoR2-expressing cells by apoptosis. Even if a small percentage of cells undergoes programmed cell death, e.g. through autophagy [244], this may lead to progressive overgrowth by keratinocytes that do not respond to OptoR2. A pilot *in vitro* experiment did not show apoptotic cells in control and OptoR2-expressing keratinocytes over time. However, if the number is very small at any given time point, this could have been missed in our analysis.

Third, it is possible that the differentiation of OptoR2-expressing keratinocytes is increased. Consistent with this hypothesis, mice expressing a dominant-negative FGFR in suprabasal keratinocytes exhibited a delay in keratinocyte differentiation [62], and early and late differentiation of HaCaT cells was induced by overexpression of FGFR2b and concomitant stimulation with FGF7 [164, 165]. Additionally, the strong keratinization of the tumours, which formed in OptoR2 mice, supports this hypothesis. Again, we did not observe a strong effect of OptoR2 expression on keratinocyte differentiation markers in pilot *in vitro* experiments. However, a continuous mild effect on differentiation may lead to the loss of some differentiated cells upon passaging.

1.1.2 Mechanism(s) underlying the loss of OptoR2 in keratinocytes

Another open question addresses the mechanisms underlying the loss of OptoR2 expression or responsiveness in keratinocytes. Deleterious effects of long-term FGFR activation in keratinocytes followed by overgrowth of cells, which have "escaped" the light-inducible activation, provides an obvious explanation for the loss of the receptor upon long-term cultivation of cells or in the mice. However, this does not explain the rapid loss of OptoR2 after continuous illumination in HaCaT keratinocytes, even in the inducible expression system. It is likely that the receptor is actively down-regulated upon illumination and the resulting FGFR kinase activation. Such an effect has been suggested before for wound keratinocytes, which are exposed to high levels of FGF7 [169]. This is achieved at the protein level by receptor ubiquitination and subsequent internalisation, or by proteasomal degradation [48]. Additional negative feedback regulation is likely to occur in response to OptoR2 activation, e.g. via overexpression/activation of endogenous signaling inhibitors, such as Dusp6, Cbl or Sprouty [48, 71, 162]. Surprisingly, we even observed reduced expression of OptoR2 at the mRNA level, which is likely a consequence of epigenetic alterations. Such mechanisms may also

explain the loss of responsiveness of keratinocytes from OptoR2 mice over time, since epigenetic modifications are well known to silence transgene expression in different mouse lines and can be tackled, for example, by targeted demethylation [166-168]. However, we observed downregulation of OptoR2 at the mRNA level already after 3-24 h of illumination – a time point that is hard to reconcile with epigenetic mechanisms. Therefore, additional mechanisms may be involved, such as reduced mRNA stability.

1.1.3 Combination of Opto-R2 expression with FGFR1/R2 knockout

To reduce the over-activation of FGFR signaling in keratinocytes, we expected that combining OptoR2 expression with knockout or knock-down of the corresponding endogenous FGFRs would reduce the problem. Therefore, we mated the K14-OptoR2 transgenic mice with keratinocyte-specific FGFR1/R2 knockout mice, and we aimed to rescue the phenotype in the triple mutant mice by illumination. However, the mice with the combined genotype (K14-OptoR2 x K5-R1/R2) showed a strong growth retardation at 4-8 weeks and thus at the onset of the skin phenotype of the K5-R1/R2 mice [65]. These mice had to be sacrificed due to animal welfare regulations, and we were therefore not able to perform a light experiment.

This observation was surprising, because we rather expected a reduction of the skin phenotype due to OptoR2 expression. There are several possible reasons for the severe phenotype: By crossing the two mouse lines, we further out-crossed the knockout mice to a pure C57/BL6 background and thereby reduced the effects of previous inbreeding. This is well known to aggravate the phenotype of many knockout mouse models. Additionally, both OptoR2 expression and loss of FGFR1/R2 may damage the epidermal barrier, but via independent mechanisms, and the triple mutant mice may therefore have a more severe phenotype compared to OptoR2 or K5-R1/R2 mice. This could be tested by analysis of transepidermal water loss in the mice with the different genotypes. Finally, the inflammation that is observed in K5-R1/R2 mice may be further aggravated, e.g. by development of an immune response to OptoR2 as has been observed when expressing channel rhodopsins in the peripheral nervous system of rats [245]. This should be tested in the future by analysis of the cutaneous immune cell infiltrate.

1.1.4 Dependence of OptoR2 down-regulation on FGFR activity

When interpreting our results, we assume that the loss of OptoR2 expression or responsiveness in keratinocytes is due to over-activation of FGFR signaling in this cell type. While our results

strongly point into this direction, this hypothesis will have to be further tested by inhibiting OptoR2 kinase activity, for example using selective FGFR kinase inhibitors such as AZD4547 or BGJ398 [181, 187]. If activation of the FGFR kinase is indeed involved in the downregulation, it would be rescued by these kinase inhibitors.

1.2 Optogenetic alternatives

For generating OptoR2, we used a light-induced dimerisation system in analogy to the systems that have been successfully applied for FGFR1 [128, 129]. However, when they applied a comparable OptoFGFR system in *Xenopus laevis* embryos, the authors observed that constitutive expression of OptoFGFR lead to developmental defects and embryonic death even in the absence of light [148]. Therefore, they modified the optogenetic system in such a way that instead of having the receptor localised at the plasma membrane and inducing its dimerisation by illumination, the light induced recruitment of the receptor to the plasma membrane, where dimerisation happened spontaneously due to the high local concentration. This modification avoided the toxicity of constitutive FGFR activation in *X. laevis* embryos and was also successfully applied for other receptor tyrosine kinases [148]. However, we did not observe activation of downstream signaling in OptoR2 cells in the dark and there was also no significant cell death (see above), indicating that toxicity of OptoR2 in the absence of light is not a problem in our system.

Another option might be to adapt the optogenetic tool. Our OptoR2 system uses LOV-domains, which are activated by blue light. However, for applying optogenetics in an organ that is exposed to the normal room light – the skin – it could be advantageous to use a tool, which is activated by light that is not in the visible spectrum, e.g. with ultraviolet (UV) or infrared light.

UV light, in particular UVB, does not penetrate the skin deeply and therefore is not expected to damage internal organs. However, UV irradiation damages the skin by inducing a sunburn reaction. Therefore, an infrared light-induced system is most likely a better choice. As infrared light is not in the visible spectrum, mice could be kept at their normal light/dark cycle without activation of the optogenetic tool. Since infrared is not visible to mice, they should not be stressed by illumination, which is important for animal welfare. There are also practical advantages of using infrared rather than blue light in cell culture: passaging and handling of the cells for experiments can be performed under normal room light, possibly with the red wavelength spectrum filtered out, which leads to easier handling and reduces contamination

problems. Furthermore, the LOV domains in our system cannot be used for brightfield live-cell imaging and cannot be combined with green flurorophores in live-cell imaging because of the overlapping excitation/activation wavelengths. An infrared light-controlled system would offer more flexibility in this regard. However, the deep tissue penetration and the generation of heat by illumination with infrared light might be challenges that would have to be tackled when applying these tools.

Indeed, near-infrared light-activated tropomyosin receptor kinases have been used to control several downstream pathways and second messenger levels in neuronal and other cell lines [124]. The same optogenetic tool has been successfully applied for EGFR and FGFR1 to modify ERK1/2, PI3K/AKT and PLCγ signaling in HeLa cells [147]. Additionally, this system can be reversibly controlled, using near-infrared light for activation and far-red light for termination of signaling. This functionality offers an additional level of control, which can be advantageous in many settings.

In summary, there are many optogenetic tools that can be combined and modified according to the research question at stage [72-74, 83, 101]. Especially for keratinocytes – a cell type that is adapted to combat the deleterious consequences of UV irradiation – other illumination systems with activation spectra further away from UV light should be better suited. This underlines the importance of tailoring the optogenetic system to the type of receptor and the target cells.

2. FGF, interferon and antiviral defence

We chose FGFR2 for optogenetic modification in keratinocytes, because we had identified FGFR2 as the most important receptor in keratinocytes using knockout approaches [65, 66]. In search for novel FGFR target genes, we investigated the transcriptome of the epidermis of mice lacking FGFR1 and FGFR2 in this cell type in comparison to control mice. Thereby, we observed an unexpected effect of FGF signaling on ISGs, which play a role in the cellular antiviral defence. Closer characterisation revealed that the down-regulation of ISG expression by FGFs occurs at the transcriptional level and is FGFR kinase dependent, but type I IFN receptor independent. The mechanism is currently being further explored in our laboratory and probably involves proteasomal degradation of a protein, which is required for ISG expression and regulated by a combination of downstream pathways. Possible mediators will be discussed later. FGF7 also suppresses ISG expression in the presence of exogenous IFN I, the IFN-inducing compound poly(I:C) and even in the presence of HSV-1. This suggests that beneficial effects of FGF7 as seen for example in wound healing [66, 67] come at the price of higher susceptibility to viral infection.

2.1 Mechanism of ISG regulation by FGFs

Up to now it is not fully clear how FGF signaling interacts with the type I IFN pathway. The first point of interaction could be that the virus enters the cell by directly docking onto FGFR. This has been suggested before for HSV-1, and stimulation with recombinant FGF decreased viral infection in this system, possibly due to competitive inhibition of binding to the receptor [210]. In contrast, FGF signaling rather increased the susceptibility to viral infection in keratinocytes, and it also promoted infection of other viruses, such as ZIKV and LCMV. This is consistent with the general antiviral properties of ISGs as effectors and argues against a virus-specific effect [211].

Using pathway inhibitors, we found that by inhibiting both MEK1/2-ERK1/2 and PI3K-AKT pathways at the same time, the effect of FGF signaling on ISG expression was significantly reduced. This is consistent with the induction of a type I IFN response in human keratinocytes by MEK inhibitors [199] and with the down-regulation of the IFN-induced antiviral response by activated Ras in cultured fibroblasts [200]. However, none of the pathway inhibitors or

inhibitor combinations could completely abolish the FGF mediated suppression of ISGs – this was only achieved with proteasome inhibitors.

In the type I IFN pathway, IFNs induce the phosphorylation of STAT1 and STAT2, which form a complex with IRF9, named IFN-stimulated gene factor 3 (ISGF 3) [201]. ISGF3 and other IRFs, including IRF1 and IRF7, bind to sequences in the promoter region of the ISGs and regulate ISG expression [184, 188, 191, 202, 206]. Since IRF and also STAT1/2 levels are frequently regulated by ubiquitination and subsequent proteasomal degradation [203-205] and since inhibition of the proteasome blocked the effect of FGF7 on ISG expression, IRFs and STATs are candidate targets of the rapid effect of FGF7. To elucidate the molecular mechanism of the pathway, we will perform proteomics studies to identify the proteins, which bind to the interferon-stimulated response elements in the promoters of ISGs, or the binding partners of STAT2, in the presence or absence of FGF7 or FGFR inhibitors.

2.2 Beneficial and detrimental FGF effects

The entry point for many viruses are surface epithelia like the skin, which form the barriers of our body against the environment. Here, viral infection often leads to disruption of the barrier and promotes inflammation. FGF7 expression is upregulated in these conditions, promoting tissue repair and protecting cells from physical and chemical insults [42, 213]. Especially during skin wound healing FGF7 and other FGFR2b ligands plays a key role, for example by stimulating migration and proliferation of keratinocytes [65, 66, 212]. However, the beneficial effects of these FGFs come with the risk of increased susceptibility for the virus. By suppressing the expression of ISGs, FGF7 promotes viral replication at the site of injury or inflammation – probably not only in the skin. Due to the ubiquitous expression of FGFRs and IFNs, our observation is likely to be relevant also for other epithelia, for example the lung or the colon.

In line with our results, FGF2 treatment suppressed ISGs and promoted Zika virus infection in human astrocytes [215]. Additionally, the titres of hepatitis C virions were increased by FGF2 in hepatoma cells [214]. Furthermore, FGF7 suppressed the expression of different ISGs in human lung epithelial cells [216]. However, there are also studies showing the opposite effect of FGFs: in certain cancer cells a subset of FGFs, which mainly act on FGFR3, inhibited infection with Vesicular stomatitis virus or Coxsackie virus via an as yet unidentified mechanism [218]. These results have to be interpreted carefully, because many cancer cells

exhibit dysregulated FGF signaling, which might lead to different signaling characteristics compared to untransformed cells [173]. Additionally, FGFs might have multiple effects on the viral life cycle, which are independent of ISGs. For example, inhibition of FGFR4 decreased the replication of Dengue virus, but it increased the infectivity of the virions that were still produced [219]. These possibilities have to be considered when using FGFR inhibitors for the treatment of viral infections (see below).

2.3 FGFR inhibition as a novel antiviral strategy

Due to their broad spectrum of effects on different viruses and on various stages of the viral life cycle [209], upregulating ISGs via FGFR inhibition is an intriguing antiviral strategy. The ISG upregulation observed under FGFR inhibition is probably self-sustained and self-potentiating, as some of the ISGs encode positive feedback regulators of their own expression [201]. Therefore, a strong effect of the treatment is to be expected and was indeed observed in our *in vitro* experiments.

However, utilizing FGFR inhibition as an antiviral treatment option can be a double-edged sword: FGFR inhibition to decrease cellular susceptibility to viruses can also impede the repair of the injuries produced by the virus, as observed for influenza virus in mouse lung [217]. Therefore, any antiviral treatment with FGFR inhibitors needs to be timed precisely and carefully to not interfere with the healing of the damaged tissue upon viral infection. Probably it should be applied early in the infection to reduce the initial virus spread and give the body time to develop an effective immune response. After reduction of the viral load, the FGFR inhibition should be terminated to allow efficient tissue repair. In addition, it is important to check if FGFR inhibition enhances the infectivity of the viruses as seen for Dengue virus in response to FGFR4 inhibition [219].

In spite of these challenges, exploring FGFR inhibitors as novel antiviral drugs offers exciting opportunities. FGFR kinase inhibitors, FGFR neutralizing antibodies or FGF ligand traps are already in clinical trials for the treatment of different cancer types, and overall they show a favourable toxicity profile [54]. However, the dosing for antiviral treatment would probably have to be higher than in the oncology trials, because most of the cancer cells that are targeted in the clinical trials exhibit increased expression of FGFRs or have FGFR activating mutations [173]. Therefore, comprehensive studies will be required regarding dosing and mode of application, but also efficacy against different viruses and side effects. However, exploring this

novel treatment option seems worth the effort as most antiviral drugs selectively target certain well-known viruses. In contrast, FGFR inhibition offers a treatment option against previously untreatable or newly emerging viruses - a great promise for future pandemics.

3. Loss of FGF signaling in keratinocytes

Apart from their decreased susceptibility to viral infection, mice with a loss of FGFR1 and FGFR2 in keratinocytes have an interesting skin phenotype [65, 66]. However, as these keratinocytes still express FGFR3, this receptor could compensate for the loss of FGFR1 and FGFR2. Therefore, to understand the individual contribution of each FGFR, we knocked them out individually and in combination. Our lab had shown before that FGFR2 is a very important FGFR in mouse epidermis, while FGFR1 has a "back-up" function [65, 66]. With additionally knocking out FGFR3, we observed that this receptor is dispensable for skin homeostasis and wound healing. However, its loss seems to enhance the barrier defect in FGFR1/2 knockout mice and the dermal fibrosis that developed in these mice.

3.1 Overlapping functions of different FGFRs in keratinocytes

Overall, out studies identified FGFR2 as the most important FGFR in keratinocytes, whereas FGFR1 has a "back-up" function [65, 66]. Surprisingly, the knockout of FGFR3 in keratinocytes did not affect skin homeostasis and wound repair. This was not expected, given the upregulation of FGFR3 in healing mouse skin wounds [212]. However, the upregulation may occur in cells other than keratinocytes, which remains to be determined. Additionally, *FGFR3* activating mutations are known to cause diseases with skin involvement, such as acanthosis nigricans, seborrheic keratosis and epidermal nevi [223-226]. However, knock-down of FGFR3 did also not affect human keratinocyte growth *in vitro* [235], although the receptor is strongly expressed in the human epidermis [236]. Hence, it seems that signaling by wild-type FGFR3 plays a minor role in keratinocyte biology.

A possible explanation for the unequal contribution of FGFR2 *vs* FGFR1 and FGFR3 *in vivo* would be a higher expression of the ligands of FGFR2 compared to the other ligands. Keratinocytes mainly express the IIIb splice variants of FGF receptors [233]. FGF7 and FGF10, the major ligands of FGFR2b, are constitutively expressed in the skin [212, 231, 237]. In contrast, FGFR3b, the predominant splice variant of FGFR3 in keratinocytes, is rather poorly activated by most FGFs [50], and expression of its major ligand, FGF9, is rather low in normal skin (our unpublished data).

Mice lacking FGFR1 or FGFR3 in keratinocytes did not show phenotypic abnormalities in normal skin and the phenotype of keratinocyte-specific FGFR2 knockout mice was very mild [65, 220]. These findings demonstrate that the function of each FGFR can be at least partially compensated by the other FGFRs. Therefore, the full phenotype is only visible in the triple knockout. However, loss of all three FGFRs expressed in keratinocytes is still compatible with life and keratinocyte growth *in vitro*. Therefore, it seems likely that other growth factors can compensate for the loss of FGFR signaling in this cell type.

3.2 Barrier defect and skin fibrosis in the absence of FGFR signaling in keratinocytes

Although the loss of FGFRs in our mouse model is specific for the epidermis and other stratified epithelia, we noticed dermal fibrosis in both the FGFR1/R2 knockout mice and even more in the triple knockout mice. This may be due to the inflammation that develops in the skin of the two mouse lines. However, additional loss of mast cells or γδ T cells, which both are strongly increased in K5-R1/R2 and K5-R1/R2/R3 skin, did not affect the phenotype in the K5-R1/R2 mice [180, 221]. Therefore, these immune cells probably do not play a major role in the development of skin fibrosis.

In contrast, the barrier defect induced by the loss of FGFR signaling in the epidermis might be an explanation for the dermal fibrosis. It has been shown that barrier defects lead to upregulation of cytokines like S100A8, S100A9 and S100A12 [238-240], which can cause fibroblast activation and fibrosis. We indeed observed upregulation of S100A8 and S100A9 in our mouse models [65, 66], together with down-regulation of follistatin. This secreted glycoprotein is the endogenous inhibitor of activin A, a potent pro-fibrotic factor [241, 242], and follistatin down-regulation may therefore promote fibrosis. Taken together, the barrier defect of K5-R1/R2 and especially K5-R1/R2/R3 mice most likely leads to increased expression and enhanced activity of pro-fibrotic cytokines that activate fibroblasts and thereby induce dermal fibrosis.

4. Complexity in biological signaling systems

Overall, my work has contributed to a deeper understanding of FGFR signaling in keratinocytes. After identifying the major FGFR in keratinocytes, FGFR2, we successfully engineered this receptor to be activated by light instead of its natural ligands. Thereby, we could gain insight into the dynamics of FGFR activation, but we faced challenges when applying this tool (Chapter 1). Additionally, we observed an unexpected interaction of FGFR signaling with IFN signaling in keratinocytes, which holds great promise for future use of FGFR inhibitors for the treatment of viral infections (Chapter 2). Last but not least, I contributed to the characterisation of mice lacking all FGF receptors in keratinocytes. This study underlined the importance of redundancy/compensation within the FGFR family, but probably also within different receptor tyrosine kinases (Chapter 3).

The main theme that spans all three projects is the complexity in biological signaling systems. Within the signaling systems, there are many factors that induce complexity: Many cellular receptors respond to a vast amount of extracellular signaling molecules in a dynamic way. The function of the different receptors partially overlaps, and therefore, the loss of one receptor is often compensated as shown in the FGFR triple knockout study. Additionally, the downstream signal transduction pathways of all these different receptors influence each other to different degrees, and many of these pathway interactions might not be known yet as highlighted by the discovery of an interaction between FGF and type I IFN signaling described in this thesis. The signaling network inside a cell is highly complex, with a great number of molecules that interact with each other. In an attempt to reduce this complexity, we decided to specifically investigate the signaling that is transduced by one FGFR without activating the others by applying a light-activatable system.

4.1 Degrees of complexity in cellular signaling networks

In order to approach a highly complex system like the intracellular signaling network, it is helpful to start with understanding a small part of the network as I did in my thesis by using optogenetics. After understanding this pathway, further complexity can be added by including more details and inter-connections [246-248].

4.1.1 Single pathway with multiple components

The simplest description of signaling can be compared to an electrical wire. Here, an external input, like the binding of a ligand, is transduced into the cell by a receptor and activates one or more intracellular signaling pathways. Regardless of how many components are involved, ultimately this leads to an output, for example the transcription of a target gene or a change in cellular behaviour. However, even if equal distribution of all factors within the cell is assumed, the activation steps have different kinetics, which have to be taken into account. This is the first degree of complexity [246, 247].

4.1.2 Compensation mechanisms

When one or more pathways are activated, usually some of the signals are partially or entirely redundant. Thereby, different receptors, as shown for FGFRs in this thesis, or downstream signaling molecules can take over certain functions of other molecules. These compensation mechanisms make it more difficult to quantitatively measure the contribution of each molecule to the cellular output – they add another level of complexity [247, 249].

4.1.3 Interaction between different pathways

Each cell expresses a large number of receptors for growth factors, cytokines and other signaling molecules, and each one of them responds to its respective ligands as described above. Additionally, there are multiple points of interaction between the different pathways as we could show in our study for the FGF and type I IFN pathways. Therefore, the observable cellular outputs are an integration of all the inputs that the cell receives. The number of possible interactions between different pathways is the exponential function of the number of pathway components to the power of the number of observed pathways – an exponential increase in complexity. Already at this level, simulations using high computing power might be needed to calculate the effects of certain inputs on the whole system as performed for neural networks [246, 247].

4.1.4 Compartmentalisation

Complexity further increases when taking into account that the cell interior is not a well-stirred reaction mix, but contains many compartments. First, there are compartments like the nucleus, other cell organelles or vesicles that play a role in signaling. Second, also within the cytoplasm

there are regions like the inside of the plasma membrane, where signaling molecules are enriched to increase interaction and reaction efficiency and specificity. Scaffold proteins like FRS2α, which bind multiple signaling molecules, have the same effect. And finally, many biological processes are regulated by translocation of proteins to different compartments. The different compartments heavily influence each other, and the same signaling molecule can have completely different functions, depending on where it is located [247, 250, 251].

4.1.5 A self-modifying system

Finally, cells are not stable systems. All their signaling components are produced from their genetic information – and this is in turn modified not only by intrinsic signals but also by external cues. Therefore, each cell is different with regard to its signaling capabilities, depending on cell type and developmental stage. Changes in the gene expression and, therefore, the signaling network itself make the whole system even more difficult to analyse [247]. Additionally, also the communication and interaction between different cells and tissues add to the complexity. As an example, in our study, the loss of FGFR signaling in keratinocytes led to phenotypic changes of fibroblasts and dermal fibrosis.

4.2 Reductionist approaches

To reduce the complexity of the signaling network, it is advantageous to combine the loss of FGFR signaling with highly controllable FGFRs, modified for example using optogenetics. Thereby, endogenous signaling is replaced by the controlled signaling tool to precisely unravel the effect of each receptor on the signaling network. By combining different light-activated FGFRs, also synergistic effects of different FGFRs can be observed and tightly controlled. For keratinocytes, expression of OptoR1 together with OptoR2 in a FGFR1/R2 knock-out background will enable researchers to gain valuable insight into keratinocyte biology. Signaling mutants with point mutations at known interaction sites or with kinase dead-mutations are another tool to further pin down the pathways that are involved in specific cellular effects or even find new pathways [252]. These variants should also be used in combination with the other tools to disentangle the signaling network.

Additionally, novel tools have to be established to be more flexible with regard to activation dynamics and modes. Engineering cellular signaling – for example using light, but also with

any other kind of stimulus – will help to unravel the effects of modulation of specific nodes in the network [115]. Therefore, biologists should team up more and more with engineers to generate more sophisticated tools to precisely manipulate the signaling network.

4.3 Holistic approaches

To understand the signaling network in all its complexity, "-omics" analyses at the single-cell level like proteomics or phospho-proteomics are performed in many experimental settings [71, 253, 254]. In addition, simulation and modelling approaches are established, in analogy to neural networks [255-257]. However, it is decisive to confirm the results of these *in silico* analyses in wet lab-experiments [258].

Other research fields like physics and mathematics already have complexity research fields, and in that regard, cell biology could learn from them [259]. Biology is now transforming from descriptive science, which observes and tries to explain effects, to a predictive science [260]. The key to these novel research fields is collaboration between different areas and interdisciplinary research to develop the tools that enable researchers to dive down even more deeply into cellular signaling. And decisive for collaborations between scientists of different research fields is communication – just like for the cells of our organism.

References

42 **Maddaluno, L., Urwyler, C. & Werner, S. (2017)** *Fibroblast growth factors: Key players in regeneration and tissue repair*. Development 144, 4047-4060.

48 **Ornitz, D. M. & Itoh, N. (2015)** *The fibroblast growth factor signaling pathway*. Wiley Interdisciplinary Reviews: Developmental Biology 4, 215-266.

50 **Zhang, X., Ibrahimi, O. A., Olsen, S. K., Umemori, H., Mohammadi, M. & Ornitz, D. M. (2006)** *Receptor specificity of the fibroblast growth factor family. The complete mammalian FGF family*. Journal of Biological Chemistry 281, 15694-15700.

54 **Touat, M., Ileana, E., Postel-Vinay, S., André, F. & Soria, J.-C. (2015)** *Targeting FGFR Signaling in Cancer*. Clinical Cancer Research 21, 2684-2694.

62 **Werner, S., Weinberg, W., Liao, X., Peters, K., Blessing, M., Yuspa, S., Weiner, R. & Williams, L. (1993)** *Targeted expression of a dominant-negative FGF receptor mutant in the epidermis of transgenic mice reveals a role of FGF in keratinocyte organization and differentiation*. The EMBO Journal 12, 2635-2643.

65 **Yang, J., Meyer, M., Muller, A. K., Bohm, F., Grose, R., Dauwalder, T., Verrey, F., Kopf, M., Partanen, J., Bloch, W., Ornitz, D. M. & Werner, S. (2010)** *Fibroblast growth factor receptors 1 and 2 in keratinocytes control the epidermal barrier and cutaneous homeostasis*. Journal of Cell Biology 188, 935-952.

66 **Meyer, M., Muller, A. K., Yang, J., Moik, D., Ponzio, G., Ornitz, D. M., Grose, R. & Werner, S. (2012)** *FGF receptors 1 and 2 are key regulators of keratinocyte migration in vitro and in wounded skin*. Journal of Cell Science 125, 5690-5701.

67 **Müller, A. K., Meyer, M. & Werner, S. (2012)** *The roles of receptor tyrosine kinases and their ligands in the wound repair process*. Seminars in Cell & Developmental Biology 23, 963-970.

71 **Francavilla, C., Rigbolt, K. T., Emdal, K. B., Carraro, G., Vernet, E., Bekker-Jensen, D. B., Streicher, W., Wikstrom, M., Sundstrom, M., Bellusci, S., Cavallaro, U., Blagoev, B. & Olsen, J. V. (2013)** *Functional proteomics defines the molecular switch underlying FGF receptor trafficking and cellular outputs*. Molecular Cell 51, 707-722.

72 **Tischer, D. & Weiner, O. D. (2014)** *Illuminating cell signalling with optogenetic tools*. Nature Reviews Molecular Cell Biology 15, 551-558.

73 **Zhang, K. & Cui, B. (2015)** *Optogenetic control of intracellular signaling pathways*. Trends in Biotechnology 33, 92-100.

74 **Kwon, E. & Heo, W. D. (2020)** *Optogenetic tools for dissecting complex intracellular signaling pathways*. Biochemical and Biophysical Research Communications 527, 331-336.

83 **Fenno, L., Yizhar, O. & Deisseroth, K. (2011)** *The development and application of optogenetics*. Annual Review of Neuroscience 34, 389-412.

101 **Rogers, K. W. & Muller, P. (2020)** *Optogenetic approaches to investigate spatiotemporal signaling during development*. Current Topics in Developmental Biology 137, 37-77.

115 **Toettcher, J. E., Voigt, C. A., Weiner, O. D. & Lim, W. A. (2011)** *The promise of optogenetics in cell biology: Interrogating molecular circuits in space and time*. Nature Methods 8, 35-38.

124 **Leopold, A. V., Chernov, K. G., Shemetov, A. A. & Verkhusha, V. V. (2019)** *Neurotrophin receptor tyrosine kinases regulated with near-infrared light*. Nature Communications 10, 1129.

128 **Grusch, M., Schelch, K., Riedler, R., Reichhart, E., Differ, C., Berger, W., Ingles-Prieto, A. & Janovjak, H. (2014)** *Spatio-temporally precise activation of engineered receptor tyrosine kinases by light*. The EMBO Journal 33, 1713-1726.

129 **Kim, N., Kim, J. M., Lee, M., Kim, C. Y., Chang, K.-Y. & Heo, W. D. (2014)** *Spatiotemporal control of fibroblast growth factor receptor signals by blue light*. Chemistry & Biology 21, 903-912.

147 **Leopold, A. V., Pletnev, S. & Verkhusha, V. V. (2020)** *Bacterial phytochrome as a scaffold for engineering of receptor tyrosine kinases controlled with near-infrared light*. Journal of Molecular Biology 432, 3749-3760.

148 **Krishnamurthy, V. V., Fu, J., Oh, T. J., Khamo, J., Yang, J. & Zhang, K. (2020)** *A generalizable optogenetic strategy to regulate receptor tyrosine kinases during vertebrate embryonic development*. Journal of Molecular Biology 432, 3149-3158.

162 **Li, C., Scott, D. A., Hatch, E., Tian, X. & Mansour, S. L. (2007)** *Dusp6 (Mkp3) is a negative feedback regulator of FGF-stimulated ERK signaling during mouse development*. Development 134, 167-176.

164 **Belleudi, F., Purpura, V. & Torrisi, M. R. (2011)** *The receptor tyrosine kinase FGFR2b/KGFR controls early differentiation of human keratinocytes*. PLoS One 6, e24194.

165 **Rosato, B., Ranieri, D., Nanni, M., Torrisi, M. R. & Belleudi, F. (2018)** *Role of FGFR2b expression and signaling in keratinocyte differentiation: Sequential involvement of PKCδ and PKCα*. Cell Death & Disease 9, 565.

166 **Calero-Nieto, F. J., Bert, A. G. & Cockerill, P. N. (2010)** *Transcription-dependent silencing of inducible convergent transgenes in transgenic mice*. Epigenetics & Chromatin 3, 3.

167 **Blewitt, M. & Whitelaw, E. (2013)** *The use of mouse models to study epigenetics*. Cold Spring Harbor Perspectives in Biology 5, a017939.

168 **Gödecke, N., Zha, L., Spencer, S., Behme, S., Riemer, P., Rehli, M., Hauser, H. & Wirth, D. (2017)** *Controlled re-activation of epigenetically silenced Tet promoter-driven transgene expression by targeted demethylation*. Nucleic Acids Research 45, e147.

169 **Marchese, C., Chedid, M., Dirsch, O. R., Csaky, K. G., Santanelli, F., Latini, C., LaRochelle, W. J., Torrisi, M. R. & Aaronson, S. A. (1995)** *Modulation of keratinocyte growth factor and its receptor in reepithelializing human skin*. Journal of Experimental Medicine 182, 1369-1376.

173 **Tanner, Y. & Grose, R. P. (2016)** *Dysregulated FGF signalling in neoplastic disorders*. Seminars in Cell and Developmental Biology 53, 126-135.

180 **Sulcova, J., Maddaluno, L., Meyer, M. & Werner, S. (2015)** *Accumulation and activation of epidermal γδ T cells in a mouse model of chronic dermatitis is not required for the inflammatory phenotype*. European Journal of Immunology 45, 2517-2528.

181 **Guagnano, V., Furet, P., Spanka, C., Bordas, V., Le Douget, M., Stamm, C., Brueggen, J., Jensen, M. R., Schnell, C., Schmid, H., Wartmann, M., Berghausen, J., Drueckes, P., Zimmerlin, A., Bussiere, D., Murray, J. & Graus Porta, D. (2011)** *Discovery of 3-(2,6-dichloro-3,5-dimethoxy-phenyl)-1-{6-[4-(4-ethyl-piperazin-1-yl)-phenylamin o]-pyrimidin-4-yl}-1-methyl-urea (NVP-BGJ398), a potent and selective inhibitor of the fibroblast growth factor receptor family of receptor tyrosine kinase*. Journal of Medicinal Chemistry 54, 7066-7083.

184 **Michalska, A., Blaszczyk, K., Wesoly, J. & Bluyssen, H. A. R. (2018)** *A positive feedback amplifier circuit that regulates interferon (IFN)-stimulated gene expression and controls type I and type II IFN responses*. Frontiers in Immunology 9, 1135.

187 **Gavine, P. R., Mooney, L., Kilgour, E., Thomas, A. P., Al-Kadhimi, K., Beck, S., Rooney, C., Coleman, T., Baker, D., Mellor, M. J., Brooks, A. N. & Klinowska, T. (2012)** *AZD4547: An orally bioavailable, potent, and selective inhibitor of the fibroblast growth factor receptor tyrosine kinase family*. Cancer Research 72, 2045-2056.

188 **Ivashkiv, L. B. & Donlin, L. T. (2014)** *Regulation of type I interferon responses*. Nature Reviews Immunology 14, 36-49.

191 **Panda, D., Gjinaj, E., Bachu, M., Squire, E., Novatt, H., Ozato, K. & Rabin, R. L. (2019)** *IRF1 maintains optimal constitutive expression of antiviral genes and regulates the early antiviral response*. Frontiers in Immunology 10, 1019.

199 **Lulli, D., Carbone, M. L. & Pastore, S. (2017)** *The MEK inhibitors trametinib and cobimetinib induce a type I interferon response in human keratinocytes*. International Journal of Molecular Sciences 18.

200 **Battcock, S. M., Collier, T. W., Zu, D. & Hirasawa, K. (2006)** *Negative regulation of the alpha interferon-induced antiviral response by the Ras/Raf/MEK pathway*. Journal of Virology 80, 4422-4430.

201 **Darnell, J. E., Jr., Kerr, I. M. & Stark, G. R. (1994)** *Jak-STAT pathways and transcriptional activation in response to IFNs and other extracellular signaling proteins*. Science 264, 1415-1421.

202 **Leviyang, S., Strawn, N. & Griva, I. (2019)** *Regulation of interferon stimulated gene expression levels at homeostasis*. Cytokine 126, 154870.

203 **Nakagawa, K. & Yokosawa, H. (2000)** *Degradation of transcription factor IRF-1 by the ubiquitin-proteasome pathway. The C-terminal region governs the protein stability*. European Journal of Biochemistry 267, 1680-1686.

204 **Barro, M. & Patton, J. T. (2007)** *Rotavirus NSP1 inhibits expression of type I interferon by antagonizing the function of interferon regulatory factors IRF3, IRF5, and IRF7*. Journal of Virology 81, 4473-4481.

205 **Zhao, X., Zhu, H., Yu, J., Li, H., Ge, J. & Chen, W. (2016)** *c-Cbl-mediated ubiquitination of IRF3 negatively regulates IFN-beta production and cellular antiviral response*. Cell Signaling 28, 1683-1693.

206 **Fujita, T., Kimura, Y., Miyamoto, M., Barsoumian, E. L. & Taniguchi, T. (1989)** *Induction of endogenous IFN-alpha and IFN-beta genes by a regulatory transcription factor, IRF-1*. Nature 337, 270-272.

209 **Schneider, W. M., Chevillotte, M. D. & Rice, C. M. (2014)** *Interferon-stimulated genes: A complex web of host defenses*. Annual Reviews Immunology 32, 513-545.

210 **Kaner, R. J., Baird, A., Mansukhani, A., Basilico, C., Summers, B. D., Florkiewicz, R. Z. & Hajjar, D. P. (1990)** *Fibroblast growth factor receptor is a portal of cellular entry for herpes simplex virus type 1*. Science 248, 1410-1413.

211 **Schoggins, J. W. & Rice, C. M. (2011)** *Interferon-stimulated genes and their antiviral effector functions*. Current Opinion in Virology 1, 519-525.

212 **Werner, S., Peters, K. G., Longaker, M. T., Fuller-Pace, F., Banda, M. J. & Williams, L. T. (1992)** *Large induction of keratinocyte growth factor expression in the dermis during wound healing*. Proceedings of the National Academy of Sciences 89, 6896-6900.

213 **Finch, P. W. & Rubin, J. S. (2004)** *Keratinocyte growth factor/fibroblast growth factor 7, a homeostatic factor with therapeutic potential for epithelial protection and repair*. Advances in Cancer Research 91, 69-136.

214 **Van, N. D., Falk, C. S., Sandmann, L., Vondran, F. W., Helfritz, F., Wedemeyer, H., Manns, M. P., Ciesek, S. & von Hahn, T. (2016)** *Modulation of HCV reinfection after orthotopic liver transplantation by fibroblast growth factor-2 and other non-interferon mediators*. Gut 65, 1015-1023.

215 **Limonta, D., Jovel, J., Kumar, A., Lu, J., Hou, S., Airo, A. M., Lopez-Orozco, J., Wong, C. P., Saito, L., Branton, W., Wong, G. K.-S., Mason, A., Power, C. & Hobman, T. C. (2019)** *Fibroblast growth factor 2 enhances zika virus infection in human fetal brain*. The Journal of Infectious Diseases 220, 1377-1387.

216 **Prince, L. S., Karp, P. H., Moninger, T. O. & Welsh, M. J. (2001)** *KGF alters gene expression in human airway epithelia: Potential regulation of the inflammatory response*. Physiological Genomics 6, 81-89.

217 **Quantius, J., Schmoldt, C., Vazquez-Armendariz, A. I., Becker, C., El Agha, E., Wilhelm, J., Morty, R. E., Vadasz, I., Mayer, K., Gattenloehner, S., Fink, L., Matrosovich, M., Li, X., Seeger, W., Lohmeyer, J., Bellusci, S. & Herold, S. (2016)** *Influenza virus infects epithelial stem/progenitor cells of the distal lung: Impact on Fgfr2b-driven epithelial repair*. PLoS Pathogens 12, e1005544.

218 **van Asten, S. D., Raaben, M., Nota, B. & Spaapen, R. M. (2018)** *Secretome screening reveals fibroblast growth factors as novel inhibitors of viral replication*. Journal of Virology 92, e00260-00218.

219 **Cortese, M., Kumar, A., Matula, P., Kaderali, L., Scaturro, P., Erfle, H., Acosta, E. G., Buehler, S., Ruggieri, A., Chatel-Chaix, L., Rohr, K. & Bartenschlager, R. (2019)** *Reciprocal effects of fibroblast growth factor receptor signaling on dengue virus replication and virion production*. Cell Reports 27, 2579-2592.

220 **Grose, R., Fantl, V., Werner, S., Chioni, A. M., Jarosz, M., Rudling, R., Cross, B., Hart, I. R. & Dickson, C. (2007)** *The role of fibroblast growth factor receptor 2b in skin homeostasis and cancer development*. The EMBO Journal 26, 1268-1278.

221 **Sulcova, J., Meyer, M., Guiducci, E., Feyerabend, T. B., Rodewald, H.-R. & Werner, S. (2015)** *Mast cells are dispensable in a genetic mouse model of chronic dermatitis*. American Journal of Pathology 185, 1575-1587.

223 **Meyers, G. A., Orlow, S. J., Munro, I. R., Przylepa, K. A. & Jabs, E. W. (1995)** *Fibroblast growth factor receptor 3 (FGFR3) transmembrane mutation in Crouzon syndrome with acanthosis nigricans*. Nature Genetics 11, 462.

224 **Wilkes, D., Rutland, P., Pulleyn, L., Reardon, W., Moss, C., Ellis, J., Winter, R. & Malcolm, S. (1996)** *A recurrent mutation, ala391glu, in the transmembrane region of*

FGFR3 causes Crouzon syndrome and acanthosis nigricans. Journal of Medical Genetics 33, 744-748.

225 **Logie, A., Dunois-Larde, C., Rosty, C., Levrel, O., Blanche, M., Ribeiro, A., Gasc, J.-M., Jorcano, J., Werner, S. & Sastre-Garau, X. (2005)** *Activating mutations of the tyrosine kinase receptor FGFR3 are associated with benign skin tumors in mice and humans*. Human Molecular Genetics 14, 1153-1160.

226 **Hafner, C., van Oers, J. M., Vogt, T., Landthaler, M., Stoehr, R., Blaszyk, H., Hofstaedter, F., Zwarthoff, E. C. & Hartmann, A. (2006)** *Mosaicism of activating FGFR3 mutations in human skin causes epidermal nevi*. Journal of Clinical Investigation 116, 2201-2207.

231 **Sennett, R., Wang, Z., Rezza, A., Grisanti, L., Roitershtein, N., Sicchio, C., Mok, K. W., Heitman, N. J., Clavel, C. & Ma'ayan, A. (2015)** *An integrated transcriptome atlas of embryonic hair follicle progenitors, their niche, and the developing skin*. Developmental Cell 34, 577-591.

233 **Chellaiah, A. T., McEwen, D. G., Werner, S., Xu, J. & Ornitz, D. M. (1994)** *Fibroblast growth factor receptor (FGFR) 3. Alternative splicing in immunoglobulin-like domain III creates a receptor highly specific for acidic FGF/FGF-1*. Journal of Biological Chemistry 269, 11620-11627.

235 **Duperret, E. K., Oh, S. J., McNeal, A., Prouty, S. M. & Ridky, T. W. (2014)** *Activating FGFR3 mutations cause mild hyperplasia in human skin, but are insufficient to drive benign or malignant skin tumors*. Cell Cycle 13, 1551-1559.

236 **Takenaka, H., Yasuno, H. & Kishimoto, S. (2002)** *Immunolocalization of fibroblast growth factor receptors in normal and wounded human skin*. Archives of Dermatological Research 294, 331-338.

237 **Beer, H.-D., Florence, C., Dammeier, J., McGuire, L., Werner, S. & Duan, D. R. (1997)** *Mouse fibroblast growth factor 10: cDNA cloning, protein characterization, and regulation of mRNA expression*. Oncogene 15, 2211.

238 **Xu, W., Hong, S. J., Zhong, A., Xie, P., Jia, S., Xie, Z., Zeitchek, M., Niknam-Bienia, S., Zhao, J. & Porterfield, D. M. (2015)** *Sodium channel Nax is a regulator in epithelial sodium homeostasis*. Science Translational Medicine 7, 312ra177-312ra177.

239 **Zhao, J., Zhong, A., Friedrich, E. E., Jia, S., Xie, P., Galiano, R. D., Mustoe, T. A. & Hong, S. J. (2017)** *S100A12 induced in the epidermis by reduced hydration activates dermal fibroblasts and causes dermal fibrosis*. Journal of Investigative Dermatology 137, 650-659.

240 **Zhong, A., Xu, W., Zhao, J., Xie, P., Jia, S., Sun, J., Galiano, R. D., Mustoe, T. A. & Hong, S. J. (2016)** *S100A8 and S100A9 are induced by decreased hydration in the*

epidermis and promote fibroblast activation and fibrosis in the dermis. American Journal of Pathology 186, 109-122.

241 **Hedger, M. P. & de Kretser, D. M. (2013)** *The activins and their binding protein, follistatin — diagnostic and therapeutic targets in inflammatory disease and fibrosis*. Cytokine & Growth factor Reviews 24, 285-295.

242 **Werner, S. & Alzheimer, C. (2006)** *Roles of activin in tissue repair, fibrosis, and inflammatory disease*. Cytokine & Growth Factor Reviews 17, 157-171.

243 **Icha, J., Weber, M., Waters, J. C. & Norden, C. (2017)** *Phototoxicity in live fluorescence microscopy, and how to avoid it*. Bioessays 39, 1700003.

244 **Nanni, M., Ranieri, D., Raffa, S., Torrisi, M. R. & Belleudi, F. (2018)** *Interplay between FGFR2b-induced autophagy and phagocytosis: Role of PLCγ-mediated signalling*. Journal of Cellular and Molecular Medicine 22, 668-683.

245 **Maimon, B. E., Diaz, M., Revol, E. C. M., Schneider, A. M., Leaker, B., Varela, C. E., Srinivasan, S., Weber, M. B. & Herr, H. M. (2018)** *Optogenetic peripheral nerve immunogenicity*. Scientific Reports 8, 14076.

246 **Bhalla, U. S. & Iyengar, R. (1999)** *Emergent properties of networks of biological signaling pathways*. Science 283, 381-387.

247 **Weng, G., Bhalla, U. S. & Iyengar, R. (1999)** *Complexity in biological signaling systems*. Science 284, 92-96.

248 **Soyer, O. S. & Bonhoeffer, S. (2006)** *Evolution of complexity in signaling pathways*. Proceedings of the National Academy of Sciences 103, 16337-16342.

249 **Edelman, G. M. & Gally, J. A. (2001)** *Degeneracy and complexity in biological systems*. Proceedings of the National Academy of Sciences 98, 13763-13768.

250 **Neves, S. R. & Iyengar, R. (2009)** *Models of spatially restricted biochemical reaction systems*. The Journal of Biological Chemistry 284, 5445-5449.

251 **Neves, S. R. (2012)** *Modeling of spatially-restricted intracellular signaling*. Wiley Interdisciplinary Reviews - Systems Biology and Medicine 4, 103-115.

252 **Ray, A. T., Mazot, P., Brewer, J. R., Catela, C., Dinsmore, C. J. & Soriano, P. (2020)** *FGF signaling regulates development by processes beyond canonical pathways*. Genes & Development 34, 1735-1752.

253 **Iadevaia, S., Lu, Y., Morales, F. C., Mills, G. B. & Ram, P. T. (2010)** *Identification of optimal drug combinations targeting cellular networks: Integrating phospho-proteomics and computational network analysis*. Cancer Research 70, 6704-6714.

254 **Likić, V. A., McConville, M. J., Lithgow, T. & Bacic, A. (2010)** *Systems biology: The next frontier for bioinformatics*. Advances in Bioinformatics 2010, 268925-268925.

255 **Eungdamrong, N. J. & Iyengar, R. (2004)** *Modeling cell signaling networks*. Biology of the Cell 96, 355-362.

256 **Qi, Y. & Ge, H. (2006)** *Modularity and dynamics of cellular networks*. PLoS Computational Biology 2, e174.

257 **Mohsenizadeh, D. N., Hua, J., Bittner, M. & Dougherty, E. R. (2015)** *Dynamical modeling of uncertain interaction-based genomic networks*. BMC bioinformatics 16, S3-S3.

258 **Rangamani, P. & Iyengar, R. (2008)** *Modelling cellular signalling systems*. Essays in Biochemistry 45, 83-94.

259 **Bizzarri, M., Naimark, O., Nieto-Villar, J., Fedeli, V. & Giuliani, A. (2020)** *Complexity in biological organization: Deconstruction (and subsequent restating) of key concepts*. Entropy 22, 885.

260 **Ma'ayan, A., Blitzer, R. D. & Iyengar, R. (2005)** *Toward predictive models of mammalian cells*. Annual Review of Biophysics and Biomolecular Structure 34, 319-349.

Appendix

Code for controlling the Arduino UNO board (“timertheresa2.0_1-15_1-60_15-0”)

```
int minutesLEDon[3]={15,60,0};// this is in real life OFF time
int minutesLEDoff[3]={1,1,15};// this is in real life ON time
int minutestostart[3]{0,0,0};
const int LEDPin[3]={12,11,10}; // LED on Pin Nr <-change the PinNr for LED here!
//dont change the rest
float timerglobal=0;        // timer in milliseconds
float millisecondsLEDon[3]={0.0,0.0,0.0};   // timecalculation LED ON from minutes to
milliseconds
float millisecondsLEDoff[3]={0.0,0.0,0.0};  // timecalculation LED OFF from minutes to
milliseconds
float millisecondstostart[3]={0.0,0.0,0.0}; // timecalculation from minutes to milliseconds
from start programm to first ON
float switchtimeLEDon[3]{0.0,0.0,0.0};      // absolute time when the LED is switched ON
for the next time
float switchtimeLEDoff[3]{0.0,0.0,0.0};     // absolute time when the LED is switched OFF
for the next time
bool LEDstate[3]={0,0,0};                   // state of each LED
void setup() {
  Serial.begin(250000);
  Serial.println("************ Begin Setup******************");
  for (int i=0;i<=2;i++){                           // for each LED...
                    pinMode(LEDPin[i], OUTPUT);       //define Pins as Output
                    digitalWrite(LEDPin[i], LOW);     // set Pins to Low
                    }
    for (int i=0;i<=2;i++){                                     // for each LED...
                    millisecondsLEDon[i]= (float)minutesLEDon[i]*60000;    // calculation
time LED ON in milliseconds
                    Serial.print("millisecondsLEDon[");                 // Print to the Serial
Monitor
                    Serial.print(i+1);
                    Serial.print("] = ");
                    Serial.println(millisecondsLEDon[i]);
                    millisecondsLEDoff[i]=(float)minutesLEDoff[i]*60000;   // calculation time
LED OFF in milliseconds
                    Serial.print("millisecondsLEDoff[");                 // Print to the Serial
Monitor
                    Serial.print(i+1);
                    Serial.print("] = ");
```

Code for controlling the Arduino UNO board (“timertheresa2.0_1-15_1-60_15-0”)

```
                Serial.println(millisecondsLEDoff[i]);
                millisecondstostart[i]=(float)minutestostart[i]*60000; // calculation time to
start in milliseconds
                Serial.print("millisecondstostart[");              // Print to the Serial Monitor
                Serial.print(i+1);
                Serial.print("] = ");
                Serial.println(millisecondstostart[i]);
                switchtimeLEDon[i]=millisecondstostart[i];          // calculation first
switchtime
                Serial.print("switchtimeLEDon[");                  // Print to the Serial
Monitor
                Serial.print(i+1);
                Serial.print("] = ");
                Serial.println(switchtimeLEDon[i]);
               }
 Serial.println("****************End Setup******************");
delay(1000);
}
void loop() {
        timerglobal=millis();// write from internal timer to variable "globaltimer"
         for (int i=0;i<=2;i++){          // for each LED...
                        switch (LEDstate[i]){      //switchcase for both LED states
                                case 0:       // if LED is off
                                    if (timerglobal>=switchtimeLEDon[i]){       // if
timer is bigger then next switchtime ON

digitalWrite(LEDPin[i],HIGH);                       //switch LED to ON
                                                            LEDstate[i]=1;
//change LED state

event(timerglobal,i,LEDstate[i]);                   // goto subprogram event
switchtimeLEDoff[i]=timerglobal+millisecondsLEDoff[i];   // calculate next switchtime
when LED is shut off again
                                                                    }
                                break;
                                case 1:
                                    if (millisecondsLEDoff[i]==0){
// if LED is always on skip the if case
                                                                goto bailout;
// skip and go to the end
                                                            }
                                    if (timerglobal>=switchtimeLEDoff[i]){
```

Code for controlling the Arduino UNO board (“timertheresa2.0_1-15_1-60_15-0”)

```
digitalWrite(LEDPin[i],LOW);                    //switch LED OFF
                                                                LEDstate[i]=0;
//change LED state

event(timerglobal,i,LEDstate[i]);                // go to subprogramm event

switchtimeLEDon[i]=timerglobal+millisecondsLEDon[i];      //calculate next switchtime
when LED is shut on again
                                                                }
                                        bailout:
// END
                                        break;
                                        }
                                }
        }
void event(float timer,int LEDnumber,bool state){
// Subprogramm event with input variables absolutetime, LED number, LED state
                                        int state1=state;                                       // take the
input variable state and write it into variable state1
                                        int LED=LEDnumber;                                      //
take the input variable LEDnumber and write it into variable LED
                                        float timesincestart=timer;                             // take
the input variable timer and write it into variable timesincestart
                                        int hours;                                      // define
variable hours
                                        int minutes;                                    // define
variable minutes
                                        int seconds;                                    // define
variable seconds

                                        hours=(int)(timesincestart/3600000);                    //
calculate hours since start
                                        minutes=(int)((timesincestart-(hours*3600000))/60000);
// calculate minutes from the full hour
                                        seconds=(int)((timesincestart-(hours*3600000)-
(minutes*60000))/1000);    // calculate seconds from the full minute
                                        Serial.print(hours);                                    // write
to the serial monitor
                                        Serial.print(":");
                                        Serial.print(minutes);
                                        Serial.print(":");
```

Code for controlling the Arduino UNO board (“timertheresa2.0_1-15_1-60_15-0”)

```
                    Serial.print(seconds);
                    Serial.print("\t");                          // tabulator
                    Serial.print("LED Number ");                 //
LED number, +1 that it is shown as LED1,2,3
                    Serial.print(LED+1);
                    Serial.print(" : ");
                    switch (state1) {
                            case 0:                             // 0 is OFF
                                Serial.println("OFF");
                            break;
                            case 1:                             // 1 is ON
                                Serial.println("ON");
                            break;
                            }
                    }
```

Abbreviations

Abbreviation	Explanation
AB	Acid box
AKT	Akt8 virus oncogene cellular homologue
APS	Ammonium persulfate
ATP	Adenosine triphosphate
BAD	BCL2 associated agonist of cell death
bp	Basepairs
BCA	Bicinchoninic acid
BM	Basement membrane
BrdU	Bromodeoxyuridine
BSA	Bovine serum albumin
C-terminal	Carboxy-terminal
Ca^{2+}	Calcium ion
CDK	Cyclin-dependent kinase
cDNA	Complementary DNA
CIB	Cryptochrome-interacting basic helix-loop-helix 1
CO_2	Carbon dioxide
CRY2	Cryptochrome 2
CT	Cycle threshold
d	Day(s)
D	Dermis
DAG	Diacylglycerol
DEPC	Diethyl pyrocarbonate
DMEM	Dulbecco's modified eagle medium
DMSO	Dimethyl sulfoxide
DNA	Deoxyribonucleic acid
dNTPs	Deoxynucleoside triphosphates
Dox	Doxycycline
DTT	Dithiothreitol
DUSP6	Dual-specific phosphatase 6
E	Epidermis
ECM	Extracellular matrix
EDTA	Ethylenediaminetetraacetic acid
EGF	Epidermal growth factor

Abbreviation	Explanation
ELISA	Enzyme-linked immunosorbent assay
EMT	Epithelial-mesenchymal transition
EPIC	ETH Phenomics Center
ER	Endoplasmatic reticulum
ERK1/2	Extracellular signal-regulated kinase 1 and 2
EV	Extended view
E. coli	*Escherichia coli*
FBS	Fetal bovine serum
FGF	Fibroblast growth factor
FGFR	FGF receptor
FRS2α	FGFR substrate 2α
GAB1	GRB2 associated binding protein 1
GDP	Guanosine 5-diphosphate
GFP	Green-fluorescent protein
GPCR	G-protein coupled receptor
GRB2	Growth factor receptor bound protein 2
GTP	Guanosine 5-triphosphate
h	Hour(s)
H&E	Hematoxylin and Eosin
HA	Hemagglutinin
HaCaT	Immortalised human keratinocyte line
HBEGF	Heparin binding EGF like growth factor
HCl	Hydrochloric acid
HD	Hypodermis
HEK	Human embryonic kidney
HF	Hair follicle
hpi	Hours post infection
HRP	Horseradish peroxidase
HSPG	Heparan sulphate proteoglycan
HSV-1	Herpes simplex virus 1
HUVECs	Human umbilical vein endothelial cells
IFN I	Type I Interferon
Ig	Immunoglobulin-like domain
IP	Immunoprecipitation
IP_3	Inositol trisphosphate
IRE	IRF response element
IRF	Interferon regulatory factor

Abbreviation	Explanation
ISG	Interferon stimulated gene
ISGF 3	Interferon stimulated gene factor 3
ISRE	Interferon stimulated response element
JNK	c-Jun N-terminal kinases
K	Keratin
KGF	Keratinocyte growth factor (FGF7)
LB	Luria-Bertani
LED	Light emitting diode
LOV	Light-oxygen-voltage domain
M	Molar
m	Milli-
µ	Mikro-
MAP	Mitogen-activated protein
MAPK	MAP kinase
MEK	MAPK/ERK kinase
min	Minute(s)
MOI	Multiplicity of infection
MTT	Thiazolyl blue tetrazolium bromide
Myr	Myristoylation anchor
n	Nano-
N-terminal	Amino-terminal
NaOH	Sodium hydroxide
NEB	New England Biolabs
NGF	Nerve growth factor
OCT	Optimum cutting temperature
OptoR2	Light-activatable FGFR2
P	Phosphorylation
PAS	Period-ARNT-Singleminded
PBS	Phosphate buffered saline
PC	*Panniculus carnosus*
PCB	Phycocyanobilin
PCR	Polymerase chain reaction
PDK	Phosphoinositide-dependent kinase
PES	Polyethersulfone
PFA	Paraformaldehyde
PH	Pleckstrin homology domain
PHYB	Phytochrome B

Abbreviation	Explanation
PI	Propidium iodide
PI3K	Phosphoinositide 3-kinase
PIF	Phytochrome interacting factor
PIP_2	Phosphatidylinositol 4,5-bisphosphate
PIP_3	Phosphatidylinositol 3,4,5-trisphosphate
PKC	Protein kinase C
PLCγ	Phospholipase Cγ
PNK	Polynucleotide kinase
POI	Protein of interest
PTB	Phosphotyrosine-binding domain
PTEN	Phosphatase and tensin homologue
PTP1B	Protein tyrosine phosphatase 1B
qPCR	Quantitative PCR
RAF	Rapidly accelerated fibrosarcoma
RAS	Rat sarcoma
RIPA	Radioimmunoprecipitation assay
rpm	Rounds per minute
RNA	Ribonucleic acid
rSAP	Recombinant shrimp alkaline phosphatase
RT	Room temperature
S	Serine
SB	*Stratum basale*
SC	*Stratum corneum*
SDS	Sodium dodecyl sulfate
sec	Second(s)
SEM	Standard error mean
SG	*Stratum granulosum*
SH2	Src homology 2 domain
SOS	Son of sevenless
SP	Signal peptide
SPF	Specific pathogen-free
SS	*Stratum spinsoum*
STAT	Signal transducer and activator of transcription
TBS-T	Tris buffered saline with Tween 20
TGFβ	Transforming growth factor β
TIRF	Total internal reflection fluorescence
TK	Tyrosine kinase domain

Abbreviation	Explanation
TM	Transmembrane domain
TRK	Tropomyosin receptor kinase
UV	Ultraviolet
VEGF	Vascular endothelial growth factor
Y	Tyrosine

Acknowledgements

First and foremost, I would like to thank Sabine for giving me the opportunity to perform my PhD thesis in your lab, for offering me to work on more than one project and for your enthusiasm that helps persevere through tough times.

Then, I would like to thank Prof. Nancy Hynes and Prof. Michael Detmar for serving in my thesis committee and for the supportive atmosphere and the helpful discussions during our meetings. Special thanks go also to our collaborator Prof. Harald Janovjak, who moved far away from Austria to Australia and still stayed close to us and our project with your great suggestions and your positive attitude.

Furthermore, I owe big thanks to all the people from the Werner group, both current or former members. First, I would like to thank the students, who joined me at different stages of my project – especially Irina and Selina, who trusted me enough to join me for your Master thesis project. I am glad that I could accompany you in such an important step of your research career and it has been an absolute pleasure to work, discuss and have fun with you. Then, thanks to Gigi and Michi for the many lunch and cake breaks together that we used to discuss science and life in general – I have learned tremendously from both of you. Next, I would like to thank the people who worked together with me on my side projects: Maya, thank you for making mouse colony maintenance a whole lot of fun and for becoming a real friend; Corinne, Debbie and Luca, thank you for collaborating on such an exciting project with me and combating viruses together. Big thanks go also to Shen and Till and the other people from F21.2 for being around and creating a feel-good atmosphere – in my opinion, our lab is the best one. Then, thank you Abbie for being such an amazing human, and Paul for being an inspiring scientist. Last but not least, thanks to all the PhDs for standing together and encouraging each other.

Next, I would like to thank the people outside the lab, who keep HPL running: Sol and Victor for taking care of my mice and keeping them as dark as possible, and Rolf for fixing absolutely everything.

Last, I would like to thank my family and friends for making this possible – Danke.

Complete bibliography

1 **Proksch, E., Brandner, J. M. & Jensen, J.-M. (2008)** *The skin: an indispensable barrier*. Experimental Dermatology 17, 1063-1072.

2 **Fuchs, E. & Raghavan, S. (2002)** *Getting under the skin of epidermal morphogenesis*. Nature Reviews Genetics 3, 199-209.

3 **Gould, J. (2018)** *Superpowered skin*. Nature 563, S84-S85.

4 **Cotsarelis, G., Sun, T. T. & Lavker, R. M. (1990)** *Label-retaining cells reside in the bulge area of pilosebaceous unit: implications for follicular stem cells, hair cycle, and skin carcinogenesis*. Cell 61, 1329-1337.

5 **Roop, D. (1995)** *Defects in the barrier*. Science 267, 474.

6 **Heenen, M. & Galand, P. (1997)** *The growth fraction of normal human epidermis*. Dermatology 194, 313-317.

7 **Webb, A., Li, A. & Kaur, P. (2004)** *Location and phenotype of human adult keratinocyte stem cells of the skin*. Differentiation 72, 387-395.

8 **Blanpain, C. & Fuchs, E. (2006)** *Epidermal stem cells of the skin*. Annual Review of Cell and Developmental Biology 22, 339-373.

9 **Blanpain, C. & Fuchs, E. (2009)** *Epidermal homeostasis: a balancing act of stem cells in the skin*. Nature Reviews Molecular Cell Biology 10, 207-217.

10 **Hsu, Y. C., Pasolli, H. A. & Fuchs, E. (2011)** *Dynamics between stem cells, niche, and progeny in the hair follicle*. Cell 144, 92-105.

11 **Baroni, A., Buommino, E., De Gregorio, V., Ruocco, E., Ruocco, V. & Wolf, R. (2012)** *Structure and function of the epidermis related to barrier properties*. Clinical Dermatology 30, 257-262.

12 **Hopkinson, S. B., Hamill, K. J., Wu, Y., Eisenberg, J. L., Hiroyasu, S. & Jones, J. C. (2014)** *Focal contact and hemidesmosomal proteins in keratinocyte migration and wound repair*. Advances in Wound Care (New Rochelle) 3, 247-263.

13 **Walko, G., Castanon, M. J. & Wiche, G. (2015)** *Molecular architecture and function of the hemidesmosome*. Cell and Tissue Research 360, 529-544.

14 **Fuchs, E. (1993)** *Epidermal differentiation and keratin gene expression*. Journal of Cell Science 17, 197-208.

15 **Simpson, C. L., Patel, D. M. & Green, K. J. (2011)** *Deconstructing the skin: cytoarchitectural determinants of epidermal morphogenesis*. Nature Reviews Molecular Cell Biology 12, 565-580.

16 **Nemes, Z. & Steinert, P. M. (1999)** *Bricks and mortar of the epidermal barrier*. Experimental & Molecular Medicine 31, 5-19.

17 **Bangert, C., Brunner, P. M. & Stingl, G. (2011)** *Immune functions of the skin*. Clinical Dermatology 29, 360-376.

18 **Richmond, J. M. & Harris, J. E. (2014)** *Immunology and skin in health and disease*. Cold Spring Harbor Perspectives in Medicine 4, a015339.

19 **Maricich, S. M., Wellnitz, S. A., Nelson, A. M., Lesniak, D. R., Gerling, G. J., Lumpkin, E. A. & Zoghbi, H. Y. (2009)** *Merkel cells are essential for light-touch responses*. Science 324, 1580-1582.

20 **Zimmerman, A., Bai, L. & Ginty, D. D. (2014)** *The gentle touch receptors of mammalian skin*. Science 346, 950-954.

21 **Dupin, E. & Le Douarin, N. M. (2003)** *Development of melanocyte precursors from the vertebrate neural crest*. Oncogene 22, 3016-3023.

22 **Brenner, M. & Hearing, V. J. (2008)** *The protective role of melanin against UV damage in human skin*. Photochemistry and Photobiology 84, 539-549.

23 **Singh, S. K., Kurfurst, R., Nizard, C., Schnebert, S., Perrier, E. & Tobin, D. J. (2010)** *Melanin transfer in human skin cells is mediated by filopodia - a model for homotypic and heterotypic lysosome-related organelle transfer*. The FASEB Journal 24, 3756-3769.

24 **Stacy, A. & Belkaid, Y. (2019)** *Microbial guardians of skin health*. Science 363, 227-228.

25 **Singer, A. J. & Clark, R. A. (1999)** *Cutaneous wound healing*. The New England Journal of Medicine 341, 738-746.

26 **Sorrell, J. M. & Caplan, A. I. (2004)** *Fibroblast heterogeneity: more than skin deep*. Journal of Cell Science 117, 667-675.

27 **Kurita, M., Okazaki, M., Kaminishi-Tanikawa, A., Niikura, M., Takushima, A. & Harii, K. (2012)** *Differential expression of wound fibrotic factors between facial and trunk dermal fibroblasts*. Connective Tissue Research 53, 349-354.

28 **Tracy, L. E., Minasian, R. A. & Caterson, E. J. (2016)** *Extracellular matrix and dermal fibroblast function in the healing wound*. Advances in Wound Care 5, 119-136.

29 **Lynch, M. D. & Watt, F. M. (2018)** *Fibroblast heterogeneity: implications for human disease*. The Journal of Clinical Investigation 128, 26-35.

30 **Proksch, E., Fölster-Holst, R. & Jensen, J.-M. (2006)** *Skin barrier function, epidermal proliferation and differentiation in eczema*. Journal of Dermatological Science 43, 159-169.

31 **O'Regan, G. M., Sandilands, A., McLean, W. H. & Irvine, A. D. (2008)** *Filaggrin in atopic dermatitis*. Journal of Allergy and Clinical Immunology 124, R2-6.

32 **Guttman-Yassky, E., Suarez-Farinas, M., Chiricozzi, A., Nograles, K. E., Shemer, A., Fuentes-Duculan, J., Cardinale, I., Lin, P., Bergman, R., Bowcock, A. M. & Krueger, J. G. (2009)** *Broad defects in epidermal cornification in atopic dermatitis identified through genomic analysis*. Journal of Allergy and Clinical Immunology 124, 1235-1244.e1258.

33 **Boguniewicz, M. & Leung, D. Y. M. (2011)** *Atopic dermatitis: A disease of altered skin barrier and immune dysregulation*. Immunological Reviews 242, 233-246.

34 **Kezic, S., Novak, N., Jakasa, I., Jungersted, J. M., Simon, M., Brandner, J. M., Middelkamp-Hup, M. A. & Weidinger, S. (2014)** *Skin barrier in atopic dermatitis*. Frontiers in Bioscience 19, 542-556.

35 **Peng, W. & Novak, N. (2015)** *Pathogenesis of atopic dermatitis*. Clinical & Experimental Allergy 45, 566-574.

36 **Härtel, E., Werner, S. & Schäfer, M. (2014)** *Transcriptional regulation of wound inflammation*. Seminars in Immunology 26, 321-328.

37 **Werner, S. & Grose, R. (2003)** *Regulation of wound healing by growth factors and cytokines*. Physiological Reviews 83, 835-870.

38 **Bünemann, E., Hoff, N. P., Buhren, B. A., Wiesner, U., Meller, S., Bolke, E., Muller-Homey, A., Kubitza, R., Ruzicka, T., Zlotnik, A., Homey, B. & Gerber, P. A. (2018)** *Chemokine ligand-receptor interactions critically regulate cutaneous wound healing*. European Journal of Medical Research 23, 4.

39 **Schäfer, M. & Werner, S. (2008)** *Cancer as an overhealing wound: an old hypothesis revisited*. Nature Reviews Molecular Cell Biology 9, 628-638.

40 **Brockes, J. P. & Kumar, A. (2008)** *Comparative aspects of animal regeneration*. Annual Review of Cell and Developmental Biology 24, 525-549.

41 **Larson, B. J., Longaker, M. T. & Lorenz, H. P. (2010)** *Scarless fetal wound healing: A basic science review*. Plastic and Reconstructive Surgery 126, 1172-1180.

42 **Maddaluno, L., Urwyler, C. & Werner, S. (2017)** *Fibroblast growth factors: Key players in regeneration and tissue repair*. Development 144, 4047-4060.

43 **Lanning, N. J. & Carter-Su, C. (2006)** *Recent advances in growth hormone signaling*. Reviews in Endocrine and Metabolic Disorders 7, 225-235.

44 **Chen, K., Liu, J. & Cao, X. (2017)** *Regulation of type I interferon signaling in immunity and inflammation: A comprehensive review*. Journal of Autoimmunity 83, 1-11.

45 **Beenken, A. & Mohammadi, M. (2009)** *The FGF family: Biology, pathophysiology and therapy*. Nature Reviews Drug Discovery 8, 235-253.

46 **Belov, A. A. & Mohammadi, M. (2013)** *Molecular mechanisms of fibroblast growth factor signaling in physiology and pathology*. Cold Spring Harbor Perspectives in Biology 5, 1-24.

47 **Makarenkova, H. P., Hoffman, M. P., Beenken, A., Eliseenkova, A. V., Meech, R., Tsau, C., Patel, V. N., Lang, R. A. & Mohammadi, M. (2009)** *Differential interactions of FGFs with heparan sulfate control gradient formation and branching morphogenesis*. Science Signaling 2, ra55.

48 **Ornitz, D. M. & Itoh, N. (2015)** *The fibroblast growth factor signaling pathway*. Wiley Interdisciplinary Reviews: Developmental Biology 4, 215-266.

49 **Eswarakumar, V. P., Lax, I. & Schlessinger, J. (2005)** *Cellular signaling by fibroblast growth factor receptors*. Cytokine & Growth Factor Reviews 16, 139-149.

50 **Zhang, X., Ibrahimi, O. A., Olsen, S. K., Umemori, H., Mohammadi, M. & Ornitz, D. M. (2006)** *Receptor specificity of the fibroblast growth factor family. The complete mammalian FGF family*. Journal of Biological Chemistry 281, 15694-15700.

51 in *Encyclopedia of Genetics, Genomics, Proteomics and Informatics* 2064-2064 (Springer Netherlands, 2008).

52 **Lemmon, M. A. & Schlessinger, J. (2010)** *Cell signaling by receptor tyrosine kinases*. Cell 141, 1117-1134.

53 **Tiong, K. H., Mah, L. Y. & Leong, C.-O. (2013)** *Functional roles of fibroblast growth factor receptors (FGFRs) signaling in human cancers*. Apoptosis 18, 1447-1468.

54 **Touat, M., Ileana, E., Postel-Vinay, S., André, F. & Soria, J.-C. (2015)** *Targeting FGFR Signaling in Cancer*. Clinical Cancer Research 21, 2684-2694.

55 **Ong, S. H., Guy, G. R., Hadari, Y. R., Laks, S., Gotoh, N., Schlessinger, J. & Lax, I. (2000)** *FRS2 Proteins Recruit Intracellular Signaling Pathways by Binding to Diverse Targets on Fibroblast Growth Factor and Nerve Growth Factor Receptors*. Molecular and Cellular Biology 20, 979-989.

56 **Hertzler-Schaefer, K., Mathew, G., Somani, A. K., Tholpady, S., Kadakia, M. P., Chen, Y., Spandau, D. F. & Zhang, X. (2014)** *Pten loss induces autocrine FGF signaling to promote skin tumorigenesis*. Cell Reports 6, 818-826.

57 **Mason, I. (2007)** *Initiation to end point: The multiple roles of fibroblast growth factors in neural development*. Nature Reviews Neuroscience 8, 583-596.

58 **Turner, N. & Grose, R. (2010)** *Fibroblast growth factor signalling: From development to cancer*. Nature Reviews Cancer 10, 116-129.

59 **Coutu, D. L. & Galipeau, J. (2011)** *Roles of FGF signaling in stem cell self-renewal, senescence and aging*. Aging 3, 920-933.

60 **Fearon, A. E., Gould, C. R. & Grose, R. P. (2013)** *FGFR signalling in women's cancers*. International Journal of Biochemistry & Cell Biology 45, 2832-2842.

61 **Aaronson, S. A., Bottaro, D. P., Miki, T., Ron, D., Finch, P. W., Fleming, T. P., Ahn, J., Taylor, W. G. & Rubin, J. S. (1991)** *Keratinocyte growth factor: A fibroblast growth factor family member with unusual target cell specificity*. Annals of the New York Academy of Sciences 638, 62-77.

62 **Werner, S., Weinberg, W., Liao, X., Peters, K., Blessing, M., Yuspa, S., Weiner, R. & Williams, L. (1993)** *Targeted expression of a dominant-negative FGF receptor mutant in the epidermis of transgenic mice reveals a role of FGF in keratinocyte organization and differentiation*. The EMBO Journal 12, 2635-2643.

63 **Boismenu, R. & Havran, W. L. (1994)** *Modulation of epithelial cell growth by intraepithelial gamma delta T cells*. Science 266, 1253-1255.

64 **Braun, S., Krampert, M., Bodo, E., Kumin, A., Born-Berclaz, C., Paus, R. & Werner, S. (2006)** *Keratinocyte growth factor protects epidermis and hair follicles from cell death induced by UV irradiation, chemotherapeutic or cytotoxic agents*. Journal of Cell Science 119, 4841-4849.

65 **Yang, J., Meyer, M., Muller, A. K., Bohm, F., Grose, R., Dauwalder, T., Verrey, F., Kopf, M., Partanen, J., Bloch, W., Ornitz, D. M. & Werner, S. (2010)** *Fibroblast growth factor receptors 1 and 2 in keratinocytes control the epidermal barrier and cutaneous homeostasis*. Journal of Cell Biology 188, 935-952.

66 **Meyer, M., Muller, A. K., Yang, J., Moik, D., Ponzio, G., Ornitz, D. M., Grose, R. & Werner, S. (2012)** *FGF receptors 1 and 2 are key regulators of keratinocyte migration in vitro and in wounded skin*. Journal of Cell Science 125, 5690-5701.

67 **Müller, A. K., Meyer, M. & Werner, S. (2012)** *The roles of receptor tyrosine kinases and their ligands in the wound repair process*. Seminars in Cell & Developmental Biology 23, 963-970.

68 **Meyer, M., Maddaluno, L. & Werner, S.** in *Fibroblast growth factors: biology and clinical application* 187-209 (2017).

69 **de Araujo, R., Lobo, M., Trindade, K., Silva, D. F. & Pereira, N. (2019)** *Fibroblast growth factors: A controlling mechanism of skin aging*. Skin Pharmacology and Physiology 32, 275-282.

70 **Dailey, L., Ambrosetti, D., Mansukhani, A. & Basilico, C. (2005)** *Mechanisms underlying differential responses to FGF signaling*. Cytokine & Growth Factor Reviews 16, 233-247.

71 **Francavilla, C., Rigbolt, K. T., Emdal, K. B., Carraro, G., Vernet, E., Bekker-Jensen, D. B., Streicher, W., Wikstrom, M., Sundstrom, M., Bellusci, S., Cavallaro, U., Blagoev, B. & Olsen, J. V. (2013)** *Functional proteomics defines the molecular switch underlying FGF receptor trafficking and cellular outputs*. Molecular Cell 51, 707-722.

72 **Tischer, D. & Weiner, O. D. (2014)** *Illuminating cell signalling with optogenetic tools*. Nature Reviews Molecular Cell Biology 15, 551-558.

73 **Zhang, K. & Cui, B. (2015)** *Optogenetic control of intracellular signaling pathways*. Trends in Biotechnology 33, 92-100.

74 **Kwon, E. & Heo, W. D. (2020)** *Optogenetic tools for dissecting complex intracellular signaling pathways*. Biochemical and Biophysical Research Communications 527, 331-336.

75 **Nagel, G., Ollig, D., Fuhrmann, M., Kateriya, S., Musti, A. M., Bamberg, E. & Hegemann, P. (2002)** *Channelrhodopsin-1: A light-gated proton channel in green algae*. Science 296, 2395-2398.

76 **Nagel, G., Szellas, T., Huhn, W., Kateriya, S., Adeishvili, N., Berthold, P., Ollig, D., Hegemann, P. & Bamberg, E. (2003)** *Channelrhodopsin-2, a directly light-gated cation-selective membrane channel*. Proceedings of the National Academy of Sciences 100, 13940-13945.

77 **Boyden, E. S., Zhang, F., Bamberg, E., Nagel, G. & Deisseroth, K. (2005)** *Millisecond-timescale, genetically targeted optical control of neural activity*. Nature Neuroscience 8, 1263-1268.

78 **Nagel, G., Brauner, M., Liewald, J. F., Adeishvili, N., Bamberg, E. & Gottschalk, A. (2005)** *Light activation of channelrhodopsin-2 in excitable cells of Caenorhabditis elegans triggers rapid behavioral responses*. Current Biology 15, 2279-2284.

79 **Ishizuka, T., Kakuda, M., Araki, R. & Yawo, H. (2006)** *Kinetic evaluation of photosensitivity in genetically engineered neurons expressing green algae light-gated channels*. Neuroscience Research 54, 85-94.

80 **Miesenböck, G. (2009)** *The optogenetic catechism*. Science 326, 395-399.

81 **Covington, H. E., 3rd, Lobo, M. K., Maze, I., Vialou, V., Hyman, J. M., Zaman, S., LaPlant, Q., Mouzon, E., Ghose, S., Tamminga, C. A., Neve, R. L., Deisseroth, K. & Nestler, E. J. (2010)** *Antidepressant effect of optogenetic stimulation of the medial prefrontal cortex*. Journal of Neuroscience 30, 16082-16090.

82 **Deisseroth, K. (2011)** *Optogenetics*. Nature Methods 8, 26-29.

83 **Fenno, L., Yizhar, O. & Deisseroth, K. (2011)** *The development and application of optogenetics*. Annual Review of Neuroscience 34, 389-412.

84 **Lin, D., Boyle, M. P., Dollar, P., Lee, H., Lein, E. S., Perona, P. & Anderson, D. J. (2011)** *Functional identification of an aggression locus in the mouse hypothalamus*. Nature 470, 221-226.

85 **Dugue, G. P., Akemann, W. & Knopfel, T. (2012)** *A comprehensive concept of optogenetics*. Progress in Brain Research 196, 1-28.

86 **Rein, M. L. & Deussing, J. M. (2012)** *The optogenetic (r)evolution*. Molecular Genetics and Genomics 287, 95-109.

87 **Yizhar, O. (2012)** *Optogenetic insights into social behavior function*. Biological Psychiatry 71, 1075-1080.

88 **Daou, I., Tuttle, A. H., Longo, G., Wieskopf, J. S., Bonin, R. P., Ase, A. R., Wood, J. N., De Koninck, Y., Ribeiro-da-Silva, A., Mogil, J. S. & Seguela, P. (2013)** *Remote optogenetic activation and sensitization of pain pathways in freely moving mice*. Journal of Neuroscience 33, 18631-18640.

89 **Bryson, J. B., Machado, C. B., Crossley, M., Stevenson, D., Bros-Facer, V., Burrone, J., Greensmith, L. & Lieberam, I. (2014)** *Optical control of muscle function by transplantation of stem cell–derived motor neurons in mice*. Science 344, 94-97.

90 **Deisseroth, K., Etkin, A. & Malenka, R. C. (2015)** *Optogenetics and the circuit dynamics of psychiatric disease*. Journal of the American Medical Association 313, 2019-2020.

91 **Lüscher, C. (2016)** *The emergence of a circuit model for addiction*. Annual Review of Neuroscience 39, 257-276.

92 **Editorial. (2010)** *Method of the year 2010*. Nature Methods 8, 1.

93 **Gorostiza, P. & Isacoff, E. Y. (2008)** *Optical switches for remote and noninvasive control of cell signaling*. Science 322, 395-399.

94 **Airan, R. D., Thompson, K. R., Fenno, L. E., Bernstein, H. & Deisseroth, K. (2009)** *Temporally precise in vivo control of intracellular signalling*. Nature 458, 1025-1029.

95 **Bacchus, W. & Fussenegger, M. (2012)** *The use of light for engineered control and reprogramming of cellular functions*. Current Opinion in Biotechnology 23, 695-702.

96 **Chow, B. Y. & Boyden, E. S. (2013)** *Optogenetics and translational medicine*. Science Translational Medicine 5, 177ps175.

97 **Ingles-Prieto, A., Reichhart, E., Schelch, K., Janovjak, H. & Grusch, M. (2014)** *The optogenetic promise for oncology: Episode I*. Molecular & Cellular Oncology 1, e964045.

98 **Iyer, S. M. & Delp, S. L. (2014)** *Optogenetic regeneration*. Science 344, 44-45.

99 **Kushibiki, T., Okawa, S., Hirasawa, T. & Ishihara, M. (2014)** *Optogenetics: Novel tools for controlling mammalian cell functions with light*. International Journal of Photoenergy 2014, 1-10.

100 **Agus, V. & Janovjak, H. (2017)** *Optogenetic methods in drug screening: Technologies and applications*. Current Opinion in Biotechnology 48, 8-14.

101 **Rogers, K. W. & Muller, P. (2020)** *Optogenetic approaches to investigate spatiotemporal signaling during development*. Current Topics in Developmental Biology 137, 37-77.

102 **Ni, M., Tepperman, J. M. & Quail, P. H. (1999)** *Binding of phytochrome B to its nuclear signalling partner PIF3 is reversibly induced by light*. Nature 400, 781-784.

103 **Shimizu-Sato, S., Huq, E., Tepperman, J. M. & Quail, P. H. (2002)** *A light-switchable gene promoter system*. Nature Biotechnology 20, 1041-1044.

104 **Levskaya, A., Weiner, O. D., Lim, W. A. & Voigt, C. A. (2009)** *Spatiotemporal control of cell signalling using a light-switchable protein interaction*. Nature 461, 997-1001.

105 **Liu, H., Yu, X., Li, K., Klejnot, J., Yang, H., Lisiero, D. & Lin, C. (2008)** *Photoexcited CRY2 interacts with CIB1 to regulate transcription and floral initiation in Arabidopsis*. Science 322, 1535-1539.

106 **Kennedy, M. J., Hughes, R. M., Peteya, L. A., Schwartz, J. W., Ehlers, M. D. & Tucker, C. L. (2010)** *Rapid blue-light-mediated induction of protein interactions in living cells*. Nature Methods 7, 973-975.

107 **Bugaj, L. J., Choksi, A. T., Mesuda, C. K., Kane, R. S. & Schaffer, D. V. (2013)** *Optogenetic protein clustering and signaling activation in mammalian cells*. Nature Methods 10, 249-252.

108 **Pudasaini, A., El-Arab, K. K. & Zoltowski, B. D. (2015)** *LOV-based optogenetic devices: Light-driven modules to impart photoregulated control of cellular signaling*. Frontiers in Molecular Biosciences 2, 18.

109 **Glantz, S. T., Carpenter, E. J., M., M., Gardner, K. H., Boydeng, E. S., Wong, G. K.-S. & Chow, B. Y. (2016)** *Functional and topological diversity of LOV domain photoreceptors*. Proceedings of the National Academy of Sciences of the United States of America 113, E1442-E1451.

110 **Christie, J. M., Salomon, M., Nozue, K., Wada, M. & Briggs, W. R. (1999)** *LOV (light, oxygen, or voltage) domains of the blue-light photoreceptor phototropin (nph1): Binding sites for the chromophore flavin mononucleotide*. Proceedings of the National Academy of Sciences 96, 8779-8783.

111 **Harper, S. M., Neil, L. C. & Gardner, K. H. (2003)** *Structural basis of a phototropin light switch*. Science 301, 1541-1544.

112 **Wu, Y. I., Frey, D., Lungu, O. I., Jaehrig, A., Schlichting, I., Kuhlman, B. & Hahn, K. M. (2009)** *A genetically encoded photoactivatable Rac controls the motility of living cells*. Nature 461, 104-108.

113 **Strickland, D., Yao, X., Gawlak, G., Rosen, M. K., Gardner, K. H. & Sosnick, T. R. (2010)** *Rationally improving LOV domain-based photoswitches*. Nature Methods 7, 623-626.

114 **Strickland, D., Lin, Y., Wagner, E., Hope, C. M., Zayner, J., Antoniou, C., Sosnick, T. R., Weiss, E. L. & Glotzer, M. (2012)** *TULIPs: Tunable, light-controlled interacting protein tags for cell biology*. Nature Methods 9, 379-384.

115 **Toettcher, J. E., Voigt, C. A., Weiner, O. D. & Lim, W. A. (2011)** *The promise of optogenetics in cell biology: Interrogating molecular circuits in space and time*. Nature Methods 8, 35-38.

116 **Prakash, R., Yizhar, O., Grewe, B., Ramakrishnan, C., Wang, N., Goshen, I., Packer, A. M., Peterka, D. S., Yuste, R., Schnitzer, M. J. & Deisseroth, K. (2012)** *Two-photon optogenetic toolbox for fast inhibition, excitation and bistable modulation*. Nature Methods 9, 1171-1179.

117 **Fish, K. N. (2009)** *Total internal reflection fluorescence (TIRF) microscopy*. Current Protocols in Cytometry 50, 12.18.11-12.18.13.

118 **Morri, M., Sanchez-Romero, I., Tichy, A. M., Kainrath, S., Gerrard, E. J., Hirschfeld, P. P., Schwarz, J. & Janovjak, H. (2018)** *Optical functionalization of human class A orphan G-protein-coupled receptors*. Nature Communications 9, 1950.

119 **Zhang, K., Duan, L., Ong, Q., Lin, Z., Varman, P. M., Sung, K. & Cui, B. (2014)** *Light-mediated kinetic control reveals the temporal effect of the Raf/MEK/ERK pathway in PC12 cell neurite outgrowth*. PLoS One 9, e92917.

120 **Toettcher, J. E., Weiner, O. D. & Lim, W. A. (2013)** *Using optogenetics to interrogate the dynamic control of signal transmission by the Ras/Erk module*. Cell 155, 1422-1434.

121 **Goglia, A. G., Wilson, M. Z., DiGiorno, D. B. & Toettcher, J. E. (2017)** *Optogenetic control of Ras/Erk signaling using the Phy-PIF system*. Methods in Molecular Biology 1636, 3-20.

122 **Johnson, H. E., Goyal, Y., Pannucci, N. L., Schupbach, T., Shvartsman, S. Y. & Toettcher, J. E. (2017)** *The spatiotemporal limits of developmental Erk signaling*. Developmental Cell 40, 185-192.

123 **Wilson, M. Z., Ravindran, P. T., Lim, W. A. & Toettcher, J. E. (2017)** *Tracing information flow from Erk to target gene induction reveals mechanisms of dynamic and combinatorial control*. Molecular Cell 67, 757-769.e755.

124 **Leopold, A. V., Chernov, K. G., Shemetov, A. A. & Verkhusha, V. V. (2019)** *Neurotrophin receptor tyrosine kinases regulated with near-infrared light*. Nature Communications 10, 1129.

125 **Hongdusit, A., Zwart, P. H., Sankaran, B. & Fox, J. M. (2020)** *Minimally disruptive optical control of protein tyrosine phosphatase 1B*. Nature Communications 11, 788.

126 **Zhou, X. X., Fan, L. Z., Li, P., Shen, K. & Lin, M. Z. (2017)** *Optical control of cell signaling by single-chain photoswitchable kinases*. Science 355, 836-842.

127 **Zhou, X., Wang, J., Chen, J., Qi, Y., Di, N., Jin, L., Qian, X., Wang, X., Chen, Q., Liu, X. & Xu, Y. (2018)** *Optogenetic control of epithelial-mesenchymal transition in cancer cells*. Scientific Reports 8, 14098.

128 **Grusch, M., Schelch, K., Riedler, R., Reichhart, E., Differ, C., Berger, W., Ingles-Prieto, A. & Janovjak, H. (2014)** *Spatio-temporally precise activation of engineered receptor tyrosine kinases by light*. The EMBO Journal 33, 1713-1726.

129 **Kim, N., Kim, J. M., Lee, M., Kim, C. Y., Chang, K.-Y. & Heo, W. D. (2014)** *Spatiotemporal control of fibroblast growth factor receptor signals by blue light*. Chemistry & Biology 21, 903-912.

130 **Kainrath, S., Stadler, M., Reichhart, E., Distel, M. & Janovjak, H. (2017)** *Green-light-induced inactivation of receptor signaling using cobalamin-binding domains*. Angewandte Chemie International Edition 56, 4608-4611.

131 **Thorey, I. S., Roth, J., Regenbogen, J., Halle, J.-P., Bittner, M., Vogl, T., Kaesler, S., Bugnon, P., Reitmaier, B. & Durka, S. (2001)** *The Ca2+-binding proteins S100A8 and S100A9 are encoded by novel injury-regulated genes*. Journal of Biological Chemistry 276, 35818-35825.

132 **Braun, S., Hanselmann, C., Gassmann, M. G., auf dem Keller, U., Born-Berclaz, C., Chan, K., Kan, Y. W. & Werner, S. (2002)** *Nrf2 transcription factor, a novel target of keratinocyte growth factor action which regulates gene expression and inflammation in the healing skin wound*. Molecular and Cellular Biology 22, 5492-5505.

133 **Graham, F. L., Smiley, J., Russell, W. C. & Nairn, R. (1977)** *Characteristics of a human cell line transformed by DNA from human adenovirus type 5*. Journal of General Virology 36, 59-72.

134 **Thomas, P. & Smart, T. G. (2005)** *HEK293 cell line: A vehicle for the expression of recombinant proteins*. Journal of Pharmacological and Toxicological Methods 51, 187-200.

135 **Boukamp, P., Petrussevska, R. T., Breitkreutz, D., Hornung, J., Markham, A. & Fusenig, N. E. (1988)** *Normal keratinization in a spontaneously immortalized aneuploid human keratinocyte cell line*. The Journal of Cell Biology 106, 761-771.

136 **Seo, E.-Y., Piao, Y.-J., Kim, J.-S., Suhr, K.-B., Park, J.-K. & Lee, J.-H. (2002)** *Identification of calcium-induced genes in HaCaT keratinocytes by polymerase chain reaction-based subtractive hybridization*. Archives of Dermatological Research 294, 411-418.

137 **Wilson, V. G.** in *Epidermal Cells: Methods and Protocols* (ed Kursad Turksen) 33-41 (Springer New York, 2014).

138 **Franken, N. A., Rodermond, H. M., Stap, J., Haveman, J. & van Bree, C. (2006)** *Clonogenic assay of cells in vitro*. Nature Protocols 1, 2315-2319.

139 **Wittekind, D. (2003)** *Traditional staining for routine diagnostic pathology including the role of tannic acid. 1. Value and limitations of the hematoxylin-eosin stain*. Biotechnic & Histochemistry 78, 261-270.

140 **Lillie, R., Tracy, R., Pizzolato, P., Donaldson, P. & Reynolds, C. (1980)** *Differential staining of collagen types in paraffin sections: A color change in degraded forms*. Virchows Archiv A 386, 153-159.

141 **Goldner, J. (1938)** *A modification of the Masson trichrome technique for routine laboratory purposes*. The American Journal of Pathology 14, 237-243.

142 **Truett, G. E., Heeger, P., Mynatt, R. L., Truett, A. A., Walker, J. A. & Warman, M. L. (2000)** *Preparation of PCR-quality mouse genomic DNA with hot sodium hydroxide and tris (HotSHOT)*. BioTechniques 29, 52-54.

143 **Strittmatter, G. E., Sand, J., Sauter, M., Seyffert, M., Steigerwald, R., Fraefel, C., Smola, S., French, L. E. & Beer, H.-D. (2016)** *IFN-γ primes keratinocytes for HSV-1–induced inflammasome activation*. Journal of Investigative Dermatology 136, 610-620.

144 **Zhang, J. D., Ruschhaupt, M. & Biczok, R.** (2010).

145 **Motulsky, H. (2007)** *Prism 5 Statistics Guide*. GraphPad Software.

146 **Reichhart, E., Ingles-Prieto, A., Tichy, A. M., McKenzie, C. & Janovjak, H. (2016)** *A phytochrome sensory domain permits receptor activation by red light*. Angewandte Chemie International Edition 55, 6339-6342.

147 **Leopold, A. V., Pletnev, S. & Verkhusha, V. V. (2020)** *Bacterial phytochrome as a scaffold for engineering of receptor tyrosine kinases controlled with near-infrared light*. Journal of Molecular Biology 432, 3749-3760.

148 **Krishnamurthy, V. V., Fu, J., Oh, T. J., Khamo, J., Yang, J. & Zhang, K. (2020)** *A generalizable optogenetic strategy to regulate receptor tyrosine kinases during vertebrate embryonic development*. Journal of Molecular Biology 432, 3149-3158.

149 **Kainrath, S. & Janovjak, H. (2020)** *Design and application of light-regulated receptor tyrosine kinases*. Methods in Molecular Biology 2173, 233-246.

150 **Zeng, H. & Madisen, L. (2012)** *Mouse transgenic approaches in optogenetics*. Progress in Brain Research 196, 193-213.

151 **Ting, J. T. & Feng, G. (2013)** *Development of transgenic animals for optogenetic manipulation of mammalian nervous system function: progress and prospects for behavioral neuroscience*. Behavioural Brain Research 255, 3-18.

152 **Nectow, A. R. & Nestler, E. J. (2020)** *Viral tools for neuroscience*. Nature Reviews Neuroscience 21, 669-681.

153 **Jansen, V., Alvarez, L., Balbach, M., Strünker, T., Hegemann, P., Kaupp, U. B. & Wachten, D. (2015)** *Controlling fertilization and cAMP signaling in sperm by optogenetics*. eLife 4.

154 **Luyben, T. T., Rai, J., Li, H., Georgiou, J., Avila, A., Zhen, M., Collingridge, G. L., Tominaga, T. & Okamoto, K. (2020)** *Optogenetic manipulation of postsynaptic cAMP using a novel transgenic mouse line enables synaptic plasticity and enhances depolarization following tetanic stimulation in the hippocampal dentate gyrus*. Frontiers in Neural Circuits 14, 24.

155 **Husson, S. J., Gottschalk, A. & Leifer, A. M. (2013)** *Optogenetic manipulation of neural activity in C. elegans: From synapse to circuits and behaviour*. Biology of the Cell 105, 235-250.

156 **Guglielmi, G., Barry, J. D., Huber, W. & De Renzis, S. (2015)** *An optogenetic method to modulate cell contractility during tissue morphogenesis*. Developmental Cell 35, 646-660.

157 **Johnson, H. E., Goyal, Y., Pannucci, N. L., Schüpbach, T., Shvartsman, S. Y. & Toettcher, J. E. (2017)** *The spatiotemporal limits of developmental Erk signaling*. Developmental Cell 40, 185-192.

158 **Bunnag, N., Tan, Q. H., Kaur, P., Ramamoorthy, A., Sung, I. C. H., Lusk, J. & Tolwinski, N. S. (2020)** *An optogenetic method to study signal transduction in intestinal stem cell homeostasis*. Journal of Molecular Biology 432, 3159-3176.

159 **Tsukada, Y. & Mori, I. (2021)** *Optogenetics in Caenorhabditis elegans*. Advances in Experimental Medicine and Biology 1293, 321-334.

160 **Welm, B. E., Freeman, K. W., Chen, M., Contreras, A., Spencer, D. M. & Rosen, J. M. (2002)** *Inducible dimerization of FGFR1: Development of a mouse model to analyze progressive transformation of the mammary gland*. Journal of Cell Biology 157, 703-714.

161 **Frank, S., Hübner, G., Breier, G., Longaker, M. T., Greenhalgh, D. G. & Werner, S. (1995)** *Regulation of vascular endothelial growth factor expression in cultured keratinocytes. Implications for normal and impaired wound healing*. Journal of Biological Chemistry 270, 12607-12613.

162 **Li, C., Scott, D. A., Hatch, E., Tian, X. & Mansour, S. L. (2007)** *Dusp6 (Mkp3) is a negative feedback regulator of FGF-stimulated ERK signaling during mouse development*. Development 134, 167-176.

163 **Maddaluno, L., Urwyler, C., Rauschendorfer, T., Meyer, M., Stefanova, D., Spörri, R., Wietecha, M., Ferrarese, L., Stoycheva, D., Bender, D., Li, N., Strittmatter, G., Nasirujjaman, K., Beer, H. D., Staeheli, P., Hildt, E., Oxenius, A. & Werner, S. (2020)** *Antagonism of interferon signaling by fibroblast growth factors promotes viral replication*. EMBO Molecular Medicine 12, e11793.

164 **Belleudi, F., Purpura, V. & Torrisi, M. R. (2011)** *The receptor tyrosine kinase FGFR2b/KGFR controls early differentiation of human keratinocytes*. PLoS One 6, e24194.

165 **Rosato, B., Ranieri, D., Nanni, M., Torrisi, M. R. & Belleudi, F. (2018)** *Role of FGFR2b expression and signaling in keratinocyte differentiation: Sequential involvement of PKCδ and PKCα*. Cell Death & Disease 9, 565.

166 **Calero-Nieto, F. J., Bert, A. G. & Cockerill, P. N. (2010)** *Transcription-dependent silencing of inducible convergent transgenes in transgenic mice*. Epigenetics & Chromatin 3, 3.

167 **Blewitt, M. & Whitelaw, E. (2013)** *The use of mouse models to study epigenetics*. Cold Spring Harbor Perspectives in Biology 5, a017939.

168 **Gödecke, N., Zha, L., Spencer, S., Behme, S., Riemer, P., Rehli, M., Hauser, H. & Wirth, D. (2017)** *Controlled re-activation of epigenetically silenced Tet promoter-driven transgene expression by targeted demethylation*. Nucleic Acids Research 45, e147.

169 **Marchese, C., Chedid, M., Dirsch, O. R., Csaky, K. G., Santanelli, F., Latini, C., LaRochelle, W. J., Torrisi, M. R. & Aaronson, S. A. (1995)** *Modulation of keratinocyte growth factor and its receptor in reepithelializing human skin*. Journal of Experimental Medicine 182, 1369-1376.

170 **Ali, J., Mansukhani, A. & Basilico, C. (1995)** *Fibroblast growth factor receptors 1 and 2 are differentially regulated in murine embryonal carcinoma cells and in response to fibroblast growth factor-4*. Journal of Cellular Physiology 165, 438-448.

171 **Nunes, Q. M., Li, Y., Sun, C., Kinnunen, T. K. & Fernig, D. G. (2016)** *Fibroblast growth factors as tissue repair and regeneration therapeutics*. PeerJ 4, e1535.

172 **Zhang, J. & Li, Y. (2016)** *Therapeutic uses of FGFs*. Seminars in Cell & Developmental Biology 53, 144-154.

173 **Tanner, Y. & Grose, R. P. (2016)** *Dysregulated FGF signalling in neoplastic disorders*. Seminars in Cell and Developmental Biology 53, 126-135.

174 **Ank, N., Iversen, M. B., Bartholdy, C., Staeheli, P., Hartmann, R., Jensen, U. B., Dagnaes-Hansen, F., Thomsen, A. R., Chen, Z., Haugen, H., Klucher, K. & Paludan, S. R. (2008)** *An important role for type III interferon (IFN-lambda/IL-28) in TLR-induced antiviral activity*. Journal of Immunology 180, 2474-2485.

175 **Mordstein, M., Kochs, G., Dumoutier, L., Renauld, J. C., Paludan, S. R., Klucher, K. & Staeheli, P. (2008)** *Interferon-lambda contributes to innate immunity of mice against influenza A virus but not against hepatotropic viruses*. PLoS Pathogens 4, e1000151.

176 **Mohn, F., Weber, M., Schubeler, D. & Roloff, T. C. (2009)** *Methylated DNA immunoprecipitation (MeDIP)*. Methods in Molecular Biology 507, 55-64.

177 **Beyer, T. A., Xu, W., Teupser, D., auf dem Keller, U., Bugnon, P., Hildt, E., Thiery, J., Kan, Y. W. & Werner, S. (2008)** *Impaired liver regeneration in Nrf2 knockout mice: Role of ROS-mediated insulin/IGF-1 resistance*. The EMBO Journal 27, 212-223.

178 **Kuleshov, M. V., Jones, M. R., Rouillard, A. D., Fernandez, N. F., Duan, Q., Wang, Z., Koplev, S., Jenkins, S. L., Jagodnik, K. M., Lachmann, A., McDermott, M. G., Monteiro, C. D., Gundersen, G. W. & Ma'ayan, A. (2016)** *Enrichr: A comprehensive gene set enrichment analysis web server 2016 update*. Nucleic Acids Research 44, W90-97.

179 **Rahn, E., Thier, K., Petermann, P. & Knebel-Mörsdorf, D. (2015)** *Ex vivo infection of murine epidermis with Herpes simplex virus type 1*. Journal of Visualized Experiments, e53046.

180 **Sulcova, J., Maddaluno, L., Meyer, M. & Werner, S. (2015)** *Accumulation and activation of epidermal γδ T cells in a mouse model of chronic dermatitis is not required for the inflammatory phenotype*. European Journal of Immunology 45, 2517-2528.

181 **Guagnano, V., Furet, P., Spanka, C., Bordas, V., Le Douget, M., Stamm, C., Brueggen, J., Jensen, M. R., Schnell, C., Schmid, H., Wartmann, M., Berghausen, J., Drueckes, P., Zimmerlin, A., Bussiere, D., Murray, J. & Graus Porta, D. (2011)** *Discovery of 3-(2,6-dichloro-3,5-dimethoxy-phenyl)-1-{6-[4-(4-ethyl-piperazin-1-yl)-phenylamin o]-pyrimidin-4-yl}-1-methyl-urea (NVP-BGJ398), a potent and selective inhibitor of the fibroblast growth factor receptor family of receptor tyrosine kinase*. Journal of Medicinal Chemistry 54, 7066-7083.

182 **Gough, D. J., Messina, N. L., Clarke, C. J., Johnstone, R. W. & Levy, D. E. (2012)** *Constitutive type I interferon modulates homeostatic balance through tonic signaling*. Immunity 36, 166-174.

183 **Blumer, T., Coto-Llerena, M., Duong, F. H. T. & Heim, M. H. (2017)** *SOCS1 is an inducible negative regulator of interferon lambda (IFN-lambda)-induced gene expression in vivo*. Journal of Biological Chemistry 292, 17928-17938.

184 **Michalska, A., Blaszczyk, K., Wesoly, J. & Bluyssen, H. A. R. (2018)** *A positive feedback amplifier circuit that regulates interferon (IFN)-stimulated gene expression and controls type I and type II IFN responses*. Frontiers in Immunology 9, 1135.

185 **Visco, V., Bava, F. A., d'Alessandro, F., Cavallini, M., Ziparo, V. & Torrisi, M. R. (2009)** *Human colon fibroblasts induce differentiation and proliferation of intestinal epithelial cells through the direct paracrine action of keratinocyte growth factor*. Journal of Cellular Physiology 220, 204-213.

186 **Bruns, A. M. & Horvath, C. M. (2014)** *Antiviral RNA recognition and assembly by RLR family innate immune sensors*. Cytokine & Growth Factor Reviews 25, 507-512.

187 **Gavine, P. R., Mooney, L., Kilgour, E., Thomas, A. P., Al-Kadhimi, K., Beck, S., Rooney, C., Coleman, T., Baker, D., Mellor, M. J., Brooks, A. N. & Klinowska, T. (2012)** *AZD4547: An orally bioavailable, potent, and selective inhibitor of the fibroblast growth factor receptor tyrosine kinase family*. Cancer Research 72, 2045-2056.

188 **Ivashkiv, L. B. & Donlin, L. T. (2014)** *Regulation of type I interferon responses*. Nature Reviews Immunology 14, 36-49.

189 **Villeneuve, N. F., Lau, A. & Zhang, D. D. (2010)** *Regulation of the Nrf2-Keap1 antioxidant response by the ubiquitin proteasome system: An insight into cullin-ring ubiquitin ligases*. Antioxidants & Redox Signaling 13, 1699-1712.

190 **Honda, K., Yanai, H., Negishi, H., Asagiri, M., Sato, M., Mizutani, T., Shimada, N., Ohba, Y., Takaoka, A., Yoshida, N. & Taniguchi, T. (2005)** *IRF-7 is the master regulator of type-I interferon-dependent immune responses*. Nature 434, 772-777.

191 **Panda, D., Gjinaj, E., Bachu, M., Squire, E., Novatt, H., Ozato, K. & Rabin, R. L. (2019)** *IRF1 maintains optimal constitutive expression of antiviral genes and regulates the early antiviral response*. Frontiers in Immunology 10, 1019.

192 **Shaw, A. E., Hughes, J., Gu, Q., Behdenna, A., Singer, J. B., Dennis, T., Orton, R. J., Varela, M., Gifford, R. J., Wilson, S. J. & Palmarini, M. (2017)** *Fundamental properties of the mammalian innate immune system revealed by multispecies comparison of type I interferon responses*. PLoS Biology 15, e2004086.

193 **Alexopoulou, L., Holt, A. C., Medzhitov, R. & Flavell, R. A. (2001)** *Recognition of double-stranded RNA and activation of NF-kappaB by Toll-like receptor 3*. Nature 413, 732-738.

194 **Petermann, P., Thier, K., Rahn, E., Rixon, F. J., Bloch, W., Ozcelik, S., Krummenacher, C., Barron, M. J., Dixon, M. J., Scheu, S., Pfeffer, K. & Knebel-Morsdorf, D. (2015)** *Entry mechanisms of herpes simplex virus 1 into murine epidermis: Involvement of nectin-1 and herpesvirus entry mediator as cellular receptors*. Journal of Virology 89, 262-274.

195 **Sayers, C. L. & Elliott, G. (2016)** *Herpes simplex virus 1 enters human keratinocytes by a nectin-1-dependent, rapid plasma membrane fusion pathway that functions at low temperature*. Journal of Virology 90, 10379-10389.

196 **Hamel, R., Dejarnac, O., Wichit, S., Ekchariyawat, P., Neyret, A., Luplertlop, N., Perera-Lecoin, M., Surasombatpattana, P., Talignani, L., Thomas, F., Cao-Lormeau, V. M., Choumet, V., Briant, L., Despres, P., Amara, A., Yssel, H. & Misse, D. (2015)** *Biology of zika virus infection in human skin cells*. Journal of Virology 89, 8880-8896.

197 **Zhu, X., He, Z., Hu, Y., Wen, W., Lin, C., Yu, J., Pan, J., Li, R., Deng, H., Liao, S., Yuan, J., Wu, J., Li, J. & Li, M. (2014)** *MicroRNA-30e* suppresses dengue virus replication by promoting NF-kappaB-dependent IFN production*. PLoS Neglected Tropical Diseases 8, e3088.

198 **Aoki, R., Kawamura, T., Goshima, F., Ogawa, Y., Nakae, S., Nakao, A., Moriishi, K., Nishiyama, Y. & Shimada, S. (2013)** *Mast cells play a key role in host defense*

against herpes simplex virus infection through TNF-alpha and IL-6 production. Journal of Investigative Dermatology 133, 2170-2179.

199 **Lulli, D., Carbone, M. L. & Pastore, S. (2017)** *The MEK inhibitors trametinib and cobimetinib induce a type I interferon response in human keratinocytes*. International Journal of Molecular Sciences 18.

200 **Battcock, S. M., Collier, T. W., Zu, D. & Hirasawa, K. (2006)** *Negative regulation of the alpha interferon-induced antiviral response by the Ras/Raf/MEK pathway*. Journal of Virology 80, 4422-4430.

201 **Darnell, J. E., Jr., Kerr, I. M. & Stark, G. R. (1994)** *Jak-STAT pathways and transcriptional activation in response to IFNs and other extracellular signaling proteins*. Science 264, 1415-1421.

202 **Leviyang, S., Strawn, N. & Griva, I. (2019)** *Regulation of interferon stimulated gene expression levels at homeostasis*. Cytokine 126, 154870.

203 **Nakagawa, K. & Yokosawa, H. (2000)** *Degradation of transcription factor IRF-1 by the ubiquitin-proteasome pathway. The C-terminal region governs the protein stability*. European Journal of Biochemistry 267, 1680-1686.

204 **Barro, M. & Patton, J. T. (2007)** *Rotavirus NSP1 inhibits expression of type I interferon by antagonizing the function of interferon regulatory factors IRF3, IRF5, and IRF7*. Journal of Virology 81, 4473-4481.

205 **Zhao, X., Zhu, H., Yu, J., Li, H., Ge, J. & Chen, W. (2016)** *c-Cbl-mediated ubiquitination of IRF3 negatively regulates IFN-beta production and cellular antiviral response*. Cell Signaling 28, 1683-1693.

206 **Fujita, T., Kimura, Y., Miyamoto, M., Barsoumian, E. L. & Taniguchi, T. (1989)** *Induction of endogenous IFN-alpha and IFN-beta genes by a regulatory transcription factor, IRF-1*. Nature 337, 270-272.

207 **Maher, S. G., Romero-Weaver, A. L., Scarzello, A. J. & Gamero, A. M. (2007)** *Interferon: cellular executioner or white knight?* Current Medicinal Chemistry 14, 1279-1289.

208 **Lasfar, A., Zloza, A., de la Torre, A. & Cohen-Solal, K. A. (2016)** *IFN-lambda: A new inducer of local immunity against cancer and infections*. Frontiers in Immunology 7, 598.

209 **Schneider, W. M., Chevillotte, M. D. & Rice, C. M. (2014)** *Interferon-stimulated genes: A complex web of host defenses*. Annual Reviews Immunology 32, 513-545.

210 **Kaner, R. J., Baird, A., Mansukhani, A., Basilico, C., Summers, B. D., Florkiewicz, R. Z. & Hajjar, D. P. (1990)** *Fibroblast growth factor receptor is a portal of cellular entry for herpes simplex virus type 1*. Science 248, 1410-1413.

211 **Schoggins, J. W. & Rice, C. M. (2011)** *Interferon-stimulated genes and their antiviral effector functions*. Current Opinion in Virology 1, 519-525.

212 **Werner, S., Peters, K. G., Longaker, M. T., Fuller-Pace, F., Banda, M. J. & Williams, L. T. (1992)** *Large induction of keratinocyte growth factor expression in the dermis during wound healing*. Proceedings of the National Academy of Sciences 89, 6896-6900.

213 **Finch, P. W. & Rubin, J. S. (2004)** *Keratinocyte growth factor/fibroblast growth factor 7, a homeostatic factor with therapeutic potential for epithelial protection and repair*. Advances in Cancer Research 91, 69-136.

214 **Van, N. D., Falk, C. S., Sandmann, L., Vondran, F. W., Helfritz, F., Wedemeyer, H., Manns, M. P., Ciesek, S. & von Hahn, T. (2016)** *Modulation of HCV reinfection after orthotopic liver transplantation by fibroblast growth factor-2 and other non-interferon mediators*. Gut 65, 1015-1023.

215 **Limonta, D., Jovel, J., Kumar, A., Lu, J., Hou, S., Airo, A. M., Lopez-Orozco, J., Wong, C. P., Saito, L., Branton, W., Wong, G. K.-S., Mason, A., Power, C. & Hobman, T. C. (2019)** *Fibroblast growth factor 2 enhances zika virus infection in human fetal brain*. The Journal of Infectious Diseases 220, 1377-1387.

216 **Prince, L. S., Karp, P. H., Moninger, T. O. & Welsh, M. J. (2001)** *KGF alters gene expression in human airway epithelia: Potential regulation of the inflammatory response*. Physiological Genomics 6, 81-89.

217 **Quantius, J., Schmoldt, C., Vazquez-Armendariz, A. I., Becker, C., El Agha, E., Wilhelm, J., Morty, R. E., Vadasz, I., Mayer, K., Gattenloehner, S., Fink, L., Matrosovich, M., Li, X., Seeger, W., Lohmeyer, J., Bellusci, S. & Herold, S. (2016)** *Influenza virus infects epithelial stem/progenitor cells of the distal lung: Impact on Fgfr2b-driven epithelial repair*. PLoS Pathogens 12, e1005544.

218 **van Asten, S. D., Raaben, M., Nota, B. & Spaapen, R. M. (2018)** *Secretome screening reveals fibroblast growth factors as novel inhibitors of viral replication*. Journal of Virology 92, e00260-00218.

219 **Cortese, M., Kumar, A., Matula, P., Kaderali, L., Scaturro, P., Erfle, H., Acosta, E. G., Buehler, S., Ruggieri, A., Chatel-Chaix, L., Rohr, K. & Bartenschlager, R. (2019)** *Reciprocal effects of fibroblast growth factor receptor signaling on dengue virus replication and virion production*. Cell Reports 27, 2579-2592.

220 **Grose, R., Fantl, V., Werner, S., Chioni, A. M., Jarosz, M., Rudling, R., Cross, B., Hart, I. R. & Dickson, C. (2007)** *The role of fibroblast growth factor receptor 2b in skin homeostasis and cancer development*. The EMBO Journal 26, 1268-1278.

221 **Sulcova, J., Meyer, M., Guiducci, E., Feyerabend, T. B., Rodewald, H.-R. & Werner, S. (2015)** *Mast cells are dispensable in a genetic mouse model of chronic dermatitis*. American Journal of Pathology 185, 1575-1587.

222 **Seltmann, K., Meyer, M., Sulcova, J., Kockmann, T., Wehkamp, U., Weidinger, S., auf dem Keller, U. & Werner, S. (2018)** *Humidity-regulated CLCA2 protects the epidermis from hyperosmotic stress*. Science Translational Medicine 10, eaao4650.

223 **Meyers, G. A., Orlow, S. J., Munro, I. R., Przylepa, K. A. & Jabs, E. W. (1995)** *Fibroblast growth factor receptor 3 (FGFR3) transmembrane mutation in Crouzon syndrome with acanthosis nigricans*. Nature Genetics 11, 462.

224 **Wilkes, D., Rutland, P., Pulleyn, L., Reardon, W., Moss, C., Ellis, J., Winter, R. & Malcolm, S. (1996)** *A recurrent mutation, ala391glu, in the transmembrane region of FGFR3 causes Crouzon syndrome and acanthosis nigricans*. Journal of Medical Genetics 33, 744-748.

225 **Logie, A., Dunois-Larde, C., Rosty, C., Levrel, O., Blanche, M., Ribeiro, A., Gasc, J.-M., Jorcano, J., Werner, S. & Sastre-Garau, X. (2005)** *Activating mutations of the tyrosine kinase receptor FGFR3 are associated with benign skin tumors in mice and humans*. Human Molecular Genetics 14, 1153-1160.

226 **Hafner, C., van Oers, J. M., Vogt, T., Landthaler, M., Stoehr, R., Blaszyk, H., Hofstaedter, F., Zwarthoff, E. C. & Hartmann, A. (2006)** *Mosaicism of activating FGFR3 mutations in human skin causes epidermal nevi*. Journal of Clinical Investigation 116, 2201-2207.

227 **Su, N., Xu, X., Li, C., He, Q., Zhao, L., Li, C., Chen, S., Luo, F., Yi, L. & Du, X. (2010)** *Generation of Fgfr3 conditional knockout mice*. International Journal of Biological Sciences 6, 327.

228 **Ramirez, A., Page, A., Gandarillas, A., Zanet, J., Pibre, S., Vidal, M., Tusell, L., Genesca, A., Whitaker, D. A. & Melton, D. W. (2004)** *A keratin K5-Cre transgenic line appropriate for tissue-specific or generalized Cre-mediated recombination*. Genesis 39, 52-57.

229 **Chrostek, A., Wu, X., Quondamatteo, F., Hu, R., Sanecka, A., Niemann, C., Langbein, L., Haase, I. & Brakebusch, C. (2006)** *Rac1 is crucial for hair follicle integrity but is not essential for maintenance of the epidermis*. Molecular and Cellular Biology 26, 6957-6970.

230 **Herovici, C. (1963)** *Picropolychrome: Histological staining technic intended for the study of normal and pathological connective tissue*. Revue francaise d'etudes cliniques et biologiques 8, 88.

231 **Sennett, R., Wang, Z., Rezza, A., Grisanti, L., Roitershtein, N., Sicchio, C., Mok, K. W., Heitman, N. J., Clavel, C. & Ma'ayan, A. (2015)** *An integrated transcriptome atlas of embryonic hair follicle progenitors, their niche, and the developing skin*. Developmental Cell 34, 577-591.

232 **Joost, S., Zeisel, A., Jacob, T., Sun, X., La Manno, G., Lönnerberg, P., Linnarsson, S. & Kasper, M. (2016)** *Single-cell transcriptomics reveals that differentiation and spatial signatures shape epidermal and hair follicle heterogeneity*. Cell Systems 3, 221-237. e229.

233 **Chellaiah, A. T., McEwen, D. G., Werner, S., Xu, J. & Ornitz, D. M. (1994)** *Fibroblast growth factor receptor (FGFR) 3. Alternative splicing in immunoglobulin-like domain III creates a receptor highly specific for acidic FGF/FGF-1*. Journal of Biological Chemistry 269, 11620-11627.

234 **McGowan, K. & Coulombe, P. (1998)** *The wound repair-associated keratins 6, 16, and 17. Insights into the role of intermediate filaments in specifying keratinocyte cytoarchitecture*. Sub-cellular Biochemistry 31, 173-204.

235 **Duperret, E. K., Oh, S. J., McNeal, A., Prouty, S. M. & Ridky, T. W. (2014)** *Activating FGFR3 mutations cause mild hyperplasia in human skin, but are insufficient to drive benign or malignant skin tumors*. Cell Cycle 13, 1551-1559.

236 **Takenaka, H., Yasuno, H. & Kishimoto, S. (2002)** *Immunolocalization of fibroblast growth factor receptors in normal and wounded human skin*. Archives of Dermatological Research 294, 331-338.

237 **Beer, H.-D., Florence, C., Dammeier, J., McGuire, L., Werner, S. & Duan, D. R. (1997)** *Mouse fibroblast growth factor 10: cDNA cloning, protein characterization, and regulation of mRNA expression*. Oncogene 15, 2211.

238 **Xu, W., Hong, S. J., Zhong, A., Xie, P., Jia, S., Xie, Z., Zeitchek, M., Niknam-Bienia, S., Zhao, J. & Porterfield, D. M. (2015)** *Sodium channel Nax is a regulator in epithelial sodium homeostasis*. Science Translational Medicine 7, 312ra177-312ra177.

239 **Zhao, J., Zhong, A., Friedrich, E. E., Jia, S., Xie, P., Galiano, R. D., Mustoe, T. A. & Hong, S. J. (2017)** *S100A12 induced in the epidermis by reduced hydration activates dermal fibroblasts and causes dermal fibrosis*. Journal of Investigative Dermatology 137, 650-659.

240 **Zhong, A., Xu, W., Zhao, J., Xie, P., Jia, S., Sun, J., Galiano, R. D., Mustoe, T. A. & Hong, S. J. (2016)** *S100A8 and S100A9 are induced by decreased hydration in the*

epidermis and promote fibroblast activation and fibrosis in the dermis. American Journal of Pathology 186, 109-122.

241 **Hedger, M. P. & de Kretser, D. M. (2013)** *The activins and their binding protein, follistatin — diagnostic and therapeutic targets in inflammatory disease and fibrosis*. Cytokine & Growth factor Reviews 24, 285-295.

242 **Werner, S. & Alzheimer, C. (2006)** *Roles of activin in tissue repair, fibrosis, and inflammatory disease*. Cytokine & Growth Factor Reviews 17, 157-171.

243 **Icha, J., Weber, M., Waters, J. C. & Norden, C. (2017)** *Phototoxicity in live fluorescence microscopy, and how to avoid it*. Bioessays 39, 1700003.

244 **Nanni, M., Ranieri, D., Raffa, S., Torrisi, M. R. & Belleudi, F. (2018)** *Interplay between FGFR2b-induced autophagy and phagocytosis: Role of PLCγ-mediated signalling*. Journal of Cellular and Molecular Medicine 22, 668-683.

245 **Maimon, B. E., Diaz, M., Revol, E. C. M., Schneider, A. M., Leaker, B., Varela, C. E., Srinivasan, S., Weber, M. B. & Herr, H. M. (2018)** *Optogenetic peripheral nerve immunogenicity*. Scientific Reports 8, 14076.

246 **Bhalla, U. S. & Iyengar, R. (1999)** *Emergent properties of networks of biological signaling pathways*. Science 283, 381-387.

247 **Weng, G., Bhalla, U. S. & Iyengar, R. (1999)** *Complexity in biological signaling systems*. Science 284, 92-96.

248 **Soyer, O. S. & Bonhoeffer, S. (2006)** *Evolution of complexity in signaling pathways*. Proceedings of the National Academy of Sciences 103, 16337-16342.

249 **Edelman, G. M. & Gally, J. A. (2001)** *Degeneracy and complexity in biological systems*. Proceedings of the National Academy of Sciences 98, 13763-13768.

250 **Neves, S. R. & Iyengar, R. (2009)** *Models of spatially restricted biochemical reaction systems*. The Journal of Biological Chemistry 284, 5445-5449.

251 **Neves, S. R. (2012)** *Modeling of spatially-restricted intracellular signaling*. Wiley Interdisciplinary Reviews - Systems Biology and Medicine 4, 103-115.

252 **Ray, A. T., Mazot, P., Brewer, J. R., Catela, C., Dinsmore, C. J. & Soriano, P. (2020)** *FGF signaling regulates development by processes beyond canonical pathways*. Genes & Development 34, 1735-1752.

253 **Iadevaia, S., Lu, Y., Morales, F. C., Mills, G. B. & Ram, P. T. (2010)** *Identification of optimal drug combinations targeting cellular networks: Integrating phospho-proteomics and computational network analysis*. Cancer Research 70, 6704-6714.

254 **Likić, V. A., McConville, M. J., Lithgow, T. & Bacic, A. (2010)** *Systems biology: The next frontier for bioinformatics*. Advances in Bioinformatics 2010, 268925-268925.

255 **Eungdamrong, N. J. & Iyengar, R. (2004)** *Modeling cell signaling networks*. Biology of the Cell 96, 355-362.

256 **Qi, Y. & Ge, H. (2006)** *Modularity and dynamics of cellular networks*. PLoS Computational Biology 2, e174.

257 **Mohsenizadeh, D. N., Hua, J., Bittner, M. & Dougherty, E. R. (2015)** *Dynamical modeling of uncertain interaction-based genomic networks*. BMC bioinformatics 16, S3-S3.

258 **Rangamani, P. & Iyengar, R. (2008)** *Modelling cellular signalling systems*. Essays in Biochemistry 45, 83-94.

259 **Bizzarri, M., Naimark, O., Nieto-Villar, J., Fedeli, V. & Giuliani, A. (2020)** *Complexity in biological organization: Deconstruction (and subsequent restating) of key concepts*. Entropy 22, 885.

260 **Ma'ayan, A., Blitzer, R. D. & Iyengar, R. (2005)** *Toward predictive models of mammalian cells*. Annual Review of Biophysics and Biomolecular Structure 34, 319-349.